Katinka Bjørhovde Rossebø

Determination of Vapour Resistance of Exterior Coatings

Impact on Moisture Drying Conditions in Wooden Claddings

NTNU
Norwegian University of
Science and Technology

Katinka Bjørhovde Rossebø

Determination of Vapour Resistance of Exterior Coatings

Impact on Moisture Drying Conditions in Wooden Claddings

Master's thesis in Civil and Environmental Engineering
Supervisor: Tore Kvande
June 2024

Norwegian University of Science and Technology
Faculty of Engineering
Department of Civil and Environmental Engineering

NTNU
Norwegian University of
Science and Technology

Abstract

The anticipated increasing frequency of precipitation and greater fluctuations in moisture levels due to global climate change pose current and future challenges for building envelopes. Wooden façades, which are common in Nordic regions, are particularly vulnerable as they are directly exposed to these climatic agents. To prevent premature degradation and decay processes of these wooden materials, proper surface protection and maintenance is known to be necessary.

This study aims to investigate the influence of exterior wood coatings' water vapour resistance on the moisture conditions and mould growth risks of ventilated wooden claddings. The vapour resistance in terms of diffusion-equivalent air layer thickness (s_d-value) is determined experimentally for nine commercial coatings (one alkyd, three emulsions, and five acrylics) by employing the wet cup method as specified in NS-EN ISO12572:2016. Further, one-dimensional simulations are conducted in WUFI Pro and post-processed in WUFI Mould Index VTT to simulate the possible influence of the coatings' vapour resistance on wood moisture conditions and evaluate the risk of mould growth. In this study, the cavity microclimate was modelled by fitting sinusoids, to represent the realistic conditions interior of the wooden cladding.

The determined s_d-values range from 0.453 to 1.350 m (three layers) and 0.690 to 2.250 m (six layers), showing a very strong correlation to dry film thickness. The simulations reveal that while the vapour resistance of coatings does not significantly influence wood moisture content in the long run (no accumulation of moisture), a coating with lower vapour resistance will facilitate slightly faster drying of embedded wood moisture. Untreated claddings show greater moisture content fluctuations and variability, as well as higher mould risks, compared to coated claddings, affirming the importance of liquid barrier properties of surface treatments. The yearly mould index of the southwest-facing wall in Stavanger is slightly accumulating over five years, which indicate favourable conditions for mould growth despite apparently sufficient drying of wood moisture. How one chooses to model the interior climate conditions is of great significance the reliability of the simulations. Fitted sinusoids can model an air cavity's temperature more precisely than relative humidity. Despite model uncertainty, it nevertheless provides insight and highlights the need for further model refinement to accurately capture the complexities of cavity microclimates.

Future research should investigate the influence of additional film supports in the wet cup-assembly on the measurements of s_d-values, as well as whether there is a definite relation between binder content and vapour resistance, by systematic experiments with larger sample sizes. The impact of other factors than vapour resistance of coatings, possibly in combination with the considered vapour resistance, should be studied more closely to develop strategies to mitigate the ever-reported rot issues in wooden claddings.

Sammendrag

Den forventede økende hyppigheten av nedbør og ekstremvær, og større fluktuasjoner i luftfuktighet på grunn av globale klimaendringer utgjør nåværende og fremtidige utfordringer for bygningskonstruksjoner. Trefasader, som er vanlige i Norden, er særlig utsatte ettersom de er direkte eksponert for disse klimapåkjenningene. For å forhindre fuktrelaterte skader og prematur nedbrytning, er riktig overflatebehandling og vedlikehold som kjent nødvendig.

Denne studien undersøker hvordan vanndampmotstanden til maling påvirker uttørkingsforhold og muggvekstrisiko i ventilerte trekledninger i to ulike norske klima. Vanndampmotstanden, i form av diffusjonsekvivalent luftlagtykkelse (s_d-verdi), blir bestemt eksperimentelt for ni kommersielle malingsprodukter (én alkyd, tre emulsjoner og fem akryl) ved å benytte våt-koppmetoden som spesifisert i NS-EN ISO12572:2016. Videre utføres én-dimensjonale simuleringer i WUFI Pro og etterbehandles i WUFI Mould Index VTT for å simulere dampmotstandens mulige påvirkning på fuktforholdene og evaluere risikoen for muggvekst. I denne studien ble luftspaltens mikroklima modellert som innendørs klima ved å tilpasse sinuskurver for å representere realistiske forhold innvendig i trekledningen.

De målte s_d-verdiene varierer fra 0.453 til 1.350 m (tre lag) og 0.690 til 2.250 m (seks lag) med lave standardavvik. s_d-verdi viser en svært sterk korrelasjon til tørrfilmtykkelse. Simuleringene avdekker at selv om malingens vanndampmotstand ikke påvirker trekledningens fuktinnhold over tid (ingen akkumulering av fukt), vil en maling med lavere dampmotstand fasilitere noe raskere uttørking av fukt. Ubehandlede kledninger viser større svingninger og variabilitet i trekledningens fuktinnhold samt høyere muggrisiko sammenlignet med de malte kledningene, noe som bekrefter viktigheten av barriereegenskapene til overflatebehandling. Den årlige muggindeksen for den sørvest-vendte veggen i Stavanger akkumuleres over fem år, noe som indikerer gunstige forhold for muggvekst til tross for tilsynelatende tilstrekkelig uttørking av trefukt. Hvordan man velger å modellere inneklimaforholdene for fuktsimuleringen er av stor betydning for påliteligheten av resultatene. Tilpassede sinuskurver kan modellere temperatur mer presist enn relative fuktighet i luftspalten. Til tross for modellusikkerhet, gir det likevel innsikt og understreker behovet for ytterligere tilpasninger for å fange kompleksiteten i luftspalteklima på en nøyaktig måte.
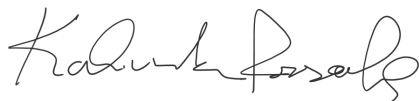
Videre studier bør undersøke hvordan bruk av ekstra film-støtte ved kopp-montasje påvirker målingene av s_d-verdi, samt om det er en korrelasjon mellom bindemiddel og dampmotstand, gjennom systematiske eksperimenter med større utvalg. Påvirkningen av andre faktorer enn malingens dampmotstand, eventuelt i kombinasjon med denne dampmotstanden, bør studeres nærmere for å utvikle strategier for å minimere de stadige rapporterte råteproblemene i trekledninger.

Preface

This master's thesis has been prepared at the Department of Civil and Environmental Engineering at the Norwegian University of Science and Technology (NTNU) during the spring semester of 2024. The scope of the thesis is 30 credits, and it constitutes the final semester of the five-year study program in Civil and Environmental Engineering.

I would like to express gratitude to my supervisor, Tore Kvande, for his presence and insightful discussions throughout the process. And for keeping my feet on the ground. A special thanks to Ole Aunrønning for his invaluable assistance with the laboratory measurements and other practical aspects of the project.

The completion of this thesis would not have been possible without the unwavering support from my family and friends over the past few months. Their encouragement and contributions have made this journey truly "No Problem et al.".

Katinka Bjørhovde Rossebø

Trondheim, June 2024

Table of Contents

List of Acronyms

MC	Moisture content
MDRY	Moisture Design Reference Year
RH	Relative humidity
RH_{cr}	Critical relative humidity
T	Temperature
TMY	Typical Meteorological Year
WUFI	Wärme Und Feuchte Instationär
ZEB	Zero Emission Building

List of Symbols

p_v	Water vapour partial pressure	Pa
δ_a	Water vapour permeability of air	kg/(msPa)
δ_p	Water vapour permeability	kg/(msPa)
Z_p	Water vapour resistance	m^2sPa/kg
W_p	Water vapour permeance	kg/m^2sPa
s_d	Water vapour diffusion equivalent air layer thickness	m
μ	Water vapour resistance factor	[-]
u	Moisture content	kg/kg (weight-%)

1 Introduction

1.1 Background

Climate change projections indicate that the already harsh Nordic climate conditions are likely to intensify, with increased precipitation and rising temperatures anticipated in the years to come (Hanssen-Bauer *et al.*, 2017). Moisture-related defects are typically issues i.e. mould growth, rot, swelling, and salt migration within materials (Lisø, Kvande and Thue, 2006). Wood is particularly vulnerable to high moisture levels and rapid fluctuations being a hygroscopic material. If not properly protected and maintained by e.g. surface coatings, favourable conditions for mould growth could occur (Edvardsen and Ramstad, 2014). The performance of wooden claddings depends on the quality of the wood material, the surface coating, the construction details and the climatic impacts to which they are exposed (Lisø *et al.*, 2006).

In recent years, there have been numerous reports of rot issues affecting wooden claddings in the Southwest region of Norway, i.e. the news articles of Heimsvik (2022a, 2022b), Håvardstein (2022) og Størksen (2022). The climate of this coastal region is known to be heavily characterised by driving rain and high outdoor humidity levels, which can aggravate moisture-related problems in the building envelopes. The rot issues could be attributed to multiple factors (and combinations of them) like climate change, variations in the quality of claddings, better insulated walls, changes in building practices, poor maintenance, and surface treatment quality.

While the focus has often been on the characteristics of exterior coatings to provide protection against liquid moisture penetration (Ekstedt and Östberg, 2001), their resistance to water vapour diffusion is equally crucial (Geving, 2021). However, manufacturers often do not explicitly provide information on the water vapour resistance properties of their coatings, and existing literature on determined vapour resistances exhibit inconsistency. This raises concerns about whether certain exterior coatings might have a vapour resistance that inhibits the drying of excessive moisture in wooden claddings, potentially accelerating the biodeterioration and shortening the material lifespans.

1.2 Preparatory Project

This master's thesis partly builds upon the specialisation project conducted Sept to Dec of 2023. The specialisation project explored whether the wet cup method, specified in NS-EN ISO 12572(2016), would be adequate for determining the vapour-diffusion equivalent air layer thickness, s_d-value, for free-standing coatings (without the need of a substrate). Coating series no. 53B and 53B2 were fully tested in this preparatory project as subjects for evaluation whether the wet cup method would yield reliable results, and to identify uncertainties regarding application, measurements, test procedure, etc. that would possibly need to be optimized before conducting the test on the full sample size of this thesis. Additionally, it initiated the literature review.

1.3 Aim and Scope

This thesis aims to determine the water vapour resistance of commercial coatings for exterior wood, in terms of the diffusion-equivalent air layer thickness (s_d-value). It also aims to investigate to what extent this vapour resistance might influence the moisture drying potential and mould growth risk of wooden claddings set in Nordic climates.

The following research questions have been formulated:

1. What does existing research say about water vapour resistance properties of coatings?
2. What is the range of water vapour resistance (s_d-value) of exterior coatings?
3. How does the vapour resistance of these coatings influence the moisture drying conditions and mould risk of the wooden cladding?

While a scientific article constitutes the central component of this thesis, this accompanying thesis document provides supplementary theory and methodology to support the discussions. Research question 2 and 3 are fully covered in the article. Research question 1 was initiated in the preliminary project, and its results are covered in the introduction of the mentioned article.

The goal of the accompanying thesis has also been to shed light on the topic of modelling field measurements of cavity climates. As it turned out more challenging and time consuming than expected, modelling of the air cavity climate became a greater focus in this document. This topic is treated to a limited extend in the article. This theme is complex and the goal with this thesis has not been to deliver a complete analysis, but rather to contribute with insights to this topic.

1.4 Limitations

The laboratory measurements were conducted under controlled laboratory conditions. The specimens were not exposed to cyclic weathering pre-weighing. All coating films (except coating no. 53 and 56) were punched and stored in a conditioned test enclosure for three months pre-assembly. The study is confined to investigate the s_d of free-standing films, excluding any possible influence of the interaction with the wood substrate. The vapour resistance measured is reported as the diffusion-equivalent air layer thickness (s_d-value). The implementation of the laboratory experiments has been the most time-consuming part of the thesis.

The hygrothermal simulations are confined to simulate realistic boundary conditions. They are based on two case buildings in Norway with different climates, and their air cavity microclimates represent the interior boundaries by the approach of curve-fitting the cavity climate. The curve-fitting that was conducted is simplified to fitting single-sinusoids. Lastly, the outcome of the mould growth model assessing the risk level is strongly affected by the end-user's choice of input parameters.

1.5   Structure of the Study

As mentioned, a scientific article constitutes the main part of this master's thesis. This article includes the laboratory experiments, as well as the moisture simulations and mould growth assessments. The full text of the article is provided in Appendix A as it was submitted the 5th of June 2024. Any methods, results, and discussions that could not be fully elaborated in the limited format of the article are included in this accompanying document. The reader is therefore encouraged to read Appendix A before prosecuting with this accompanying thesis document.

Chapter 2 addresses the theoretical framework necessary for evaluating the research questions.

Chapter 3 briefly explains the initial literature review that was conducted to investigate the existing research of water vapour resistance of coatings. The method of the laboratory measurements is fully covered in the article, but an introduction of the chosen materials is provided. Then a thorough elaboration of the hygrothermal simulations' input parameters and boundary conditions, as well as the mould growth criteria assessed by the VTT model, is presented, as this was only briefly included in the article. As a part of the moisture simulation assessment, the approach of modelling the air cavity microclimate to fit the interior climate boundary format of WUFI is explained. Lastly, it explains the extended parametric study to evaluate the mould growth risk with different approaches of interior boundary conditions.

In Chapter 4, the resulting measured vapour resistances and corresponding dry film thicknesses is reproduced from the article, supplied with a validation of the measurement method by a comparison of the retested product. The resulting curve-fitted models are presented and analysed. Supplementary results of the WUFI simulations are provided. After which this chapter presents the results of the extended parametric study of mould growth risk.

The discussion in Chapter 5 addresses the findings of the laboratory experiments and the suitability of the measurement method. Then, applicability of curve-fitting an air cavity microclimate to the interior climate boundary conditions of WUFI is discussed. Discussions regarding the simulated water content and mould growth risk are fully covered in the article. The uncertainties introduced by several aspects in this study are discussed. Finally, the thesis concludes in Chapter 6 with the conclusion from the article supplied with further insights and suggestions for future research.

Appendix A contains the scientific article. Appendix B shows the literature review matrix. Appendix C displays the spreadsheet of dry film thickness calculations. Appendix D presents the full-scale test reports, including graphs and input data for each of the tested coating series.

2 Theoretical Framework

This chapter presents theory necessary for assessing the research questions, forming the basis for further analysis of the results from the laboratory measurements, hygrothermal simulations, and mould risk assessments. Fundamental principles of moisture transport by vapour diffusion, two-stage weatherproofing, protective surface coatings, as well as key factors for mould growth are elaborated.

2.1 Moisture Transport

2.1.1 Sources and Transport Mechanisms

Controlling the moisture transport is crucial when designing buildings, as moisture related problems account for approximately 75% of building defects (Lisø, Kvande and Thue, 2006) and are the primary agent of building deterioration (Straube, 2002). The primary moisture sources are liquid moisture such as precipitation and snow-melt, water vapour both from exterior air and from processes within the building, moisture from the ground, and built-in moisture in the materials (Geving and Thue, 2002; Straube, 2002).

The four main moisture transport mechanisms are water vapour diffusion due to differences in vapour pressure, moisture convection caused by air movement, capillary suction driven by capillary forces in material pores, and liquid flow i.e. water leakage (Geving and Thue, 2002; Bøhlerengen, 2018).

2.1.2 Moisture Transport by Diffusion

Water vapour diffusion is driven by the difference in water vapour pressure Δp_v across a material layer, causing vapour molecules to diffuse from higher to lower concentration, as described by Fick's law (Thue, 2016). Fick's Law can be expressed by several combinations of the different water vapour properties of permeance, resistance, and diffusion-equivalent air layer thickness s_d-value, as shown in Equation (1). These properties are more expedient than vapour permeability when assessing the vapour resistance of thin materials i.e. coatings and films, precisely because of to the material thinness (Bøhlerengen, 2018).

$$g = \frac{\delta_a \cdot \Delta p_v}{s_d} = W_p \cdot \Delta p_v = \frac{\Delta p_v}{Z_p} \quad [kg/m^2 s] \tag{1}$$

where g is the rate of water vapour flow in kg/(m²s) representing the mass of water vapour passing through a unit area per second, and δ_a is the water vapour permeability of air (1.95e-10 kg/(msPa)). The other properties are presented with definitions and relationships to each other in Table 2.1 below.

Table 2.1: Relevant properties for vapour diffusion calculations

Property		Definitions by NS:EN ISO 12572:(2016)
Difference in partial vapour pressure (Pa)	Δp_v	The difference in partial vapour pressure across the material. This is the driving force of moisture transport by diffusion.
Water vapour permeability (kg/msPa)	$\delta_p = W_p \cdot d$	The material's ability to allow water vapour to pass through due to the gradient in water vapour pressure in the material.
Water vapour permeance (kg/(m^{2}sPa))	$W_p = \dfrac{\delta_p}{d}$	Density of water vapour flow rate divided by the thickness of the material.
Water vapour resistance ((m^{2}sPa)/kg)	$Z_p = \dfrac{1}{W_p}$	The resistance to the diffusion of water vapour due to the pressure difference across the material layer. The reciprocal of permeance.
Water vapour diffusion equivalent air layer thickness (m)	$s_d = \delta_a \cdot Z_p = \mu \cdot d$	The thickness of a motionless air layer which has the same vapour resistance as the material concerned.
Water vapour resistance factor (-)	$\mu = \dfrac{\delta_a}{\delta_p} = \dfrac{s_d}{d}$	The water vapour permeability of air divided by that of the material concerned. Relates the permeability to the diffusion coefficient of a stagnant air layer.

The water vapour resistance of materials influences the extent to which moisture within a building component can dry out. If moisture is trapped, condensation of the vapour could occur, and it is therefore desirable to have an increasing vapour permeability towards the exterior of the construction to facilitate outward drying (Thue, 2016; Bøhlerengen, 2018; Geving, 2021). If both the interior vapour barrier and exterior wind barrier have high vapour resistances, moisture stresses and condensation risk is very high due to the entrapment of moisture and organic material (wood framework) between these impermeable layers (Geving, 2021).

It is the layers that either form the surface of a building component or are close to the surface that determine the component's water vapour transmission (Geving, 2021), i.e. cardboard, foils, plasters, paint films, cladding materials. A material is considered highly "vapour diffusion tight" with an equivalent air layer thickness $s_d > 10$ m (e.g. vapour barriers) and "vapour diffusion open" for s_d-values < than 0.5 m, which is typical for wind barriers that are intended to be as vapour-permeable as possible to facilitate outward drying (Geving and Thue, 2002; Geving, 2021). There exists no explicit recommendation of s_d-values separately for coatings.

2.2 Materials and Principles for Weatherproofing

2.2.1 Two-Stage Weatherproofing

Ventilated façades employ the two-stage weatherproofing concept illustrated in Figure 2.1. The exterior cladding acts like the outer rain barrier, while the wind barrier is an airtight membrane primarily to prevent air infiltration (Kvande, 2013; Edvardsen and Ramstad, 2014; Thue, 2016). The two are separated by an air cavity ventilated outwards to ensure proper drainage and drying of embedded or intruded moisture. And even if some liquid water would penetrate the rain barrier, this ventilated cavity would facilitate drainage and ventilation to avoid wetting of the wind barrier and other vital inner parts of the wall (Svendsen, 1967).
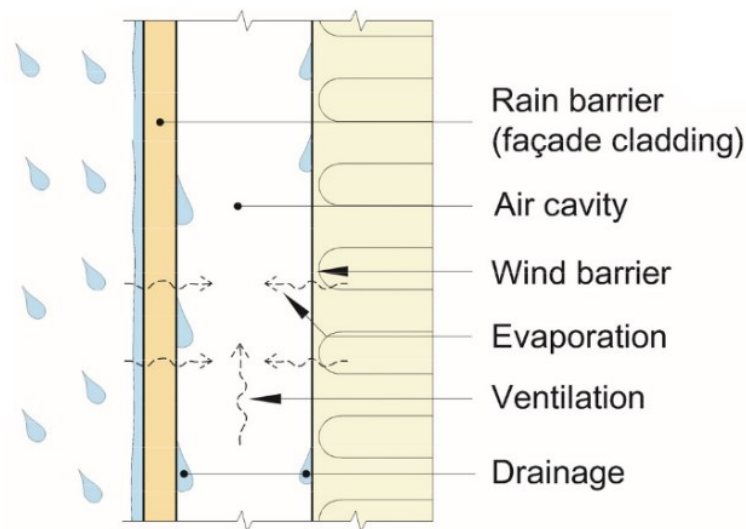
Figure 2.1: Schematic illustration of a ventilated façade with "two-stage-weatherproofing" and drying mechanisms. Reprinted with permission (Kvande, 2013).

The way of designing a wooden ventilated façade, means having the cladding be battened out in such a way to provide ventilation and drainage for the (Edvardsen and Ramstad, 2014; Elvebakk and Gullbrekken, 2020). The ventilation rate behind the cladding is determined by the cavity design i.e. the openings in the lower and upper ends, and type of convection (Nore, 2010), and is acknowledged to be crucial for reducing risk of moisture-related problems. Despite its importance, it is not within the scope of this study to assess this directly.

2.2.2 Wooden Claddings and Protective Surface Coatings

The two softwoods spruce (Picea abies) and pine (Pinus sylvestris) are the most common wood species used for exterior claddings in Norway (Flæte and Alfredsen, 2004; Edvardsen and Ramstad, 2014). Historically, this is due to local availability and production, and more now due to material characteristics, i.e. versatility and ratio strength/self-weight. Spruce is less permeable to liquid water and better for paint adhesion compared to pine (Jourdain *et al.*, 1999; Flæte and Alfredsen, 2004; Gobakken and Westin, 2008). Wetting and subsequent drying can

cause swelling, shrinkage, cracking, and moisture penetration in wood over time (Plesser, 2009; Edvardsen and Ramstad, 2014), which highlights the importance of surface maintenance.

Surface coatings on exterior wood serves two primary purposes: achieving the desired appearance, and protecting the wood from UV radiation, moisture stresses, and fungal attacks (Ekstedt, 2002; Plesser, 2009; Edvardsen and Ramstad, 2014; Thue, 2016). Hjort (1997) found a strong correlation between rot and surface treatment of wood, noting that the best-performing wood panels had several layers, including impregnate, primer and paint. The application of coatings forms a protective film, offering superior protection and longer service life compared to untreated wood (Geving and Thue, 2002).

The water vapour permeability of coatings is crucial because low-permeability coatings, while effective at preventing liquid moisture ingress, may impede moisture drying from the substrate (Huldén and Hansen, 1985; Ekstedt, 2002). This might create favourable conditions for microbiological growth and decay in the wood interface. A surface coating must therefore be liquid water repellent yet vapour diffusion-open to enable adequate drying of excess moisture (Geving and Thue, 2002; Nore, 2010). The modern waterborne coatings generally prevent less water ingress compared to more "traditional" solvent-borne coatings due to their water-solubility and surface-active substances (van Meel *et al.*, 2011).

Coatings may erode and lose their protective characteristics (liquid transport properties) or adhesion to the wood due to weathering (de Meijer, 2001). Regular reapplication of coating will help avoiding premature deterioration when executed with quality and by manufacturer specifications. Nore (2010) reports maintenance periods typically ranging from 2 to 15 years. Though, in regions with extreme weather fluctuations and driving rain like the southwestern part of Norway, entire claddings may need to be replaced every 20-25 years regardless.

2.3 Moisture Content of Wood

The moisture content (MC) of wood materials is normally evaluated as the weight of moisture per weight of dry matter u (kg/kg) and expressed as a percentage of the woods mass in a dry state (weight-%) (Thue, 2016). At a given RH and temperature, wood will reach for an equilibrium moisture content, where the rate of moisture absorption and desorption from the surrounding air is balanced (Bøhlerengen, 2018). This relationship of is shown by the wood's sorption curve, see Figure 2.2.
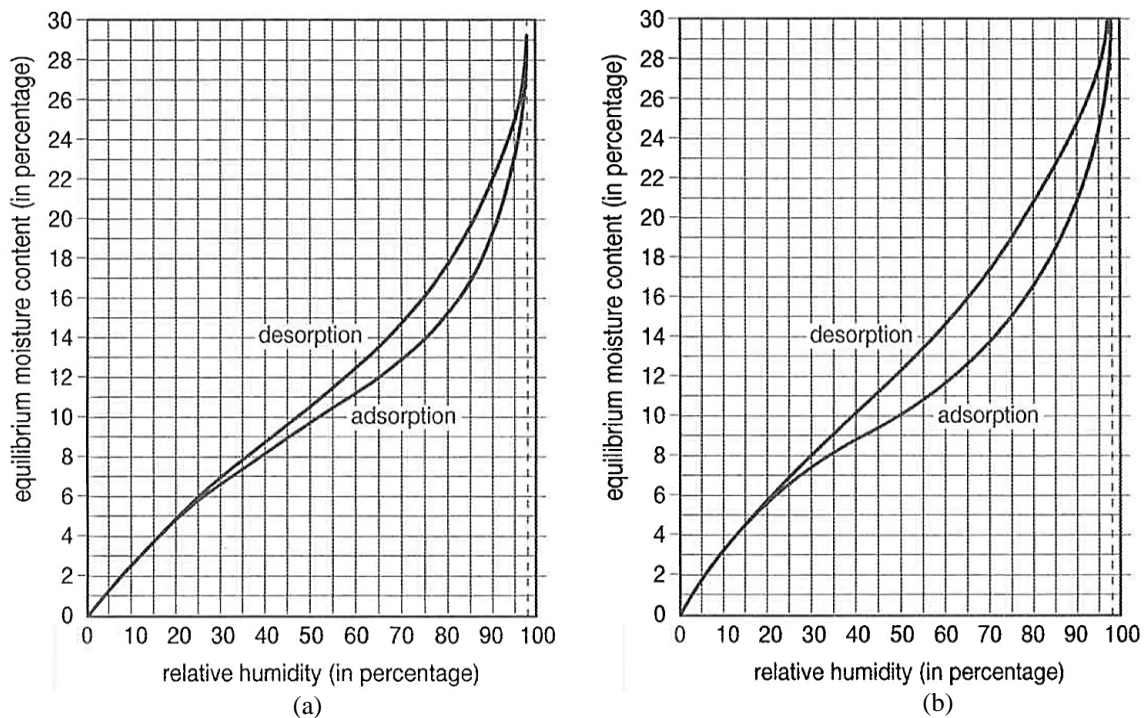
Figure 2.2: Sorption isotherms of (a) Norway spruce and (b) pine. Obtained from (van Meel *et al.*, 2011)

As a hygroscopic material, wood absorbs or releases moisture to achieve this mentioned equilibrium with the surrounding air conditions (Thue, 2016). Ekstedt and Östberg (2001) explain how moisture uptake in wood occurs through absorption of liquid water, water vapour absorption, and water vapour desorption. Also, due to its anisotropic nature, the moisture absorption and desorption behaviour varies depending on the direction of the wood grain (tangential, radial, or longitudinal) (Thue, 2016)

The fibre saturation point of wood occurs at approximately MC 28-30 wt% and marks the level where the cell walls are saturated with bound water. Exceeding this level, excess moisture exists as free water in cell cavities, which is more accessible for fungal and bacterial growth (Geving and Thue, 2002; Bøhlerengen, 2018).

The critical moisture content of wood can be expressed in weight-% (wt%) or as a relative humidity (RH_{cr}) and is the recommended threshold for maximum moisture content to avoid moisture issues (Bøhlerengen, 2018). For facilitating growth of decay fungi in spruce and pine, the critical MC is 18 wt% (~80% RH) (Viitanen, 1994; Edvardsen and Ramstad, 2014). Geving and Thue (2002) suggest a critical level of 20 wt%, though they consider it unnecessarily conservative.

2.4 Factors for Mould Growth

Development of fungi requires organic material, moisture, the right temperature, and sufficient exposure time in favourable conditions to grow (Viitanen, 1994; Magnussen and Mattsson, 2005; Edvardsen and Ramstad, 2014). Different organisms have specific growth criteria. For instance, rot typically requires the wood moisture content to be near the fibre saturation point, which for spruce and pine is approximately 28-30 wt% (Geving and Thue, 2002). As shown in Figure 2.3, the favourable temperature range for mould growth is approximately 20-50°C, with an RH exceeding 80 to 85%, which corresponds to a wood MC above 20 wt% (Viitanen & Ritschkoff, 1991).
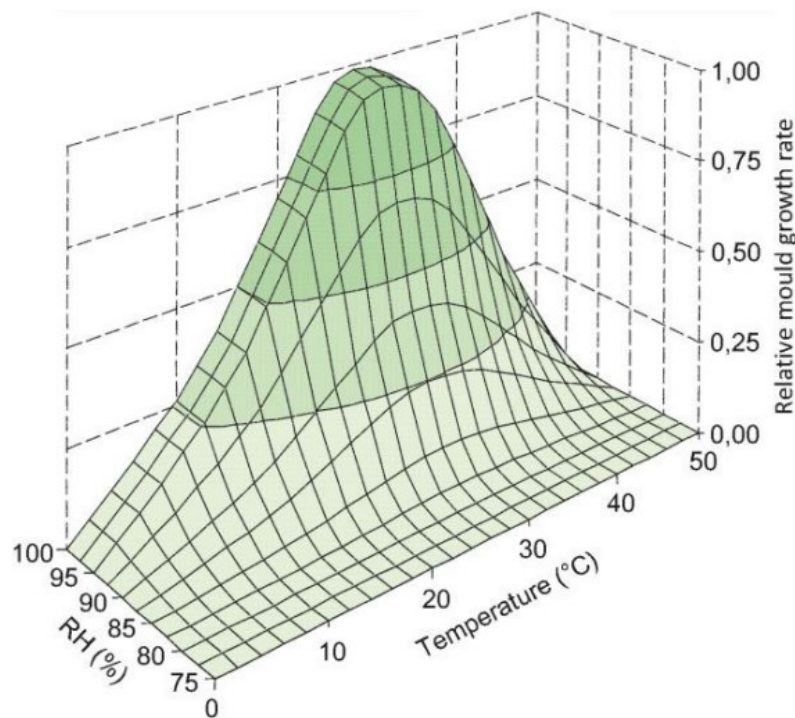
Figure 2.3: Relative mould growth rate for the most common mould species as a function of T and RH (Magnussen and Mattsson, 2005)

Prolonged exposure time in these conditions can result in rapid mould growth and material decay, which should be avoided. In some materials when the conditions are unfavourable for growth, the growth may decline in these periods (Viitanen, 1994). Another crucial aspect of mould growth is its persistence; once growth has established at 20 wt%, it can continue to grow even if the MC later drops to 16 wt% (Geving and Thue, 2002). This underscores the importance of effective drying and continuous maintenance of wooden materials from the very start.

3 Methodology

3.1 Literature Review

A literature review, initiated in the preparatory specialisation project, was conducted to examine what existing research said about methods and established values of water vapour resistance properties for exterior coatings for wood creating a basis of reference. The review aimed to identify possible knowledge gaps in the existing research field.

A database search was initially carried out in the library databases of Scopus, ScienceDirect and Google Scholar, with predefined keywords in different combinations. However, as it was inefficient due to scarce relevant literature, a "snowballing" technique was quickly adopted as the main reviewing method.

This search strategy finds relevant literature by starting with a small set of known papers and expanding the search based on references and citations (Wohlin, 2014). This approach was more efficient at accessing relevant studies. Also rather advantageous, as credible sources would tend to cite similar credible works, and it naturally provides a peer-reviewed filtration (Greenhalgh and Peacock, 2005). To facilitate filtering of the identified literature, a search matrix was created. Primarily it was filtered by methodology employed (wet cup method), reported vapour resistance (s_d-value), and type of substrate (wood). However, due to limited sampling of studies meeting all criteria, the scope was broadened to include several methods, vapour transmission properties, and substrates in the findings, to collect research and insights in the greater context. The search matrix is displayed in Appendix B.

The review revealed knowledge gaps, particularly regarding the determination of s_d-values of free-standing exterior wood coatings using the wet cup method. While some studies reported s_d-values for wood coatings, descriptions of experimental methodology, sample sizes, and standard deviations were often not present, making it challenging to establish reliable and reproducible comparisons. The results of the literature review are presented in the introduction of the article in Appendix A, and briefly discussed in Chapter 5.1.1.

3.2 Laboratory Measurements

The measurements of water vapour resistance of coatings were carried out using the wet cup method as described in NS-EN ISO 12572:(2016) and in detail for paints and varnishes in NS-EN ISO 7783:(2018). This method is fully presented in the article. However, the materials are introduced here to provide the context and scope of the measurements.

A total of nine commercial coatings intended for use on exterior wooden claddings were chosen for testing based on their relevancy on the Norwegian market. The coatings tested are all advertised to prevent liquid water intrusion into the wood, being long-lasting, and "withstanding harsh Nordic weather". Each coating was tested for three and six layers (of each

5 specimens), making the total of 100 tested specimens. Three and six layers were approximated to resemble one and two rounds of surface treatment, with the intent to account for uncertainties in estimating the number of previous coating layers and the eroding effects of weathering in real-life. The coatings are all waterborne, semi-glossy/semi-matt, and white hued, and are displayed in Table 3.1.

Table 3.1: Overview of the nine tested coatings, tested as. "B" and "B2" signifies the three and six layers of coating, respectively. This table is reproduced from the article (Appendix A).

Coating	Series	Binder type	Bulk density [kg/m^3]	Additional film support in assembly
51	B	Alkyd resin	1260	metal grid
	B2			metal grid
52	B	Emulsion (alkyd/ acrylic)	1260	metal grid
	B2			metal grid
53	B	Emulsion (alkyd/ acrylic)	1230	none
	B2			none
53X	B	Emulsion (alkyd/ acrylic)	1230	none
	B2			none
54	B	Acrylic resin	1200	none
	B2			none
55	B	Acrylic resin	1200	metal grid
	B2			metal grid
56*	B	Emulsion (alkyd/ acrylic)	1200	plastic cylinder
	B2			none
57	B	Acrylic resin	1250	none
	B2			none
58	B	Acrylic resin	1200	plastic cylinder
	B2			none
59	B	Acrylic resin	1260	none
	B2			none

*Series no.56 was fully tested anew March 24 due to large leakages of the B-series of the previous (salt rash on 3 of 5 samples). The "original" 56 was discarded.

3.3 Hygrothermal Simulations

The aim of the simulations is to investigate whether the drying conditions of a considered wooden cladding construction is influenced by the water vapour resistance of the applied coating. The simulations are conducted as a parametric study of both measured s_d-values and other parameters, to assess the influence and sensitivity of the parameters in combinations with the vapour resistance.

3.3.1 WUFI Pro Software

The hygrothermal software WUFI Pro (version 6.7) developed by the Fraunhofer Institute for Building Physics (Kuenzel, 1994; Fraunhofer IBP, 2021) was used for the simulating the moisture conditions. WUFI Pro is a well-known tool which simulates one-dimensional coupled heat and moisture transport in steady state conditions, and complies with all requirements of

standard EN 15026 (Fraunhofer IBP, 2024a). Several studies provides details and validation of the WUFI simulation software i.e. Mundt-Pettersen and Harderup (2013) and Hägerstedt and Arfvidsson (2010) to mention some.

3.3.2 Climate Boundary Conditions

This study aims to investigate the simulated moisture conditions and mould growth risk under realistic environmental conditions. Therefore, Typical Meteorological Year (TMY) weather files were used to represent the outdoor climate conditions, while the air cavity microclimate data of temperature and RH represents the indoor conditions. The modelled component and climate boundaries considered is simplistically illustrated in Figure 3.1.
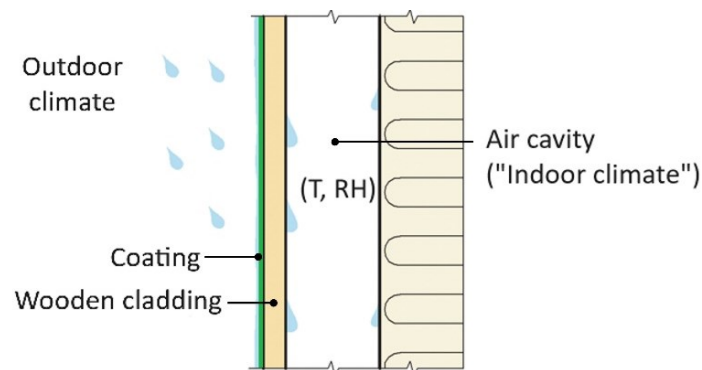
Figure 3.1: Illustration of the considered construction with the outer and inner climatic boundaries. Modified and reprinted with permission (Kvande, 2013) with added components and text.

The boundary conditions were defined based on field measurements from two sensor-monitored case buildings: Fjogstad-Hus in Stavanger and ZEB-Laboratory in Trondheim. These case buildings were selected as a continuation of the thorough analysis work on the air cavity by Ingebretsen (2022) and Ingebretsen et al. (2022). In the current study, one representative sensor from each building was chosen.

Typically, when assessing entire wall assemblies, the air cavity is modelled as an air layer with added heat and moisture sources/sinks and air flows (Fraunhofer IBP, 2021). In this study, the cavity microclimate is assumed to inherently reflect the influence of any real-world sources, sinks, and ventilation conditions. Thus, additionally modeling these factors could possibly apply their impact twice, which would be redundant. Despite the uncertainties of this possible simplification, the microclimate is assumed to mirror the climate boundary realistically.

The coating's material properties are assumed to restrict liquid moisture transportation and capillary uptake into the wood from the outer climate boundary. Consequently, the moisture in these simulations is mainly provided from the interior boundary side which could be a factor of uncertainty. While this is a simplification, the aim of the study is to investigate the effect of the coating's s_d-value on the drying potential. This effect will be captured in the results despite uncertainties of some boundary conditions, as long as the simulations are set to the same

conditions when varying the s_d-parameter in the material property. The simulated levels of wood MC and mould risk must though be evaluated with this aspect in mind.

Choice of Sensors

For Fjogstad-Hus, sensor SW1 (Figure 3.2a) on the southwest-facing wooden façade was chosen based off the findings of Ingebretsen et al. (2022) that exhibited the most unfavourable T, RH, and mould growth risk conditions compared to other sensors, with wood MC > 25 wt% for 36% of the time, and RH > RH_{cr} for 40% of the time. In the case of ZEB-Laboratory, sensor MN5 (Figure 3.2b) on the north-facing wooden facade was selected to serve as a reference building with acceptable mould risk in their analysis, the north façade being the only wooden one. MN5 yielded the best data completeness of the sensors on this wall, and recorded wood MC between 15-20 wt% for 57% of the time, RH > RH_{cr} for 1% of the time. Usually a north facing wall would be considered the worst case because it has almost no direct solar radiation during the winter months and the drying capability of the cladding in this period is limited (Nore, 2010), though southwest-facing façades have more extreme moisture exposure due to driving rain.
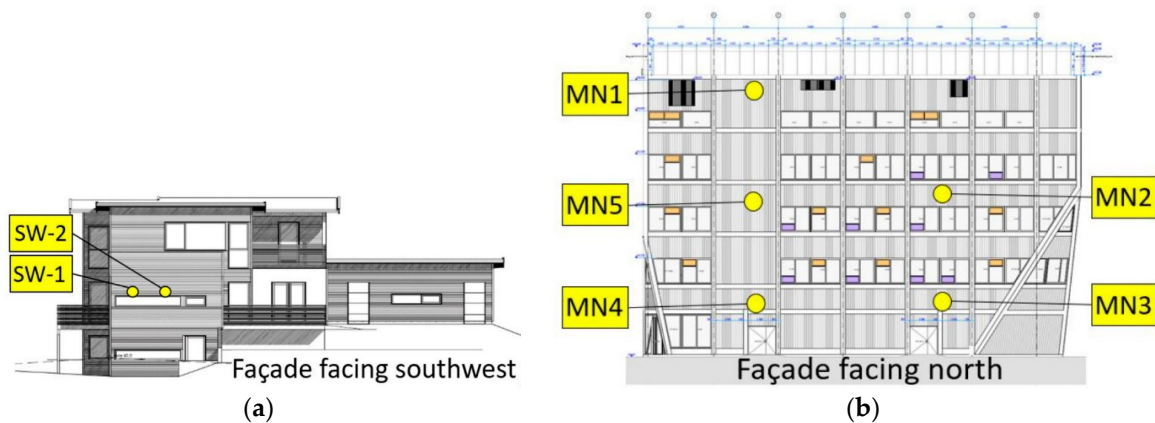
Figure 3.2. The wall positions of (**a**) SW1 of Fjogstad-Hus, and (**b**) MN5 of ZEB-Laboratory. Reprinted with permission (Ingebretsen *et al.*, 2022).

Outdoor climate

As mentioned, TMY weather files were imported to the WUFI Software to describe the outdoor climates. TMY data are condensed into a year of the most usual conditions (Betti *et al.*, 2024). Contrastingly, the Moisture Design Reference Year (MDRY) weather files are developed for design purposes and simulation of worst-case moisture conditions (Fraunhofer IBP, 2024b), and is usually more recommended when assessing risks. As the realistic conditions are opted for, typical weather data which are representative for the locations are appropriate (Fraunhofer IBP, 2024b). This approach also stemmed from the fact that there was no MDRY file available for Stavanger within WUFI.

A summary of the weather file data of Trondheim and Stavanger are shown in Table 3.2 below. The driving rain situations calculated and visualised by WUFI, are shown in **Figure 3.3**. Note that TMY climate data represent a typical year, meaning that for longer simulation periods these

data will be used cyclically by WUFI. Optimally, climatic data of the full period would provide the most reliable boundary conditions. Some uncertainties are also introduced by the fact that neither of the two case buildings are located exactly at the weather stations.

Table 3.2. Climatic data summaries of the TMY weather files for Trondheim and Stavanger. Obtained from WUFI Pro.

Data Information		
Location	Trondheim Voll	Stavanger Våland
Latitude [°]	63.41 North	58.96 North
Longitude [°]	10.45 East	5.73 East
Altitude [m]	131	72
Number of data lines	8760	8760
Climate Summary		
Mean T [°C]	6.2	8.8
Max T [°C]	27.2	25.7
Min T [°C]	-14.1	-5.3
Counter radiation sum [kWh/m^{2}a]	2509.4	2661.8
Mean cloud index [-]	0.65	0.7
Mean RH [%]	74.1	78
Max RH [%]	100	100
Min RH [%]	21	29
Mean wind speed [m/s]	2.7	5
Normal rain sum [mm/a]	1250	2074

(**a**) (**b**)
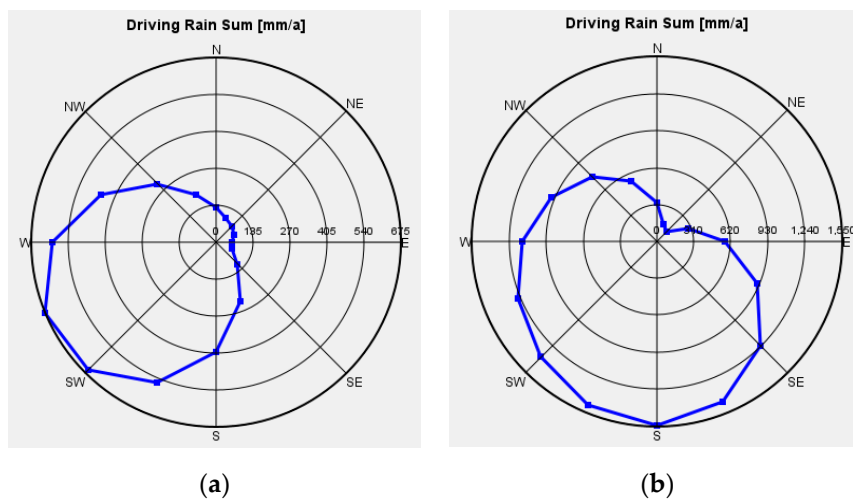
Figure 3.3: The driving rain of the locations (**a**) Trondheim and (**b**) Stavanger. Obtained from the WUFI Pro.

Indoor Climate

The microclimate of the air cavity was chosen to represent the conditions of the indoor climate conditions, as shown in Figure 3.1. See Section 3.4 for the approach of this modelling.

3.3.3 Elaboration of Input Parameters

Material properties

Material properties were obtained from the material database of WUFI (Fraunhofer IBP, 2021), expect for water vapour resistance properties and bulk densities that were obtained from personal laboratory measurements. Table 3.3 shows details on material data for both the cladding and the coating. Initial attempts of inserting the coating merely as an s_d-value did not successfully include the liquid transport properties. The coating was therefore modelled as a separate material layer, utilising the liquid transport properties of an existing Korean waterborne paint. The personal s_d-values were converted to vapour resistance factors μ to fit the input format, together with respective bulk density, included in the modelled coating layer.

Table 3.3. Component material properties retrieved by WUFI and laboratory measurements.

	Thickness [m]	Bulk density [kg/m³]	Porosity [m³/m³]	Heat capacity [J/kgK]	Thermal conductivity [W/mK]	Vapour resistance factor μ [-]
Scandinavian spruce transversal direction II	0.022	390	0.75	1600	0.13	108
Waterborne Coating	0.001*	1260, 1200	0.001	990	0.2	2225*, 1350*, 690*, 453*

*Thicknesses inserted as 1 mm to minimize convergence errors in the simulation software, the s_d (thus μ) values are scaled accordingly. The actual measured thicknesses of the coatings are available in Table 3.1.

Surface transfer coefficients

The exterior surface heat transfer resistance R_{si} remains unchanged from the WUFI default 0.0588 (m²K)/W for exterior walls. The short-wave and long-wave absorptivity factors are set to 0.4 and 0.9, respectively, based on the white bright hue of the coating. The ground short-wave reflectivity is set to the standard value of 0.2. The adhering fraction of rain remains unchanged from 0.7, although when the coating film restricts capillary absorption, this factor is not of any influence.

The interior surface heat resistance R_{si} of the interface between the cladding and the ventilated air cavity was varied between WUFI's default 0.125 (m²K)/W and the standard for R_{se} of 0.0588 (m²K)/W, due to uncertainty of how well-ventilated the façades of the case buildings were. No measurements of cavity air flow were available. The realistic value is expected to lie within this range, likely much closer to 0.125 (m²K)/W. Midway through the iterations of the parametric study, it was acknowledged that 0.125 (m²K)/W was a more realistic and conservative choice, leading the study to disregard discussing the cases of 0.0588 (m²K)/W.

Initial conditions

The parameter regarding initial moisture content of the spruce layer was initially tested for all 20- and 15 wt% as these represent critical and standard RH values of built-in wood. The 20 wt% resembles an unusually high level for initial built-in moisture, not in line with the aim of simulation of realistic parameters. However, the intention was to enhance the potential efficacy the coatings' water vapour resistance might have on the moisture drying of the wooden cladding.

Calculation period

The calculation period is set to five years. In this way, the evaluation of the long-term trend is more prominent. A ten-year period was initially also simulated, but eventually discarded as of redundancy. The simulation start was chosen to be the 1st of October which is the beginning of the wetting season in Norway. Simulating with this setting is intended to enhance the efficacy of the coating's vapour resistance on the drying potential, because of the humid and wet conditions that worsen the moisture conditions in this season.

3.4 Curve-Fitting of the Cavity Microclimate

3.4.1 Reasoning of Modelling

The options for modelling the microclimate as "indoor climate" in WUFI is limited to either creating a compatible file or defining the temperature and RH as sine curves with inputted "amplitude", "mean", and "date of max". Initially, the sine curve option was chosen. During the later stages of the work, the alternative approach of creating a WUFI-compatible Weather and Climate (WAC) file was discovered. This type of file would directly represent the measured temperature and RH data, providing greater accuracy compared to when simplifying the cavity climate into a sinusoid. As a substantial amount of work was already invested in simulations using the sinusoidal models at the time of this discovery, it was decided to retain this curve-fitting approach as the primary method of defining the interior climatic boundary. However, recognizing the potential of the WAC file, the scope was extended to include its use as a validation tool for the curve-fitted sine models.

3.4.2 Sinusoidal Regression Model

To utilise WUFI's "Sine Curve" option, the hourly temperature and RH data of the sensors required curve-fitting, and a least-squares regression model was adopted (Rawlings, Pantula and Dickey, 1998; Bloomfield, 2000). This method minimizes the sum of the squared residuals between predicted values of the model and observed data to ensure optimal agreement. Fitting sinusoids to data is thoroughly elaborated by e.g. Bloomberg (2000).

The data sets of sensors SW1 and MN5 (described in Section 3.3.2) used in the curve-fitting were hourly monitored data. The periods were three years for SW1 (from 12/05/2021 to 03/02/2024) and five years for MN5 (from 01/02/2019 to 03/02/2024). The statistical summaries of each data set are presented below in Table 3.4.

Table 3.4: Statistical data of sensor measured T and RH data.

Measured Data		Mean	St.dev.	Min.	25%	50%	75%	Max.
SW1	T	10.20	6.25	-8.8	5.5	10.3	14.8	32.9
SW1	RH	78.68	10.28	28.3	72	78.8	86.6	99.8
MN5	T	7.36	8.89	-19	1.6	6.9	13.9	33.6
MN5	RH	70.38	11.84	27.5	63	71.6	79.7	100

The single-sinusoid models of T and RH are coded in Python 3.4 with SciPy (Virtanen *et al.*, 2020) and NumPy (Harris *et al.*, 2020) packages. As coding was partly unfamiliar to the author, the AI tool ChatGPT Python by Barker (2024) was employed for assistance on both code interpretation, code debugging, and data analysis/plotting. The mathematical equation around which the models are coded is given in Equation (2):

$$y(t) = A \sin(Bt + C) + D \tag{2}$$

where A is the amplitude of the curve, B is the angular frequency, C is the phase shift, and D is the vertical offset value.

These single-sinusoid models for temperature and RH, while aiming at capturing general seasonal trends, are rather simplistic due to the scope of this thesis. The author is aware that the simplification introduces uncertainties in the models and hygrothermal simulations. Bloomfield (2000) states that climatic data often require multiple sinusoidal components to be optimized and account for finer seasonal fluctuations. The choice of using single-sinusoid models likely oversimplifies, thus missing potential secondary seasonal effects. However, the uncertainties will be reflected and quantified in the coefficients of determination (R^2) presented together with the sinusoid models in Section 4.2.1.

After iterations of coding and testing the best-fit model, it was observed that the RH sinusoid inadequately captured winter extremes of both Fjogstad-Hus SW1 and ZEB-Laboratory MN5. To account for a greater portion of these extreme RH levels, the original best-fit curve was vertically shifted with +5 offsets (parameter D of the above Equation (2). To separate these two models, this new one will hereafter be referred to as the "offset-shifted curve" though note that only the RH curve of this model was shifted.

3.5 Mould Growth Risk Assessment

The following section details the assessment criteria of the VTT Model that has been applied in the mould risk assessments. It regards both the original and the extended parametric studies conducted.

3.5.1 The VTT Model

The VTT model (Hukka and Viitanen, 1999) was utilised through the post-processor program of WUFI denoted "WUFI Mould Index VTT" version 2.3 (Fraunhofer IBP, 2018). The model predicts the risk of mould growth as a function of surface material, temperature, RH and

exposure time, and the outcome of the VTT model is the dimensionless "Mould Index" which describes the intensity of mould growth (Hukka and Viitanen, 1999). The Index ranges as shown in Table 3.5.

Table 3.5. Mould Index for modelling (Hukka and Viitanen, 1999)

Mould Index	Description of the growth rate
0	No growth
1	Small amounts of mould on surface (microscope), initial stages
2	Several local mould growth colonies on surface (microscope)
3	Visual findings of mould on surface, < 10% coverage
4	Visual findings of mould on surface, $10 - 50\%$ coverage
5	Plenty of growth on surface, > 50% coverage (visual)
6	Heavy and tight growth, coverage about 100%

The risk is further interpreted by employing a traffic light interpretation: green meaning no risk, red meaning an unacceptable risk, whereas yellow indicates a possible risk that needs further investigation (Viitanen *et al.*, 2015). The thresholds for these risks depend on the chosen "occupant exposition class" by which the thresholds are adjusted (Hukka and Viitanen, 1999).

The decline coefficient C_{mat} resembles the model to account for a reduction in the mould index when environmental conditions of temperature and RH are unfavourable for mould growth. In this case, the growth factor of "exposure time" is essential part of the analysis (Viitanen *et al.*, 2015). The different material classes these decline coefficients represent are shown in Table 3.6. The sensitivity classes are presented in

Table **3.7** with material examples.

Table 3.6. Material classes of the VTT model with examples of materials (Viitanen *et al.*, 2015)

Material class	C_{mat}	Typical materials
Significant decline	1	Untreated wood
Relevant decline	0.5	Lightweight concrete
Relatively low decline	0.25	Concrete, laminated wood, PUR, mineral fibres
Almost no decline	0.1	EPS, polyester fibres, lightweight concrete

Table 3.7. Sensitivity classes with examples of materials (Viitanen *et al.*, 2015)

Sensitivity class	Typical materials
Very sensitive	Untreated wood, pine sapwood, material which contain large amounts of nutrients for biological growth.
Sensitive	Glued wood-based boards, PUR with paper surface, spruce, planed wood.
Medium resistant	Concrete, aerated and cellular concrete, glass wool, polyester wool.
Resistant	Glass and metal products, PUR with polished surface, materials with efficient protective compound treatments

Whether the moisture conditions are categorized as critical for mould growth in the calculation program is defined, among other things, based on the function for critical RH dependent on the temperature (Hukka and H.A. Viitanen, 1999) shown in Equation (3):

$$RH_{cr}(T) = \begin{cases} -0.00267T^3 + 0.16T^2 - 3.13T + 100, & T \leq 20\,°\text{C} \\ RH_{min} = 80\%, & T > 20\,°\text{C} \end{cases} \qquad (3)$$

The factor RH$_{cr}$ is, as introduced in the theoretical framework, the threshold RH level of where mould growth may begin (under the temperature conditions and with the selected material). For wood and wood based products the RH$_{min}$ is 80% RH (~MC 18%wt) (Hukka and Viitanen, 1999). Thereby, the criterion RH > RH$_{cr}$ showcase the humidity conditions for when mould growth is possible.

3.5.2 Risk Assessment

As the cladding is exterior and separated by the envelope with a ventilated cavity, the exposition class considered is not expecting to have any impact on the occupants of the building. The assessed risk thresholds are given in Table 3.8.

Table 3.8: Traffic light interpretation of the VTT Model's mould risk for this specific occupant exposition class.

Mould Index	Risk Thresholds for Exposition Class "No expected impact on occupants"
(red)	(Not evaluated)
> 3 (yellow)	Additional criteria or investigations are needed for assessing acceptability
≤ 3 (green)	Usually acceptable

However, it is important to note that relying solely on the traffic light interpretation of the risk thresholds could potentially underestimate the actual risk, as the Mould Index itself suggests the amount of growth, regardless of the assigned color-coding.

The WUFI VTT Mould Model settings chosen is summarised in Table 3.9.

Table 3.9: Summary of parameter settings in WUFI Mould Index VTT Model. Reprinted from Appendix A.

VTT Model parameter	Chosen setting
Occupant exposition class	"No impact on occupants expected"
Material category	Wooden or natural materials
Material sub-category	Untreated pine or spruce (Heartwood)
Sensitivity class	Sensitive
Decline coefficient (C_{mat})	Almost no decline (0.1)
Type of surface	Planed
Type of wood	Softwood

3.6 Extended Parametric Study

In addition to the main parametric study presented in the article, an extended study was conducted to validate the accuracy in simulation by the curve-fitting approach against the self-composed WAC file approach. The cases I, II, and III represent the ZEB-Laboratory, while cases IV, V, and VI represent Fjogstad-Hus. The cavity model approaches considered are the best-fit curve (T_0, RH_0), the offset-shifted curve (T_0, RH_{+5}), and the WAC file (measured data), see Table 3.10 for the combinations.

The previously varied WUFI parameters are here constant: Coating's vapour resistance $s_d = 2.25$ m, initial wood MC 20 wt%, $R_{si} = 0.125$ (m^{2}K)/W, simulation start the 1st of October, and simulation duration of five years. See Appendix A for clarity.

Table 3.10: Parameter combinations of the extended parametric study.

WUFI Input Parameters		I	II	III	IV	V	VI
Outdoor climate	Trondheim	x	x	x			
	Stavanger				x	x	x
Cavity Climate Model	Best-fit curve (T_0, RH_0)	x			x		
	Offset-shifted (T_0, RH_{+5})		x			x	
	WAC file (Measured data)			x			x

4 Results

This chapter aims to present either new or supplementary results, extending beyond the space limitations of the article.

Section 4.1 reproduces the article's key laboratory results before continuing with a comparison of the coating that was tested twice. Section 4.2 presents the curve-fitted cavity climate models, and the validation of accuracy against the WAC file approach. Section 4.3 provides supplementary results on simulated wood moisture content, data that space limitations precluded from the article. Lastly, comparing the approaches for modelling the cavity climates, Section 4.4 offers an extended parametric study of the mould growth indices.

4.1 Laboratory Measurements

4.1.1 Determined Vapour Resistances

A summary of the main laboratory results as well as a comparison of the measured s_d-values and dry film thickness are displayed in Table 4.1. See Appendix D for the full-scale laboratory test reports for all 20 tested series. Regardless of number layers it is to be observed that coating no. 51 is the least vapour permeable with s_d of 1.35 (0.083) m and 2.25 (0.048) m, and contrarily coating no. 56 is the most vapour permeable with s_d of 0.453 (0.019) m and 0.690 (0.012) m.

Table 4.1: Results of laboratory measurements both dry film thicknesses and s_d, and standard deviation of the mean is shown in brackets. Retrieved form the scientific article of (Rossebø and Kvande, 2024 submitted).

Coating no.	Binder type	Three layers (series B)		Six layers (series B2)	
		Dry film thickness [mm]	s_d [m]	Dry film thickness [mm]	s_d [m]
51	Alkyd	0.34 (0.02)	1.350 (0.083)	0.56 (0.02)	2.250 (0.048)
52	Emulsion	0.28 (0.01)	0.836 (0.042)	0.48 (0.02)	1.280 (0.020)
53	Emulsion	0.26 (0.01)	0.669 (0.031)	0.52 (0.02)	1.090 (0.049)
53X	Emulsion	0.25 (0.01)	0.602 (0.026)	0.42 (0.02)	0.925 (0.047)
54	Acrylic	0.28 (0.01)	0.787 (0.037)	0.41 (0.02)	1.110 (0.058)
55	Acrylic	0.26 (0.01)	1.090 (0.027)	0.41 (0.02)	1.530 (0.065)
56	Emulsion	0.25 (0.01)	0.453 (0.019)	0.45 (0.01)	0.690 (0.012)
57	Acrylic	0.24 (0.01)	0.999 (0.051)	0.44 (0.03	1.480 (0.063)
58	Acrylic	0.20 (0.01)	0.472 (0.024)	0.45 (0.02)	0.932 (0.019)
59	Acrylic	0.26 (0.01)	0.559 (0.006)	0.38 (0.01)	0.724 (0.023)

4.1.2 Comparison of Retested Coating

Coating series no. 53B and 53B2 were fully tested in the preliminary project conducted Sept to Nov 2023, while no. 53BX and 53B2X were painted and conditioned during this same period though assembly and weight measurements occurred from Jan to Feb 2024.

The Figure 4.1 show the developments of the s_d-values over the test periods for the two different rounds of testing product "53". It is observed that the fall test-rounds (53) exhibit a higher level of vapour resistance throughout the measurement period than the spring retest-rounds (53X). This is due to the differences in dry film thickness, no. 53 having a thicker film both for the three-layer series and the six-layer series. Neither of the series show any discrepancies during testing, and the results show the s_d stabilising. No. 53B2X show somewhat more variability towards the end of the testing than the others.
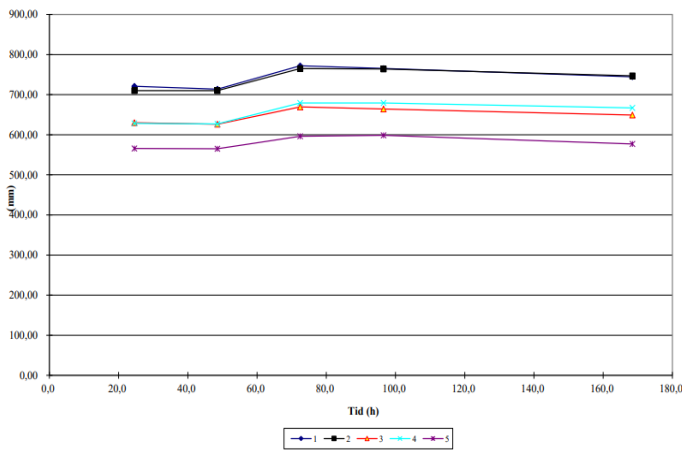
(**a**) 53B (Fall)
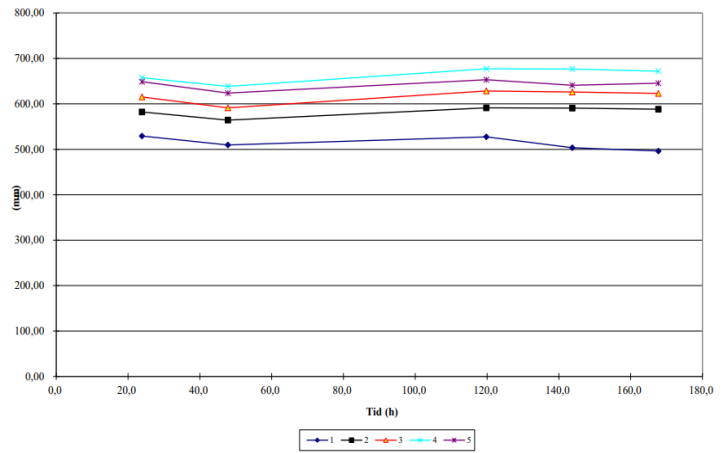
(**b**) 53BX (Spring)
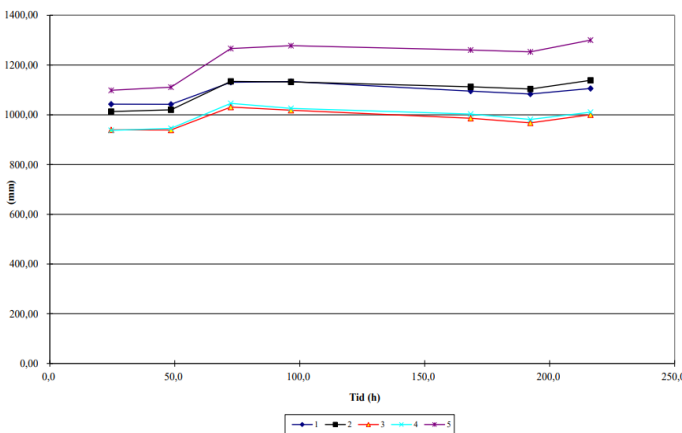
(**c**) 53B2 (Fall)
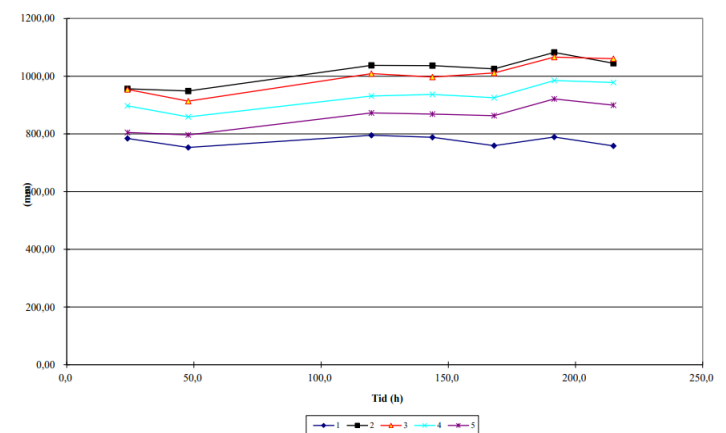
(**d**) 53B2X (Spring)

Figure 4.1: The measured equivalent air layer thicknesses s_d-values over the period for each specimen of no. 53 and 53X.

A linear regression analysis of no. 53 and 53X are presented separately in Figure 4.2a and Figure 4.2b. Both R^2 values are high, 0.9039 for 53 and 0.9204 for 53X, confirming that dry

film thickness is a significant predictor of the s_d-value in both cases. The plotted residuals (Figure 4.2c) and (Figure 4.2d) appear randomly scattered around zero and no clear pattern, which indicates that the wet cup method's performance is consistent across the two rounds of testing. This demonstrates a well-fitted and reliable approach for measuring the vapour resistance of the coatings.
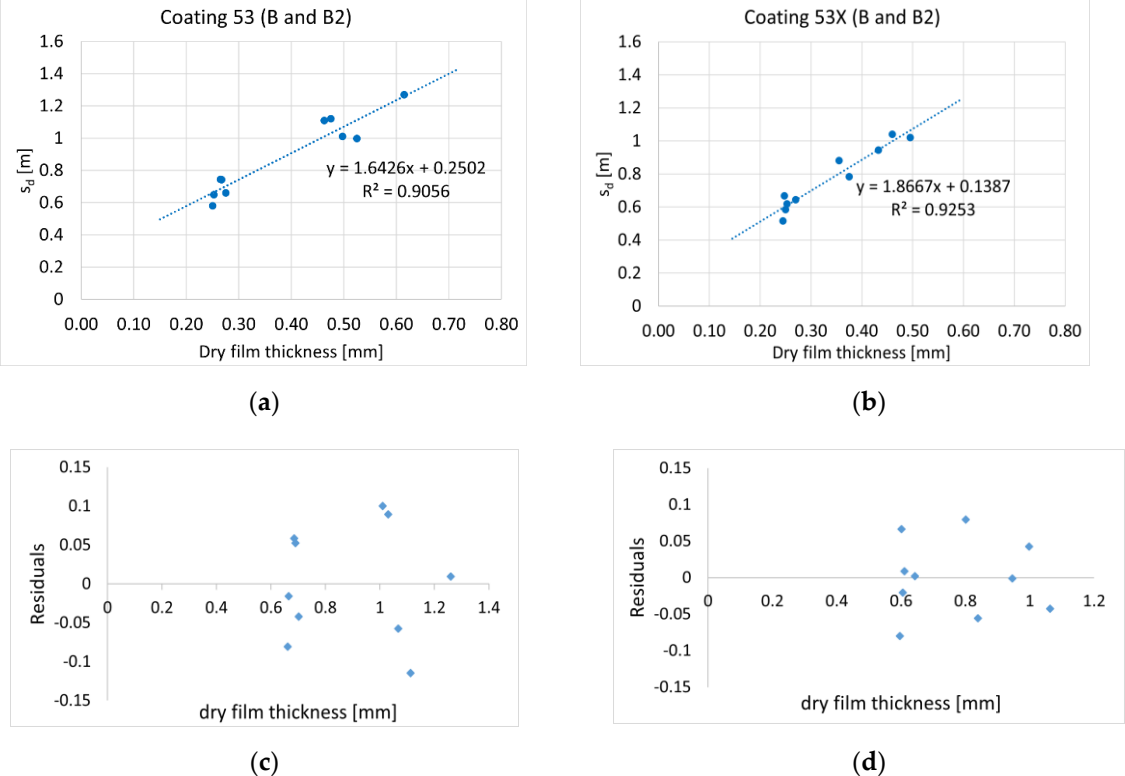
Figure 4.2: Linear correlation (**a**) coating 53 and (**b**) coating 53X. Plotted residuals of (**c**) 53, and (**d**) 53X

4.2   Curve-Fitting the Cavity Microclimate

4.2.1   Resulting Models

The resulting sinusoid models are presented in Figure 4.3 for SW1 (Fjogstad-Hus), and Figure 4.4 for MN5 (ZEB-Laboratory). The least-square optimized curve parameters and R^2 coefficients are presented in Table 4.2 and Table 4.3.

The best-fit model for temperature showed R² of 0.6751 for SW1 and 0.7058 for MN5, indicating a moderate fit to the measured data. The best-fit model for RH had lower R² values of 0.4225 for SW1 and 0.5689 for MN5, suggesting a weaker fit compared to the temperature models. The offset-shifted model for RH demonstrated even poorer fits to the measured data, with R² values of 0.1859 for SW1 and 0.3907 for MN5. Despite the varying degrees of fit, all models clearly capture the general fluctuating trend of the temperature and RH data.
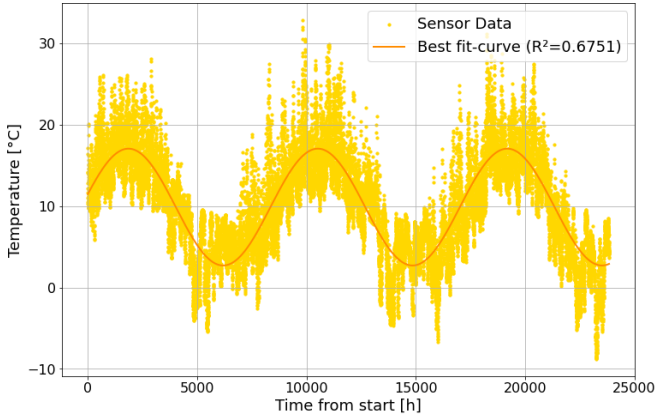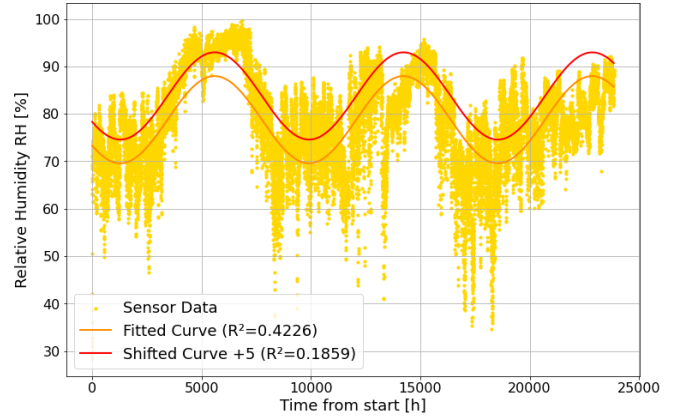
Figure 4.3. Scatterplots of SW1's sensor data with (**a**) Best-fit temperature curve T_0, and (**b**) Relative humidity best-fit curve RH_0 and offset-shifted curve RH_{+5}

Table 4.2. Results of parameters of the best-fit and offset-shifted curves for SW1.

SW1 Fitted Curve	Amplitude A	Angular frequency B	Phase shift C	Vertical offset D	Date of Max.	R²
T_0	7.18	0.02	0.224	9.89	28th July	0.6751
RH_0	9.20	0.02	-2.51	78.77	31st Dec	0.4226
RH_{+5}	9.20	0.02	-2.51	83.77	31st Dec	0.1859
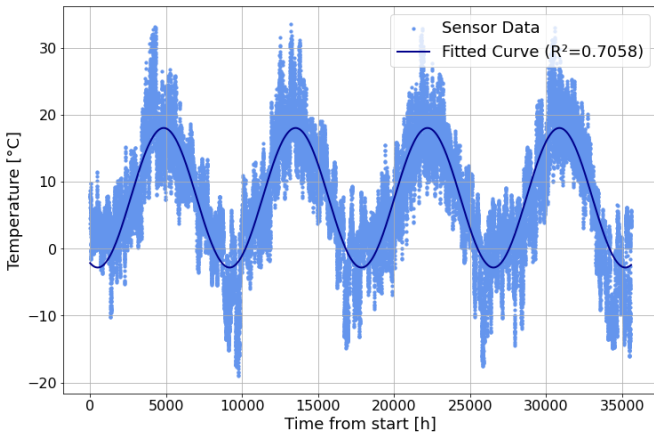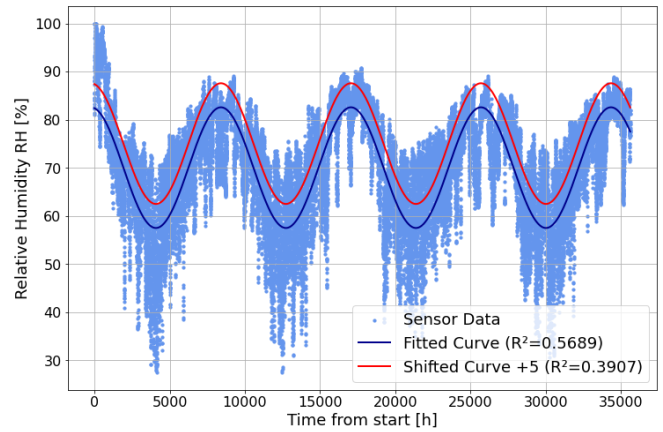
Figure 4.4. Scatterplots of MN5's sensor data with (**a**) Temperature best-fit curve T_0, and (**b**) Relative humidity best-fit curve RH_0 and offset-shifted curve RH_{+5}

Table 4.3. Regression-estimated parameters of the Best-fit curves and offset-shifted curve for MN5.

MN5 Fitted Curve	Amplitude A	Angular frequency B	Phase shift C	Vertical Offset D	Date of Max.	R²
T_0	10.43	0.02	-1.93	7.60	20th July	0.7058
RH_0	12.54	0.02	1.74	70.05	16th Dec	0.5689
RH_{+5}	12.54	0.02	1.74	75.05	16th Dec	0.3907

24

4.2.2 Comparison of Different Cavity Climate Approaches

The simulated temperature and RH data on the interior side of the cladding were compared between the two approaches of inputting the cavity microclimate of the offset-shifted curve (T_0, RH_{+5}) and composed WAC file (measured data).

For both Fjogstad-Hus (Figure 4.5) and ZEB-Laboratory (Figure 4.6), the simulated temperature and RH profiles follow similar seasonal trend when using the two approaches. However, the WAC files yield more variability and extreme values of simulated RH (both higher and lower) compared to the offset-shifted models.

For Fjogstad-Hus, the simulated temperature and RH using the offset-shifted curve showed strong correlations with the simulated temperature and RH using the WAC file, with correlation coefficients (R) of 0.9548 and 0.8679, respectively. The mean absolute error (MAE) for simulated temperature was approximately 1.5°C, while the simulated RH deviated between the two by an average of 5.8%RH (percentage points).
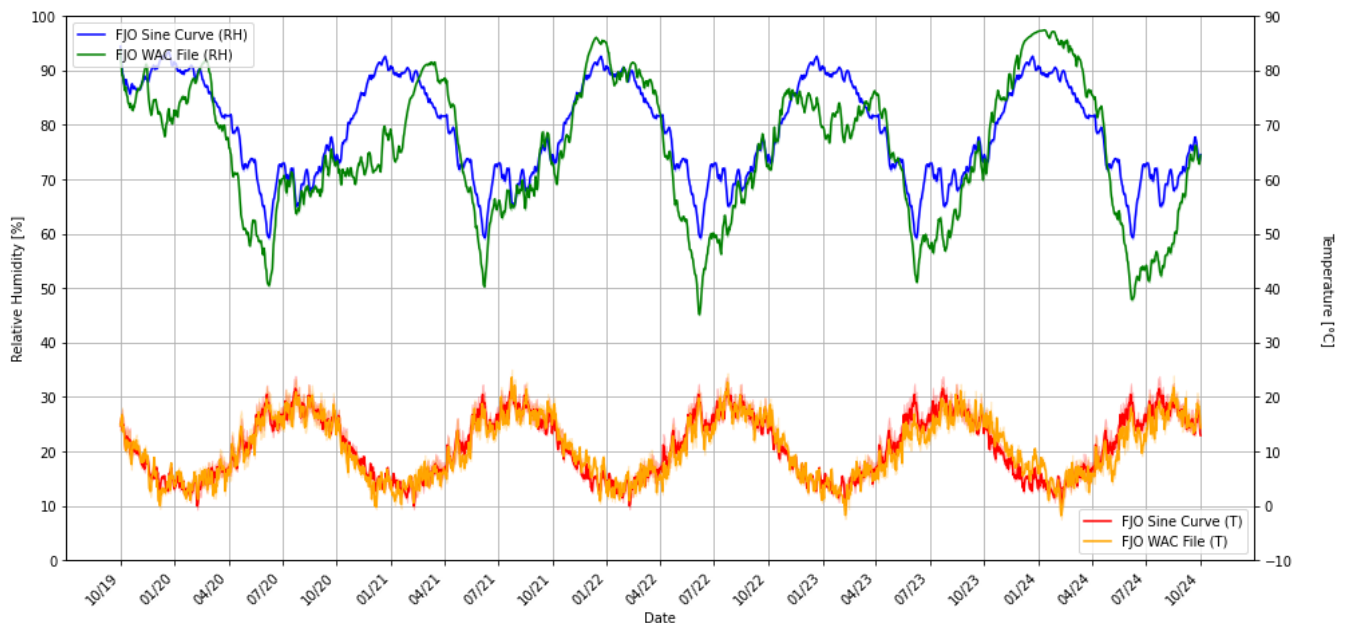
Figure 4.5: Simulated T and RH in the wooden cladding in Fjogstad-Hus. Comparison of offset-shifted curve RH_{+5} and the self-composed WAC file.

For ZEB-Laboratory, the temperature correlation was slightly stronger (R = 0.9639) than at Fjogstad-Hus, while the RH correlation was lower (R = 0.8317). The lower RH correlation may be attributed to a discontinuation of the data in the WAC file around year three as seen in Figure 4.6. The MAEs for the ZEB-Laboratory simulations were approx. 1.6°C and 4.5% RH.
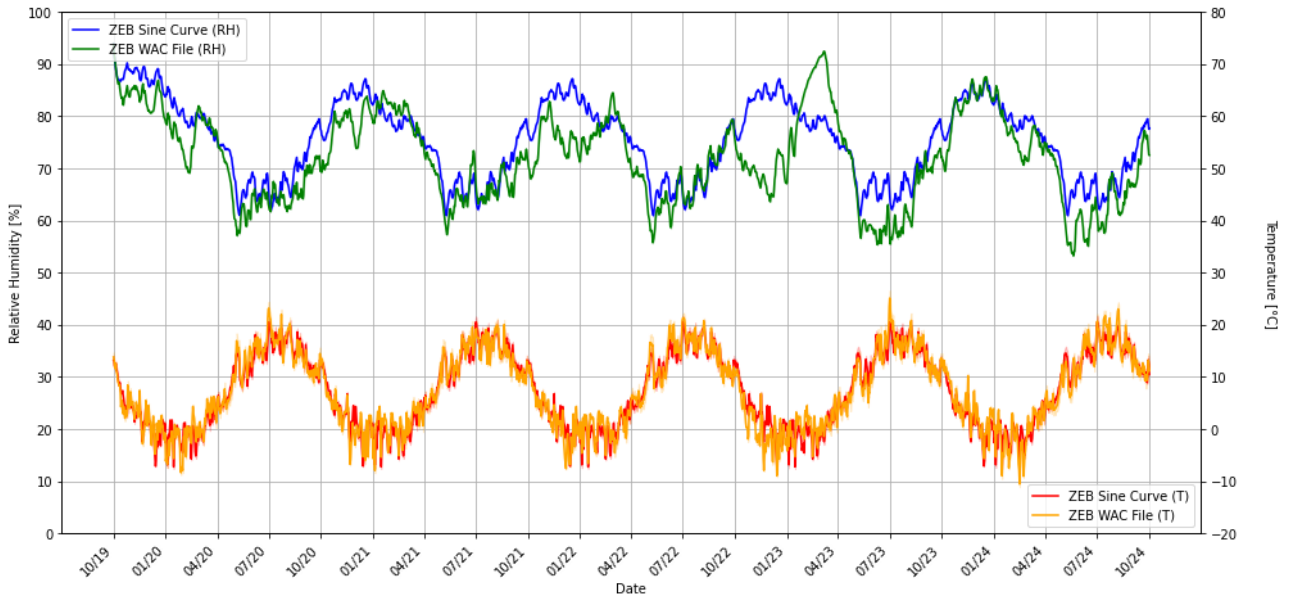
Figure 4.6: Comparison of simulated T and RH for offset-shifted curve RH_{+5} and the self-composed WAC file at the monitor position in Fjogstad-Hus.

4.3 Supplementary Simulations of Wood Moisture Content

4.3.1 Effect of Layers of Coating

The effects of the different maximum and minimum s_d-values for three and six layers of coating were plotted and are displayed in Figure 4.7 for both the five- and one-year period. The MC still do not show any moisture accumulation. The cases of s_d 0.453 m and 0.690 m lay approx. 1 wt% below the less permeable coatings (1.35 m and 2.25 m) throughout the drying period, indicating faster drying of moisture when the coating is more vapour permeable. These observations affirm the results of the article (Appendix A).

(a)

(b)
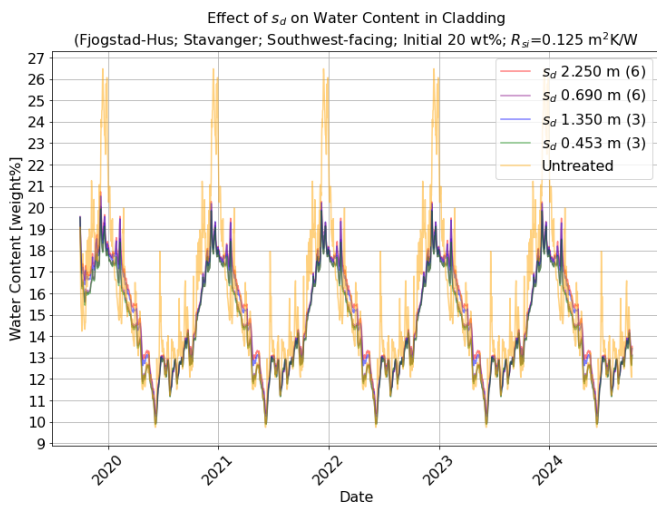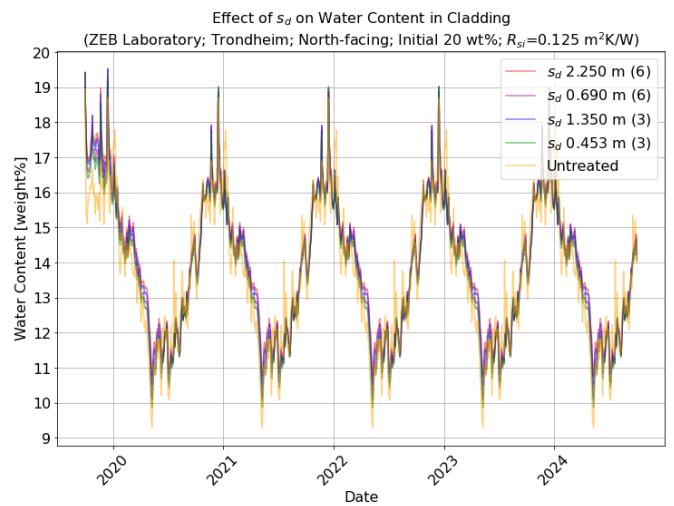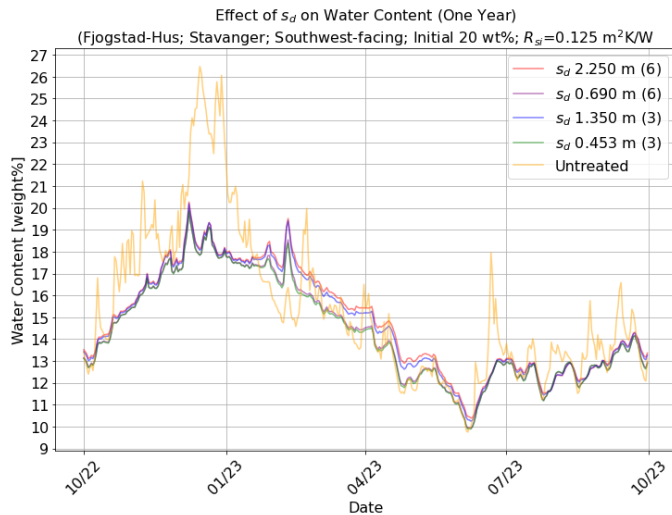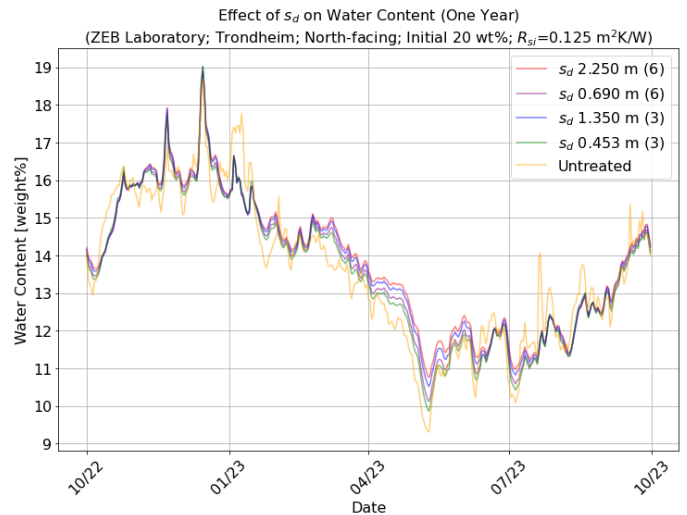
Figure 4.7: Comparison of the effect of different sd-values and coating layers on the wood MC. (**a**) Fjogstad-Hus five-year period, (**b**) ZEB-Lab five-year period, (**c**) Fjogstad-Hus one year, (**d**) ZEB-Lab one year.

4.3.2 Effect of Vapour Resistance and Initial Wood Moisture Content

Figure 4.8 show the effect of having the initial wood MC 15 wt%, instead of 20 wt%. As the effect of the initial MC was negligible over time, the period visualised below is the first six months of simulation start, to observe the immediate effect. It is observed in Figure 4.8 that for 20 wt% cases the wood MC quickly drops the first weeks to a level of 16-17 wt% (approximately the same as for 15 wt% cases) for both Fjogstad-Hus and ZEB-Laboratory. This could be due to the wood's hygroscopicity, as well as the thinness (22 mm), quickly adapting its moisture content to the surrounding RH.
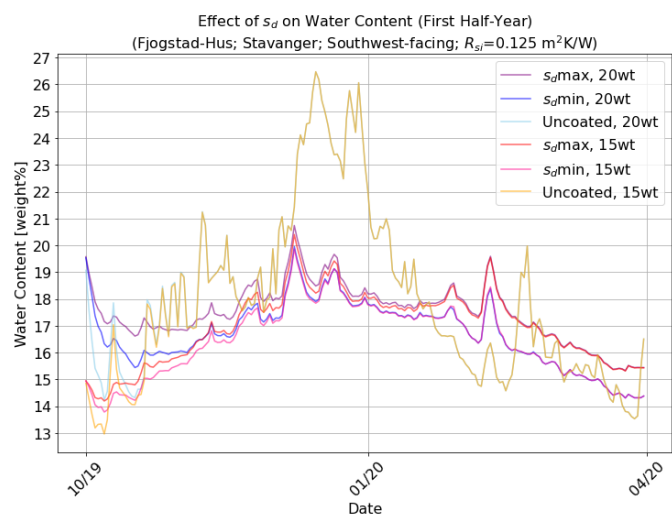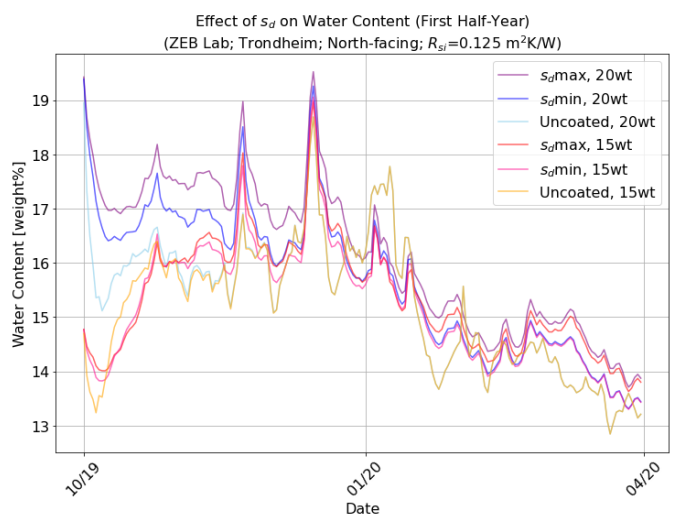
Figure 4.8: Effect of initial MC 15 wt% for the wooden cladding in (**a**) Fjogstad-Hus, (**b**) ZEB-Lab.

4.4 Extended Parametric Study on Mould Growth Risk

The resulting yearly mould growth indices of the extended parametric study considering are presented in the Table 4.4. considering different combinations of cavity climate input and outdoor climate. The yearly mould growth indices range from 0.02 (case I) to 4.79 (case VI). Both cases V and VI of Fjogstad-Hus yield indices of yellow risk, indicating that "Additional criteria or investigations are needed for assessing acceptability". This is expected due to the harsh climatic conditions of the Stavanger and the sensor being of the southwest-facing façade.

Table 4.4 Parametric study of which "indoor climate" is used, for both case buildings.

Input Parameters		I	II	III	IV	V	VI
Outdoor Climate	Trondheim	x	x	x			
	Stavanger				x	x	x
Cavity Climate Model	Best-fit curve (T_0, RH_0)	x			x		
	Offset-shifted (T_0, RH_{+5})		x			x	
	WAC file (Measured data)			x			x
Yearly Mould Index M		0.02	0.15	0.37	0.82	3.30	4.79

Figure 4.9 visually presents the development of the mould growth index over time for the six cases considered. The graph clearly shows the differences in mould growth risk based on chosen approach of inputting the cavity climate model to the simulation software. The results exhibit that using the WAC file leads to higher predicted mould growth risk compared to using the best-fit or offset-shifted curves. Besides, one observes that the offset-shifted model mirrors the performance of the WAC file better than the original least-squares best-fit curve does, making it a more reliable model for this type of climate than the least-squares best-fit model. The results show that how one choose to model the interior climate conditions is of great significance for the mould risk prediction.
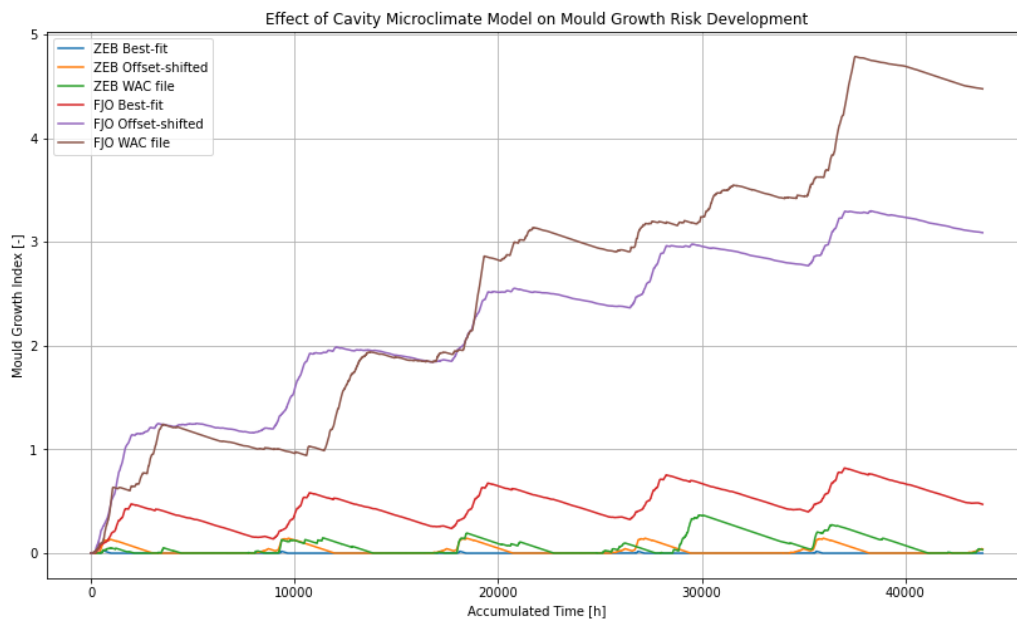
Figure 4.9: Development of Mould Growth Index for the considered cases I to VI.

5 Discussion

5.1 Laboratory Measurements

5.1.1 Consideration of Vapour Resistance Range

The range of s_d-values regardless of layers was 0.453 m for the most permeable to 2.250 m for the least permeable. When evaluating these coatings' values against the recommended thresholds detailed by e.g. Geving (2021) with the "diffusion open" wind barrier ($s_d < 0.5$ m) and "diffusion tight" vapour barrier ($s_d > 10$ m), only series no. 56B and 58B fall under the category "diffusion open". Several of the three-layers are below s_d of 1 m. Not even the least vapour permeable no. 51B2 (s_d of 2.250) m is "diffusion tight" according to these thresholds.

Comparing measured s_d-values to each other is challenging due to several reasons. Manufacturers simply not stating their coatings' vapour resistance in technical datasheets and denying providing these data when requested being the first. Secondly, there are limited scientifically published articles reporting s_d-values, and reported values vary both in explicit value, method and substrate used. When conducting the simulations in WUFI, it was observed that the default s_d-value for "acrylic façade paint" (inserted as surface transfer coefficient) was 0.3 m, which is lower than this study's laboratory findings. An s_d of 0.1 m for emulsion coatings is reported in NS-EN ISO 10456:(2007), with no mention of film thickness, which is much lower than the current findings. Some reported s_d-values for coatings for exterior wooden claddings that were identified in the literature review were 1.3 m and 2.5 m (wet cup method) by Geving et al. (2006) and 1.6 m and 2.8 m by Nore and Hundhausen (2016). These show a somewhat similar range compared to this study. However, Geving et al. (2006) mentions own method uncertainties due to insufficient sample size. Also, they tested the coating together with the wood substrate, which could potentially affect the results. This basis of comparison emphasize the variability and uncertainties in established s_d-values. As the dry film thickness is correlating so strong to the and more research should aim to develop standardised values for quantifying the vapour resistance of thin coatings and films.

5.1.2 Validation of Method

The low standard deviations of the s_d-values and dry film thicknesses across all coatings demonstrate the consistency and precision of the measurements by this wet cup method. Considering the sample size of 100 specimens, the consistency and low variability ensures reproducibility of the results. The retest of no. 53 affirms these findings that use of the wet cup method in this way is highly accurate for determining the vapour resistance of the coating films.

As discussed briefly in the article (Appendix A) a trend was observed regarding the potential additional support in the cup assembly. To recall, this was conducted for specimens that were too elastic to carry their own self-weight before sealing. If the film had accidentally touched the KNO_3 solution below, the test would need to have been discarded, and the intention with

these additional supports was therefore to avoid retesting of many series. Generally, coatings with a metal grid support (no. 51, 52, and 55) exhibited greater s_d-values, indicating less vapour permeability compared to those with either plastic cylinder support or no extra support. There was only two series (no. 56B and 58B) which used the plastic cylinder, both of which exhibit the two lowest s_d-values of the sample size. The rest of the series were conducted as completely according to the standard NS:EN ISO7783:(2018) for wet cup method on paints and varnishes. There was no specific reason for the differentiation of support type, it was merely selected based on availability in the lab of the day of assembly. The measurement uncertainties are greater for no. 51, 52, and 55 (all series B+B2) than for no. 56 and 58 (only B series) because the two latter were validated by *not* having their B2-series with the support. Thus, the low standard deviations and proved strong linear relationships suggest that the measured s_d-value is reliable despite these plastic supports. Additionally, during the weighing process, one specimen from both coating no. 55 and 52 had leakage incidents. These were promptly resealed, ensuring minimal impact on the overall results. The extent of the leaks and the subsequent readaptation back to stable water vapour transmission after sealing is evident in Figures D.4.2 and D.12.2 in Appendix D. The readaptation of the vapour transmission rates following the sealing indicates that the leakages did not significantly compromise the overall experiment or the integrity of the data.

5.2   Applicability of Curve-Fitting the Cavity Climate

The limitations of using single-sinusoid models for estimating the cavity microclimate are evident from the results. While the models capture the general fluctuating trend of temperature and RH, they struggle to accurately represent the extreme values. The best-fit models for temperature showed moderate fits, with R^2 values (approx. 0.7) for both the SW1 and MN5 sensor data indicating that the sinusoidal curve is able to capture a significant portion of the temperature variability. Considering RH, the best-fit model had low R^2 values and offset-shifted model had of course even lower R^2, suggesting that the sinusoidal curve is less effective in representing the humidity fluctuations within the cavity. This could be attributed to the sligthly different seasonal pattern of the fluctuating RH datapoints than just a sine trend (Figure 4.3 and Figure 4.4). The poor fits underscores the study of Bloomberg (2000) which recommends optimizing the model with multiple sinusoids to account for the complexity of several affecting factors.

Despite of the offset-shifted (RH_{+5}) curves poor fit to the sensor data, it simulated temperature and RH surprisingly well compared to the simulated temperature and RH of the WAC file-approach, with R above 0.8 for all the simulated data. The higher mould growth risk predictions obtained when using the WAC file (measured data) compared to the best-fit and offset-shifted curves is attributed to the fact that the WAC file provides the actual fluctuations and extreme values of temperature and relative humidity in the cavity, in contrast to the curve-fittings.

5.3   Other Uncertainties

Firstly, uncertainties are introduced by using a simplified sinusoid model as "indoor climate". Although the offset-shifted model captures the general seasonal fluctuations, the extreme levels of especially relative humidity are not accounted for, not even when offset-shifting the least-squares best-fit curve. The approach of composing the WUFI-compatible WAC file also poses uncertainty, as all models representing the reality tend to do. However, by ensuring completeness of datasets and analysing the sensor measurements preliminary, a large portion of such uncertainties could be controlled and thereby reduced.

Secondly, uncertainty in the simulations concerning the material properties of the coatings have been identified. While the vapour resistance value was determined experimentally and the bulk density was obtained from the manufacturer's technical datasheet, the remaining properties were sourced from an existing waterborne paint in the WUFI material database. Whether these properties accurately represent the coatings investigated in this study remains uncertain and has not been thoroughly evaluated.

In the simulations, the liquid moisture uptake from the exterior climate was limited by the coating's liquid moisture barrier properties. Yet the extent of this limitation has not been investigated thoroughly. Some uncertainty is thereby introduced regarding whether the influence of the outdoor precipitation and driving rain is realistically captured in the simulated wood MC and mould growth risk. Limiting the liquid water absorption on the exterior boundary would practically mean that the moisture source would merely be the RH of the air cavity. As the southwest-facing Fjogstad-Hus in Stavanger is highly exposed to driving rain, this restriction of the precipitation could seem like an oversimplification that would not capture the realistic amount of penetrating rain. For all simulated Fjogstad-Hus, this could indicate that the mould situation is underestimated. On the other hand, the sensor measured RH of the air cavities could possibly reflect the outdoor conditions of the measurement period to some extent, but this remains uncertain.

However, considering that this study aims to evaluate the different influences of coatings' vapour resistance on the claddings, the uncertainty regarding the simulations does not necessarily affect the results. As long as different boundary and material conditions are consistent across all simulation cases, the effect of the s_d-value will still be effectively shown in the results.

Furthermore, the simulations employed a simplification by not differentiating between the coatings based on their binder content (maximum and minimum solid content). While these adjustments would likely have minimal impact on the predicted wood MC and mould growth, a comprehensive sensitivity analysis study of coating properties in WUFI and update standardised tables could be useful for both the industry as well as homeowners to understand which characteristics are sensitive for potentially impeding the drying of moisture in claddings.

6 Conclusion

The laboratory experiments revealed that water vapour resistance (s_d) ranged from 0.453 m to 1.350 m (three layers), and from 0.690 m to 2.250 m (six layers). There is a strong linear relationship between s_d-value and dry film thickness. The alkyd (only one) exhibited higher s_d-values than the emulsions and acrylics, though the sample size is insufficient to determine this relationship. It might be due to factors i.e. higher bulk density and solid content or influence of the additional support. Despite some uncertainties of the assembly, the results anyhow show minimal deviations and high reliability of the method.

Over the five-year simulation, the wood MC fluctuates seasonally. The more vapour-resistant coatings showed a slightly slower drying than the more vapour permeable ones. However, their different impact on the moisture conditions is insignificant over the five-year period as no moisture is accumulating. Untreated claddings showcased both greater MC fluctuations with more variability and higher mould risk than for the coated claddings, which affirms the importance of surface coating. The cases of Fjogstad-Hus exhibited greater wood MC levels and greater mould risks than the cases of ZEB-Laboratory, due to the more extreme climatic conditions in this region.

The sinusoidal regression models provide initial cavity microclimate estimates but lack accuracy, especially for extreme values. The offset-shifted model deviated more for RH than temperature at both sites. The extended parametric study demonstrated that the choice of cavity climate model has a significant impact on the mould growth risk. Further model refinement and alternative approaches are needed for improved hygrothermal simulations.

Future research should investigate the influence of the additional film support of the wet cup assembly when doing measurements on thin films or coatings. This investigation should aim to isolate and quantify the efficacy of the additional support by e.g. controlled and systematic experiments with various supports. To establish a more definitive correlation between binder type and vapour resistance, more targeted experiments with a larger number of samples and various types of coatings are necessary, as the current findings only provide an indication of this relationship. Further assessment of the significance and accuracy of realistically modelling the climate boundary conditions, especially of the microclimate, as this study tried to shed some light on. The work could develop more advanced, multiple-sinusoid models but also to investigate which simplified models could be sufficient for the considered situation.

The study shows that the vapour density of wood cladding paint on the Norwegian market today does not appear to be the critical factor in terms of rot risk in external wood cladding. The unobserved trend of increasing rot problems in external wooden cladding in South-West Norway probably has other primary causes, be it climate change, the principle of ventilation, better heat-insulated houses, cladding quality, etc. This should be studied more closely.

References

Ahola, P. (1991) 'Moisture transport in wood coated with joinery paints', *Holz als Roh- und Werkstoff: European Journal of Wood and Wood Industries*, 49(11), pp. 428–432. Available at: https://doi.org/10.1007/BF02619465.

Altinkaya, S.A. *et al.* (2010) 'The influence of binder content on the water transport properties of waterborne acrylic paints', *Progress in Organic Coatings*, 69(4), pp. 417–425. Available at: https://doi.org/10.1016/j.porgcoat.2010.08.005.

Barker, N. (2024) 'ChatGPT Python'. OpenAI. Available at: https://chatgpt.com/g/g-cKXjWStaE-python (Accessed: 3 February 2024).

Betti, G. *et al.* (2024) 'CBE Clima Tool: A free and open-source web application for climate analysis tailored to sustainable building design', *Building Simulation*, 17(3), pp. 493–508. Available at: https://doi.org/10.1007/s12273-023-1090-5.

Bloomfield, P. (2000) 'Fitting Sinusoids', in *Fourier Analysis of Time Series*. Raleigh, North Carolina: John Wiley & Sons, Ltd (Wiley Series in Probability and Statistics), pp. 9–24. Available at: https://doi.org/10.1002/0471722235.ch2.

Bøhlerengen, T. (2018) *Byggforskserien 421.132 Fukt i bygninger. Teorigrunnlag.* Oslo, Norway: SINTEF Byggforsk. Available at: https://www.byggforsk.no/dokument/184/fukt_i_bygninger_teorigrunnlag (Accessed: 19 October 2023).

Brito, V., Diaz Gonçalves, T. and Faria, P. (2011) 'Coatings applied on damp building substrates: Performance and influence on moisture transport', *J. Coating. Tech. Res.*, 8, pp. 513–525. Available at: https://doi.org/10.1007/s11998-010-9319-5.

Edvardsen, K.I. and Ramstad, T.Ø. (2014) *Trehus Håndbok 5*. Oslo, Norway: SINTEF akademisk forlag.

Ekstedt, J. (2002) *Studies on the barrier properties of exterior wood coatings*. Doctoral Thesis. KTH- Royal Institute of Technology. Available at: https://www.diva-portal.org/smash/get/diva2:9254/FULLTEXT01.pdf (Accessed: 12 July 2023).

Ekstedt, J. and Östberg, G. (2001) 'Liquid water permeability of exterior wood coatings-testing according to a proposed European standard method', *Journal of Coatings Technology*, 73(914), pp. 53–59. Available at: https://doi.org/10.1007/BF02698438.

Elvebakk, K. and Gullbrekken, L. (2020) *Byggforskserien 523.255 Yttervegger av bindingsverk. Varmeisolering og tetting.* Oslo, Norway: SINTEF Byggforsk. Available at: https://www.byggforsk.no/dokument/361/yttervegger_av_bindingsverk_varmeisolering_og_te tting (Accessed: 7 May 2024).

Flæte, P.O. and Alfredsen, G. (2004) *Gran som ubehandlet utvendig kledning.* Ås, Norway: Norsk Institutt for Skogforskning. Available at: https://nibio.brage.unit.no/nibio-xmlui/handle/11250/2558468 (Accessed: 18 March 2024).

Fraunhofer IBP (2018) *WUFI® Mould Index VTT*, *WUFI® Software Add-ons*. Available at: https://wufi.de/en/software/wufi-add-ons/ (Accessed: 28 March 2024).

Fraunhofer IBP (2021) *WUFI® Pro*, *WUFI®*. Available at: https://wufi.de/en/software/wufi-pro/ (Accessed: 29 March 2024).

Fraunhofer IBP (2024a) *Benchmark test of EN 15026*, *WUFI®*. Available at: https://wufi.de/en/2015/04/09/benchmark-test-of-en-15026/ (Accessed: 8 June 2024).

Fraunhofer IBP (2024b) *Creating weather files*, *WUFI*. Available at: https://wufi.de/en/service/downloads/creating-weather-files/ (Accessed: 21 March 2024).

Geving, S. *et al.* (2006) *Hygrothermal conditions in wooden claddings*. Oslo, Norway: Norwegian Building Research Institute. Available at: https://sintef.brage.unit.no/sintef-xmlui/handle/11250/2418978 (Accessed: 13 May 2024).

Geving, S. (2021) *Praktisk bygningsfysikk*. 1.utgave. Bergen, Norway: Fagbokforlaget.

Geving, S. and Thue, J.V. (2002) *Fukt i bygninger*. Norges byggforskningsinstitutt (Håndbok).

Gezici-Koç, Ö. *et al.* (2018) 'Understanding the influence of wood as a substrate on the permeability of coatings by NMR imaging and wet-cup', *Progress in Organic Coatings*, 114, pp. 135–144. Available at: https://doi.org/10.1016/j.porgcoat.2017.10.013.

Gobakken, L.R. and Westin, M. (2008) 'Surface mould growth on five modified wood substrates coated with three different coating systems when exposed outdoors', *International Biodeterioration and Biodegradation*, 62(4), pp. 397–402. Available at: https://doi.org/10.1016/j.ibiod.2008.03.004.

Goossens, E.L.J., Van der Zanden, A.J.J. and Van der Spoel, W.H. (2004) 'The measurement of the moisture transfer properties of paint films using the cup method', *Progress in Organic Coatings*, 49(3), pp. 270–274. Available at: https://doi.org/10.1016/j.porgcoat.2003.10.008.

Greenhalgh, T. and Peacock, R. (2005) 'Effectiveness and efficiency of search methods in systematic reviews of complex evidence: audit of primary sources', *BMJ (Clinical research ed.)*, 331(7524), pp. 1064–1065. Available at: https://doi.org/10.1136/bmj.38636.593461.68.

Grüll, G. and Truskaller, M. (2014) 'Moisture protection of wood coatings and its sensitivity to mechanical defects depending on surface hydrophobicity and solid content', *International Wood Products Journal*, 5(2), pp. 74–82. Available at: https://doi.org/10.1179/2042645313Y.0000000048.

Hägerstedt, S.O. and Arfvidsson, J. (2010) 'Comparison of Field Measurements and Calculations of Relative humidity and Temperature in Wood Framed Walls', in O. Zmeskal (ed.) *Conference proceedings - Thermophysics 2010. Thermophysics 2010*, Valtice, Czech Republic: Brno University of Technology, Faculty of Chemistry, pp. 93–101.

Hanssen-Bauer, I. *et al.* (2017) *Climate in Norway 2100.*

Harris, C.R. *et al.* (2020) 'Array programming with NumPy', *Nature*, 585(7825), pp. 357–362. Available at: https://doi.org/10.1038/s41586-020-2649-2.

Håvardstein, E. (2022) 'Huset råtnet etter mindre enn ti år: - Som pulled pork', *TV 2*, 30 October. Available at: https://www.tv2.no/nyheter/innenriks/huset-ratnet-etter-mindre-enn-ti-ar-som-pulled-pork/15217737/ (Accessed: 20 February 2024).

Heimsvik, O. (2022a) '14 år etter at husene var nye må kledningen skiftes – Skanska avviser ansvar', 8 May. Available at: https://www.aftenbladet.no/i/pWeJ7W (Accessed: 20 February 2024).

Heimsvik, O. (2022b) 'Når du legger deg om kvelden og hører det plasker på vinduene, da lurer du på om det går bra denne gangen', *Aftenbladet*, 27 January. Available at: https://www.aftenbladet.no/i/jaM1qn (Accessed: 20 February 2024).

Hjort, S. (1997) *Moisture Balance in Painted Wood Panelling*. Doctoral Thesis. Chalmers University of Technology. Available at: https://www.semanticscholar.org/paper/Moisture-Balance-in-Painted-Wood-Panelling-Hjort/9ccd761d89e5f011e93a62836d323c3b53a4a9cc (Accessed: 8 June 2024).

Hukka, A. and Viitanen, H.A. (1999) 'A mathematical model of mould growth on wooden material', *Wood Science and Technology*, 33(6), pp. 475–485. Available at: https://doi.org/10.1007/s002260050131.

Huldén, M. and Hansen, C.M. (1985) 'Water permeation in coatings', *Progress in Organic Coatings*, 13(3–4), pp. 171–194. Available at: https://doi.org/10.1016/0033-0655(85)80025-X.

Hýsek, Š. *et al.* (2018) 'Water permeability of exterior wood coatings: Waterborne acrylate dispersions for windows', *Journal of Green Building*, 13(3), pp. 1–16. Available at: https://doi.org/10.3992/1943-4618.13.3.1.

Ingebretsen, S.B. *et al.* (2022) 'Microclimate and Mould Growth Potential of Air Cavities in Ventilated Wooden Façade and Roof Systems—Case Studies from Norway', *Buildings*, 12(10), p. 1739. Available at: https://doi.org/10.3390/buildings12101739.

Ingebretsen, S.B. (2022) *Mikroklima i luftespalter i luftede fasader og skråtak*. Master thesis. NTNU. Available at: https://ntnuopen.ntnu.no/ntnu-xmlui/handle/11250/3020989.

Jourdain, C. *et al.* (1999) 'Changing nature of wood products—what does it mean for coatings and finish performance?', *Journal of Coatings Technology*, 71(890), pp. 61–66. Available at: https://doi.org/10.1007/BF02697900.

Kuenzel, H. (1994) *Methods for one- and two-dimensional calculations of the coupled heat and moisture transport in components with simple characteristics*. Doctoral Thesis. Universität Stuttgart. Available at: https://www.ibp.fraunhofer.de/content/dam/ibp/ibp-neu/de/dokumente/dissertationen/hk_dissertation_tcm45-30727.pdf (Accessed: 29 April 2024).

Kvande, T. (2013) *Byggforskserien 542.003 Totrinnstetning mot slagregn på fasader. Luftede kledninger og fuger*. Oslo, Norway: SINTEF Byggforsk. Available at:

https://www.byggforsk.no/dokument/470/totrinnstetning_mot_slagregn_paa_fasader_luftede_ kledninger_og_fuger (Accessed: 20 March 2024).

Lisø, K.R. *et al.* (2006) 'Decay potential in wood structures using climate data', *Building Research & Information*, 34(6), pp. 546–551. Available at: https://doi.org/10.1080/09613210600736248.

Lisø, K.R., Kvande, T. and Thue, J.V. (2006) 'Learning from experience – an analysis of process induced building defects in Norway', in *Research in Building Physics and Building Engineering*. CRC Press.

Magnussen, K. and Mattsson, J. (2005) *Byggforskserien 701.401 Muggsopp i bygninger. Forekomst og konsekvenser for inneklimaet.* Oslo, Norway: SINTEF Byggforsk. Available at: https://www.byggforsk.no/dokument/3231/muggsopp_i_bygninger_forekomst_og_konsekven ser_for_inneklimaet (Accessed: 18 December 2023).

van Meel, P.A. *et al.* (2011) 'Moisture transport in coated wood', *Progress in Organic Coatings*, 72(4), pp. 686–694. Available at: https://doi.org/10.1016/j.porgcoat.2011.07.011.

de Meijer, M. (2001) 'Review on the durability of exterior wood coatings with reduced VOC-content', *Progress in Organic Coatings*, 43(4), pp. 217–225. Available at: https://doi.org/10.1016/S0300-9440(01)00170-9.

Mundt-Petersen, S.O. and Harderup, L.-E. (2013) 'Validation of a One-Dimensional Transient Heat and Moisture Calculation Tool under Real Conditions', in. *Thermal Performance of the Exterior Envelopes of Whole Buildings XII International Conference*, ASHRAE.

Nore, K. (2010) *Hygrothermal performance of ventilated wooden cladding*. Doctoral thesis. NTNU. Available at: https://ntnuopen.ntnu.no/ntnu-xmlui/handle/11250/231575 (Accessed: 13 May 2024).

Nore, K. and Hundhausen, U. (2016) 'Hygrothermal performance of ventilated wooden cladding', in. *47th IRG Annual Meeting*, Lisbon, Portugal. Available at: https://www.researchgate.net/publication/329216688_Hygrothermal_performance_of_ventilat ed_wooden_cladding.

NS-EN ISO 7783:2018 (2018) *Paints and varnishes - Determination of water-vapour transmission properties - Cup method (ISO 7783:2018)*. Oslo, Norway: Standard Norge. Available at: https://online.standard.no/nb/ns-en-iso-7783-2018 (Accessed: 10 September 2023).

NS-EN ISO 10456:2007 (2007) *Building materials and products - Hygrothermal properties - Tabulated design values and procedures for determining declared and design thermal values (ISO 10456:2007)*. Oslo, Norway: Standard Norge.

NS-EN ISO 12572:2016 (2016) *Hygrothermal performance of building materials and products - Determination of water vapour transmission properties - Cup method (ISO 12572:2016)*. Oslo, Norway: Standard Norge. Available at: https://www.iso.org/standard/64988.html#lifecycle.

Plesser, T. (2009) *Byggforskserien 542.640 Overflatebehandling av utvendig trevirke.* Oslo, Norway: SINTEF Byggforsk. Available at: https://www.byggforsk.no/dokument/482/overflatebehandling_av_utvendig_trevirke (Accessed: 7 December 2023).

Rawlings, J.O., Pantula, S.G. and Dickey, D.A. (eds) (1998) 'Review of Simple Regression', in *Applied Regression Analysis: A Research Tool*. New York, NY: Springer, pp. 1–36. Available at: https://doi.org/10.1007/0-387-22753-9_1.

Ruus, A. *et al.* (2011) 'Water vapour transmission properties of natural paints', *Agronomy Research*, 9(SPPL. ISS. 1), pp. 197–201.

Šadauskienė, J. *et al.* (2008) 'Linear-Regression-Equation-Based Prognosis of the Dependence of the Thickness of the Air Layer Equivalent to the Paint Coating's Water Vapour Permeability on the Type of the Paint and Number of the Paint Coating Layers', *Materials Science*, 14.

Šadauskiene, J., Monstvilas, E. and Stankevičius, V. (2007) 'The impact of exterior finish vapour resistance on the moisture state of building walls', *Technological and Economic Development of Economy*, 13(1), pp. 73–82. Available at: https://doi.org/10.3846/13928619.2007.9637779.

Størksen, T. (2022) 'Råteskader ødelegger idyllen på Hemmingstad', *Haugesunds Avis*, 15 February. Available at: https://www.h-avis.no/5-62-1302165 (Accessed: 20 February 2024).

Straube, J. (2002) 'Moisture in buildings', *ASHRAE Journal*, 44, pp. 15–19.

Svendsen, S. (1967) 'Principles of One-Stage and Two-Stage Seals', in *Proceedings of the International CIB Symposium*. Oslo, Norway, pp. 25–28. Available at: https://www.scribd.com/document/446309302/Svendsen-1967-Drained-PE-Joint-Wall-Principles-of-One-stage-and-Two-stage-Seals.

Thue, J.V. (2016) *Bygningsfysikk grunnlag*. 1st edn. Bergen, Norway: Fagbokforlaget.

Tomren, J.H. *et al.* (2023) 'Water Vapour Resistance of Ceiling Paints - Implications for the Use of Smart Vapour Barriers in Compact Wooden Roofs'. Available at: https://doi.org/10.3390/buildings13092185.

Topçuoğlu, O., Altinkaya, S.A. and Balköse, D. (2006) 'Characterization of waterborne acrylic based paint films and measurement of their water vapor permeabilities', *Progress in Organic Coatings*, 56(4), pp. 269–278. Available at: https://doi.org/10.1016/j.porgcoat.2006.02.003.

Viitanen, H. (1994) 'Factors affecting the development of biodeterioration in wooden constructions', *Materials and Structures*, 27(8), pp. 483–493. Available at: https://doi.org/10.1007/BF02473453.

Viitanen, H. *et al.* (2015) 'Mold Risk Classification Based on Comparative Evaluation of Two Established Growth Models', *Energy Procedia*, 78, pp. 1425–1430. Available at: https://doi.org/10.1016/j.egypro.2015.11.165.

Virtanen, P. *et al.* (2020) 'SciPy 1.0: fundamental algorithms for scientific computing in Python', *Nature Methods*, 17(3), pp. 261–272. Available at: https://doi.org/10.1038/s41592-019-0686-2.

Wohlin, C. (2014) 'Guidelines for snowballing in systematic literature studies and a replication in software engineering', in *Proceedings of the 18th International Conference on Evaluation and Assessment in Software Engineering. EASE '14: 18th International Conference on Evaluation and Assessment in Software Engineering*, London England United Kingdom: ACM, pp. 1–10. Available at: https://doi.org/10.1145/2601248.2601268.

Appendices

List of Appendices:

Appendix A: Scientific Article

Appendix B: Literature Search Matrix

Appendix C: Dry Film Thickness Calculations

Appendix D: Official Laboratory Test Reports

A Scientific Article

This Appendix A contains the article Water Vapour Resistance of Exterior Coatings – Influence on Moisture Conditions in Ventilated Wooden Claddings is shown as it was submitted to the scientific journal Buildings the 5th of June 2024.

Rossebø, K.B., Kvande, T. (2024). Water Vapour Resistance of Exterior Coatings – Influence on Moisture Conditions in Ventilated Wooden Claddings. Submitted.

Author contribution

Confirmation on paper contribution

Katinka Bjørhovde Rossebø[1] og Tore Kvande[1]

Water Vapour Resistance of Exterior Coatings – Influence on Moisture Conditions in Ventilated Wooden Claddings

[1] Institutt for bygg- og miljøteknikk (NTNU)
www.ntnu.no

ABSTRACT: *Increasing climate fluctuations and extremes due to climate change are particularly concerning for wooden building envelopes, especially in the Nordic region with harsh climatic conditions. The exterior coating's barrier properties are crucial for maintaining building envelopes' intended lifespans. This study investigates the influence of water vapour resistance of exterior coatings on the moisture conditions and mould growth risk of ventilated wooden claddings. The s_d-value (vapour diffusion-equivalent air layer thickness) is determined for nine free-standing coatings (alkyds, emulsions, and acrylics), in total 100 specimens tested with the wet cup method Additionally with WUFI Pro, one-dimensional hygrothermal simulations under Nordic climatic conditions investigate how coatings' vapour resistance might influence the moisture dynamics of wood. The mould risk is assessed by the add-on WUFI VTT Model. The determined s_d-values for the coatings range from 0.453 to 1.350 m (three layers) and from 0.690 to 2.250 m (six layers), showing a strong correlation with dry film thickness. The vapour resistance of coatings does not significantly influence the wood moisture content, but lower resistance may cause slightly faster drying. The importance of surface-treatment is confirmed. Mould risk is notably higher in a Stavanger climate on a southwest-facing wall compared to Trondheim on a north-facing wall.*

AUTHOR CONTRIBUTIONS: **Katinka Bjørhovde Rossebø**: Conceptualization, methodology, validation, formal analysis, investigation, writing—original draft preparation, writing—review and editing. **Tore Kvande**: Conceptualization, methodology, validation, writing—review and editing, supervision.

Both authors have read and agreed to the published version of the manuscript. We hereby confirm the work process and the sharing of work.

Katinka Bjørhovde Rossebø   Tore Kvande

Article

Water Vapour Resistance of Exterior Coatings – Influence on Moisture Conditions in Ventilated Wooden Claddings

Katinka Bjørhovde Rossebø [1] and Tore Kvande [2,*]

1   Department of Civil and Environmental Engineering, Norwegian University of Science and Technology (NTNU), 7034 Trondheim, Norway; katinkar@stud.ntnu.no
2   Department of Civil and Environmental Engineering, Norwegian University of Science and Technology (NTNU), 7034 Trondheim, Norway; tore.kvande@ntnu.no
*   Correspondence: tore.kvande@ntnu.no

Abstract:

Increasing climate fluctuations and extremes due to climate change are particularly concerning for wooden building envelopes, especially in the Nordic region with harsh climatic conditions. The exterior coating's barrier properties are crucial for maintaining building envelopes' intended lifespans. This study investigates the influence of water vapour resistance of exterior coatings on the moisture conditions and mould growth risk of ventilated wooden claddings. The s_d-value (vapour diffusion-equivalent air layer thickness) is determined for nine free-standing coatings (alkyds, emulsions, and acrylics), in total 100 specimens tested with the wet cup method Additionally with WUFI Pro, one-dimensional hygrothermal simulations under Nordic climatic conditions investigate how coatings' vapour resistance might influence the moisture dynamics of wood. The mould risk is assessed by the add-on WUFI VTT Model. The determined s_d-values for the coatings range from 0.453 to 1.350 m (three layers) and from 0.690 to 2.250 m (six layers), showing a strong correlation with dry film thickness. The vapour resistance of coatings does not significantly influence the wood moisture content, but lower resistance may cause slightly faster drying. The importance of surface-treatment is confirmed. Mould risk is notably higher in a Stavanger climate on a southwest-facing wall compared to Trondheim on a north-facing wall.

Keywords: diffusion equivalent air layer thickness; sd-value; wet cup method; moisture drying; mould growth risk

1. Introduction

The hygrothermal performance of buildings is affected by urban and local microclimates, considering the impacts on façade surfaces and surrounding air temperatures [1]. Due to global climate change, increasing frequency and intensity of extreme weather and climate events is expected [2], as well as increased fluctuations in moisture levels, which is likely to implicate the degradation of the building envelopes that are especially vulnerable as directly exposed to the climate agents [1,3]. The Nordic region already experiences a particularly harsh climate with strong seasonal variations, driving rain, freeze-thaw cycles, strong winds etc. For this region, anticipated climate change implies even more precipitation and rising temperature in the years to come [4].

Historically, wood has been an important construction material in Nordic countries due to its simple production and the local availability of raw materials [5]. Wood as a building material is of ever-rising global importance considering the necessary implementation of climate change adaptation strategies, favoured especially for its versatile characteristics [5] and low carbon footprint [6]. However, increasing weather fluctuations are creating unfavourable circumstances for building with wood [7–9] as wood is a

hygroscopic material highly affected by surrounding moisture conditions, as well as vulnerably to attacking microorganisms. Mould growth criteria involve temperature, RH, exposure time and wood moisture content [10–12]. Wood moisture content is typically stated as a percentage of the wood's dry state mass in "weight-%" [13]. Air temperature, global radiation, wind velocity, and driving rain are the most significant contributors to fluctuating moisture content in wood [14]. It is recognised that 75% of building defects are related to moisture, leading to problems such as mould growth, rot, swelling, and salt migration within the materials [15]. It is essential to conduct designs and good quality maintenance to withstand the future climate exposures and ensure intended material lifespans.

Executional quality of the building envelope may be varied. The principle of "two-stage weatherproofing" shown in Figure 1 is common in Scandinavia and recommended for façades exposed to the harsh Nordic and coastal climates, thoroughly described by several studies i.e. [16–18]. In short, this is a ventilated façade system featuring an outer cladding separated from the wind barrier by an air cavity. It is primarily designed for avoiding driving rain penetration while still facilitating proper drainage and drying of embedded moisture that may have entered.
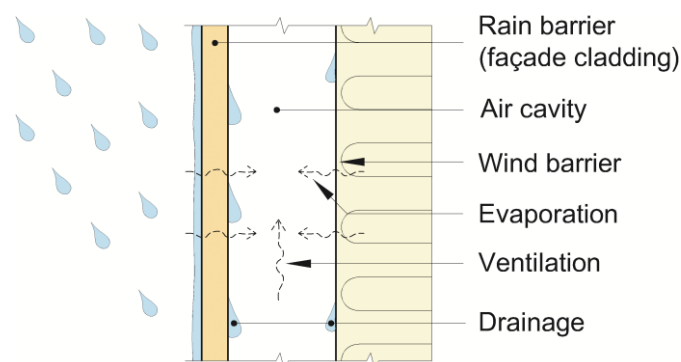
Figure 1. Schematic illustration of "two-stage weatherproofing" (ventilated façade) and moist. Reprinted with permission from Refs. [18].

The most commonly used wood type exterior cladding material in Norway is spruce (Picea abies) [19–21], among other reasons because it absorbs less moisture and adheres better to paint compared to other wood types (i.e. pine) [5,21,22]. Maintenance and treatment of the outdoor wood surfaces (e.g. by application of paint) is necessary to protect against harsh climate conditions that may cause biodeterioration [5,14,23]. Coatings on exterior wooden claddings not only provide an aesthetic appeal, but also form a protective barrier of the wood [8,24–26] when executed and maintained properly. Protective properties of exterior coatings are addressed in several studies e.g. [24,26–28].

The ever-reported issues of rot damage in wooden claddings in Southwest Norway may be attributed to multiple factors, i.e. climate change, changes in the quality of wooden cladding, alterations in building practices, better insulated walls, reduced maintenance, and variations in surface coating quality. Commercial exterior coatings are typically proclaimed by manufacturers to be "rainwater impermeable" with intend to withstand the Nordic weather conditions. However, their water vapour resistance performance are not addressed in technical declaration sheets. A question arises whether these exterior coatings might be so vapour impermeable that they potentially impede the drying of embedded moisture in wooden claddings, and thus, accelerating the biodeterioration processes. In this context, a common way to assess coatings' resistance to water vapour diffusion is by the equivalent air layer thickness, s_d-value, which resembles the thickness in m of a motionless air layer with the same water vapour resistance as the material [29].

Existing literature recognizes factors influencing the moisture protection of coatings as binder type, dry film thickness, surfactants, weathering, and the age and condition of

the paint film [8,22,30,31]. Hu et al. [32] tested highly permeable films with the wet cup method and found that the water vapour transmission rate depends on film thickness. Brito et al. [33] found that the coating's impact on substrate drying significantly varies with the substrate's moisture content. A substrate is the surface to which a coating material is applied [34]. Gezici-Koc et al. [35] found that the interaction between wooden substrate and coating did not affect water vapour permeability, yet contradictory conclusions were drawn by Yaseen and Raju [36] who found that choice of substrate significantly affect the films' water vapour permeability. The study of Hysek et al. [31] revealed that water vapour uptake were affected by film thickness and coating composition. Topçuoğlu et al. [37] found that the moisture barrier properties of acrylic coatings decrease with decreasing binder content.

Some studies explicitly measuring or mentioning the s_d-value for coatings were identified. According to Table 5 of NS-EN ISO 10456:2007 [38], the s_d is 0.1 m for emulsion paints and 3 m for glossy paints, no mentioning of layer thicknesses. Table B1.3 of Geving and Thue [39] reports an s_d-range of 0.049 to 0.49 for alkyds with two layers. The wet cup measurements of combined coating and spruce board by Geving et al. [23] indicates an s_d-value of 2.5 m for oil-dilutable coatings and of 1.3 m for waterborne acrylic/alkyd, however, with large uncertainties due to few specimens. Nore and Hundhausen [40] use in their study an alkyd coating with measured s_d of 2.8 (0.23) m and an acrylic coating with s_d of 1.6 (0.15) m, however the measurement method remains unexplained. They concluded that surface treatments did not influence the hygrothermal performance. Grüll and Truskaller [30] tested both liquid- and water vapour permeability of coatings on wood substrate, and reported a strong correlation of these properties. Šadauskiene et al. [41] measured that s_d-value of coatings on exterior render façades should be less than 0.6 m to allow proper drying. The results also showed increasing s_d for increased number of layers (i.e. film thickness), yet not linearly. Of these, acrylic coatings were the least vapour permeable of the different types. Tomren et al. [42] measured the s_d of ceiling coatings on gypsum substrate, finding a range between 0.1 to 0.5 m depending on the number of paint layers. Conclusions were drawn that s_d did not linearly increase with the number of layers. Note that the substrate types of these abovementioned studies vary beyond solely wood which is due to the limited number of identified studies focusing exclusively on coatings for wood.

The review of existing literature confirms anticipation of some knowledge gaps in determining the vapour resistance (in terms of s_d-value) of exterior coatings on wood. How these coatings' diffusion properties may influence the moisture conditions of wooden panels in Nordic climates should be studied as well.

The current study aims to determine the vapour resistance (s_d-value) for various commercial coatings for exterior wooden claddings, and to investigate to which extent this vapour resistance affects the moisture drying conditions of wooden claddings set in two Nordic climates. The following research questions have been formulated:

- What is the range of water vapour resistance s_d for exterior coatings?
- How does water vapour resistance of coatings affect the moisture drying conditions and mould growth risk of wooden claddings?

Limitations of this study include reporting only the water vapour resistance in terms of the s_d-value by the "wet cup method" in NS:EN ISO 12572 [29], disregarding characteristics i.e. surfactants, contact angle, and liquid transport. The test did not involve cyclic weathering exposure. The study is confined to investigate the s_d og free-standing films, excluding any possible influence of the interaction with the wood substrate. Secondly, the hygrothermal simulations are one-dimensional. The simulations are based on two case buildings in Norway, with some parameters chosen to reflect more realistic environmental conditions rather than those that typically would produce more extreme moisture conditions. The mould growth model used is highly sensitive to the end-user's parameter choices.

2. Materials and Methods

2.1. Laboratory Measurements

Laboratory measurements for determining the water vapour resistance of commercial coating products intended for exterior wood have been carried out at the Laboratory of Building Physics at the Institute of Civil and Environmental Engineering at NTNU. The wet cup method, as specified in NS-EN ISO 12572:2016 [29] and in detail for paints and varnishes in NS-EN ISO 7783:2018 [43], has been applied for determining the properties describing the coatings abilities to resist water vapour diffusion. A total of 110 specimens were comprehended. Paint sampling and test conditioning were performed Oct to Dec 2023, while test assembly and weighing procedure were conducted Jan to May 2024 for all coatings apart from

- no. 53, which was fully tested fall of 2023 as a subject for method evaluation in the preliminary project, and
- no. 56, which suffered substantial leakage and therefore was resampled and conditioned anew spring of 2024.

2.1.1. Materials

Nine commercial products were chosen for their relevance in the Norwegian market of exterior coatings for wooden claddings that are advertised for being "impermeable to rain" and "withstanding harsh Nordic weather". They are detailed along with technical specifications in Table 1. All coating products are waterborne, semi-glossy, and white hued. Binder type varies between alkyd resin, acrylic resin, and emulsion of acrylic/alkyd. Three and six layers were approximated to resemble respectively one and two rounds of surface treatment. The intend was to account for uncertainties in estimating the number of previous coating layers and the eroding effects of weathering.

Table 1. Overview of tested coatings. Each product consists of one series of three layers, and one series of six layers, labelled respectively -B and -B2.

Coating		Layers	Binder Type	Bulk Density [kg/m³]	Additional Film Support**
51	B	3	Alkyd resin	1260	Metal grid
	B2	6			Metal grid
52	B	3	Emulsion (Alkyd/Acrylic)	1260	Metal grid
	B2	6			Metal grid
53	B	3	Emulsion (Alkyd/Acrylic)	1230	-
	B2	6			-
53X*	B	3	Emulsion (Alkyd/Acrylic)	1230	-
	B2	6			-
54	B	3	Acrylic resin	1200	-
	B2	6			-
55	B	3	Acrylic resin	1200	Metal grid
	B2	6			Metal grid
56	B	3	Emulsion (Alkyd/Acrylic)	1200	Plastic cylinder
	B2	6			-
57	B	3	Acrylic resin	1250	-
	B2	6			-
58	B	3	Acrylic resin	1200	Plastic cylinder
	B2	6			-
59	B	3	Acrylic resin	1260	-
	B2	6			-

*The "X" signifies the second test of an already tested coating.
** Explained in Section 2.1.2.

2.1.2. Test Preparation and Assembly

The coating application process (e.g. application method by brush, uniform direction, consistent repaint intervals, etc.) was executed by a skilled laboratory technician and accords with NS-EN 927-10:2019 [44] and manufacturer specifications. The re-paintable intervals between layers were sufficient to allow proper drying. Each product had a separate brush and stirrer to prevent sample contamination. A teflon film substrate was used to allow easy detachment [43]. Of each product, in total twelve specimens were painted, six of which were of three layers and six of which were of six layers, then cured for seven days in freely circulating air, before being punched out to the circular specimens of 0.174 m diameter, see Figure 2. After which, they were stored in the controlled test enclosure for at least 28 days [43] until further cup assembly.

(**a**) (**b**)
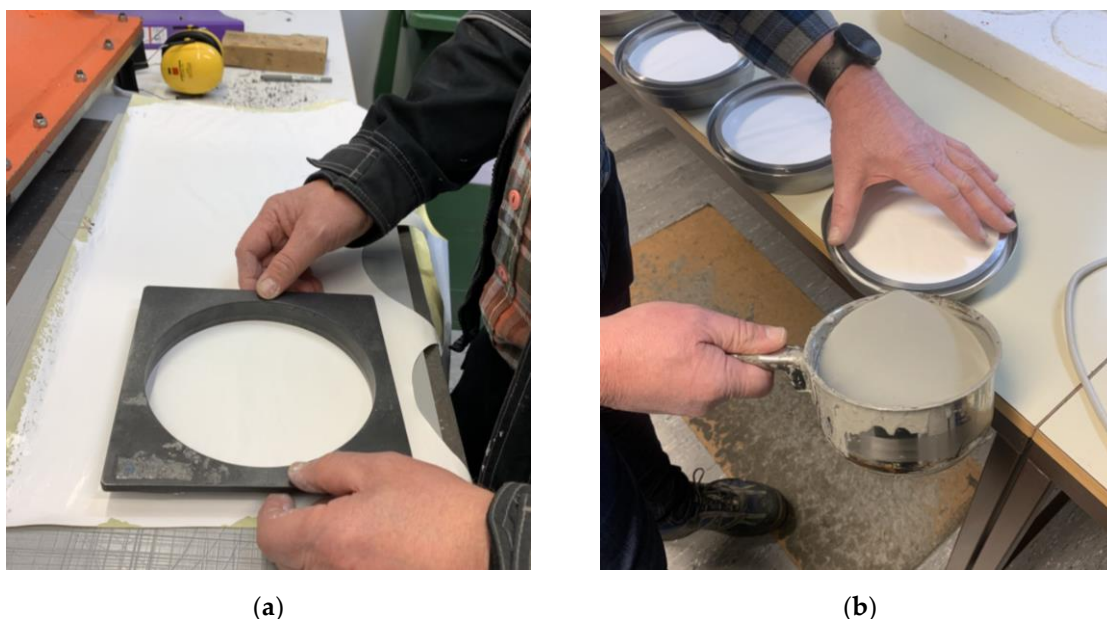
Figure 2. (**a**) Punching of a specimens. (**b**) Sealing procedure with molten wax and ring template

The teflon substrate was after the curation time removed, and dry film thickness was measured with a thickness gauge of 0.01 mm accuracy. The thickness reported in Table 6 is the mean of five random measurements f or each specimen of a series.

In total ten specimens of each product (five with three layers, five with six layers) were assembled. Molten wax and a ring template was used for sealing, in accordance with Annex B of NS-EN ISO 7783:2018 [43]. The specimen was sealed to the rim of a metal cup containing a saturated aqueous solution of KNO_3. This liquid was poured until measured 10 mm below the specimen surface. The KNO_3 creates a relative humidity 94% RH inside the test cup, thus a lower partial vapour pressure p_v than in the surrounding test enclosure [43]. Note that the diameter of the test surface after the sealing is changed to be 0.164 m.

(**a**) (**b**)
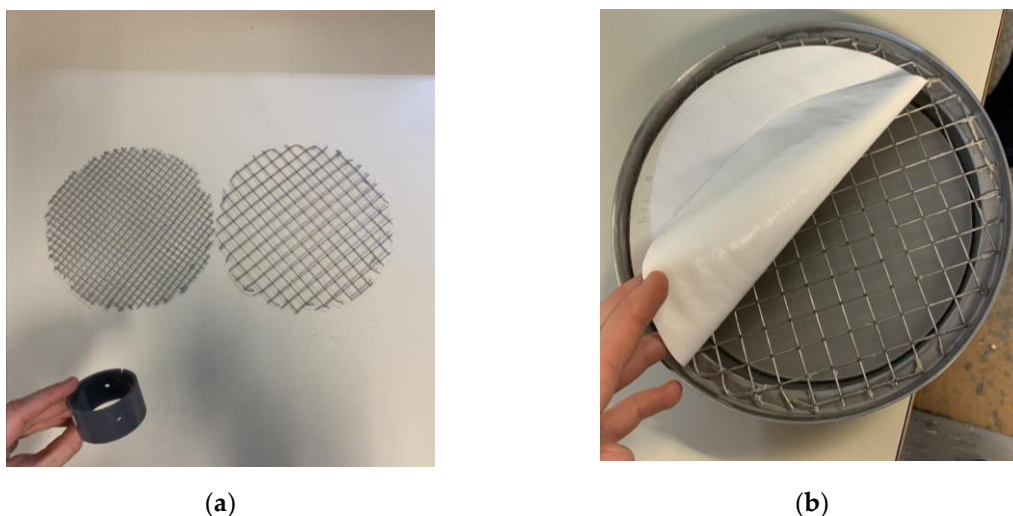
Figure 3. The types of additional film support, in (**a**) metal grids and plastic cylinder , and (**b**) shows it under the film in the cup assembly.

Some coatings were too elastic to allow for self-support and needed a stabilizing support to give enough stiffness to seal them on the cups' rims, see Figure 3. This is not part of the standardised method, and may yield uncertaintiy for the measurements. Table 1 displays the coatings to which this applies. For some specimens, the additional cup support created difficulties in sealing tightly. Though, upon any suspicion of leakage during the test, the specimen was sealed promptly.

2.1.3. Test Procedure

During testing, the cups were stored in the conditioned test enclosure of (23 ± 2) °C and (50 ± 5) % RH, as shown in Figure 4.

Figure 4. Storing of cups during weighing.

The difference in the partial vapour pressure across the specimen, Δp_v, is the driving force of the vapour flow (from higher to lower partial pressure) [29,45]. As a result of this rate of vapour flow through the specimen, periodic weighings are conducted to determine the rate of mass change over time. From this, the water vapour transmission rate through the specimen, V, is found and finally the diffusion-equivalent air layer thickness in meters is calculated using Equation (1):

$$s_d = \frac{\delta_a \cdot \Delta p_v}{V} \tag{1}$$

where δ_a is the water vapour permeation coefficient of air at standard temperature and pressure [43].

It is worth mentioning that the s_d-value is only one of several ways of expressing the results of the wet cup method.

The first weighing occurred 24-48 hours post-assembly to accommodate the initial stabilization of water vapour transmission. The time interval for subsequent measurements was then set at 24 hours, based on the expected range of the product's s_d-value, which was between 0.5 - 2 m [29,43]. Weight measurements were carried out using a high-precision balance with accuracy of 0.001 g placed inside a plastic chamber to prevent disturbances from the surroundings, see Figure 5. The balance was calibrated with a control weight of 1000 g before each individual weighing.

Figure 5. Set-up of test procedure of a specimen on the high-precision balance

The test concluded when the mass change across the last five consecutive measurements remained constant within ± 5% of its average rate of change [29]. Temperature (T), relative humidity (RH), and partial vapour pressure p_v of the test enclosure were monitored hourly by sensors and logged in the calculation spreadsheet alongside the weight measurements for calculations.

The results are corrected for the surface heat resistance above the sample, the vapour transport through the overlapping zone, and the resistance of the air layer in the cup. The reader is referred to the two abovementioned standards for other specific details.

2.2. Hygrothermal Simulations and Mould Growth Risk Assessment

2.2.1. WUFI® Pro

The simulated moisture conditions of the considered cladding construction have been performed with the one-dimensional software WUFI® Pro 6.7 by the Fraunhofer-Institut für Bauphysik [46], which is validated by several studies.

The simulations are based on the climatic conditions of two case buildings Fjogstad-Hus and ZEB-Laboratory, located respectively Stavanger and Trondheim in Norway, previously analysed by Ingebretsen [47] and Ingebretsen et al. [48]. One sensor from each building was selected based on Ingebretsen's results: SW1 for Fjogstad-Hus, due to extreme moisture conditions (southwest orientation), and MN5 for ZEB-Laboratory, as a reference line. Note that MN5 is on the north façade which was the only wooden one. Southwest orientation is more exposed to driving rain, while north usually reflects the poorest winter drying conditions due to lack of solar radiation [5]. Table 2 shows the parameters which depend on climate and orientation of case building.

Table 2. Input parameters dependent on case building.

Parameters Dependent on Case Building	Fjogstad-Hus	ZEB-Laboratory
Outdoor climate	Stavanger	Trondheim
Sensor	SW1	MN5
Indoor climate "Sine Curve"	Curve fit of SW1 data	Curve fit of MN5 data
Wall orientation	Southwest	North
Building height	Short building (< 10 m)	Tall building (10 to 20 m)
Driving rain coefficients	R1 = 0, R2 = 0.07	R1 = 0, R2 = 0.1

As this study aims to investigate realistic climate boundary conditions, Typical Meteorological Year (TMY) weather files were used for the outdoor climate [49–51], and the cavity microclimate represents the indoor climate boundaries. To use WUFI's "Sine Curve" option, least-square sinusoidal regression [52] was performed to estimate the best-fit sinusoids for the temperature (T) and relative humidity (RH) data of the cavities. To account for the most humid periods, the RH-curve's vertical offset D was eventually shifted by +5 offset. A thorough methodology and uncertainty assessment of the sinusoid-fitting is available in the referenced master thesis, see Data Availability Statement. The resulting parameters of the four fitted sinusoids that are representing the cavity microclimate in the simulation are presented below in Table 3.

Table 3. Sinusoid-fitted model parameters for WUFIs indoor climate option "Sine Curve".

Cavity Model	WUFI Parameter "Sine Curve"	Sensor SW1	Sensor MN5
Temperature T (Best-fit)	Mean	9.89	7.6
	Amplitude	7.2	10.43
	Date of max	28th of July	20th of July
	R^2	0.6751	0.7058
Relative Humidity RH* (Offset shifted +5)	Mean*	83.77	75.05
	Amplitude	9.2	12.54
	Date of max	31st of Dec	16th of Dec
	R^2	0.1859	0.3907

*The shift of +5 offset only affects the "mean" which resembles the parameter D of the sinusoid-fit

Most parameters are set as constants throughout the simulations, others are varied to understand how different parameters and combinations might influence the moisture and mould contitions. The parameters and variations are presented in Table 4 while the combinations are presented in the results section Table 8 and Table 9

The modelled component consists of the coating and the wooden cladding material. The cladding is 22 mm Scandinavian spruce with density 390 kg/m³. Initial attempts of inserting the coating merely as an s_d-value did not successfully include the liquid transport properties. The coating was therefore modeled as a separate material layer, utilizing the liquid transport properties of a waterborne acrylic coating found in the built-in WUFI material database [53]. Personal measurements of vapour resistance s_d were adjusted to thickness 1 mm due to converted to vapour resistance factor μ and included, together with respective bulk density (see Table 1), in the modelled component layer. Note that the coatings needed to be inserted with thickness 1 mm, due to numerical convergence reasons, and that the μ are adjusted accordingly.

The interior surface heat resistance R_{si} on the inside of the cladding has been varied between the WUFIs standard exterior value R_{se} of 0.0588 (m²K)/W and standard interior value of 0.125 (m²K)/W due to unknown cavity ventilation. However, a realistic value for

the ventilated façade considered in this study is expected to lie within this range, though possibly closer to 0.125 (m²K)/W (which is also anticipated to yield more conservatively).

Table 4. Input parameters and variations for WUFI Pro simulations.

Parameters	Setting	Variation(s)
Monitor position	Interior side of cladding	
Cladding material	Scandinavian spruce transversal direction II	
	Wall inclination	90°
Initial wood moisture content	20 wt%	15 wt%
Coating's vapour resistance s_d	2.25 m (max$_{B2}$*)	0.453 m (min$_B$*); 1.35 m (max$_B$*); 0.69m (min$_{B2}$*); Untreated
Exterior surface heat resistance R_{se}	0.0588 (m²K)/W	
Interior surface heat resistance R_{si}	0.125 (m²K)/W	0.0588 (m²K)/W
Short wave radiation absorptivity	0.4 (White hue)	
Ground short wave reflectivity	0.2	
	Adhering fraction of rain	0.7
Simulation start	October (Beginning of wetting season)	April
Simulation duration	Five years	

*B and B2 signifies number of layers

2.2.2. WUFI® Mould Index VTT

The simulated T and RH conditions on the interior side of the cladding were evaluated for mould growth risk using the additional plugin WUFI® Mould Index VTT originally developed by Viitanen et al. [54]. The VTT Model is thoroughly described by several studies, e.g. Ojanen et al. [55] and Vereecken and Roels [56]. In short, it generates a mould growth index ranging from 0 to 6. The model considers factors such as humidity and temperature, exposure time, decline during unfavourable conditions, and material qualities. Risk levels are indicated using a traffic light interpretation: green for acceptable risk, yellow for further evaluation needed, and red for unacceptable risk requiring action. However, thresholds of the mould risk vary by structure and so-called "occupant exposure class". This study evaluates spruce material stationed outdoors and is not expected to impact the occupants directly. Thus, the risk level thresholds of this current study are limited to solely green (0 to 3) and yellow (index 3 to 6), never showing any level of unacceptable risk [54].

The parameters chosen for simulating the planed wooden cladding are shown in Table 5. Sensitivity class and decline coefficient regarding the evaluated spruce material are based on literature by the model developers [54,55,57], as well as affirmative studies [47,56,58] for a realistic yet conservative model set-up. For the untreated wood cases, the sensitivity class "very sensitive" and mould decline coefficient "Significant decline (1.0)" were set [57].

In total there are 64 different possible combinations of the parameter value choices in the VTT model; four values of class, two of surface, two of wood type and four values of C_{mat} [58]. The end-user's choices of input parameters can significantly impact the results [9,58]. A sensitivity analysis should be conducted to identify parameters affecting mould growth risk, though, this is outside the scope of the current study and should be explored in future research.

Table 5. Parameter settings in WUFI Mould Index VTT model.

Parameter	Chosen setting
Occupant exposition class	No impact on occupants expected
Material category	Wooden or natural materials
Material sub-category	Untreated pine or spruce (Heartwood)
Sensitivity Class	Sensitive
Decline Coeff. (C_{mat})	Almost no decline (0.1)
Type of Surface	Planed
Type of Wood	Softwood

3. Results

3.1. Laboratory Measurements

3.1.1. Range of water vapour resistance for exterior coatings

The measured dry film thicknesses and vapour resistances (s_d-values) of the wet cup experiments are presented in Table 6. Official laboratory reports for each tested series can be found in the Data Availability Statement. The measured range of s_d-values for B-series was from 0.453 (0.024) m for the most vapour permeable to 1.350 (0.083) m for the least vapour permeable. For B2-series, the range was 0.690 (0.022) m for the most vapour permeable to 2.250 (0.048) m for the least vapour permeable. The standard deviations of both s_d-values and dry film thicknesses are small, which suggests precision and consistency in measurement technique and instruments used.

Table 6. Measured s_d-values for the coatings and dry film thicknesses. Differentiated by number of layers. Standard deviation of the mean in brackets.

Coating	Binder	Three layers (B)		Six layers (B2)	
		Dry film thickness [mm]	s_d-value [m]	Dry film thickness [mm]	s_d-value [m]
51	Alkyd	0.34 (0.02)	1.350 (0.083)	0.56 (0.02)	2.250 (0.048)
52	Emulsion	0.28 (0.01)	0.836 (0.042)	0.48 (0.02)	1.280 (0.020)
53	Emulsion	0.26 (0.01)	0.669 (0.031)	0.52 (0.02)	1.090 (0.049)
53X	Emulsion	0.25 (0.01)	0.602 (0.026)	0.42 (0.02)	0.925 (0.047)
54	Acrylic	0.28 (0.01)	0.787 (0.037)	0.41 (0.02)	1.110 (0.058)
55	Acrylic	0.26 (0.01)	1.090 (0.027)	0.41 (0.02)	1.530 (0.065)
56	Emulsion	0.25 (0.01)	0.453 (0.024)	0.45 (0.01)	0.690 (0.022)
57	Acrylic	0.24 (0.01)	0.999 (0.051)	0.44 (0.03)	1.480 (0.063)
58	Acrylic	0.20 (0.01)	0.472 (0.024)	0.45 (0.02)	0.932 (0.019)
59	Acrylic	0.26 (0.01)	0.559 (0.006)	0.38 (0.01)	0.724 (0.023)

3.1.2 Correlation of Dry Film Thickness and Vapour Resistance

In Figure 6 the linear correlation between dry film thickness and s_d in for the nine coatings are shown. For each product, both series (B + B2) are displayed. The coefficients of determination R² are provided in Table 7. The high R² values it indicate that 81 to 98 % of the variance in the s_d-value can be explained by the dry film thickness, suggesting a strong linear relationship for all coatings. Higher dry film thickness generally resulting in a greater resistance against vapour diffusion.
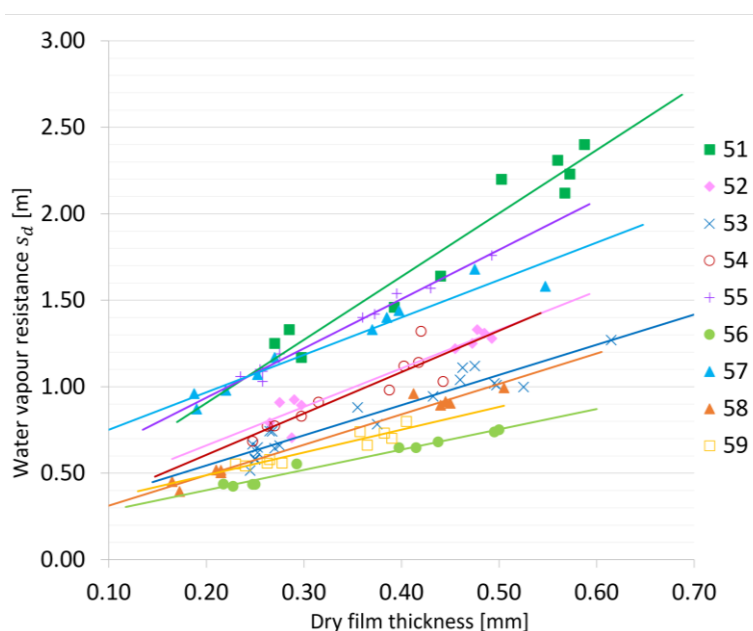
Figure 6. Correlation between dry film thickness and s_d. Both series (B + B2) of each product are displayed. No. 53 includes both 53 and 53X.

Table 7. Coefficients of determination for the tested coatings.

Coating	51	52	53+53X	54	55	56	57	58	59
R²	0.9345	0.9254	0.9113	0.8088	0.9827	0.977	0.934	0.9734	0.8926

3.1.3. Effect of Binder Type

The measured values in Table 6 suggests a relationship between the binder type and vapour resistance of the coatings, as depicted in Figure 7 below. The alkyd coating no. 51 exhibited higher vapour resistance compared to emulsions and acrylics; this is assessed further in the discussion.
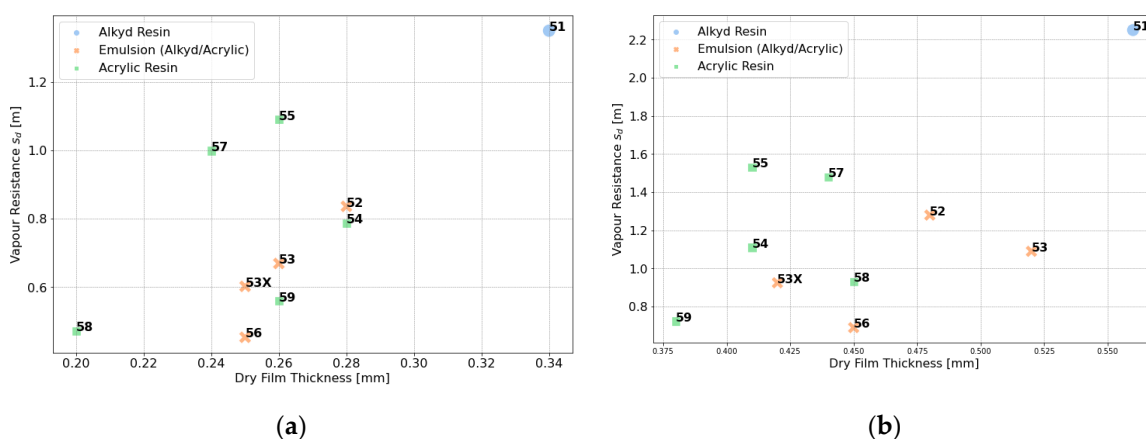
Figure 7. Correlation of binder type and s_d-value of (**a**) three layers, and (**b**) six layers of coating.

3.2. Simulated Moisture Contents and Mould Growth Risk

3.2.1. Parametric Study and Mould Growth Indices

The results present the combinations of moisture simulations in WUFI Pro along with the corresponding mould indices for each considered case. Table 8 and Table 9 display the results of Fjogstad-Hus and ZEB-Laboratory, respectively. The interior heat resistance was initially varied due to uncertainties regarding the cavity ventilation conditions. However, after further assessment, the value of 0.125 m²K/W was deemed more realistic for this study and confirmed also more conservative by the simulated yearly mould indices. Consequently, cases with an R_{si} of 0.0588 m²K/W have been set aside, as the ventilation of the claddings is not within the scope of this study.

In Table 8 all cases with R_{si} of 0.125 (m²K)/W exhibit yellow risk levels ranging from 3.28 to 3.30 for coated claddings, and 5.20 for the untreated cladding. Table 9 shows that with the same interior heat resistance, the mould index ranges from 0.11 to 0.15 for coated surfaces and 0.18 for the untreated case. For both case buildings, the simulation start as the wetting or drying season was insignificant, and the initial wood moisture content (MC) of 20 wt% versus 15 wt% had no significant effect on the mould index.

Table 8. Parametric study and resulting yearly mould growth indices of Fjogstad-Hus cases.

		Case													
Input Parameters		1	2	3	4	5	6	7	8	9	10	11	12	13	14
Outdoor Climate	Trondheim														
	Stavanger	x	x	x	x	x	x	x	x	x	x	x	x	x	x
Cavity Climate Model	MN5 (T₀, RH₊₅)														
	SW1 (T₀, RH₊₅)	x	x	x	x	x	x	x	x	x	x	x	x	x	x
Vapour Resistance s_d [m]	2.250 (max-B2)	x					x					x		x	x
	0.690 (min-B)		x					x							
	1.350 (max-B2)			x					x						
	0.453 (min-B)				x					x			x		
	Untreated					x					x				
Initial Wood MC [wt%]	20	x	x	x	x	x	x	x	x	x	x			x	x
	15											x	x		
Simulation Start	1st of October	x	x	x	x	x	x	x	x	x	x	x	x		
	1st of April													x	x
R_{si} [m²K/W]	0.125						x	x	x	x	x			x	
	0.0588	x	x	x	x	x						x	x		x
Yearly Mould Growth Index [-]		2.64	2.63	2.64	2.63	4.54	3.30	3.28	3.30	3.28	5.20	2.63	2.63	3.30	2.64

Table 9. Parametric study and resulting yearly mould growth indices of the ZEB-Laboratory cases.

Input Parameters		Case 15	16	17	18	19	20	21	22	23	24	25	26	27	28
Outdoor Climate	Trondheim	x	x	x	x	x	x	x	x	x	x	x	x	x	x
	Stavanger														
Cavity Climate Model	MN5 (T_0, RH_{+5})	x	x	x	x	x	x	x	x	x	x	x	x	x	x
	SW1 (T_0, RH_{+5})														
Vapour Resistance s_d [m]	2.250 (max-B2)*	x					x					x	x	x	x
	0.690 (min-B)		x					x							
	1.350 (max-B2)			x					x						
	0.453 (min-B)				x					x					
	Untreated					x					x				
Initial Wood MC [wt%]	20	x	x	x	x	x	x	x	x	x	x	x			x
	15												x	x	
Simulation Start	1st of October	x	x	x	x	x	x	x	x	x	x		x	x	
	1st of April											x			x
R_{si} [m²K/W]	0.125						x	x	x	x	x			x	x
	0.0588	x	x	x	x	x						x	x		
Yearly Mould Growth Index [-]		0.06	0.06	0.05	0.06	0.10	0.15	0.15	0.11	0.15	0.18	0.05	0.05	0.15	0.15

The development of the yearly mould growth indices when comparing the most and least vapour permeable-coated wood, as well as untreated wood, are shown in Figure 8. There are noticeable seasonal fluctuations in the mould growth index, with peaks corresponding to the winter months when moisture levels are higher. During the summer months, the indices tends to decrease for all cases in both locations. Fjogstad-Hus shows an increasing annual risk of mould growth for the coated claddings.

(**a**)

(**b**)
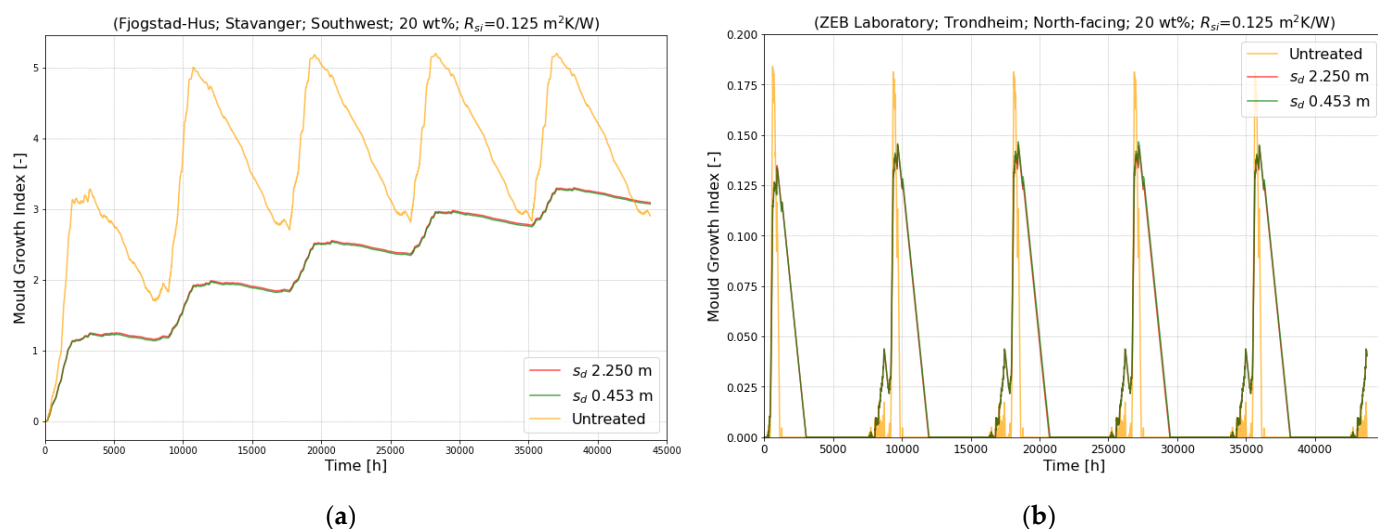
Figure 8. The effect of the coating's vapour resistance on the development of mould growth index of (**a**) Fjogstad-Hus, Stavanger, and (**b**) ZEB-Laboratory. The extremal s_d-values of 2.25 m and 0.453 m, and displayed together with untreated. Note the difference scale of the the y-axis.

3.2.2. Wood Moisture Conditions 387

The simulated wood MC for both locations over five-year and one-year periods are 388
shown below. The effects of maximum and minimum vapour resistance s_d of the lab 389
measurements are compared in Figure 9, while the other s_d-values as suspected will yield 390
within this MC range. The other parameters that were varied have remain constant. 391
Observes fluctuating trends in the course of the MC for all three cases. The peaks in the 392
winter and the lowest MC during summer. Despite the initial wood MC 20 wt%, the MCs 393
for the coated claddings stabilize around the intervals 10 to 20 wt% and 10 to 19 wt% (for 394
Fjogstad-Hus and ZEB-Laboratory, respectively). 395
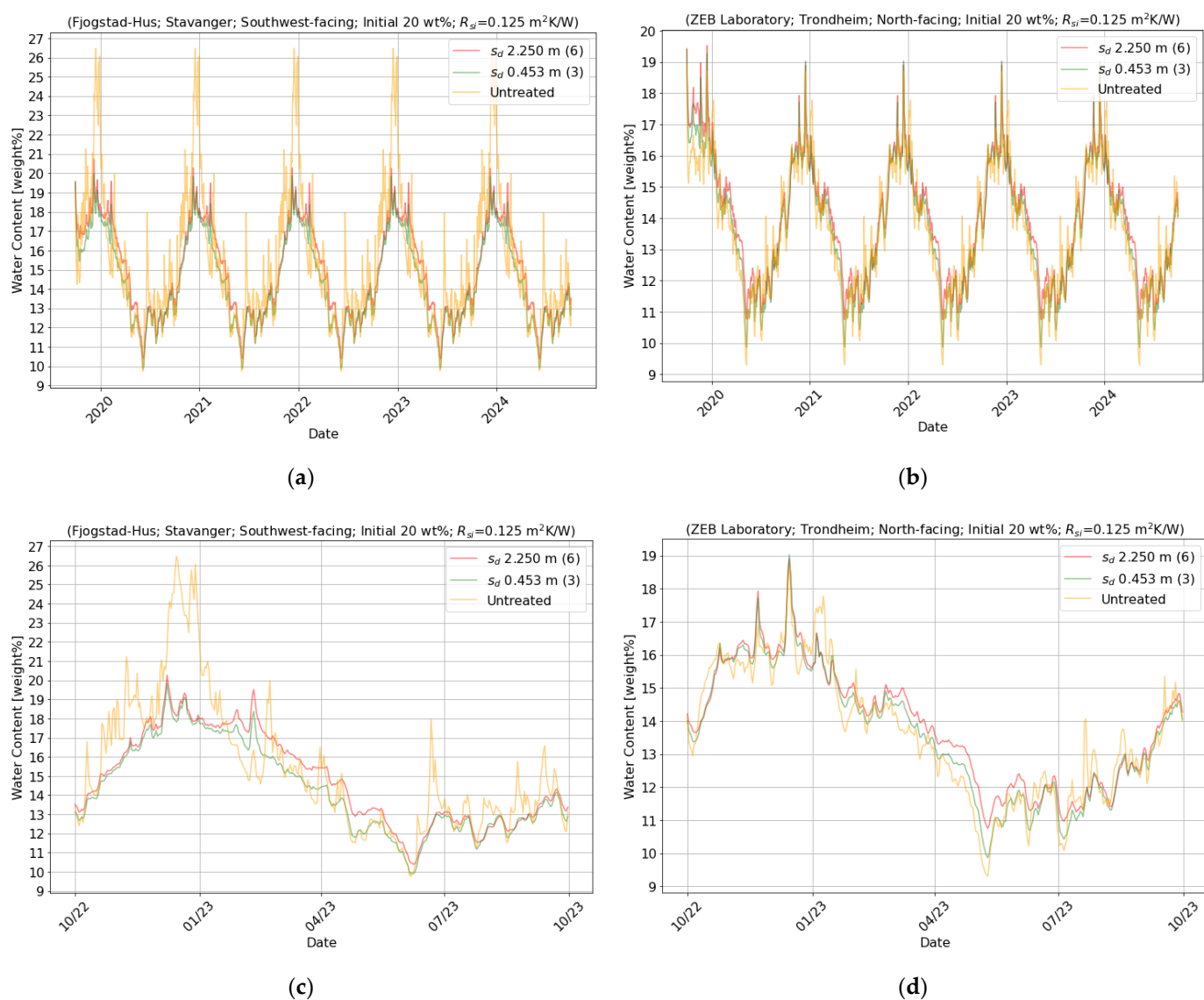
Figure 9. The effect of the coating's s_d-value (absolute max and min) on the moisture conditions of 396
the cladding. "(6)" and "(3)" in the data labels signifies six and three layers of coating, respectively. 397
(**a**) Five-year period of Fjogstad-Hus, (**b**) five-year period of ZEB-Laboratory, (**c**) one-year period of 398
Fjogstad-Hus, (**d**) one-year period of ZEB-Laboratory. 399

4. Discussion 400

4.1. Laboratory Measurements 401

The range of s_d-value was found to be 0.453 m to 1.350 m (three layers) and 0.690 m 402
to 2.250 m (six layers). Regardless of the number of layers, coating no. 51 exhibited the 403

highest vapour resistance, and no. 56 showed the lowest resistance among all the products. Some measured s_d-values are higher than identified in previously reported values [23,39,40]. The low standard deviations in both s_d-values and in dry film thicknesses across all coatings indicate consistency and precision in the measurements. This consistency enhances the reliability of the results and the miportance of accurate application methods for achieveing a predictable vapour resistance in a coating.

The high R² (ranging from 0.8088 to 0.9770) suggest that 81 to 98% of the variability in the s_d-value can be explained by the dry film thickness, and that the relationship between these two variables is strong and consistent across different samples. The strongest linear relationship was observed for coatings no. 55 and 56 (R² 0.9827 and 0.9770, respectively), while no. 54 had the weakest, yet still significant, linear relationship (R² 0.8088), possibly due to variability in the application process or thickness measurements.

The additional film support of the cup assembly (metal grid or plastic cylinder) listed in Table 1 indicates a trend that coatings with a metal grid support (no. 51, 52 and 55) have higher s_d-values suggesting a greater vapour resistance. Coatings with plastic cylinder support and those without support generally show lower s_d-values. This trend suggest that assembling with an additional support may influence measured vapour resistance, and introduces uncertainty into the results.

The most vapour-resistant coating was no. 51, an alkyd resin coating. Alkyds being more vapour resistant than acrylics and emulsions confirms the work of Geving et al. [23] and Nore and Hundhausen [40]. However, neither the acrylics nor emulsions showed any clear trends of the binder type and s_d-value. The variability might bedue to differences in either formulation or film thickness, or simply by other factors than binder content. And with no. 51 being the only tested alkyd, this study cannot with certainty determine any such relationship of binder type. Its high vapour resistancy may be related to other factors i.e. the higher bulk density, or the additional metal grid support.

4.2. Moisture Content and Mould Growth Risk in Ventilated Wooden Claddings.

Over the simulation period, one observes that the wood MC fluctuates with seasonable variations as anticipated, with the highest MC in the winter. During fall and winter, the MC increases, but desiccates over the summer months, without signs of moisture accumulation over the simulated five-year period. This suggests that the vapour resistance of the coating does not significantly impede the drying of moisture.

During the drying period, however, Figure 9c and Figure 9d indicate a slightly faster drying for the vapour-permeable coating, as indicated by the green line having a more rapid decline in MC compared to the red line during this specific period. Untreated claddings (yellow) show both the fastest drying and wetting, as well as more variablity and occasional spikes, indicating that they retain more moisture compared to treated wood-cases. The amplitude of the MC fluctuations is notably greater for untreated cladding compared to coated cladding, in line with findings from several studies [14,23,40] regarding the positive effects of surface treatment of wood.

The variations of initial wood MC of 20- and 15 wt% yield similar MC projections and mould indices for both Fjogstad-Hus and ZEB-Laboratory. This is probably due to the thinness of the cladding which facilitates fast moisture drying regardless of factors i.e. the vapour resistance of the coating. Similarly, simulation start in April versus in October does not affect the results. This confirms the effect of the thin cladding's ability to quickly dry towards the air cavity, with the cladding being uncoated on this interior side.

The seasonal fluctuations in the mould growth risk mirrors the fluctuations of the wood MC, the with a peak in the winter, and a declining risk in during the drying period (Figure 8). The two different vapour resistances of the coatings yield similar mould risk developments, which underscores that either the difference in s_d is too small or the value itself is insignificant. It is observed for Fjogstad-Hus that the coated claddings have an slightly annual increase in mould risk, indicating that the moisture exposure and

conditions of this wall over time does not fully dry out, causing favourable conditions for mould growth. Which confirms the analysis of Ingebretsetsen et al. [48].

The notably higher mould growth indices and MC levels of Fjogstad-Hus compared to ZEB-Laboratory supports the previous findings of Ingebretsen [47,48], and were expected due to the drying conditions being the worse (i.e. orientation and climate conditions in Stavanger climate). While north-facing orientations usually are considered worst-case for winter drying due to lack of direct solar radiation, the southwest façade of Fjogstad-Hus is more exposed to driving rain.

Both Fjogstad-Hus and ZEB-Laboratory show higher risk of mould growth of untreated claddings compared to coated claddings. This is because the exterior surface coating, after all, protects against liquid moisture absorption in the cladding. These results confirms the importance of applying coating to façade cladding to protect against biodeteoriation thereby achieving longer lifespans.

5. Conclusions

The laboratory experiments revealed that the water vapour resistance (in terms of s_d-value) for three layers ranged from 0.453 m to 1.350 m, and from 0.690 m to 2.250 m for six layers. There is a strong linear relationships between s_d-value and dry film thickness. The alkyd exhibited higher s_d-vlaues than emulsions and acrylics, though the sample size is not sufficient to determine this relationship..

Over the five-year simulation, the wood MC fluctuates seasonally. The vapour-resistant coating showed a slightly slower drying than the more vapour-permeable one. However, their different impact on MC is insignificant over the five-year period as no moisture is accumulating. Untreated claddings showcased both greater MC fluctuations with more variability and higher mould risk than for the two coated claddings, which affirms the importance of surface coating. The cases of Fjogstad-Hus exhibited greater wood MC levels and greater mould risks than the cases of ZEB-Laboratory, due to the more extreme climatic conditions.

Future studies should aim to isolate and quantify the impact of additional film supports by conducting controlled experiments where coatings are tested systematically with and without various supports, to help understand the extent of their influence on the water vapour permeability and resistance measurements. To establish a more definitive correlation between binder type and vapour resistance, more targeted experiments with a larger number of samples and various types of coatings are necessary, as the current findings only provide an indication of this relationship.

Author Contributions: Conceptualization, K.B.R. and T.K.; methodology, K.B.R. and T.K.; validation, K.B.R. and T.K.; formal analysis, K.B.R.; investigation, K.B.R.; writing—original draft preparation, K.B.R.; writing—review and editing, K.B.R. and T.K.; visualization, K.B.R.; supervision, T.K. All authors have read and agreed to the published version of the manuscript.

References

1. Barrelas, J.; Ren, Q.; Pereira, C. Implications of Climate Change in the Implementation of Maintenance Planning and Use of Building Inspection Systems. *J. Build. Eng.* **2021**, *40*, 102777, doi:10.1016/j.jobe.2021.102777.

2. Weather and Climate Extreme Events in a Changing Climate. In *Climate Change 2021 – The Physical Science Basis: Working Group I Contribution to the Sixth Assessment Report of the Intergovernmental Panel on Climate Change*; Intergovernmental Panel on Climate Change (IPCC), Ed.; Cambridge University Press: Cambridge, 2023; pp. 1513–1766 ISBN 978-1-00-915788-9.

3. Almås, A.-J.; Lisø, K.R.; Hygen, H.O.; Øyen, C.F.; Thue, J.V. An Approach to Impact Assessments of Buildings in a Changing Climate. *Build. Res. Inf.* **2011**, *39*, 227–238, doi:10.1080/09613218.2011.562025.

4. Hanssen-Bauer, I.; Førland, E.; Haddeland, I.; Hisdal, H.; Lawrence, D.; Mayer, S.; Nesje, A.; Nilsen, J.E.; Sandven, S.; Sandø, A.; et al. *Climate in Norway 2100*; 2017;

5. Edvardsen, K.I.; Ramstad, T.Ø. *Trehus Håndbok 5*; SINTEF akademisk forlag: Oslo, Norway, 2014; ISBN 978-82-536-1391-8.

6. Oliver, C.D.; Nassar, N.T.; Lippke, B.R.; McCarter, J.B. Carbon, Fossil Fuel, and Biodiversity Mitigation With Wood and Forests. *J. Sustain. For.* **2014**, *33*, 248–275, doi:10.1080/10549811.2013.839386.

7. Lisø, K.R.; Hygen, H.O.; Kvande, T.; Thue, J.T. Decay Potential in Wood Structures Using Climate Data. *Build. Res. Inf.* **2006**, *34*, 546–551, doi:10.1080/09613210600736248.

8. Viitanen, H. Factors Affecting the Development of Biodeterioration in Wooden Constructions. *Mater. Struct.* **1994**, *27*, 483–493, doi:10.1007/BF02473453.

9. Lie, S.K.; Vestøl, G.I.; Høibø, O.; Gobakken, L.R. Surface Mould Growth on Wooden Claddings – Effects of Transient Wetting, Relative Humidity, Temperature and Material Properties. *Wood Mater. Sci. Eng.* **2019**, *14*, 129–141, doi:10.1080/17480272.2018.1424239.

10. Holme, J. Mould Growth in Buildings.

11. Gradeci, K.; Labonnote, N.; Time, B.; Köhler, J. Mould Growth Criteria and Design Avoidance Approaches in Wood-Based Materials – A Systematic Review. *Constr. Build. Mater.* **2017**, *150*, 77–88, doi:10.1016/j.conbuildmat.2017.05.204.

12. Viitanen, H. The Critical Conditions Causing Mould and Decay Problems in Buildings.; 1996.

13. Thue, J.V. *Bygningsfysikk grunnlag*; 1st ed.; Fagbokforlaget: Bergen, Norway, 2016; ISBN 978-82-450-1994-0.

14. Nore, K. Hygrothermal Performance of Ventilated Wooden Cladding. Doctoral thesis, NTNU, 2010.

15. Lisø, K.R.; Kvande, T.; Thue, J.V. Learning from Experience – an Analysis of Process Induced Building Defects in Norway. In *Research in Building Physics and Building Engineering*; CRC Press, 2006 ISBN 978-1-00-306082-6.

16. Ingebretsen, S.B.; Andenæs, E.; Kvande, T. Microclimate of Air Cavities in Ventilated Roof and Façade Systems in Nordic Climates. *Buildings* **2022**, *12*, 683, doi:10.3390/buildings12050683.

17. Svendsen, S. Principles of One-Stage and Two-Stage Seals. In Proceedings of the Proceedings of the International CIB Symposium; Oslo, Norway, 1967; pp. 25–28.

18. Kvande, T. *Byggforskserien 542.003 Totrinnstetning mot slagregn på fasader. Luftede kledninger og fuger.*; SINTEF Byggforsk: Oslo, Norway, 2013;

19. Larsen, K.E. *Byggforskserien 542.645 Kledninger av ubehandlet tre.*; SINTEF Byggforsk: Oslo, Norway, 2008;

20. Plesser, T. *Byggforskserien 542.640 Overflatebehandling av utvendig trevirke.*; SINTEF Byggforsk: Oslo, Norway, 2009;

21. Flæte, P.O.; Alfredsen, G. *Gran som ubehandlet utvendig kledning.*; Norsk Institutt for Skogforskning: Ås, Norway, 2004;

22. Ahola, P. Moisture Transport in Wood Coated with Joinery Paints. *Holz Als Roh- Werkst. Eur. J. Wood Wood Ind.* **1991**, *49*, 428–432, doi:10.1007/BF02619465.

23. Geving, S.; Erichsen, T.H.; Nore, K.; Time, B. *Hygrothermal Conditions in Wooden Claddings*; Norwegian Building Research Institute: Oslo, Norway, 2006; ISBN 82-536-0931-0.

24. Ekstedt, J. Studies on the Barrier Properties of Exterior Wood Coatings. Doctoral Thesis, KTH- Royal Institute of Technology: Stockholm, Sweden, 2002.

25. Copak, A.; Jirouš-Rajković, V.; Živković, V.; Miklečić, J. Water Vapour Transmission Properties of Uncoated and Coated Wood-Based Panels. *Wood Mater. Sci. Eng.* **2023**, *18*, 1086–1093, doi:10.1080/17480272.2022.2106582.

26. de Meijer, M. Review on the Durability of Exterior Wood Coatings with Reduced VOC-Content. *Prog. Org. Coat.* **2001**, *43*, 217–225, doi:10.1016/S0300-9440(01)00170-9.

27. Topçuoğlu, O.; Altinkaya, S.A.; Balköse, D. Characterization of Waterborne Acrylic Based Paint Films and Measurement of Their Water Vapor Permeabilities. *Prog. Org. Coat.* **2006**, *56*, 269–278, doi:10.1016/j.porgcoat.2006.02.003.

28. Altinkaya, S.A.; Topcuoglu, O.; Yurekli, Y.; Balkose, D. The Influence of Binder Content on the Water Transport Properties of Waterborne Acrylic Paints. *Prog. Org. Coat.* **2010**, *69*, 417–425, doi:10.1016/j.porgcoat.2010.08.005.

29. NS-EN ISO 12572:2016 *Hygrothermal Performance of Building Materials and Products - Determination of Water Vapour Transmission Properties - Cup Method (ISO 12572:2016)*; Standard Norge: Oslo, Norway, 2016;

30. Grüll, G.; Truskaller, M. Moisture Protection of Wood Coatings and Its Sensitivity to Mechanical Defects Depending on Surface Hydrophobicity and Solid Content. *Int. Wood Prod. J.* **2014**, *5*, 74–82, doi:10.1179/2042645313Y.0000000048.

31. Hýsek, Š.; Fidan, H.; Pánek, M.; Böhm, M.; Trgala, K. Water Permeability of Exterior Wood Coatings: Waterborne Acrylate Dispersions for Windows. *J. Green Build.* **2018**, *13*, 1–16, doi:10.3992/1943-4618.13.3.1.

32. Hu, Y.; Topolkaraev, V.; Hiltner, A.; Baer, E. Measurement of Water Vapor Transmission Rate in Highly Permeable Films. *J. Appl. Polym. Sci.* **2001**, *81*, 1624–1633, doi:10.1002/app.1593.

33. Brito, V.; Diaz Gonçalves, T.; Faria, P. Coatings Applied on Damp Building Substrates: Performance and Influence on Moisture Transport. *J Coat. Tech Res* **2011**, *8*, 513–525, doi:10.1007/s11998-010-9319-5.

34. NS-EN ISO 4618:2023 *Paints and Varnishes - Vocabulary (ISO 4618:2023)*; Standard Norge: Oslo, Norway, 2023;

35. Gezici-Koç, Ö.; Erich, S.J.F.; Huinink, H.P.; van der Ven, L.G.J.; Adan, O.C.G. Understanding the Influence of Wood as a Substrate on the Permeability of Coatings by NMR Imaging and Wet-Cup. *Prog. Org. Coat.* **2018**, *114*, 135–144, doi:10.1016/j.porgcoat.2017.10.013.

36. Kothapalli, R.V.; Yaseen, M. A CRITICAL ANALYSIS OF VARIOUS METHODS FOR   PREPARATION OF FREE FILMS OF ORGANIC COATINGS. *Prog. Org. Coat.* **1982**.

37. Topçuoğlu, O.; Altinkaya, S.A.; Balköse, D. Characterization of Waterborne Acrylic Based Paint Films and Measurement of Their Water Vapor Permeabilities. *Prog. Org. Coat.* **2006**, *56*, 269–278, doi:10.1016/j.porgcoat.2006.02.003.

38. NS-EN ISO 10456:2007+NA:2010 *Building materials and products - Hygrothermal properties - Tabulated design values and procedures for determining declared and design thermal values (ISO 10456:2007)*; Standard Norge: Oslo, Norway, 2010;

39. Geving, S.; Thue, J.V. *Fukt i Bygninger*; Håndbok; Norges byggforskningsinstitutt, 2002; ISBN 82-536-0747-4.

40. Nore, K.; Hundhausen, U. Hygrothermal Performance of Ventilated Wooden Cladding.; May 17 2016.

41. Šadauskiene, J.; Monstvilas, E.; Stankevičius, V. The Impact of Exterior Finish Vapour Resistance on the Moisture State of Building Walls. *Technol. Econ. Dev. Econ.* **2007**, *13*, 73–82, doi:10.3846/13928619.2007.9637779.

42. Tomren, J.H.; Andenæs, E.; Geving, S.; Kvande, T. Water Vapour Resistance of Ceiling Paints - Implications for the Use of Smart Vapour Barriers in Compact Wooden Roofs. **2023**, doi:https://doi.org/10.3390/buildings13092185.

43. NS-EN ISO 7783:2018 *Paints and Varnishes - Determination of Water-Vapour Transmission Properties - Cup Method (ISO 7783:2018)*; Standard Norge: Oslo, Norway, 2018;

44. NS-EN 927-10:2019 *Paints and Varnishes - Coating Materials and Coating Systems for Exterior Wood - Part 10: Resistance to Blocking of Paints and Varnishes on Wood*; Standard Norge: Oslo, Norway, 2019;

45. Geving, S. *Praktisk Bygningsfysikk*; 1.utgave.; Fagbokforlaget: Bergen, Norway, 2021; ISBN 978-82-450-2801-0.

46. Fraunhofer Institute for Building Physics WUFI® Pro | WUFI (En).

47. Ingebretsen, S.B. Mikroklima i luftespalter i luftede fasader og skråtak. Master thesis, NTNU, 2022.

48. Ingebretsen, S.B.; Andenæs, E.; Gullbrekken, L.; Kvande, T. Microclimate and Mould Growth Potential of Air Cavities in Ventilated Wooden Façade and Roof Systems—Case Studies from Norway. *Buildings* **2022**, *12*, 1739, doi:10.3390/buildings12101739.

49. Panico, S.; Larcher, M.; Herrera Avellanosa, D.; Baglivo, C.; Troi, A.; Maria Congedo, P. Hygrothermal Simulation Challenges: Assessing Boundary Condition Choices in Retrofitting Historic European Buildings. *Energy Build.* **2023**, *297*, 113464, doi:10.1016/j.enbuild.2023.113464.

50. Betti, G.; Tartarini, F.; Nguyen, C.; Schiavon, S. CBE Clima Tool: A Free and Open-Source Web Application for Climate Analysis Tailored to Sustainable Building Design. *Build. Simul.* **2024**, *17*, 493–508, doi:10.1007/s12273-023-1090-5.

51. Fraunhofer IBP Creating Weather Files Available online: https://wufi.de/en/service/downloads/creating-weather-files/ (accessed on 21 March 2024).

52. Bloomfield, P. Fitting Sinusoids. In *Fourier Analysis of Time Series*; Wiley Series in Probability and Statistics; John Wiley & Sons, Ltd: Raleigh, North Carolina, 2000; pp. 9–24 ISBN 978-0-471-72223-6.

53. Fraunhofer Institute for Building Physics WUFI® Pro.

54. Hukka, A.; Viitanen, H.A. A Mathematical Model of Mould Growth on Wooden Material. *Wood Sci. Technol.* **1999**, *33*, 475–485, doi:10.1007/s002260050131.

55. Ojanen, T.; Viitanen, H.; Peuhkuri, R.; Lähdesmäki, K.; Vinha, J.; Salminen, K. Mold Growth Modeling of Building Structures Using Sensitivity Classes of Materials. **2010**.

56. Vereecken, E.; Roels, S. Review of Mould Prediction Models and Their Influence on Mould Risk Evaluation. *Build. Environ.* **2012**, *51*, 296–310, doi:10.1016/j.buildenv.2011.11.003.

57. Viitanen, H.; Krus, M.; Ojanen, T.; Eitner, V.; Zirkelbach, D. Mold Risk Classification Based on Comparative Evaluation of Two Established Growth Models. *Energy Procedia* **2015**, *78*, 1425–1430, doi:10.1016/j.egypro.2015.11.165.

58. Johansson, P.; Lång, L.; Capener, C.-M. How Well Do Mould Models Predict Mould Growth in Buildings, Considering the End-User Perspective? *J. Build. Eng.* **2021**, *40*, 102301, doi:10.1016/j.jobe.2021.102301.

B Literature Search Matrix

This appendix contains the search matrix of the literature review.

Table B.1: Literature Search Matrix

Type of study	Author	Year	Title	Method	Short description + main finding	Reported property	Type of substrate
Journal Article	Brito et al.	(2011)	Coatings applied on damp building substrates: Performance and influence on moisture transport	Water vapour permeability tests and evaporative drying tests.	Correlation between «Drying Index" and sd for dry substrates. The impact paint has on the drying of the substrate vary significantly depending on the moisture content of the substrate.	sd = 2.24 (0.47) m (emulsion)	Damp mortar substrate
Journal Article	Topçuoğlu, et al.	(2006)	Characterization of waterborne acrylic based paint films and measurement of their water vapour permeabilities	Permeation cell for measuring water vapour permeability	The moisture barrier properties of acrylic coatings decrease with decreasing binder content		
Journal Article	Šadauskiene et al.	(2008)	Linear-Regression-Equation-Based Prognosis of the Dependence of the Thickness of the Air Layer Equivalent to the Coating's Water Vapour Permeability	Linear regression equation that can be used to predict the sd value	Determined the correlation between the number of the coating layers and water vapour resistance The major inadequacy of the s d value is determined for the acrylic paint.	mean sd = 0.639 m (acrylic)	NA
Journal Article	Grüll and Truskaller	(2014)	Moisture protection of wood coatings and its sensitivity to mechanical defects depending on surface hydrophobicity and solid content	Wet cup method for sd value, Liquid water uptake measurements	Film forming coating systems had significantly lower water permeability than the non-film forming. A strong correlation between liquid- and water vapour permeability.	sd between 0.02-0.25 m	Wood
Journal Article	Ahola	(1991)	Moisture transport in wood coated with joinery paints	Immersion of wood in water, absorption-desorption method	Moisture uptake is affected by wooden substrate, where coated spruce panels absorbed less water than coated pine panels. Most of the paints were very impermeable.	Water vapour flux [kg/m2s]	Wood
Journal Article	de Meijer	(2001)	Review on the durability of exterior wood coatings with reduced VOC-content	Outdoor weathering studies	Durability of a coating under outdoor weathering is determined by photochemical degradation, and vapour transmission in relation to the wood's moisture content		Wood
Journal Article	Šadauskiene et al.	(2007)	The impact of exterior finish vapour resistance on the moisture state of building walls	Calculations, laboratory experiments	sd indicate that as the number of paint coatings or the thickness of each coating increases, the sd value of the paint coatings also increase. The extent of the increase in sd depends on the type of paint and the binder used.	sd < 0.6 m to allow proper drying	Render substrate
Journal Article	Altinkaya	(2010)	The influence of binder content on the water transport properties of waterborne acrylic paints	Gravimetric sorption method	The binder content in the waterborne acrylic paint films significantly affects water transport.	Diffusion coefficient D [cm2/s]	
Journal Article	Goossens et al.	(2004)	The measurement of the moisture transfer properties of paint films using the cup method	Cup method	The diffusion coefficient depends strongly on the RH.	Diffusion coefficient D [cm2/s]	No substrate
Journal Article	Tomren et al.	(2023)	Water Vapour Resistance of Ceiling Paints—Implications for the Use of Smart Vapour Barriers in Compact Wooden Roofs	Wet cup method	Paint can affect the drying rate somewhat, but it does not lead to a significantly higher risk of mould growth. sd did not linearly increase with the number of layers.	sd = 0.1 to 0.5 m	Gypsum

Project report	Geving et al.	(2006)	Hygrothermal conditions in wooden claddings – Test house measurements	Wet cup method. Note that sd-value is not the main focus of this study	Regarding untreated claddings we found that the risk for decay and microbiological growth was generally higher for these cladding types compared to painted claddings.	sd 2.5 m (oil-dilutable), 1.3 m (waterborne acrylic/alkyd)	Spruce panels
Journal Article	Ruus et al.	(2011)	Water vapour transmission properties of natural paints	ISO 7783-1:2001 the dish method (now: wet cup method)	Linseed oil paint transmits up to 2.5 times more vapour than alkyd, enhancing building moisture management, and casein paint allows effective moisture regulation.	Water vapour transmission rate g	Mortar and plaster
Journal Article	Hýsek et al.	(2018)	Water permeability of exterior wood coatings: Waterborne acrylate dispersions for windows	Absorption-desorption method	The results clearly revealed that liquid water and water vapour uptake were affected by coating film thickness, number of coats, and coating composition. The values for water vapour absorption were much higher than for free water absorption.	Absorption and desorption [g/m2]	Spruce panels
Conference Paper	Nore and Hundhausen	(2016)	Hygrothermal performance of ventilated wooden cladding	Note: sd-value not focus of this study	No significant conclusion could be drawn of the surface treatment (acryl vs. alkyd) influence on hygrothermal performance	sd 2.8 (0.23) m (alkyd), 1.6 (0.15) m (acrylic)	Spruce panels
Journal Article	Gezici-Koc et al.	(2018)	Understanding the influence of wood as a substrate on the permeability of coatings by NMR imaging and wet-cup	NMR imaging, wet cup method	For all combinations of wood and coating the water transport was limited by the coating. The interaction between wood and coating had no effect on water vapour permeability.		NA
Book	Geving and Thue	(2002)	Fukt i bygninger	Tabulated values for sd		sd 0.049 m to 0.49 m for alkyds with two layers	NA
Standard	NS-EN ISO 10456:2007	(2007)	NS-EN ISO 10456:2007	Tabulated values for sd		sd 0.1 m (emulsion), 3 m (glossy)	NA

C.   Dry Film Thickness Calculations

The appendix shows measurements for thicknesses of the specimens. For each of the five specimens in each coating series, four randomly placed thickness measurements were done. The mean thickness reported in the thesis and in the article is the mean of these five means. The reported standard deviation is the "standard error of the mean" (SME).

Semester: Fall 23 — 53B — Date:

	Measured thicknesses [mm]				Mean
Test 1	0.27	0.25	0.3	0.24	**0.27**
Test 2	0.26	0.23	0.33	0.25	**0.27**
Test 3	0.27	0.22	0.27	0.25	**0.25**
Test 4	0.21	0.22	0.33	0.34	**0.28**
Test 5	0.3	0.24	0.25	0.21	**0.25**
Test 6 (ekstra)					-
			Overall mean (test 1 to 5)		0.26
			Std.dev of the mean		0.01

Semester: Fall 23 — 53B2 — Date:

	Measured thicknesses [mm]				Mean
Test 1	0.43	0.42	0.53	0.47	**0.46**
Test 2	0.44	0.42	0.54	0.50	**0.48**
Test 3	0.50	0.48	0.51	0.61	**0.53**
Test 4	0.49	0.44	0.52	0.54	**0.50**
Test 5	0.69	0.71	0.49	0.57	**0.62**
Test 6 (ekstra)					-
			Overall mean (test 1 to 5)		0.52
			Std.dev of the mean		0.02

Semester: Spring 24 — 51B — Date: 10.jan

	Measured thicknesses [mm]				Mean
Test 6 (1)	0.5	0.48	0.33	0.45	**0.44**
Test 2	0.28	0.3	0.22	0.28	**0.27**
Test 3	0.3	0.28	0.3	0.31	**0.30**
Test 4	0.32	0.28	0.32	0.22	**0.29**
Test 5	0.42	0.36	0.47	0.32	**0.39**
Test 1 (ekstr)	0.34	0.35	0.4	0.35	0.36
			Overall mean (test 1 to 5)		0.34
			Std.dev of the mean		0.02

Semester: Spring 24 — 51B2 — Date: 10.jan

	Measured thicknesses [mm]				Mean
Test 1	0.55	0.48	0.63	0.58	**0.56**
Test 2	0.65	0.6	0.49	0.53	**0.57**
Test 3	0.59	0.49	0.6	0.67	**0.59**
Test 4	0.75	0.38	0.68	0.48	**0.57**
Test 5	0.54	0.48	0.59	0.4	**0.50**
Test 6	0.47	0.47	0.51	0.4	0.46
			Overall mean (test 1 to 5)		0.56
			Std.dev of the mean		0.02

Semester: Spring 24 — 52B — Date: 11.jan

	Measured thicknesses [mm]				Mean
Test 1	0.25	0.31	0.26	0.33	**0.29**
Test 2	0.3	0.31	0.22	0.27	**0.28**
Test 3	0.22	0.27	0.33	0.37	**0.30**
Test 4	0.22	0.34	0.27	0.23	**0.27**
Test 5	0.31	0.22	0.25	0.38	**0.29**
Test 6	0.38	0.44	0.25	0.4	0.37
			Overall mean (test 1 to 5)		0.28
			Std.dev of the mean		0.01

Semester: Spring 24 — 52B2 — Date: 11.jan

	Measured thicknesses [mm]				Mean
Test 1	0.47	0.4	0.44	0.51	**0.46**
Test 2	0.44	0.46	0.63	0.41	**0.49**
Test 3	0.57	0.39	0.45	0.5	**0.48**
Test 4	0.39	0.48	0.57	0.45	**0.47**
Test 5	0.37	0.49	0.62	0.49	**0.49**
Test 6	0.4	0.41	0.46	0.49	0.44
			Overall mean (test 1 to 5)		0.48
			Std.dev of the mean		0.02

Semester: V24 — 53BX — Date: 23.jan

	Measured thicknesses [mm]				Mean
Test 1	0.17	0.21	0.25	0.35	**0.25**
Test 2	0.25	0.23	0.28	0.24	**0.25**
Test 3	0.21	0.35	0.25	0.20	**0.25**
Test 4	0.25	0.20	0.31	0.23	**0.25**
Test 5	0.36	0.26	0.21	0.25	**0.27**
Test 6	0.22	0.18	0.19	0.20	0.20
			Overall mean (test 1 to 5)		0.25
			Std.dev of the mean		0.01

Semester: Spring 24 — 53B2X — Date: 23.jan

	Measured thicknesses [mm]				Mean
Test 1	0.29	0.49	0.29	0.43	**0.38**
Test 2	0.50	0.43	0.49	0.42	**0.46**
Test 3	0.70	0.32	0.38	0.58	**0.50**
Test 4	0.43	0.42	0.36	0.52	**0.43**
Test 5	0.42	0.30	0.28	0.42	**0.36**
Test 6	0.50	0.66	0.59	0.71	0.62
			Overall mean (test 1 to 5)		0.42
			Std.dev of the mean		0.02

Semester: Spring 24 — 54B — Date: 23.jan

	Measured thicknesses [mm]				Mean
Test 1	0.26	0.19	0.22	0.32	**0.25**
Test 2	0.35	0.36	0.18	0.30	**0.30**
Test 3	0.24	0.29	0.30	0.25	**0.27**
Test 4	0.32	0.29	0.21	0.23	**0.26**
Test 5	0.33	0.25	0.35	0.33	**0.32**
Test 6	0.20	0.20	0.18	0.21	0.20
			Overall mean (test 1 to 5)		0.28
			Std.dev of the mean		0.01

Semester: Spring 24 — 54B2 — Date: 23.jan

	Measured thicknesses [mm]				Mean
Test 1	0.38	0.44	0.28	0.45	**0.39**
Test 2	0.46	0.42	0.36	0.37	**0.40**
Test 3	0.50	0.22	0.36	0.60	**0.42**
Test 4	0.61	0.50	0.22	0.44	**0.44**
Test 5	0.32	0.45	0.55	0.35	**0.42**
Test 6	0.33	0.23	0.26	0.36	0.30
			Overall mean (test 1 to 5)		0.41
			Std.dev of the mean		0.02

Semester: Spring 24 — 55B — Date: 1.feb

	Measured thicknesses [mm]				Mean
Test 1	0.20	0.32	0.24	0.27	**0.26**
Test 2	0.26	0.27	0.20	0.21	**0.24**
Test 3	0.21	0.30	0.27	0.25	**0.26**
Test 4	0.35	0.30	0.22	0.23	**0.28**
Test 5	0.23	0.28	0.23	0.28	**0.26**
Test 6	0.30	0.42	0.25	0.31	0.32
			Overall mean (test 1 to 5)		0.26
			Std.dev of the mean		0.01

Semester: Spring 24 — 55B2 — Date: 1.feb

	Measured thicknesses [mm]				Mean
Test 1	0.39	0.39	0.41	0.39	**0.40**
Test 2	0.35	0.42	0.31	0.36	**0.36**
Test 3	0.59	0.40	0.51	0.47	**0.49**
Test 4	0.42	0.38	0.42	0.50	**0.43**
Test 5	0.45	0.29	0.28	0.47	**0.37**
Test 6	0.34	0.33	0.30	0.40	0.34
			Overall mean (test 1 to 5)		0.41
			Std.dev of the mean		0.02

Semester:	Spring 24			Dato:	8.feb
57B	Measured thicknesses [mm]				Mean
Test 1	0.16	0.16	0.19	0.24	**0.19**
Test 2	0.32	0.27	0.26	0.23	**0.27**
Test 3	0.21	0.22	0.16	0.17	**0.19**
Test 4	0.25	0.24	0.20	0.19	**0.22**
Test 5	0.20	0.29	0.35	0.17	**0.25**
Test 6	0.35	0.36	0.31	0.17	0.30
			Overall mean (test 1 to 5)		0.24
			Std.dev of the mean		0.01

Semester:	Spring 24			Date:	8.feb
57B2	Measured thicknesses [mm]				Mean
Test 1	0.30	0.33	0.45	0.40	**0.37**
Test 2	0.49	0.39	0.54	0.77	**0.55**
Test 3	0.31	0.41	0.57	0.61	**0.48**
Test 4	0.30	0.44	0.49	0.31	**0.39**
Test 5	0.44	0.43	0.33	0.39	**0.40**
Test 6	0.41	0.85	0.35	0.79	0.60
			Overall mean (test 1 to 5)		0.44
			Std.dev of the mean		0.03

Semester:	V24			Date:	13.feb
58B	d thicknesses [mm]				Mean
Test 1	0.19	0.15	0.25	0.27	**0.22**
Test 2	0.17	0.18	0.16	0.15	**0.17**
Test 3	0.16	0.18	0.20	0.15	**0.17**
Test 4	0.22	0.18	0.20	0.24	**0.21**
Test 5	0.21	0.21	0.22	0.22	**0.22**
Test 6	0.16	0.37	0.25	0.26	0.26
			Overall mean (test 1 to 5)		0.20
			Std.dev of the mean		0.01

Semester:	Spring 24			Date:	13.feb
58B2	Measured thicknesses [mm]				Mean
Test 1	0.55	0.42	0.42	0.39	**0.45**
Test 2	0.39	0.41	0.42	0.54	**0.44**
Test 3	0.35	0.42	0.37	0.51	**0.41**
Test 4	0.70	0.30	0.48	0.54	**0.51**
Test 5	0.42	0.48	0.55	0.35	**0.45**
Test 6	0.30	0.34	0.25	0.27	0.29
			Overall mean (test 1 to 5)		0.45
			Std.dev of the mean		0.02

Semester:	Spring 24			Date:	13.feb
59B	Measured thicknesses [mm]				Mean
Test 1	0.19	0.21	0.34	0.37	**0.28**
Test 2	0.24	0.23	0.33	0.25	**0.26**
Test 3	0.22	0.25	0.25	0.20	**0.23**
Test 4	0.26	0.21	0.17	0.32	**0.24**
Test 5	0.23	0.25	0.28	0.30	**0.27**
Test 6	0.35	0.23	0.32	0.38	0.32
			Overall mean (test 1 to 5)		0.26
			Std.dev of the mean		0.01

Semester:	Spring 24			Date:	13.feb
59B2	Measured thicknesses [mm]				Mean
Test 1	0.30	0.40	0.38	0.35	**0.36**
Test 2	0.30	0.40	0.40	0.36	**0.37**
Test 3	0.41	0.42	0.35	0.44	**0.41**
Test 4	0.44	0.44	0.35	0.30	**0.38**
Test 5	0.44	0.36	0.35	0.41	**0.39**
Test 6	0.34	0.34	0.26	0.41	0.34
			Overall mean (test 1 to 5)		0.38
			Std.dev of the mean		0.01

Semester:	Spring 24			Date:	28.feb
56B	Measured thicknesses [mm]				Mean
Test 1	0.23	0.22	0.25	0.21	**0.23**
Test 2	0.32	0.31	0.3	0.24	**0.29**
Test 3	0.36	0.27	0.21	0.16	**0.25**
Test 4	0.25	0.17	0.19	0.26	**0.22**
Test 5	0.2	0.19	0.32	0.28	**0.25**
Test 6	0.21	0.18	0.24	0.2	0.21
			Overall mean (test 1 to 5)		0.25
			Std.dev of the mean		0.01

Semester:	Spring 24			Date:	28.feb
56B2	Measured thicknesses [mm]				Mean
Test 1	0.53	0.41	0.51	0.53	**0.50**
Test 2	0.41	0.37	0.44	0.37	**0.40**
Test 3	0.5	0.42	0.43	0.4	**0.44**
Test 4	0.46	0.37	0.43	0.4	**0.42**
Test 5	0.49	0.48	0.49	0.54	**0.50**
Test 6	0.36	0.37	0.35	0.36	0.36
			Overall mean (test 1 to 5)		0.45
			Std.dev of the mean		0.01

D Official Laboratory Test Reports

This appendix presents the full-scale results from the laboratory measurements carried out in accordance with NS-EN ISO 12572:2016, the wet cup method. All products names are anonymised with black boxes.

Each individual coating series' sub-appendix contains three components: an official test report, graphs of mass reduction, water vapour transmission, and equivalent air layer thickness over the testing period, and input data of the wet cup method

D.1. Coating 51B (Three layers)

SINTEF

Produktnavn:	███████████	Tykkelse, mm:	0,34
Oppdragsgiver:	Masteroppgave_Katinka	Målenummer:	51B
Prosjektnummer:	51B	Prøvediameter: (mm)	164
Produkttype:	Maling	Salttype i boksen:	KNO3
		Prøveperiode: fra:	15.01.2024
		til:	19.01.2024

	Middel i prøveperioden
Relativ luftfuktighet i boksen (%RF)	94,1
Relativ luftfuktighet i rommet (%RF)	50,7
Temperatur i boksen (°C)	23,0
Temperatur i rommet (°C)	23,0
Barometertrykk (hPa)	987,1

Lufth. over pr.(m/s): 0,3

Tykkelse prøve nr

1	0,44
2	0,27
3	0,30
4	0,29
5	0,39
6	0,36

Tabell 1   Temperatur, relativ luftfuktighet og barometertrykk i prøveperioden.

Prøve nummer	Vanndamppermeans Wp	Vanndampmotstand	
		sd	Zp
	(kg/m²sPa)	(m)	(m²sPa/kg)
1	1,22E-10	1,640	8,20E+09
2	1,61E-10	1,250	6,22E+09
3	1,71E-10	1,170	5,84E+09
4	1,51E-10	1,330	6,64E+09
5	1,38E-10	1,460	7,27E+09
Middel	1,48E-10	1,350	6,74E+09
Std. dev. mean. value	8,66561E-12	0,083	4,16E+08

Tabell 2   Vanndamppermeans og vanndampmotstand for de fem prøvestykkene.
                     Enkeltresultatene er et middel over fem tidsintervall med stabil fukttransport.
                     Resultatene er korrigert for overgangsmotstanden over prøven,
                     damptransport gjennom overlappsonen, og motstanden i luftlaget i boksen.

SIGN:

Vektendring siden start for de enkelte prøvene

Figure D.1.1: Mass reduction during the period

Ekvivalent luftlagstykkelse i perioden

Figure D.1.2: Equivalent air layer thickness sd-value during the period

Vanndampgjennomgang i perioden

Figure D.1.3: Water vapour transmission during the period

Table D.1.1: Input data of the wet cup method

				Salttype:		KNO3	Prøvestykke:		1	2	3
Masteroppgave_Katinka		Katinka		Prøvediameter (mm):		0,164	Tykkelse:	0,44		0,27	0,30
51B				Luftlag salt/prøve (mm):		15	Side mot saltløsning:			Hvit side	
Maling				Prøvest. diameter(mm):		0,174	Ferkst/Aldret:			Ferskt	
0,3400				Lufth. over pr.(m/s):		0,3	Start kondisjonering:			27-10-2023	
51B				RF/Temp:		Vekt:		Tykkelsesmåler:			Stanse:
	11.01.2024	12.01.2024	15.01.2024	16.01.2024	17.01.2024	18.01.2024	19.01.2024				
	09:45	09:10	09:10	09:04	09:05	09:03	09:06				
3											
	1026,55	1017,1	989,9	987,05	980,88	983,3	987,79				
	1026,55	1023,34	994,58	991,39	983,22	981,54	984,81				
	23	23,05	23,03	23,02	23,01	23,02	23,02				
	23	23,05	23,03	23,02	23,01	23,02	23,02				
	50	50,62	50,74	50,65	50,67	50,67	50,59				
	1	2	3	4	5	6	7	8	9	10	
	999,999	1000	1000,001	1000,004	1000,002	1000,003	1000,002				
1	530,131	529,865	529,051	528,783	528,517	528,248	527,979				
2	561,787	561,44	560,379	560,028	559,675	559,321	558,965				
3	529,322	528,953	527,814	527,433	527,055	526,69	526,318				
4	566,982	566,66	565,675	565,348	565,018	564,689	564,339				
5	564,706	564,383	563,463	563,161	562,861	562,563	562,26				
	1000	1000,003	1000,003	1000,003	1000,004	1000,004	1000,002				

D.2. Coating 51B2 (Six Layers)

SINTEF

Produktnavn:	▮▮▮▮▮▮▮▮
Oppdragsgiver:	Masteroppgave_Katinka
Prosjektnummer:	51B2
Produkttype:	Maling

Tykkelse, mm:	0,56
Målenummer:	51B2
Prøvediameter: (mm)	164
Salttype i boksen:	KNO3
Prøveperiode: fra:	12.01.2024
til:	18.01.2024

	Middel i prøveperioden
Relativ luftfuktighet i boksen (%RF)	94,1
Relativ luftfuktighet i rommet (%RF)	50,7
Temperatur i boksen (°C)	23,0
Temperatur i rommet (°C)	23,0
Barometertrykk (hPa)	994,8

Lufth. over pr.(m/s):	0,3

Tykkelse prøve nr	
1	0,56
2	0,57
3	0,59
4	0,57
5	0,50
6	0,46

Tabell 1   Temperatur, relativ luftfuktighet og barometertrykk i prøveperioden.

Prøve nummer	Vanndamppermeans Wp	Vanndampmotstand	
		sd	Zp
	(kg/m²sPa)	(m)	(m²sPa/kg)
1	8,62E-11	2,310	1,16E+10
2	9,39E-11	2,120	1,07E+10
3	8,30E-11	2,400	1,20E+10
4	8,92E-11	2,230	1,12E+10
5	9,04E-11	2,200	1,11E+10
Middel	8,85E-11	2,250	1,13E+10
Std. dev. mean. value	1,8477E-12	0,048	2,38E+08

Tabell 2   Vanndamppermeans og vanndampmotstand for de fem prøvestykkene.
Enkeltresultatene er et middel over fem tidsintervall med stabil fukttransport.
Resultatene er korrigert for overgangsmotstanden over prøven,
damptransport gjennom overlappsonen, og motstanden i luftlaget i boksen.

SIGN:

Vektendring siden start for de enkelte prøvene

Figure D.2.1: Mass reduction during the period

Ekvivalent luftlagstykkelse i perioden

Figure D.2.2: Equivalent air layer thickness sd-value during the period

Vanndampgjennomgang i perioden
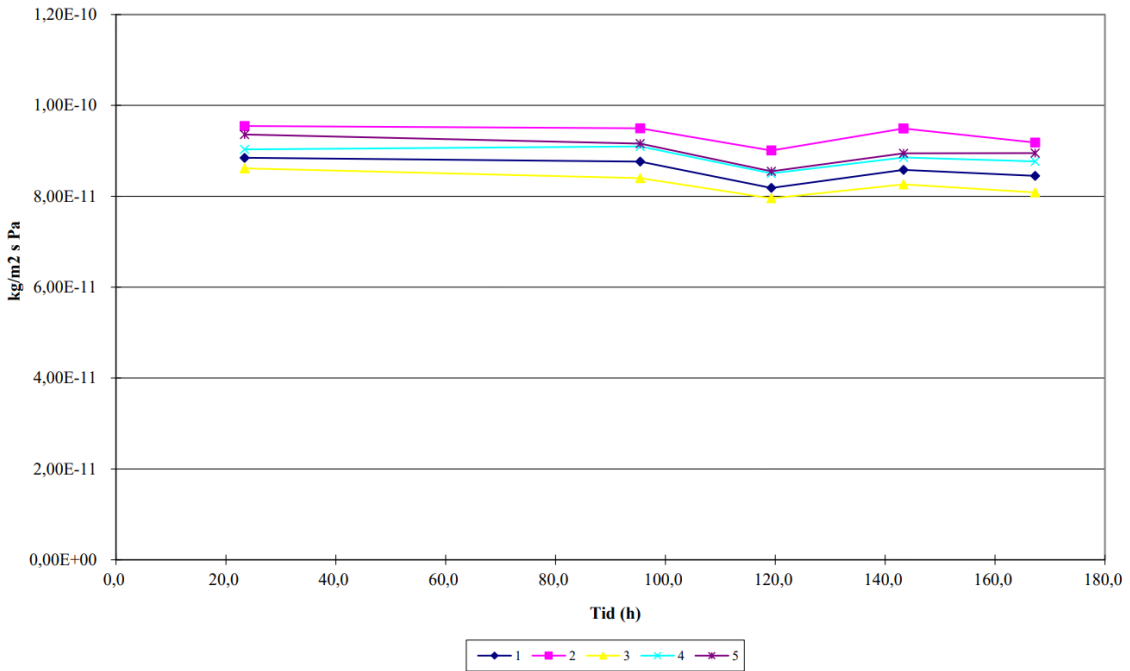
Figure D.2.3: Water vapour transmission during the period

Table D.2.1: Input data of the wet cup method

				Salttype:		KNO3	Prøvestykke:		1	2	3
Masteroppgave_Katinka		Katinka		Prøvediameter (mm):		0,164	Tykkelse:	0,56	0,57	0,59	
51B2				Luftlag salt/prøve (mm):		15	Side mot saltløsning:		Hvit side		
Maling				Prøvest. diameter(mm):		0,174	Ferkst/Aldret:		Ferskt		
	0,5600			Lufth. over pr.(m/s):		0,3	Start kondisjonering:			11.01.2023	
51B2				RF/Temp:		Vekt:		Tykkelsesmåler:			Stanse:
	11.01.2024	12.01.2024	15.01.2024	16.01.2024	17.01.2024	18.01.2024					
	09:52	09:17	09:17	09:10	09:12	09:10					
2											
	1026,54	1017,1	989,9	987,05	980,88	983,3					
	1026,54	1023,34	994,58	991,39	983,22	981,54					
	23	23,05	23,03	23,02	23,01	23,02					
	23	23,05	23,03	23,02	23,01	23,02					
	50	50,62	50,74	50,65	50,67	50,67					
	1	2	3	4	5	6	7		8	9	10
	1000	1000	1000,003	1000,003	1000,003	1000,003					
1	587,281	587,093	586,519	586,329	586,14	585,95					
2	596,800	596,597	595,975	595,767	595,558	595,352					
3	521,623	521,44	520,89	520,705	520,523	520,341					
4	478,952	478,76	478,164	477,967	477,772	477,575					
5	554,110	553,911	553,311	553,113	552,916	552,715					
	1000,004	1000,004	1000,004	1000,004	1000,004	1000,005					

D.3. Coating 52B (Three layers)

SINTEF

<div style="border:1px solid">

PRØVINGS RAPPORT
Prøving av vanndamppermeans etter ISO/DIS 12572

</div>

Produktnavn:	███████████████		Tykkelse, mm:	0,28
Oppdragsgiver:	Masteroppgave_Katinka		Målenummer:	52B
Prosjektnummer:	52B		Prøvediameter: (mm)	164
Produkttype:	Maling		Salttype i boksen:	KNO3
			Prøveperiode: fra:	16.01.2024
			til:	22.01.2024

	Middel i prøveperioden
Relativ luftfuktighet i boksen (%RF)	94,1
Relativ luftfuktighet i rommet (%RF)	50,6
Temperatur i boksen (°C)	23,0
Temperatur i rommet (°C)	23,0
Barometertrykk (hPa)	986,2

Lufth. over pr.(m/s): 0,3

Tykkelse prøve nr

1 0,29
2 0,28
3 0,30
4 0,27
5 0,29
6 0,37

Tabell 1   Temperatur, relativ luftfuktighet og barometertrykk i prøveperioden.

Prøve nummer	Vanndamppermeans	Vanndampmotstand	
	Wp	sd	Zp
	(kg/m²sPa)	(m)	(m²sPa/kg)
1	2,85E-10	0,705	3,51E+09
2	2,20E-10	0,910	4,54E+09
3	2,25E-10	0,893	4,45E+09
4	2,53E-10	0,791	3,95E+09
5	2,17E-10	0,925	4,61E+09
Middel	2,40E-10	0,836	4,17E+09
Std. dev. mean. value	1,2887E-11	0,042	2,10E+08

Tabell 2   Vanndamppermeans og vanndampmotstand for de fem prøvestykkene.
Enkeltresultatene er et middel over fem tidsintervall med stabil fukttransport.
Resultatene er korrigert for overgangsmotstanden over prøven,
damptransport gjennom overlappsonen, og motstanden i luftlaget i boksen.

SIGN:

Vektendring siden start for de enkelte prøvene

Figure D.3.1: Mass reduction during the period

Ekvivalent luftlagstykkelse i perioden

Figure D.3.2: Equivalent air layer thickness sd-value during the period

Vanndampgjennomgang i perioden

Figure D.3.3: Water vapour transmission during the period

Table D.3.1: Input data of the wet cup method

				Salttype:		KNO3	Prøvestykke:		1	2	3
Masteroppgave_Katinka		Katinka		Prøvediameter (mm):		0,164	Tykkelse:	0,29	0,28	0,30	
52B				Luftlag salt/prøve (mm):		15	Side mot saltløsning:		Hvit side		
Maling				Prøvest. diameter(mm):		0,174	Ferkst/Aldret:		Ferskt		
0,2800				Lufth. over pr.(m/s):		0,3	Start kondisjonering:		25-10-2023		
52B				RF/Temp:		Vekt:		Tykkelsesmåler:		Stanse:	
	12.01.2024	15.01.2024	16.01.2024	17.01.2024	18.01.2024	19.01.2024	22.01.2024				
	09:24	09:23	09:16	09:18	09:15	09:17	08:33				
3											
	1017,1	989,9	987,05	980,88	983,3	987,79	958,19				
	1017,1	994,58	991,39	983,22	981,54	984,81	989,98				
	23	23,03	23,02	23,01	23,02	23,02	23,02				
	23	23,03	23,02	23,01	23,02	23,02	23,02				
	50	50,74	50,65	50,67	50,67	50,59	50,63				
	1	2	3	4	5	6	7	8	9	10	
	1000,001	1000,001	1000,002	1000,003	1000,003	1000,003	1000,004				
1	524,566	522,094	521,469	520,841	520,226	519,609	517,796				
2	510,229	508,698	508,204	507,718	507,232	506,748	505,348				
3	562,837	561,299	560,797	560,302	559,807	559,314	557,886				
4	523,489	521,745	521,18	520,62	520,064	519,51	517,905				
5	602,837	601,332	600,844	600,366	599,886	599,408	598,036				
	1000,002	1000,003	1000,003	1000,005	1000,003	1000,002	1000,007				

D.4. Coating 52B (Six Layers)

SINTEF

Produktnavn:	██████████	Tykkelse, mm:	0,48
Oppdragsgiver:	Masteroppgave_Katinka	Målenummer:	52B2
Prosjektnummer:	52B2	Prøvediameter: (mm)	164
Produktype:	Maling	Salttype i boksen:	KNO3
		Prøveperiode: fra:	18.01.2024
		til:	25.01.2024

	Middel i prøveperioden
Relativ luftfuktighet i boksen (%RF)	94,1
Relativ luftfuktighet i rommet (%RF)	50,7
Temperatur i boksen (°C)	23,0
Temperatur i rommet (°C)	23,0
Barometertrykk (hPa)	983,9

Lufth. over pr.(m/s): 0,3

Tykkelse prøve nr

1	0,46
2	0,49
3	0,48
4	0,47
5	0,49
6	0,44

Tabell 1   Temperatur, relativ luftfuktighet og barometertrykk i prøveperioden.

Prøve nummer	Vanndamppermeans	Vanndampmotstand	
	Wp	sd	Zp
	(kg/m²sPa)	(m)	(m²sPa/kg)
1	1,64E-10	1,220	6,09E+09
2	1,53E-10	1,310	6,54E+09
3	1,51E-10	1,330	6,62E+09
4	1,61E-10	1,250	6,21E+09
5	1,57E-10	1,280	6,36E+09
Middel	1,57E-10	1,280	6,36E+09
Std. dev. mean. value	2,42525E-12	0,020	9,79E+07

Tabell 2   Vanndamppermeans og vanndampmotstand for de fem prøvestykkene.
Enkeltresultatene er et middel over fem tidsintervall med stabil fukttransport.
Resultatene er korrigert for overgangsmotstanden over prøven,
damptransport gjennom overlappsonen, og motstanden i luftlaget i boksen.

SIGN:

Vektendring siden start for de enkelte prøvene

Figure D.4.1: Mass reduction during the period

Ekvivalent luftlagstykkelse i perioden

Figure D.4.2: Equivalent air layer thickness sd-value during the period

Vanndampgjennomgang i perioden
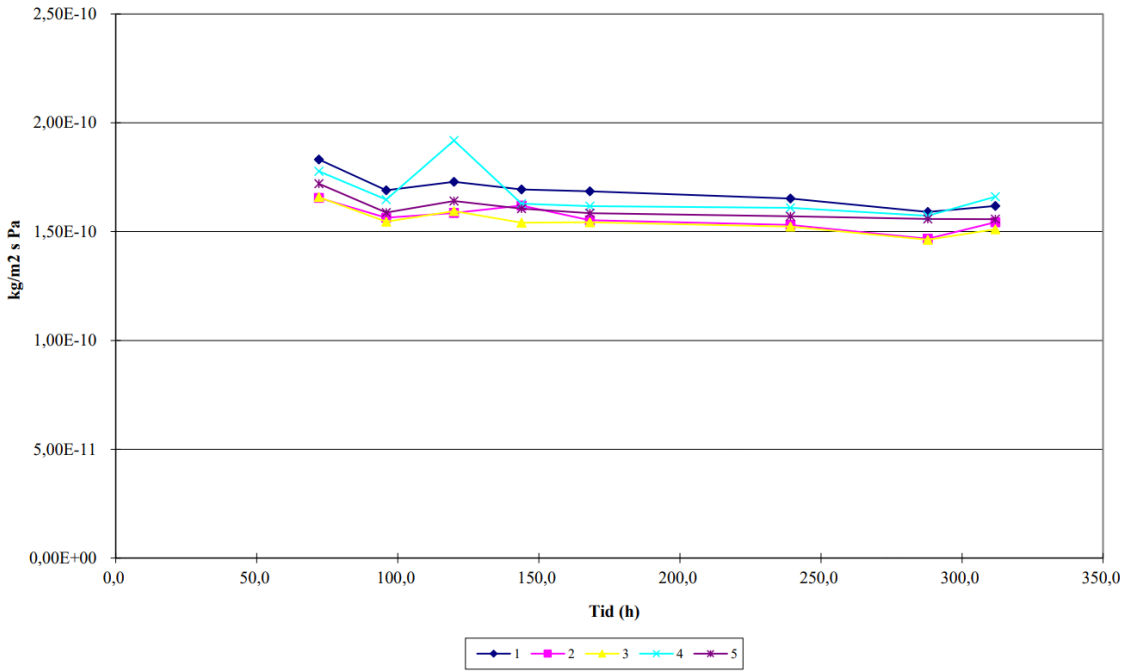
Figure D.4.3: Water vapour transmission during the period

Table D.4.1: Input data of the wet cup method

				Salttype:		KNO3	Prøvestykke:		1	2	3
Masteroppgave_Katinka		Katinka		Prøvediameter (mm):		0,164	Tykkelse:	0,46		0,49	0,48
52B2				Luftlag salt/prøve (mm):		15	Side mot saltløsning:			Hvit side	
Maling				Prøvest. diameter(mm):		0,174	Ferkst/Aldret:			Ferskt	
0,4800				Lufth. over pr.(m/s):		0,3	Start kondisjonering:			27-10-2023	
52B2				RF/Temp:		Vekt:		Tykkelsesmåler:			Stanse:
	12.01.2024	15.01.2024	16.01.2024	17.01.2024	18.01.2024	19.01.2024	22.01.2024		24.01.2024	25.01.2024	
	09:29	09:31	09:23	09:25	09:21	09:33	08:40		09:22	09:18	
5											
	1017,1	989,9	987,05	980,88	983,3	987,79	958,19		974,1	1009,9	
	1017,1	994,58	991,39	983,22	981,54	984,81	989,98		973,44	989,95	
	23	23,03	23,02	23,01	23,02	23,02	23,02		23,03	23,04	
	23	23,03	23,02	23,01	23,02	23,02	23,02		23,03	23,04	
	50	50,74	50,65	50,67	50,67	50,59	50,63		50,74	50,84	
	1	2	3	4	5	6	7		8	9	10
	1000,001	1000	1000,001	1000,003	1000,002	1000,002	1000,007		1000,003	1000,000	
1	564,943	563,749	563,371	562,993	562,619	562,244	561,184		560,455	560,092	
2	582,277	581,197	580,846	580,499	580,141	579,795	578,813		578,138	577,791	
3	578,921	577,839	577,492	577,143	576,802	576,458	575,481		574,808	574,468	
4	521,252	520,093	519,724	519,305	518,945	518,585	517,552		516,831	516,459	
5	560,834	559,712	559,356	558,997	558,642	558,289	557,281		556,566	556,216	
	1000,001	1000,001	1000,002	1000,002	1000,004	1000,003	1000,01		1000,004	1000	

D.5. Coating 53B (Three Layers)

SINTEF

Produktnavn:	███████████	Tykkelse, mm:	0,26
Oppdragsgiver:	Masteroppgave_Katinka	Målenummer:	53B
Prosjektnummer:	53B	Prøvediameter: (mm)	164
Produkttype:	Maling	Salttype i boksen:	KNO3
		Prøveperiode: fra:	21.11.2023
		til:	27.11.2023

	Middel i prøveperioden
Relativ luftfuktighet i boksen (%RF)	94,1
Relativ luftfuktighet i rommet (%RF)	50,9
Temperatur i boksen (°C)	23,0
Temperatur i rommet (°C)	23,0
Barometertrykk (hPa)	999,2

Lufth. over pr.(m/s): 0,3

Tykkelse prøve nr

1	0,27
2	0,27
3	0,25
4	0,28
5	0,25
6	0

Tabell 1   Temperatur, relativ luftfuktighet og barometertrykk i prøveperioden.

Prøve nummer	Vanndamppermeans Wp	Vanndampmotstand	
		sd	Zp
	(kg/m²sPa)	(m)	(m²sPa/kg)
1	2,66E-10	0,744	3,76E+09
2	2,67E-10	0,742	3,75E+09
3	3,05E-10	0,649	3,28E+09
4	3,00E-10	0,660	3,33E+09
5	3,41E-10	0,580	2,93E+09
Middel	2,96E-10	0,669	3,38E+09
Std. dev. mean. value	1,39503E-11	0,031	1,56E+08

Tabell 2   Vanndamppermeans og vanndampmotstand for de fem prøvestykkene.
Enkeltresultatene er et middel over fem tidsintervall med stabil fukttransport.
Resultatene er korrigert for overgangsmotstanden over prøven,
damptransport gjennom overlappsonen, og motstanden i luftlaget i boksen.

SIGN:

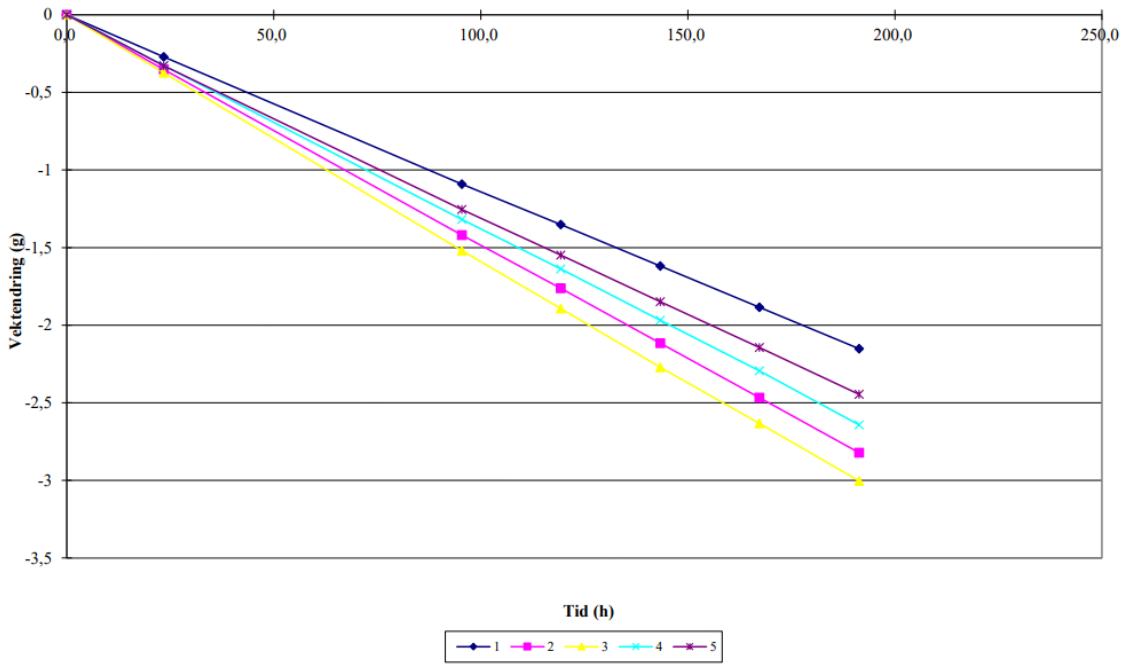Vektendring siden start for de enkelte prøvene

Figure D.5.1: Mass reduction during the period
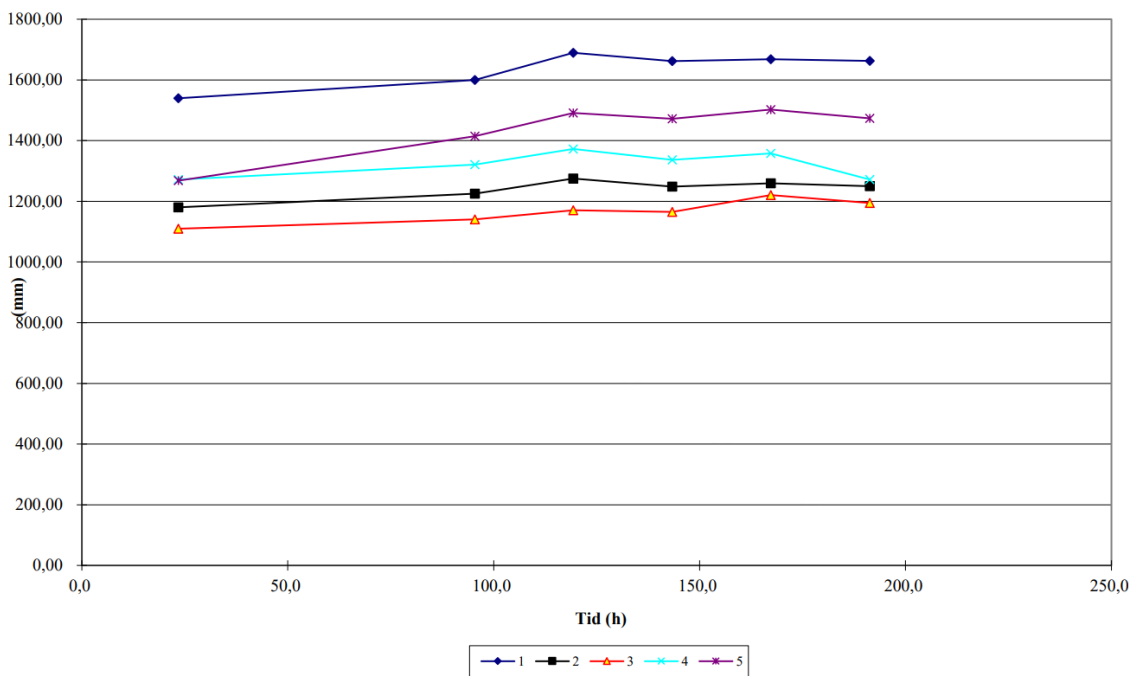
Ekvivalent luftlagstykkelse i perioden

Figure D.5.2: Equivalent air layer thickness sd-value during the period
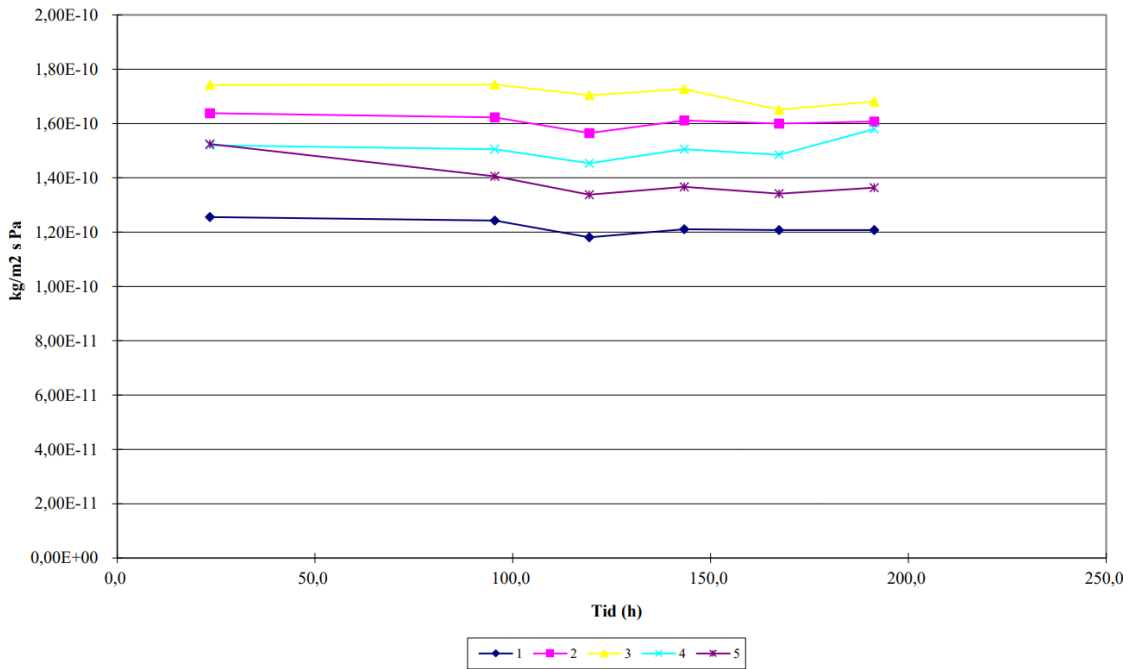
Vanndampgjennomgang i perioden

kg/m2 s Pa

Tid (h)

Legend: 1 | 2 | 3 | 4 | 5

Figure D.5.3: Water vapour transmission during the period

Table D.5.1: Input data of the wet cup method

					Salttype:		KNO3	Prøvestykke:	1	2	3	4	5
(1)Produktnavn:					Salttype:		KNO3	Prøvestykke:	1	2	3	4	5
(2)Oppdragsgiver:	Masteroppgave_Katinka		Katinka		Prøvediameter (mm):		0,164	Tykkelse:	0,27	0,27	0,25	0,28	0,25
(3)Prosjektnummer:	53B				Luftlag salt/prøve (mm):		15	Side mot saltløsning:		Hvit side			
(4)Produktype:	Maling				Prøvest. diameter(mm):		0,174	Ferkst/Aldret:		Ferskt			
(5)Tykkelse, mm:		0,2600			Lufth. over pr.(m/s):		0,3	Start kondisjonering:		17-10-2023			
(6)Målenummer:	53B				RF/Temp:		Vekt:		Tykkelsesmåler:			Stanse:	
(12)Dato (CTRL+SHIFT+ ;)		20.11.2023	21.11.2023	22.11.2023	23.11.2023	24.11.2023	27.11.2023						
(13)Tid (CTRL+SHIFT+ :)		08:35	09:09	09:07	09:03	09:07	09:01						
(14)Beregning fra veiing:	2												
(15)Barometertrykk ved veiing, hPa:		1009,46	1020,51	989,62	974,89	992,29	1015,19						
(16)Barometertrykk i perioden, hPa:		1009,46	1015,28	1012,79	982,92	980,08	1004,85						
(17)Temperatur luft over boks,°C:		23	23,09	23,06	23,01	23,01	23,02						
(18)Temperatur i saltløsning, °C:		23	23,09	23,06	23,01	23,01	23,02						
(19)RF i rommet, %		50	50,82	50,9	50,67	51,2	51,13						
(20)Veiing nummer:		1	2	3	4	5	6	7	8	9	10	11	12
(21)Vekt,g kontrolllodd før veiing:		1000	1000,001	1000,005	1000,004	1000,002	1000,002						
(22)Vekt,g prøve nr:	1	463,595	462,991	462,417	461,846	461,266	459,561						
(23)Vekt,g prøve nr:	2	459,387	458,774	458,197	457,621	457,04	455,34						
(24)Vekt,g prøve nr:	3	467,263	466,575	465,921	465,266	464,602	462,654						
(25)Vekt,g prøve nr:	4	510,261	509,571	508,918	508,272	507,622	505,725						
(26)Vekt,g prøve nr:	5	513,425	512,662	511,938	511,206	510,473	508,291						
(27)Vekt,g kontrolllodd etter veiing:		999,999	1000,002	1000,004	1000,005	1000,005	1000,001						

D.6 Coating 53B2 (Six Layers)

◉ SINTEF

Produktnavn:	████████████	Tykkelse, mm:	0,52
Oppdragsgiver:	Masteroppgave_Katinka	Målenummer:	53B2
Prosjektnummer:	53B2	Prøvediameter: (mm)	164
Produkttype:	Maling	Salttype i boksen:	KNO3
		Prøveperiode: fra:	23.11.2023
		til:	29.11.2023

	Middel i prøveperioden
Relativ luftfuktighet i boksen (%RF)	94,1
Relativ luftfuktighet i rommet (%RF)	51,0
Temperatur i boksen (°C)	23,0
Temperatur i rommet (°C)	23,0
Barometertrykk (hPa)	999,0

Lufth. over pr.(m/s):	0,3

Tykkelse prøve nr	
1	0,46
2	0,48
3	0,53
4	0,5
5	0,62
6	0

Tabell 1   Temperatur, relativ luftfuktighet og barometertrykk i prøveperioden.

Prøve nummer	Vanndamppermeans Wp	Vanndampmotstand	
		sd	Zp
	(kg/m²sPa)	(m)	(m²sPa/kg)
1	1,79E-10	1,110	5,59E+09
2	1,76E-10	1,120	5,67E+09
3	1,98E-10	0,998	5,04E+09
4	1,96E-10	1,010	5,11E+09
5	1,56E-10	1,270	6,42E+09
Middel	1,81E-10	1,090	5,52E+09
Std. dev. mean. value	7,67813E-12	0,049	2,47E+08

Tabell 2   Vanndamppermeans og vanndampmotstand for de fem prøvestykkene.
Enkeltresultatene er et middel over fem tidsintervall med stabil fukttransport.
Resultatene er korrigert for overgangsmotstanden over prøven,
damptransport gjennom overlappsonen, og motstanden i luftlaget i boksen.

SIGN:

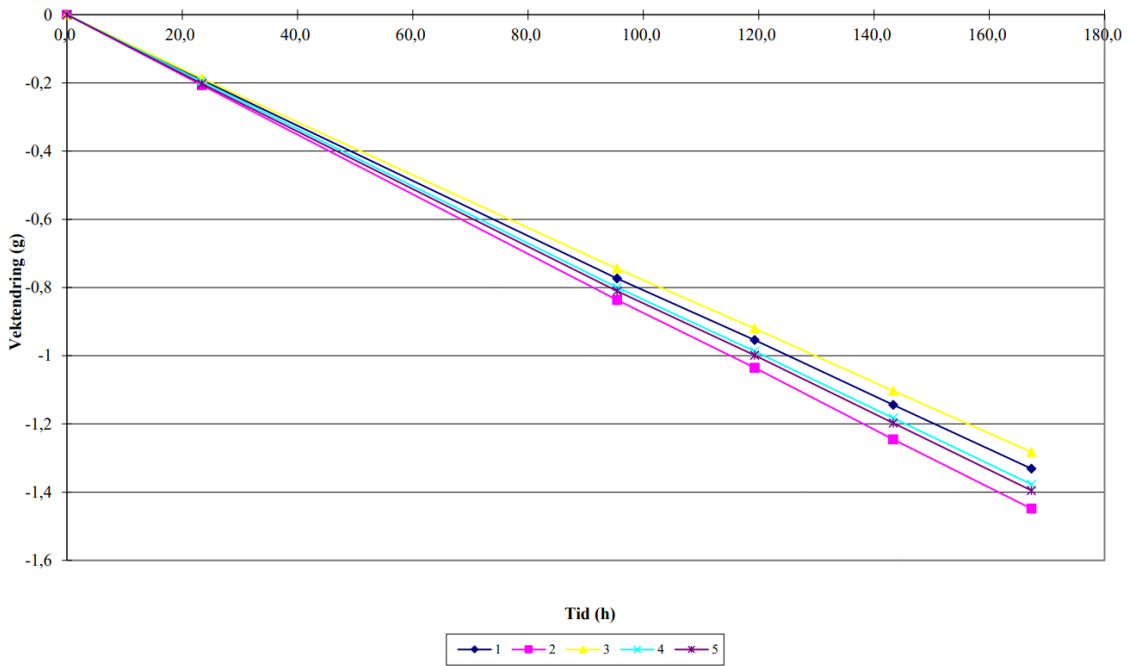Vektendring siden start for de enkelte prøvene

Figure D.6.1: Mass reduction during the period
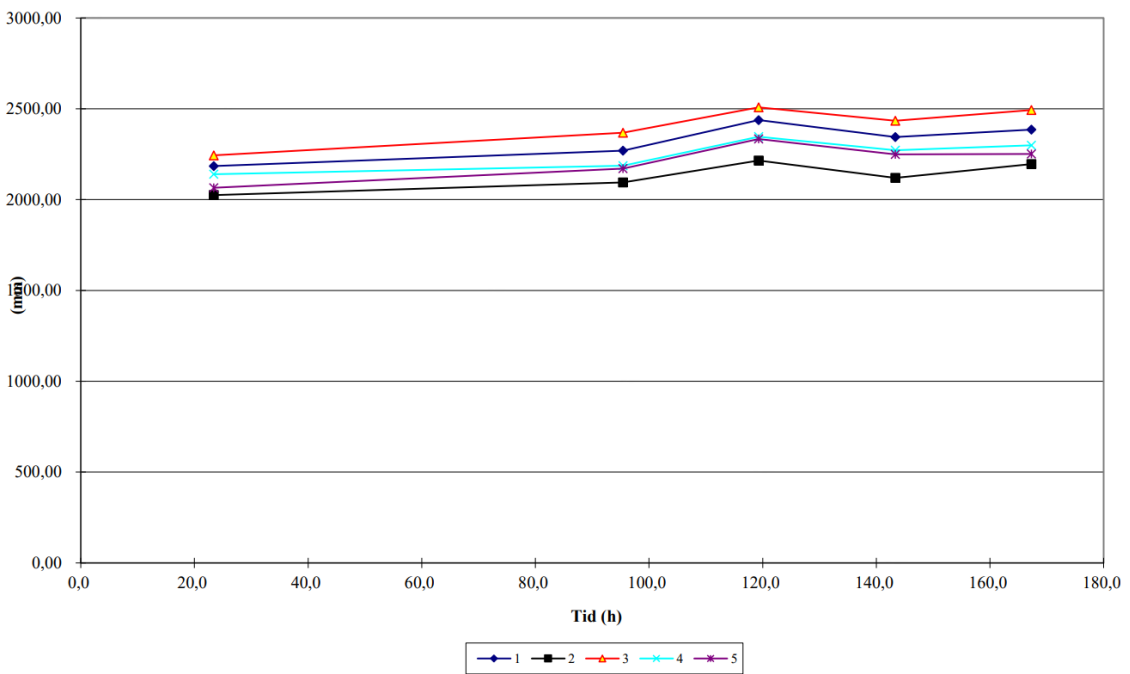
Ekvivalent luftlagstykkelse i perioden

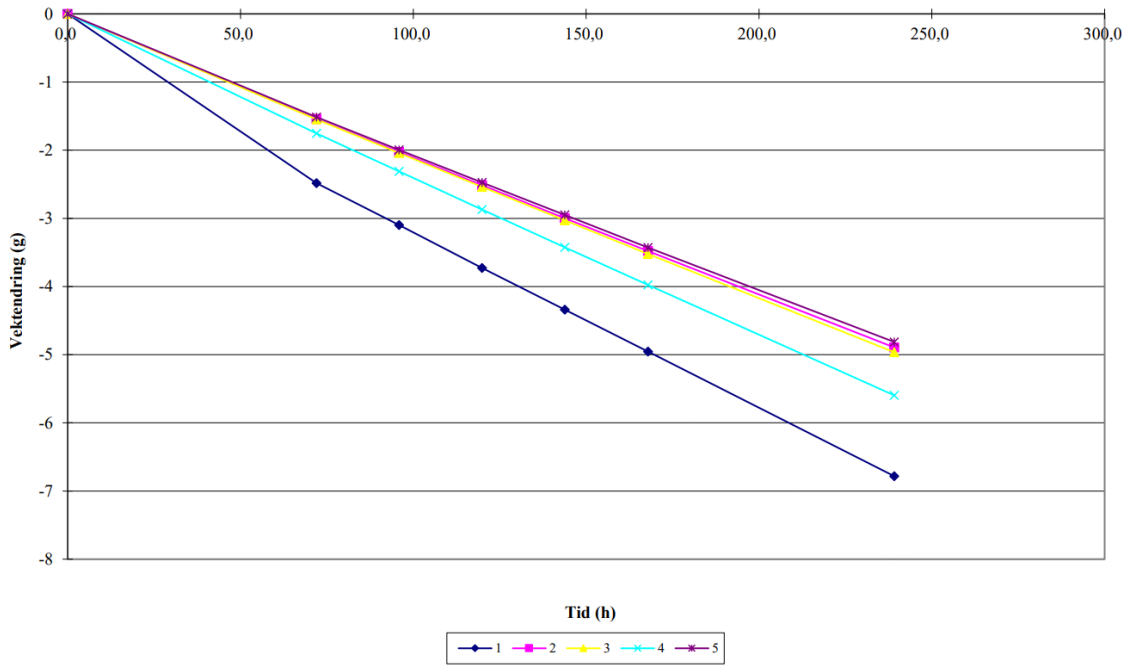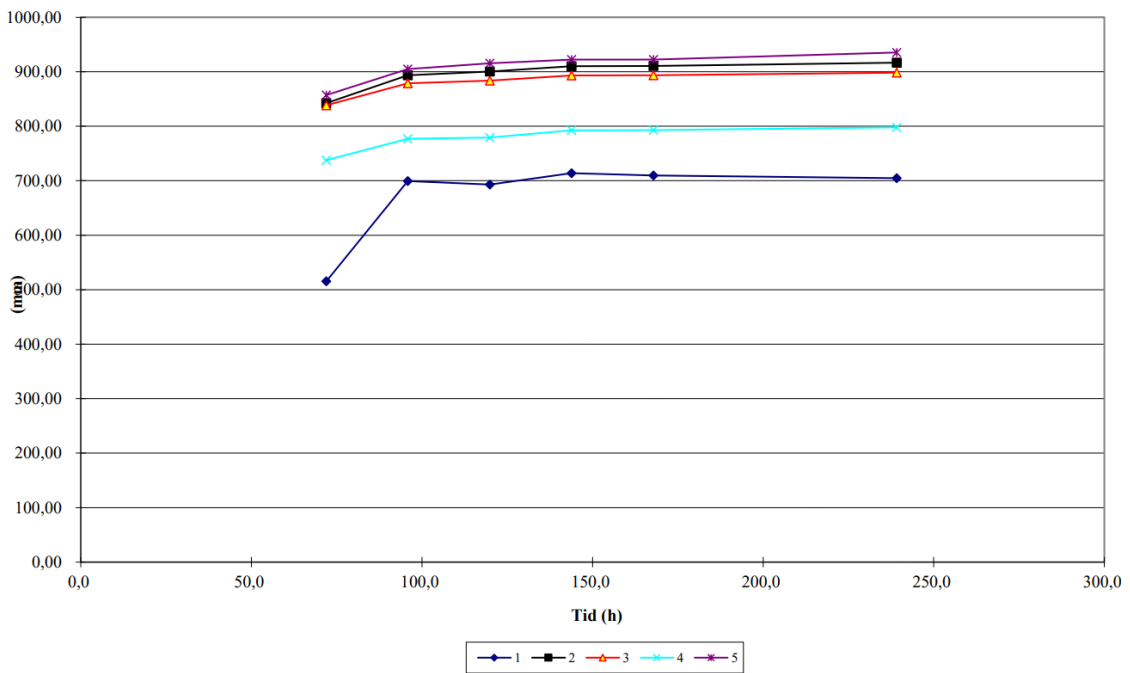**Figure D.6.2:** Equivalent air layer thickness sd-value during the period

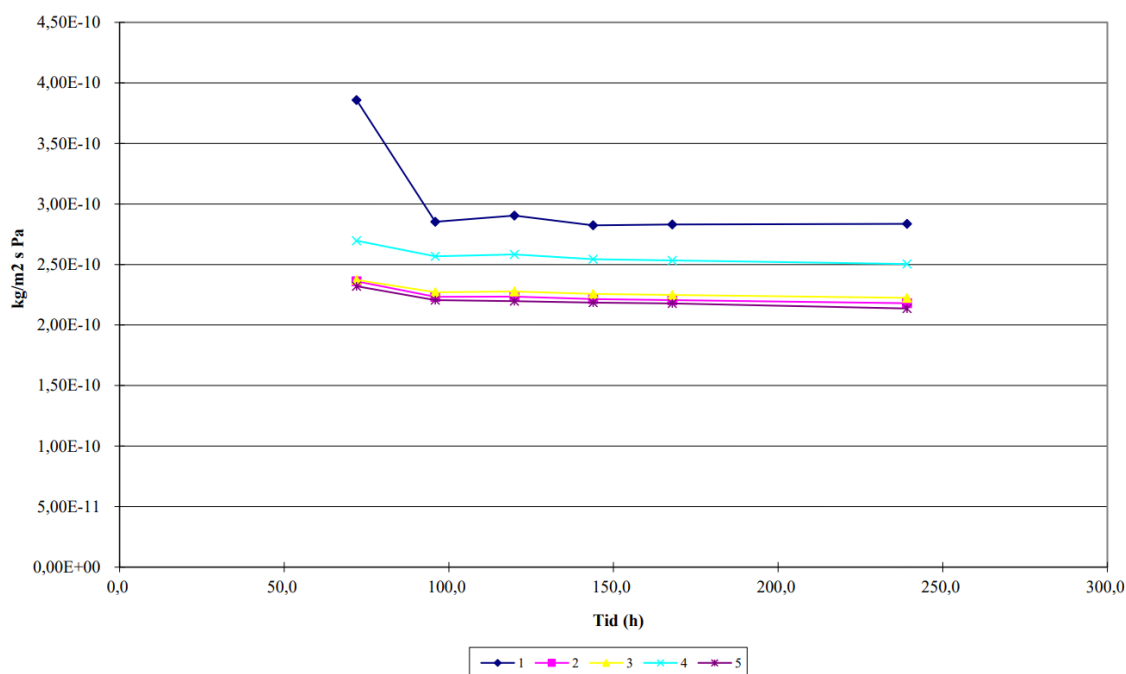**Figure D.6.3**: Water vapour transmission during the period

Table D.6.1: Input data of the wet cup method

											1	2	3	4	5
(1)Produktnavn:	Jotun Drygolin Nordic Extreme				Salttype:		KNO3	Prøvestykke:			1	2	3	4	5
(2)Oppdragsgiver:	Masteroppgave_Katinka	Katinka			Prøvediameter (mm):		0,164	Tykkelse:			0,46	0,48	0,53	0,5	0,62
(3)Prosjektnummer:	53B2				Luftlag salt/prøve (mm):		15	Side mot saltløsning:		hvit					
(4)Produktype:	Maling				Prøvest. diameter(mm):		0,174	Ferkst/Aldret:		Ferskt					
(5)Tykkelse, mm:	0,5200				Lufth. over pr.(m/s):		0,3	Start kondisjonering:		17-10-2023					
(6)Målenummer:	53B2				RF/Temp:		Vekt:		Tykkelsesmåler:		Stanse:				
(12)Dato (CTRL+SHIFT+ ;)		20.11.2023	21.11.2023	22.11.2023	23.11.2023	24.11.2023	27.11.2023	28.11.2023	29.11.2023						
(13)Tid (CTRL+SHIFT+ :)		08:45	09:17	09:15	09:11	09:15	09:08	09:03	09:07						
(14)Beregning fra veiing:	4														
(15)Barometertrykk ved veiing, hPa:		1009,46	1020,51	989,62	974,89	992,29	1015,19	1015,14	1009,76						
(16)Barometertrykk i perioden, hPa:		1009,46	1015,28	1012,79	982,92	980,08	1004,85	1016,19	1010,85						
(17)Temperatur luft over boks,°C:		23	23,09	23,06	23,01	23,01	23,02	23,02	23,02						
(18)Temperatur i saltløsning, °C:		23	23,09	23,06	23,01	23,01	23,02	23,02	23,02						
(19)RF i rommet, %		50	50,82	50,9	50,67	51,2	51,13	50,92	50,86						
(20)Veiing nummer:		1	2	3	4	5	6	7	8	9	10	11	12		
(21)Vekt,g kontrolllodd før veiing:		1000	1000	1000,005	1000,007	1000,004	1000,001	1000,001	1000						
(22)Vekt,g prøve nr:	1	504,906	504,483	504,092	503,698	503,296	502,125	501,743	501,357						
(23)Vekt,g prøve nr:	2	431,746	431,311	430,911	430,518	430,116	428,963	428,588	428,213						
(24)Vekt,g prøve nr:	3	506,416	505,948	505,513	505,082	504,637	503,339	502,911	502,485						
(25)Vekt,g prøve nr:	4	520,608	520,139	519,707	519,282	518,84	517,564	517,142	516,72						
(26)Vekt,g prøve nr:	5	511,567	511,165	510,799	510,446	510,087	509,067	508,737	508,408						
(27)Vekt,g kontrolllodd etter veiing:		1000,003	1000,004	1000,006	1000,01	1000,002	1000,003	1000,001	1000						
Tekst i diagrammet Vektendring															

D.7. Coating 53BX (Three Layers)

SINTEF

Produktnavn:	▊▊▊▊▊▊▊▊▊	
Oppdragsgiver:	Masteroppgave_Katinka	
Prosjektnummer:	53BX	
Produkttype:	Maling	

Tykkelse, mm:		0,25
Målenummer:		53BX
Prøvediameter: (mm)		164
Salttype i boksen:		KNO3
Prøveperiode:	fra:	25.01.2024
	til:	31.01.2024

	Middel i prøveperioden
Relativ luftfuktighet i boksen (%RF)	94,1
Relativ luftfuktighet i rommet (%RF)	50,7
Temperatur i boksen (°C)	23,0
Temperatur i rommet (°C)	23,0
Barometertrykk (hPa)	1003,4

Lufth. over pr.(m/s):	0,3

Tykkelse prøve nr

1	0,25
2	0,25
3	0,25
4	0,25
5	0,27
6	0,20

Tabell 1   Temperatur, relativ luftfuktighet og barometertrykk i prøveperioden.

Prøve nummer	Vanndamppermeans	Vanndampmotstand	
	Wp	sd	Zp
	(kg/m²sPa)	(m)	(m²sPa/kg)
1	3,82E-10	0,516	2,62E+09
2	3,37E-10	0,585	2,97E+09
3	3,18E-10	0,619	3,14E+09
4	2,96E-10	0,667	3,38E+09
5	3,06E-10	0,645	3,27E+09
Middel	3,28E-10	0,602	3,05E+09
Std. dev. mean. value	1,51802E-11	0,026	1,34E+08

Tabell 2   Vanndamppermeans og vanndampmotstand for de fem prøvestykkene.
Enkeltresultatene er et middel over fem tidsintervall med stabil fukttransport.
Resultatene er korrigert for overgangsmotstanden over prøven,
damptransport gjennom overlappsonen, og motstanden i luftlaget i boksen.

SIGN:

VEKTENDRING

Vektendring siden start for de enkelte prøvene
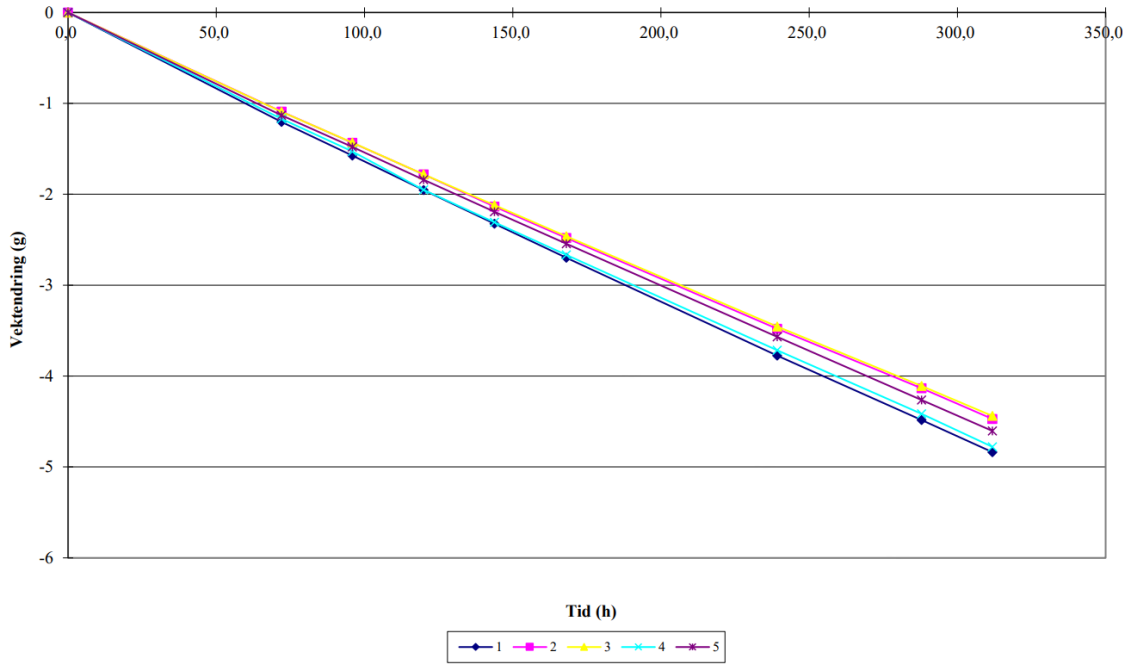

Figure D.7.1: Mass reduction during the period
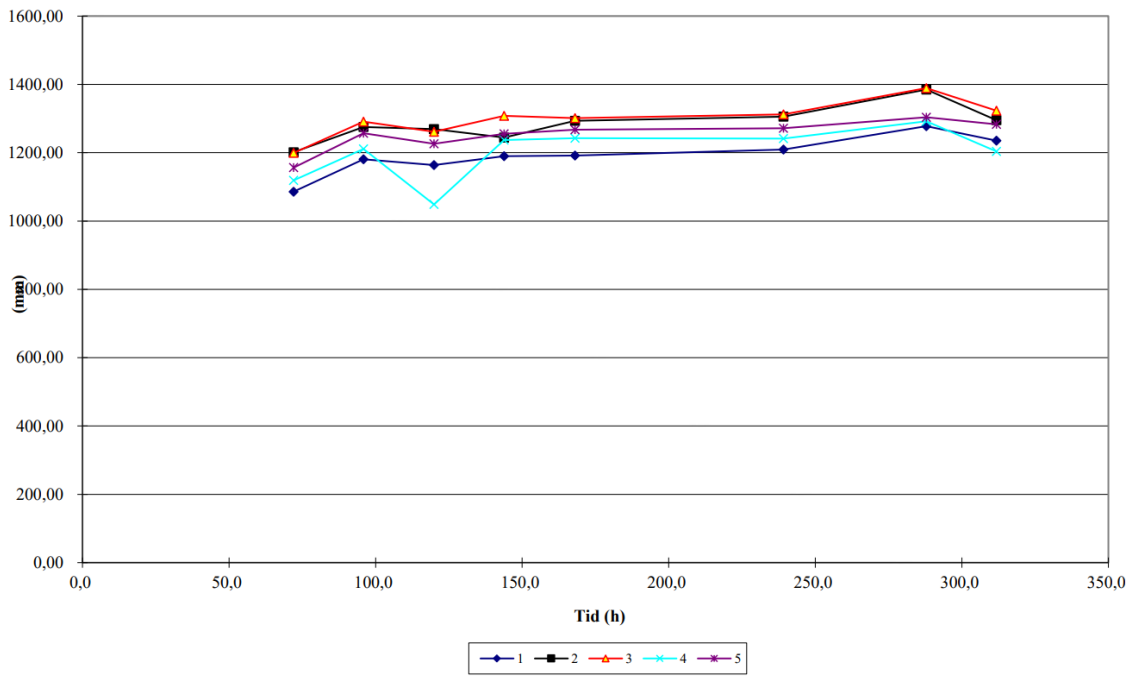
Ekvivalent luftlagstykkelse i perioden

Figure D.7.2: Equivalent air layer thickness sd-value during the period
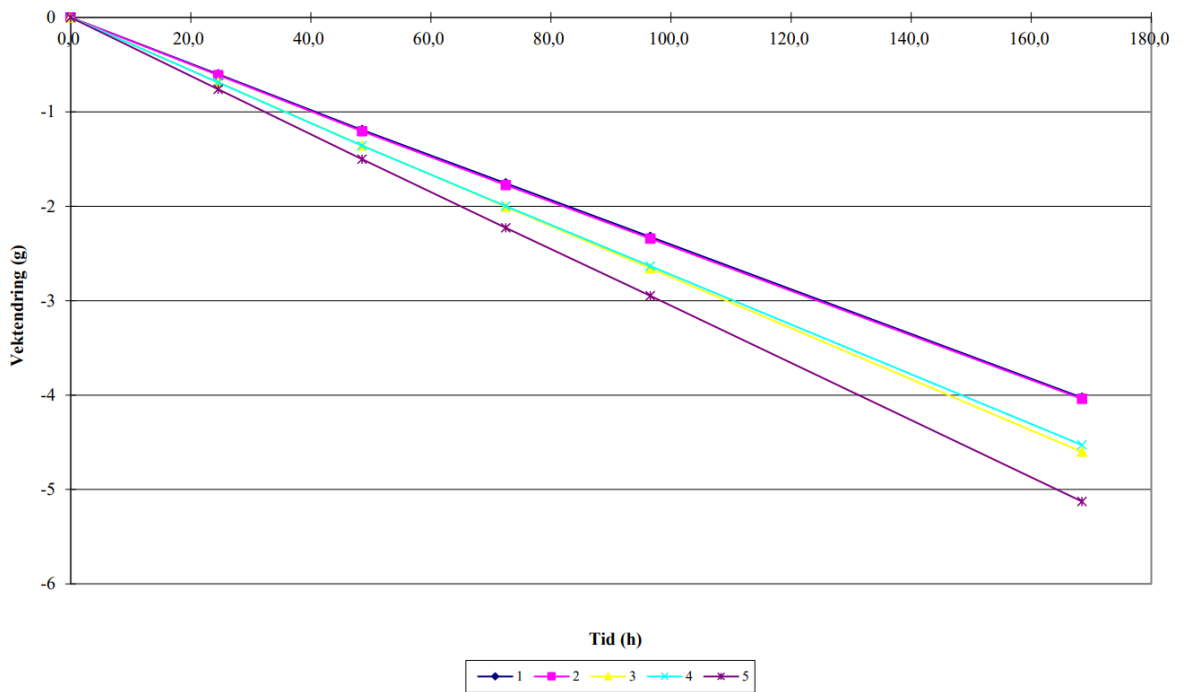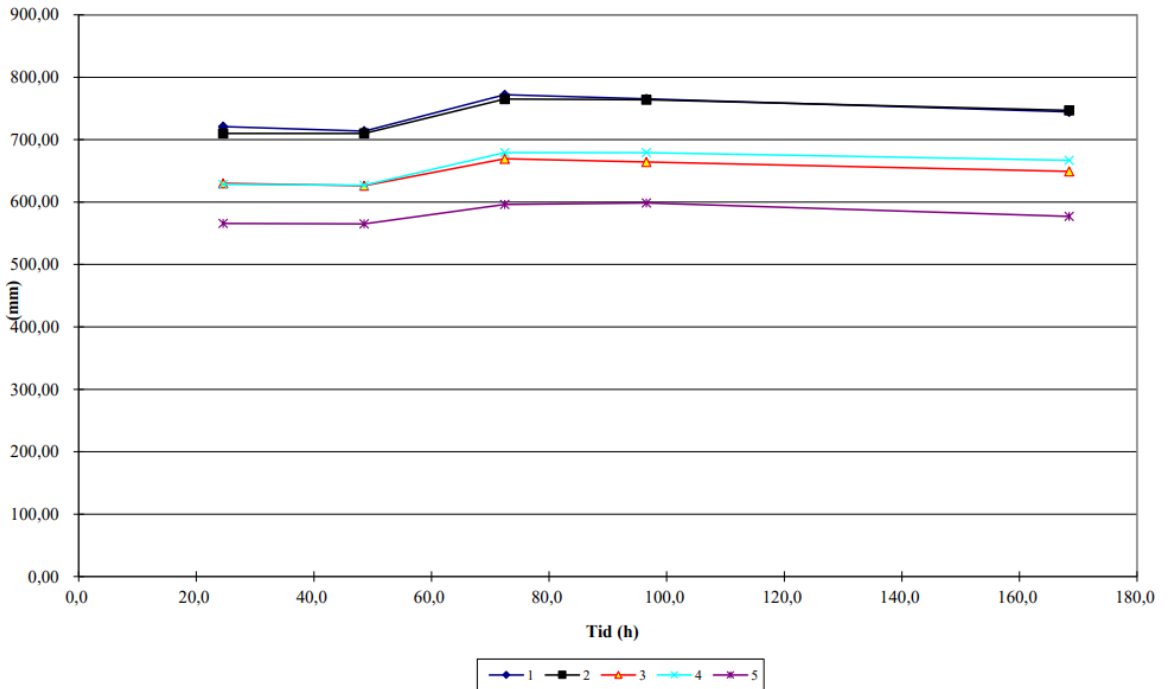
Vanndampgjennomgang i perioden

Figure D.7.3: Water vapour transmission during the period

Table D.7.1: Input data of the wet cup method

(1)Produktnavn:					Salttype:		KNO3
(2)Oppdragsgiver:	Masteroppgave_Katinka		Katinka		Prøvediameter (mm):		0,164
(3)Prosjektnummer:	53BX				Luftlag salt/prøve (mm):		15
(4)Produktype:	Maling				Prøvest. diameter(mm):		0,174
(5)Tykkelse, mm:	0,2500				Lufth. over pr.(m/s):		0,3
(6)Målenummer:	53BX				RF/Temp:		Vekt:
(12)Dato (CTRL+SHIFT+ ;)		24.01.2024	25.01.2024	26.01.2024	29.01.2024	30.01.2024	31.01.2024
(13)Tid (CTRL+SHIFT+ :)		09:31	09:24	09:20	09:19	09:16	09:14
(14)Beregning fra veiing:	2						
(15)Barometertrykk ved veiing, hPa:		973,97	1009,9	990,93	1003	1016,32	997,12
(16)Barometertrykk i perioden, hPa:		973,97	989,95	1006,39	999,1	1012,66	1008,85
(17)Temperatur luft over boks,°C:		23	23,04	23,04	23,03	23,02	23,03
(18)Temperatur i saltløsning, °C:		23	23,04	23,04	23,03	23,02	23,03
(19)RF i rommet, %		50	50,84	50,84	50,74	50,6	50,6
(20)Veiing nummer:		1	2	3	4	5	6
(21)Vekt,g kontrollodd før veiing:		1000,004	999,999	1000,002	1000,001	1000,002	1000,001
(22)Vekt,g prøve nr:	1	506,483	505,661	504,86	502,432	501,599	500,764
(23)Vekt,g prøve nr:	2	491,848	491,097	490,373	488,197	487,483	486,776
(24)Vekt,g prøve nr:	3	490,756	490,043	489,352	487,3	486,625	485,957
(25)Vekt,g prøve nr:	4	451,303	450,634	449,994	448,085	447,459	446,839
(26)Vekt,g prøve nr:	5	479,461	478,783	478,128	476,151	475,491	474,846
(27)Vekt,g kontrollodd etter veiing:		1000,005	999,998	1000,001	1000,002	999,998	1000

Prøvestykke:		1		2		3
Tykkelse:	0,25		0,25		0,25	
Side mot saltløsning:			Hvit side			
Ferkst/Aldret:			Ferskt			
Start kondisjonering:			11.01.2023			
	Tykkelsesmåler:			Stanse:		

D.8. Coating 53BX2 (Six Layers)

SINTEF

Produktnavn:	███████████	Tykkelse, mm:	0,42
Oppdragsgiver:	Masteroppgave_Katinka	Målenummer:	53BX2
Prosjektnummer:	53BX2	Prøvediameter: (mm)	164
Produkttype:	Maling	Salttype i boksen:	KNO3
		Prøveperiode: fra:	29.01.2024
		til:	02.02.2024

	Middel i prøveperioden		Lufth. over pr.(m/s):	0,3
Relativ luftfuktighet i boksen (%RF)	94,1		Tykkelse prøve nr	
Relativ luftfuktighet i rommet (%RF)	50,6		1	0,38
			2	0,46
Temperatur i boksen (°C)	23,0		3	0,50
Temperatur i rommet (°C)	23,0		4	0,43
			5	0,36
Barometertrykk (hPa)	999,0		6	0,62

Tabell 1   Temperatur, relativ luftfuktighet og barometertrykk i prøveperioden.

Prøve nummer	Vanndamppermeans Wp	Vanndampmotstand	
		sd	Zp
	(kg/m^2sPa)	(m)	(m^2sPa/kg)
1	2,53E-10	0,783	3,95E+09
2	1,90E-10	1,040	5,27E+09
3	1,94E-10	1,020	5,16E+09
4	2,10E-10	0,945	4,77E+09
5	2,25E-10	0,881	4,45E+09
Middel	2,14E-10	0,925	4,67E+09
Std. dev. mean. value	1,15079E-11	0,047	2,41E+08

Tabell 2   Vanndamppermeans og vanndampmotstand for de fem prøvestykkene.
Enkeltresultatene er et middel over fem tidsintervall med stabil fukttransport.
Resultatene er korrigert for overgangsmotstanden over prøven,
damptransport gjennom overlappsonen, og motstanden i luftlaget i boksen.

SIGN:

Vektendring siden start for de enkelte prøvene

Figure D.8.1: Mass reduction during the period

Ekvivalent luftlagstykkelse i perioden

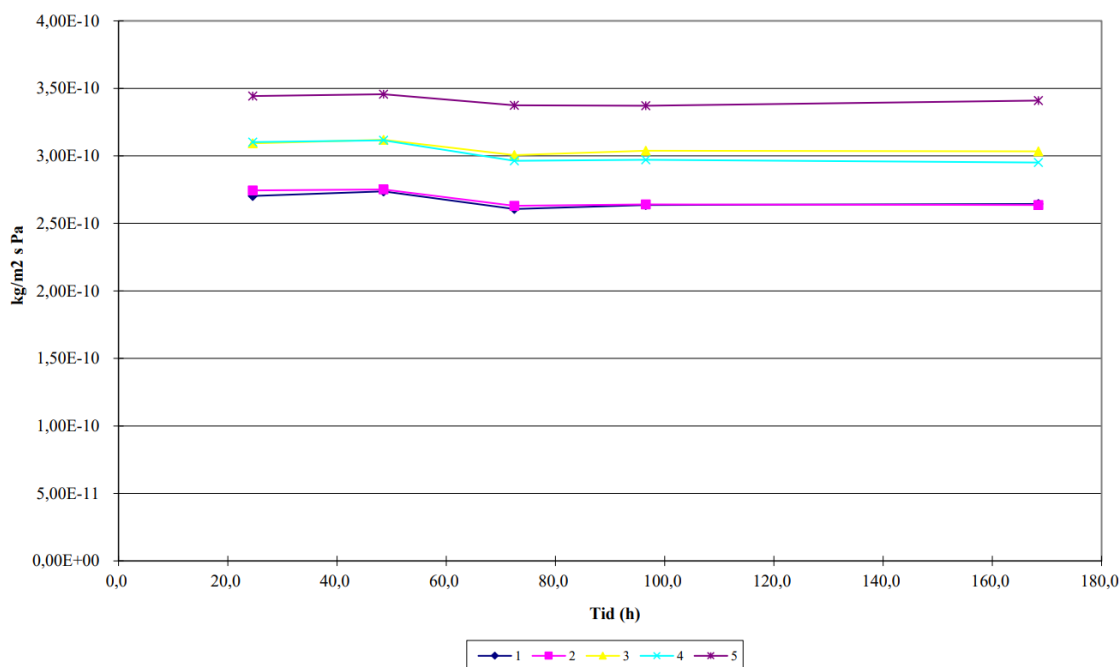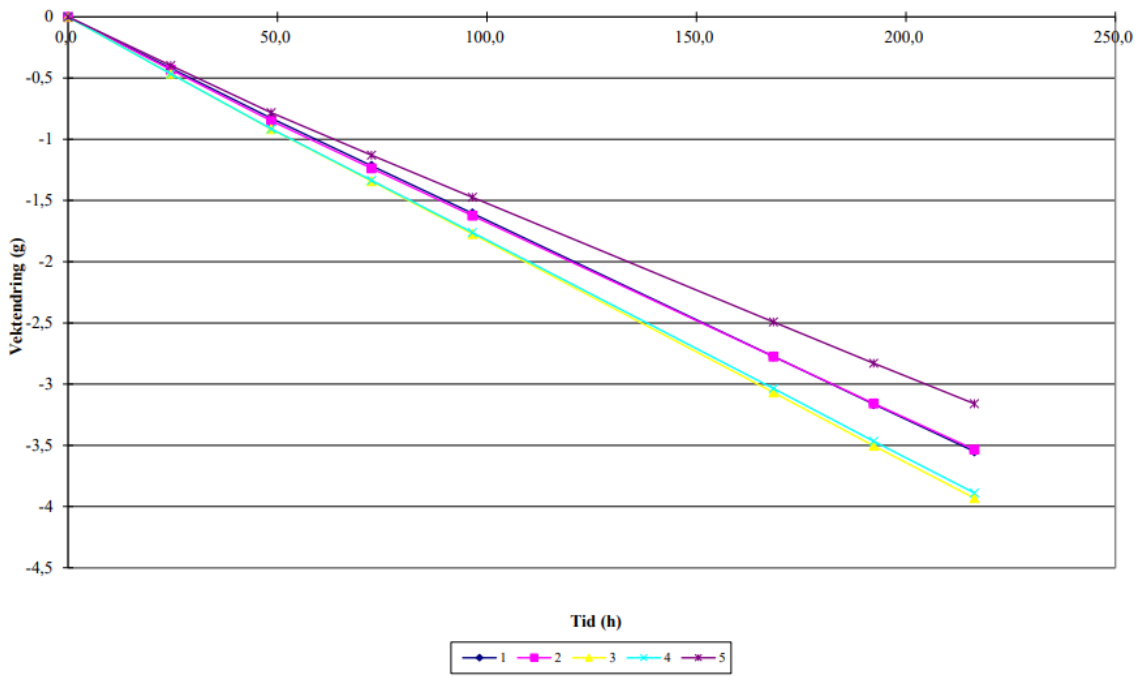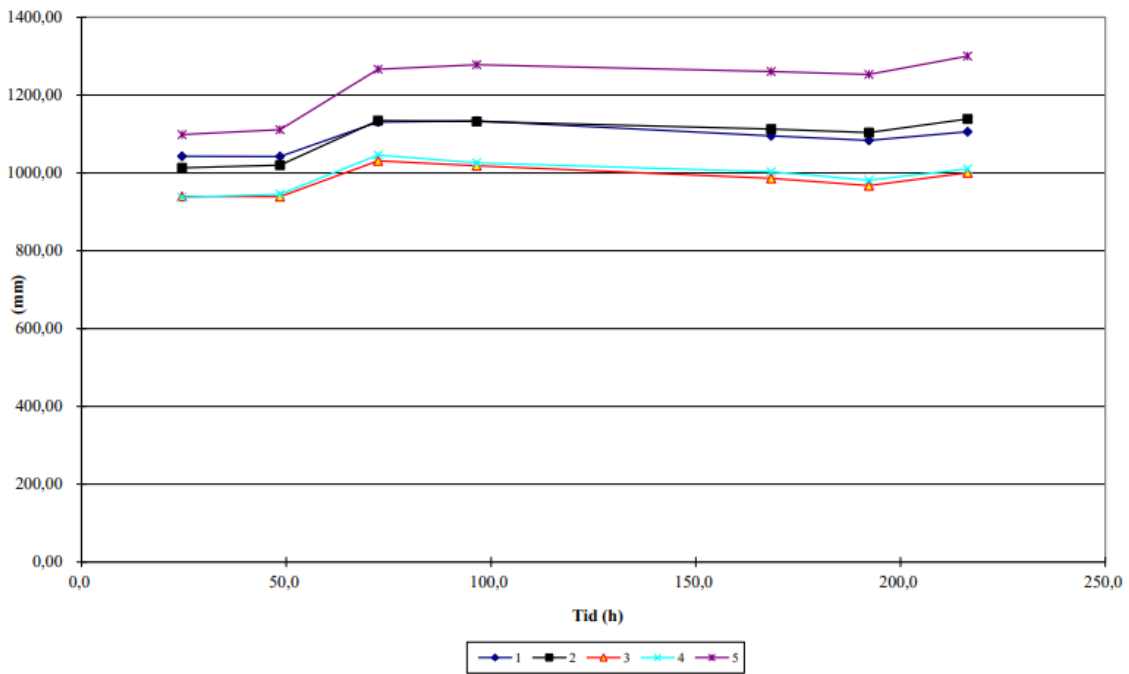**Figure D.8.2:** Equivalent air layer thickness sd-value during the period

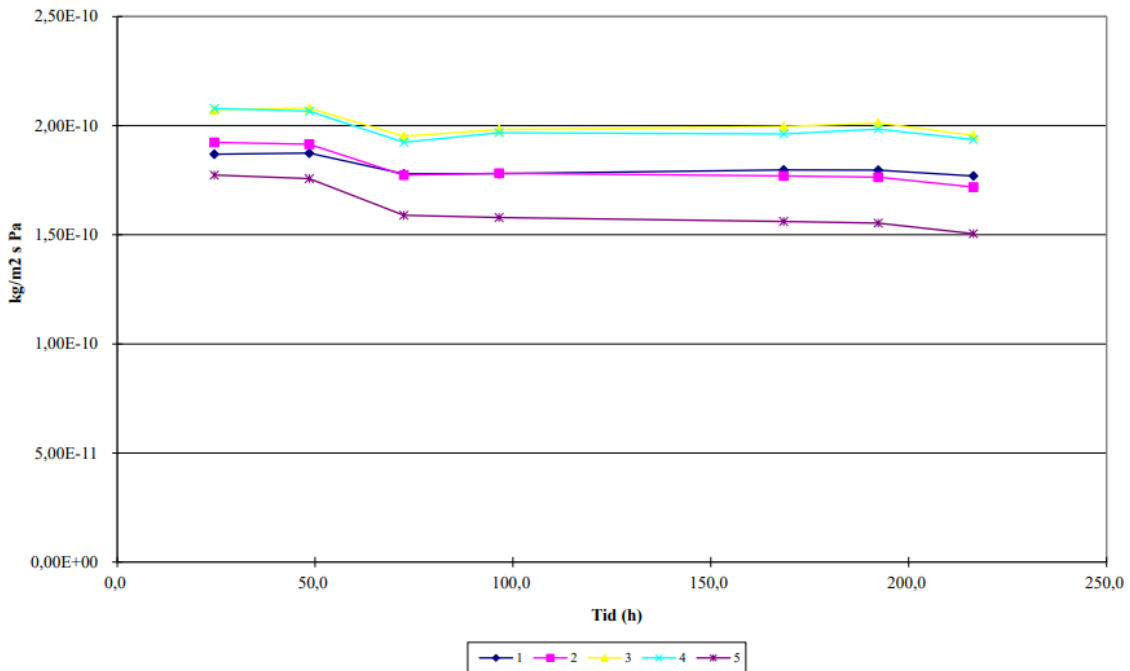**Figure D.8.3**: Water vapour transmission during the period

Table D.8.1: Input data of the wet cup method

(1)Produktnavn:						Salttype:		KNO3	Prøvestykke:		1	2	3
(2)Oppdragsgiver:	Masteroppgave_Katinka		Katinka			Prøvediameter (mm):		0,164	Tykkelse:	0,38		0,46	0,50
(3)Prosjektnummer:	53BX2					Luftlag salt/prøve (mm):		15	Side mot saltløsning:			Hvit side	
(4)Produkttype:	Maling					Prøvest. diameter(mm):		0,174	Ferkst/Aldret:			Ferskt	
(5)Tykkelse, mm:	0,4200					Lufth. over pr.(m/s):		0,3	Start kondisjonering:		11.03.2023		
(6)Målenummer:	53BX2					RF/Temp:			Vekt:		Tykkelsesmåler:		Stanse:
(12)Dato (CTRL+SHIFT+ ;)		24.01.2024	25.01.2024	26.01.2024	29.01.2024	30.01.2024	31.01.2024	01.02.2024	02.02.2024				
(13)Tid (CTRL+SHIFT+ :)		09:38	09:30	09:25	09:24	09:23	09:39	09:17	08:33				
(14)Beregning fra veiing:	4												
(15)Barometertrykk ved veiing, hPa:		973,97	1009,9	990,93	1003	1016,32	997,12	985,17	990,69				
(16)Barometertrykk i perioden, hPa:		973,97	989,95	1006,39	999,1	1012,66	1008,85	979,4	995,15				
(17)Temperatur luft over boks,°C:		23	23,04	23,04	23,03	23,02	23,03	23,04	23,03				
(18)Temperatur i saltløsning, °C:		23	23,04	23,04	23,03	23,02	23,03	23,04	23,03				
(19)RF i rommet, %		50	50,84	50,84	50,74	50,6	50,6	50,69	50,55				
(20)Veiing nummer:		1	2	3	4	5	6	7	8	9			10
(21)Vekt,g kontrollodd før veiing:		1000,004	1000,001	1000,002	1000,002	999,998	1000,004	1000,003	1000,002				
(22)Vekt,g prøve nr:	1	523,596	523,03	522,487	520,852	520,309	519,755	519,203	518,641				
(23)Vekt,g prøve nr:	2	515,169	514,7	514,271	513,008	512,592	512,183	511,777	511,364				
(24)Vekt,g prøve nr:	3	490,251	489,781	489,335	488,037	487,605	487,19	486,778	486,371				
(25)Vekt,g prøve nr:	4	475,063	474,565	474,09	472,687	472,228	471,774	471,329	470,889				
(26)Vekt,g prøve nr:	5	501,588	501,036	500,523	499,029	498,535	498,048	497,573	497,096				
(27)Vekt,g kontrollodd etter veiing:		1000,007	1000,002	1000,001	1000,005	999,999	1000,004	1000,004	1000,001				

D.9. Coating 54B (Three Layers)

SINTEF

Produktnavn:	████████████	Tykkelse, mm:	0,28
Oppdragsgiver:	Masteroppgave_Katinka	Målenummer:	54B
Prosjektnummer:	54B	Prøvediameter: (mm)	164
Produkttype:	Maling	Salttype i boksen:	KNO3
		Prøveperiode: fra:	25.01.2024
		til:	31.01.2024

	Middel i prøveperioden
Relativ luftfuktighet i boksen (%RF)	94,1
Relativ luftfuktighet i rommet (%RF)	50,7
Temperatur i boksen (°C)	23,0
Temperatur i rommet (°C)	23,0
Barometertrykk (hPa)	1003,4

Lufth. over pr.(m/s): 0,3

Tykkelse prøve nr

1	0,25
2	0,30
3	0,27
4	0,26
5	0,32
6	0,20

Tabell 1   Temperatur, relativ luftfuktighet og barometertrykk i prøveperioden.

Prøve nummer	Vanndamppermeans Wp	Vanndampmotstand	
		sd	Zp
	(kg/m²sPa)	(m)	(m²sPa/kg)
1	2,88E-10	0,684	3,47E+09
2	2,38E-10	0,829	4,21E+09
3	2,55E-10	0,773	3,92E+09
4	2,55E-10	0,772	3,92E+09
5	2,16E-10	0,911	4,62E+09
Middel	2,51E-10	0,787	3,99E+09
Std. dev. mean. value	1,18236E-11	0,037	1,90E+08

Tabell 2   Vanndamppermeans og vanndampmotstand for de fem prøvestykkene.
Enkeltresultatene er et middel over fem tidsintervall med stabil fukttransport.
Resultatene er korrigert for overgangsmotstanden over prøven,
damptransport gjennom overlappsonen, og motstanden i luftlaget i boksen.

SIGN:

Vektendring siden start for de enkelte prøvene

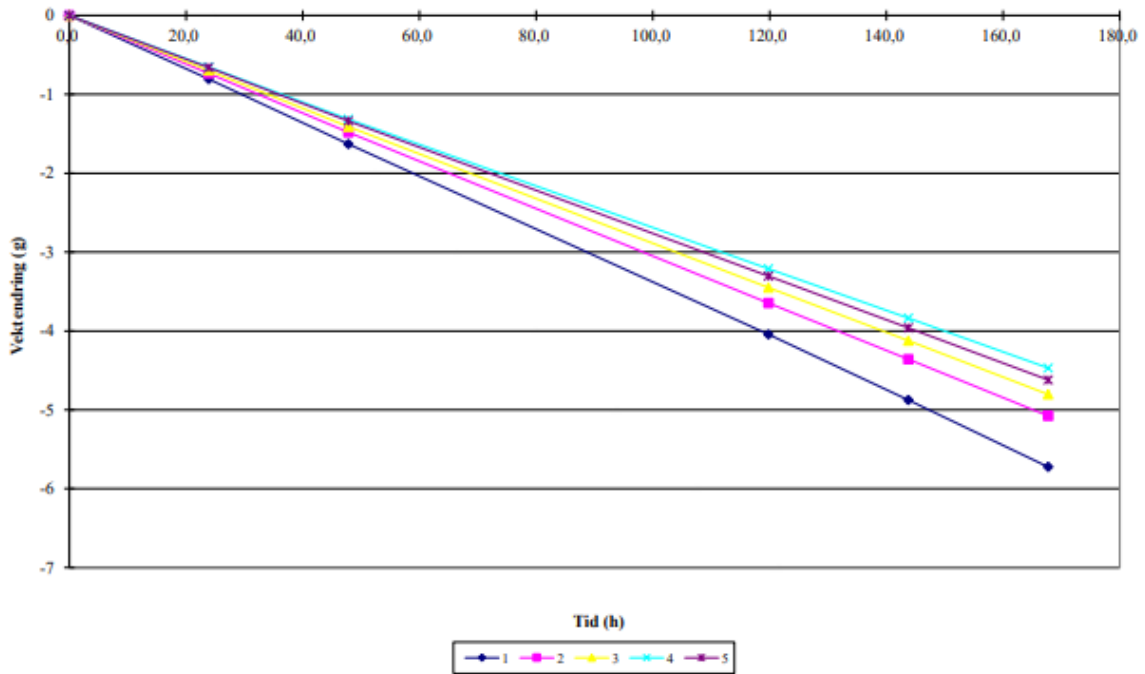**Figure D.9.1**: Mass reduction during the period

Ekvivalent luftlagstykkelse i perioden

Figure D.9.2: Equivalent air layer thickness sd-value during the period
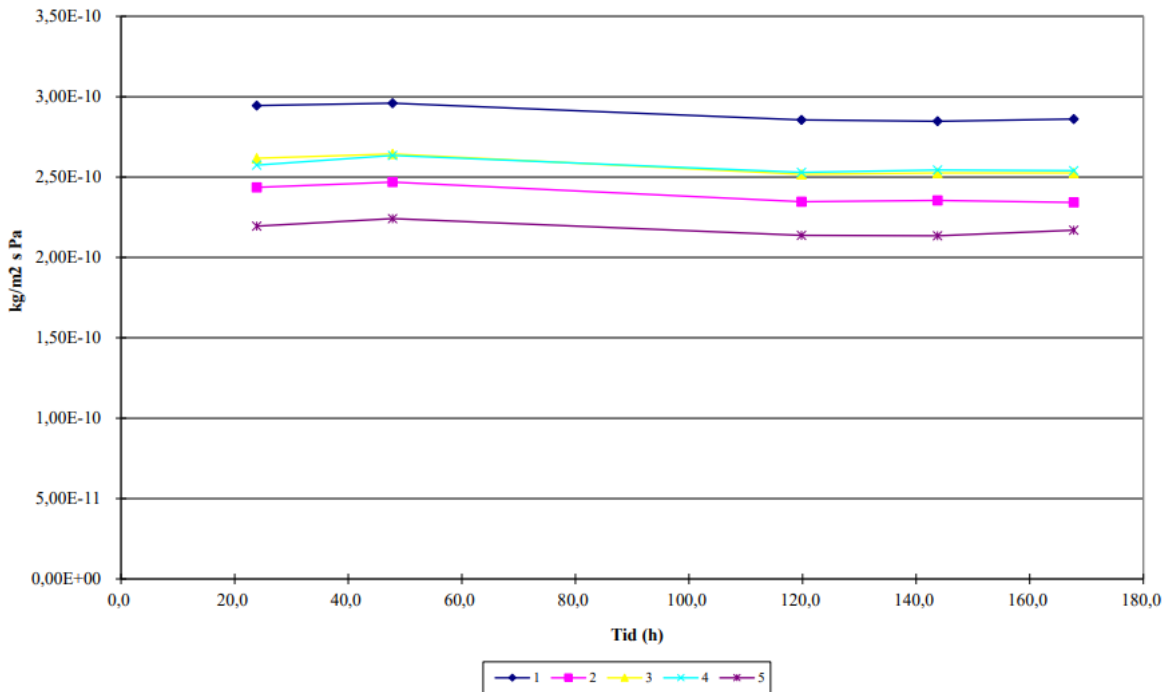
Figure D.9.3: Water vapour transmission during the period

Table D.9.1: Input data of the wet cup method

(1)Produktnavn:	███████████			Salttype:		KNO3
(2)Oppdragsgiver:	Masteroppgave_Katinka	Katina		Prøvediameter (mm):		0,164
(3)Prosjektnummer:	54B			Luftlag salt/prøve (mm):		15
(4)Produkttype:	Maling			Prøvest. diameter(mm):		0,174
(5)Tykkelse, mm:	0,2800			Lufth. over pr.(m/s):		0,3
(6)Målenummer:	54B			RF/Temp:		Vekt:
(12)Dato (CTRL+SHIFT+ ;)		24.01.2024	25.01.2024	26.01.2024	29.01.2024	30.01.2024	31.01.2024
(13)Tid (CTRL+SHIFT+ :)		09:42	09:35	09:30	09:30	09:27	09:26
(14)Beregning fra veiing:	2					
(15)Barometertrykk ved veiing, hPa:		973,97	1009,9	990,93	1003	1016,32	997,12
(16)Barometertrykk i perioden, hPa:		973,97	989,95	1006,39	999,1	1012,66	1008,85
(17)Temperatur luft over boks,°C:		23	23,04	23,04	23,03	23,02	23,03
(18)Temperatur i saltløsning, °C:		23	23,04	23,04	23,03	23,02	23,03
(19)RF i rommet, %		50	50,84	50,84	50,74	50,6	50,6
(20)Veiing nummer:		1	2	3	4	5	6
(21)Vekt,g kontrolllodd før veiing:		1000,004	999,999	1000,002	1000,002	999,998	1000,004
(22)Vekt,g prøve nr:	1	524,166	523,516	522,902	521,033	520,415	519,808
(23)Vekt,g prøve nr:	2	505,781	505,238	504,727	503,181	502,667	502,17
(24)Vekt,g prøve nr:	3	475,743	475,162	474,614	472,96	472,41	471,874
(25)Vekt,g prøve nr:	4	494,082	493,51	492,964	491,302	490,748	490,209
(26)Vekt,g prøve nr:	5	506,313	505,821	505,358	503,946	503,479	503,019
(27)Vekt,g kontrollodd etter veiing:		1000,006	1000	1000,005	999,999	1000	1000,001

Prøvestykke:		1		2		3
Tykkelse:	0,25		0,30		0,27	
Side mot saltløsning:			Hvit side			
Ferkst/Aldret:			Ferskt			
Start kondisjonering:			25-10-2023			
	Tykkelsesmåler:				Stanse:	

D.10. Coating 54B2 (Six Layers)

SINTEF

Produktnavn:	▬▬▬▬▬▬
Oppdragsgiver:	Masteroppgave_Katinka
Prosjektnummer:	54B2
Produkttype:	Maling

Tykkelse, mm:	0,41
Målenummer:	54B2
Prøvediameter: (mm)	164
Salttype i boksen:	KNO3
Prøveperiode: fra:	25.01.2024
til:	31.01.2024

	Middel i prøveperioden
Relativ luftfuktighet i boksen (%RF)	94,1
Relativ luftfuktighet i rommet (%RF)	50,7
Temperatur i boksen (°C)	23,0
Temperatur i rommet (°C)	23,0
Barometertrykk (hPa)	1003,4

Lufth. over pr.(m/s): 0,3

Tykkelse prøve nr

1	0,39
2	0,40
3	0,42
4	0,44
5	0,42
6	0,30

Tabell 1   Temperatur, relativ luftfuktighet og barometertrykk i prøveperioden.

Prøve nummer	Vanndamppermeans Wp (kg/m²sPa)	Vanndampmotstand	
		sd (m)	Zp (m²sPa/kg)
1	2,01E-10	0,981	4,98E+09
2	1,75E-10	1,120	5,71E+09
3	1,49E-10	1,320	6,70E+09
4	1,90E-10	1,030	5,25E+09
5	1,73E-10	1,140	5,79E+09
Middel	1,78E-10	1,110	5,63E+09
Std. dev. mean. value	8,79532E-12	0,058	2,95E+08

Tabell 2   Vanndamppermeans og vanndampmotstand for de fem prøvestykkene.
Enkeltresultatene er et middel over fem tidsintervall med stabil fukttransport.
Resultatene er korrigert for overgangsmotstanden over prøven,
damptransport gjennom overlappsonen, og motstanden i luftlaget i boksen.

SIGN:

Vektendring siden start for de enkelte prøvene

Figure D.10.1: Mass reduction during the period
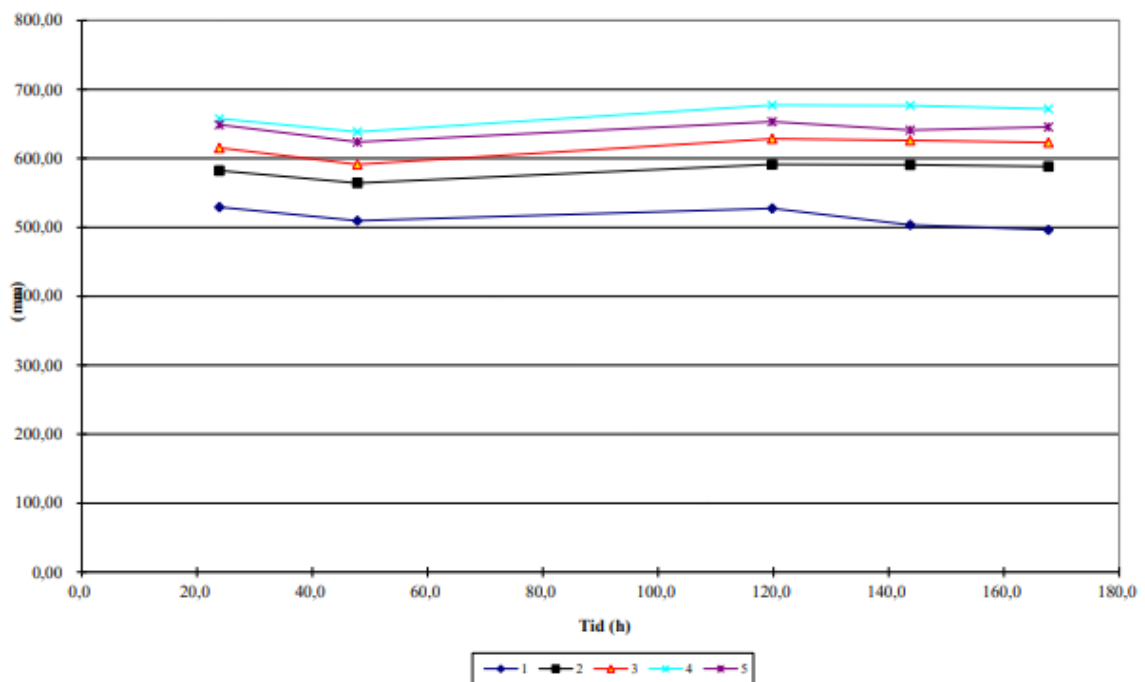
Ekvivalent luftlagstykkelse i perioden

Figure D.10.2: Equivalent air layer thickness sd-value during the period
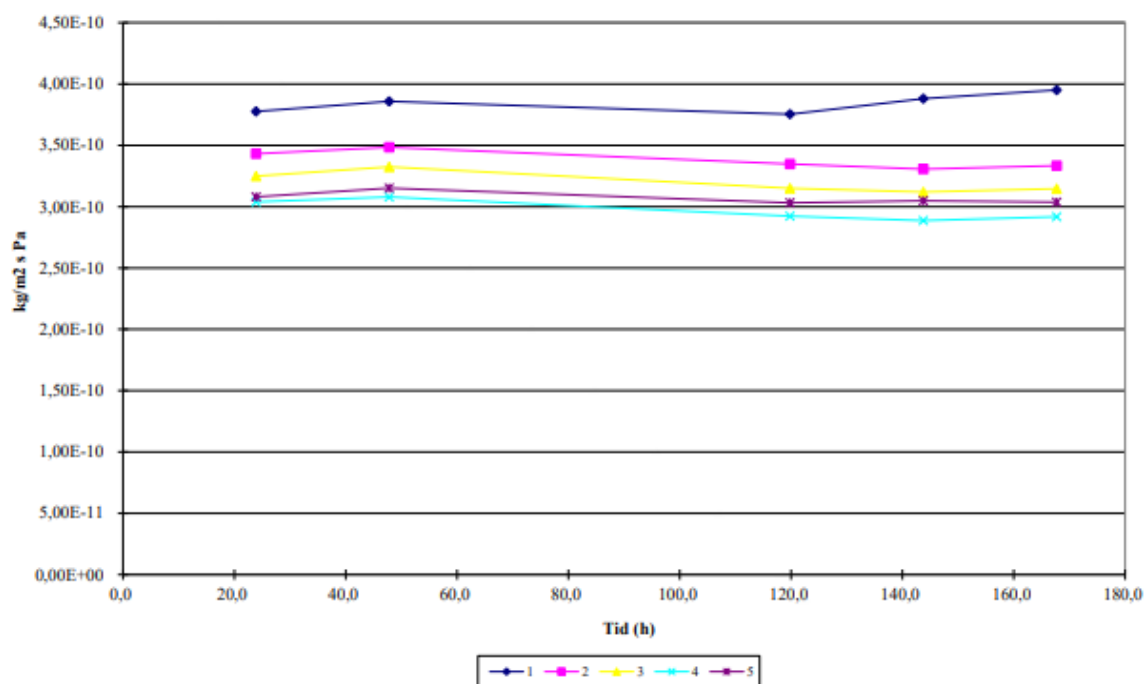
Vanndampgjennomgang i perioden

Figure D.10.3: Water vapour transmission during the period

Table D.10.1: Input data of the wet cup method

(1)Produktnavn:		███████			Salttype:			KNO3
(2)Oppdragsgiver:		Masteroppgave_Katinka		Katinka	Prøvediameter (mm):			0,164
(3)Prosjektnummer:		54B2			Luftlag salt/prøve (mm):			15
(4)Produktype:		Maling			Prøvest. diameter(mm):			0,174
(5)Tykkelse, mm:		0,4100			Lufth. over pr.(m/s):			0,3
(6)Målenummer:		54B2			RF/Temp:		Vekt:	
(12)Dato (CTRL+SHIFT+ ;)			24.01.2024	25.01.2024	26.01.2024	29.01.2024	30.01.2024	31.01.2024
(13)Tid (CTRL+SHIFT+ :)			09:49	09:40	09:35	09:36	09:32	09:33
(14)Beregning fra veiing:	2							
(15)Barometertrykk ved veiing, hPa:			973,97	1009,9	990,93	1003	1016,32	997,12
(16)Barometertrykk i perioden, hPa:			973,97	989,95	1006,39	999,1	1012,66	1008,85
(17)Temperatur luft over boks,°C:			23	23,04	23,04	23,03	23,02	23,03
(18)Temperatur i saltløsning, °C:			23	23,04	23,04	23,03	23,02	23,03
(19)RF i rommet, %			50	50,84	50,84	50,74	50,6	50,6
(20)Veiing nummer:			1	2	3	4	5	6
(21)Vekt,g kontrollodd før veiing:			1000,003	1000	1000,001	1000,001	999,999	1000,002
(22)Vekt,g prøve nr:		1	513,184	512,719	512,28	510,973	510,541	510,12
(23)Vekt,g prøve nr:		2	495,886	495,485	495,107	493,958	493,574	493,208
(24)Vekt,g prøve nr:		3	519,339	519,007	518,686	517,698	517,371	517,054
(25)Vekt,g prøve nr:		4	524,836	524,397	523,987	522,741	522,33	521,929
(26)Vekt,g prøve nr:		5	585,578	585,184	584,812	583,679	583,302	582,937
(27)Vekt,g kontrollodd etter veiing:			1000,004	1000,002	1000,004	1000,002	1000	1000,002

Prøvestykke:	1	2	3
Tykkelse:	0,39	0,40	0,42
Side mot saltløsning:		Hvit side	
Ferkst/Aldret:		Ferskt	
Start kondisjonering:		27-10-2023	
Tykkelsesmåler:		Stanse:	

D.11. Coating 55B (Three Layers)

SINTEF

Produktnavn:	▉▉▉▉▉	Tykkelse, mm:	0,26
Oppdragsgiver:	Masteroppgave_Katinka	Målenummer:	55B
Prosjektnummer:	55B	Prøvediameter: (mm)	164
Produkttype:	Maling	Salttype i boksen:	KNO3
		Prøveperiode: fra:	06.02.2024
		til:	12.02.2024

	Middel i prøveperioden
Relativ luftfuktighet i boksen (%RF)	94,1
Relativ luftfuktighet i rommet (%RF)	50,5
Temperatur i boksen (°C)	23,0
Temperatur i rommet (°C)	23,0
Barometertrykk (hPa)	993,6

Lufth. over pr.(m/s): 0,3

Tykkelse prøve nr

1 0,26
2 0,24
3 0,26
4 0,28
5 0,26
6 0,32

Tabell 1   Temperatur, relativ luftfuktighet og barometertrykk i prøveperioden.

Prøve nummer	Vanndamppermeans W_p	Vanndampmotstand	
		sd	Z_p
	(kg/m²sPa)	(m)	(m²sPa/kg)
1	1,82E-10	1,090	5,50E+09
2	1,88E-10	1,060	5,33E+09
3	1,94E-10	1,030	5,16E+09
4	1,68E-10	1,190	5,96E+09
5	1,81E-10	1,100	5,52E+09
Middel	1,82E-10	1,090	5,48E+09
Std. dev. mean. value	4,31434E-12	0,027	1,34E+08

Tabell 2   Vanndamppermeans og vanndampmotstand for de fem prøvestykkene.
Enkeltresultatene er et middel over fem tidsintervall med stabil fukttransport.
Resultatene er korrigert for overgangsmotstanden over prøven,
damptransport gjennom overlappsonen, og motstanden i luftlaget i boksen.

SIGN:

Vektendring siden start for de enkelte prøvene

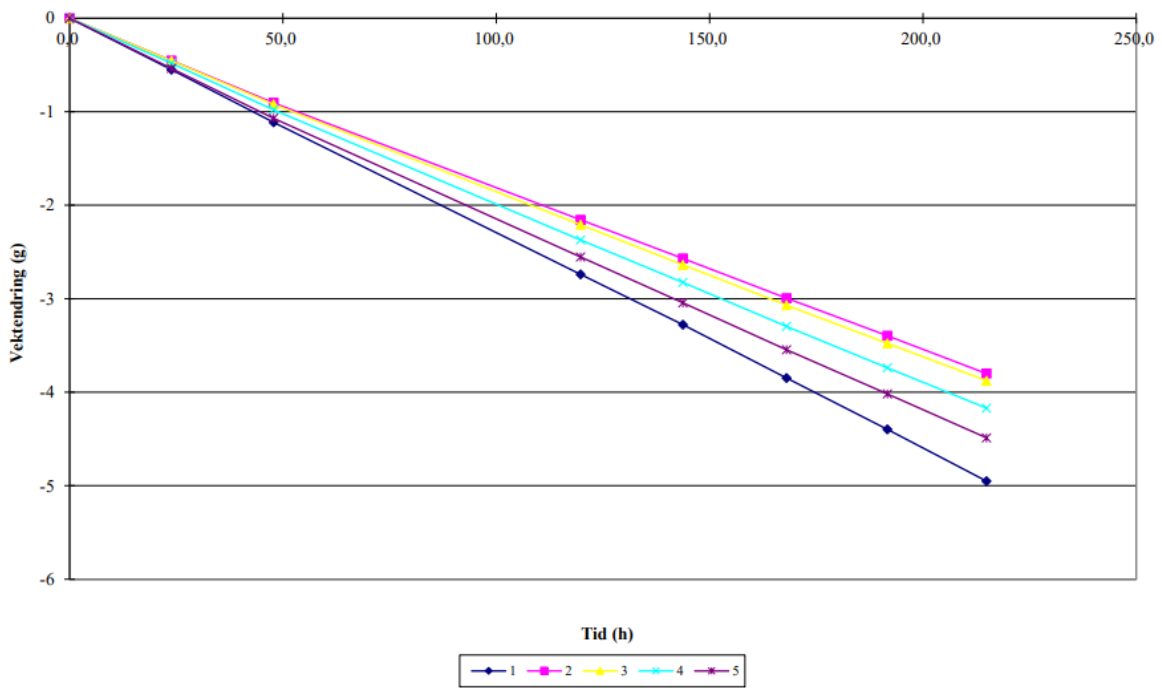**Figure D.11.1**: Mass reduction during the period
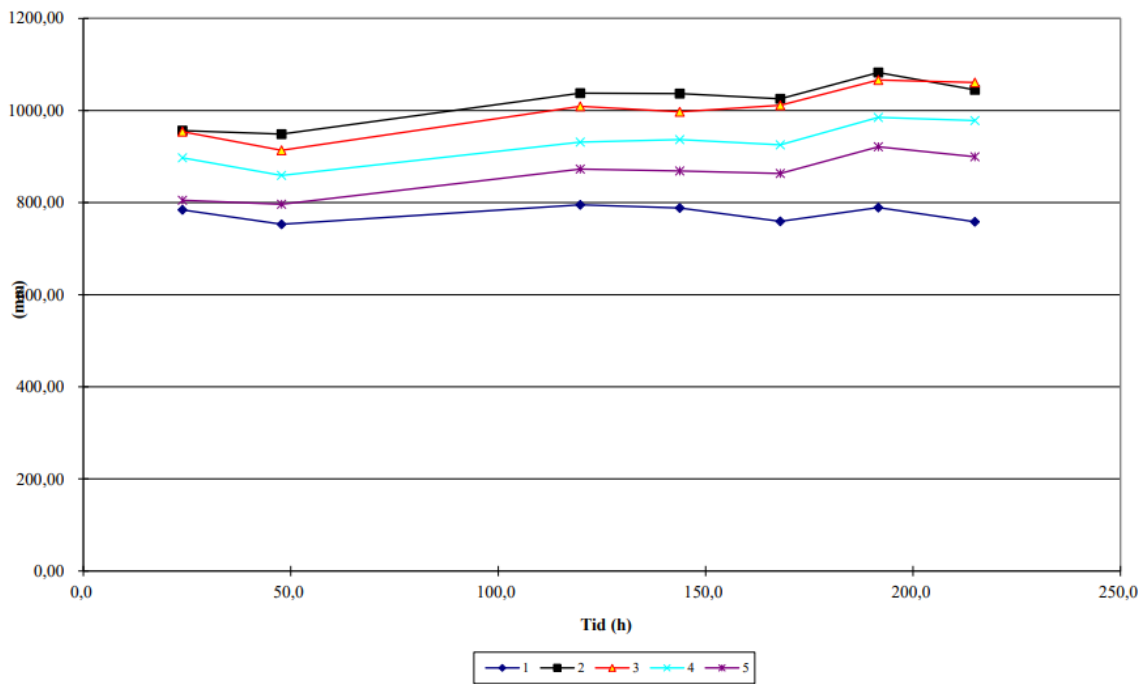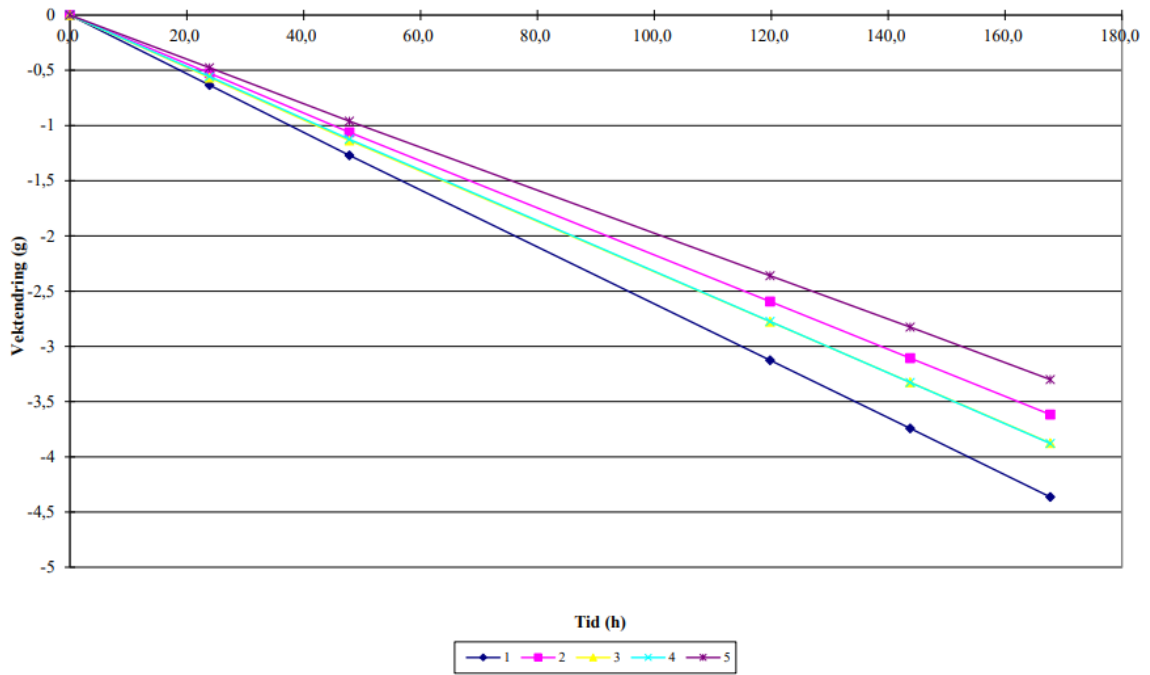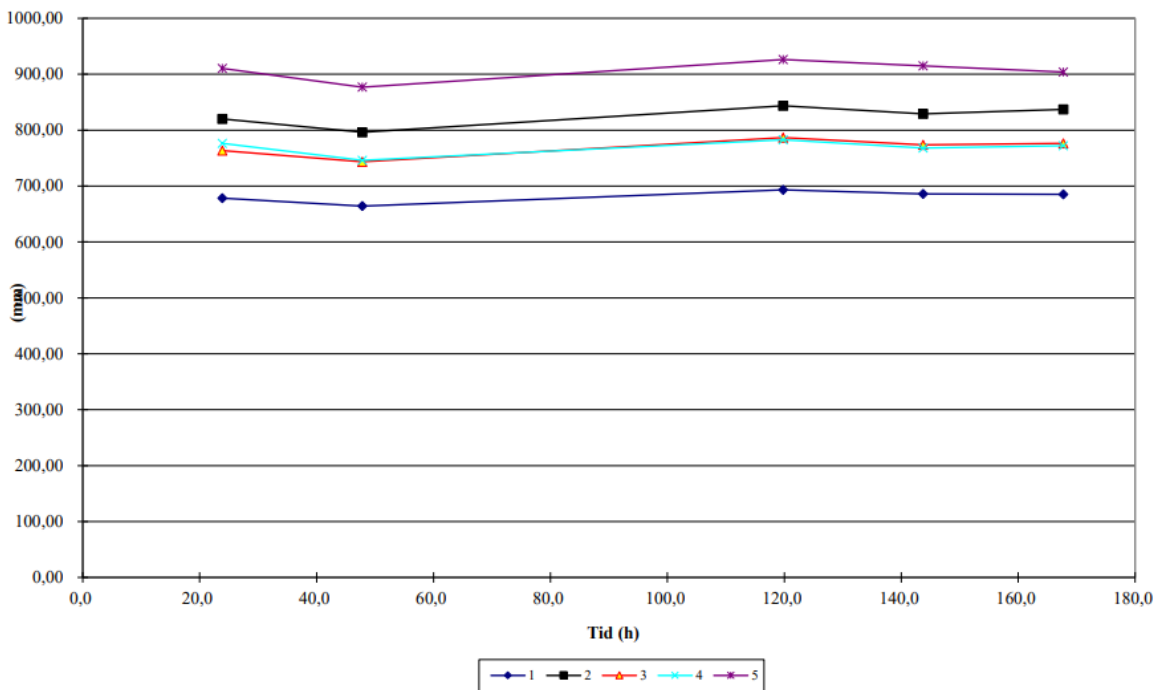
Ekvivalent luftlagstykkelse i perioden

Figure D.11.2: Equivalent air layer thickness sd-value during the period

Vanndampgjennomgang i perioden

Figure D.11.3: Water vapour transmission during the period

Table D.11.1: Input data of the wet cup method

					Salttype:		KNO3	Prøvestykke:		1		2	3
(1)Produktnavn:	███████												
(2)Oppdragsgiver:	Masteroppgave Katinka		Katinka		Prøvediameter (mm):		0,164	Tykkelse:	0,26			0,24	0,26
(3)Prosjektnummer:	55B				Luftlag salt/prøve (mm):		15	Side mot saltløsning:		Hvit side			
(4)Produkttype:	Maling				Prøvest. diameter(mm):		0,174	Ferskt/Aldret:		Ferskt			
(5)Tykkelse, mm:	0,2600				Lufth. over pr.(m/s):		0,3	Start kondisjonering:		01.11.2023			
(6)Målenummer:	55B				RF/Temp:			Vekt:		Tykkelsesmåler:			Stanse:

(12)Dato (CTRL+SHIFT+ ;)		02.02.2024	05.02.2024	06.02.2024	07.02.2024	08.02.2024	09.02.2024	12.02.2024					
(13)Tid (CTRL+SHIFT+ :)		08:39	09:20	09:45	09:24	09:14	09:12	09:14					
(14)Beregning fra veiing:	3												
(15)Barometertrykk ved veiing, hPa:		990,69	989,17	991,52	991,07	990,94	998,82	1000,01					
(16)Barometertrykk i perioden, hPa:		990,69	981,49	993,28	989,43	990,2	994,47	1000,84					
(17)Temperatur luft over boks,°C:		23	23,03	23,03	23,02	23,03	23,02	23,02					
(18)Temperatur i saltløsning, °C:		23	23,03	23,03	23,02	23,03	23,02	23,02					
(19)RF i rommet, %:		50	50,78	50,67	50,47	50,47	50,34	50,34					
(20)Veiing nummer:		1	2	3	4	5	6	7	8		9		10
(21)Vekt,g kontrollodd før veiing:		1000,003	1000,006	1000,004	1000,003	1000	1000,000	1000,001					
(22)Vekt,g prøve nr:	1	582,624	581,374	580,953	580,558	580,155	579,754	578,568					
(23)Vekt,g prøve nr:	2	493,59	492,279	491,848	491,435	491,02	490,604	489,385					
(24)Vekt,g prøve nr:	3	511,29	509,901	509,452	509,025	508,597	508,172	506,916					
(25)Vekt,g prøve nr:	4	509,912	508,718	508,327	507,957	507,588	507,217	506,126					
(26)Vekt,g prøve nr:	5	538,55	537,296	536,878	536,486	536,086	535,682	534,499					
(27)Vekt,g kontrolllodd etter veiing:		1000,004	1000,006	1000,003	1000,003	1000,006	1000,002	1000,001					

D.12. Coating 55B2 (Six Layers)

◯ SINTEF

PRØVINGS RAPPORT
Prøving av vanndamppermeans etter ISO/DIS 12572

Produktnavn:	████████████	Tykkelse, mm:	0,41
Oppdragsgiver:	Masteroppgave_Katinka	Målenummer:	55B2
Prosjektnummer:	55B2	Prøvediameter: (mm)	164
Produkttype:	Maling	Salttype i boksen:	KNO3
		Prøveperiode: fra:	07.02.2024
		til:	13.02.2024

	Middel i prøveperioden
Relativ luftfuktighet i boksen (%RF)	94,1
Relativ luftfuktighet i rommet (%RF)	50,5
Temperatur i boksen (°C)	23,0
Temperatur i rommet (°C)	23,0
Barometertrykk (hPa)	995,2

Lufth. over pr.(m/s): 0,3

Tykkelse prøve nr

1 0,40
2 0,36
3 0,49
4 0,43
5 0,37
6 0,34

Tabell 1   Temperatur, relativ luftfuktighet og barometertrykk i prøveperioden.

Prøve nummer	Vanndamppermeans W_p	Vanndampmotstand	
		sd	Z_p
	(kg/m²sPa)	(m)	(m²sPa/kg)
1	1,29E-10	1,540	7,72E+09
2	1,42E-10	1,400	7,04E+09
3	1,13E-10	1,760	8,85E+09
4	1,26E-10	1,570	7,91E+09
5	1,40E-10	1,420	7,14E+09
Middel	1,30E-10	1,530	7,68E+09
Std. dev. mean. value	5,23718E-12	0,065	3,25E+08

Tabell 2   Vanndamppermeans og vanndampmotstand for de fem prøvestykkene.
Enkeltresultatene er et middel over fem tidsintervall med stabil fukttransport.
Resultatene er korrigert for overgangsmotstanden over prøven,
damptransport gjennom overlappsonen, og motstanden i luftlaget i boksen.

SIGN:

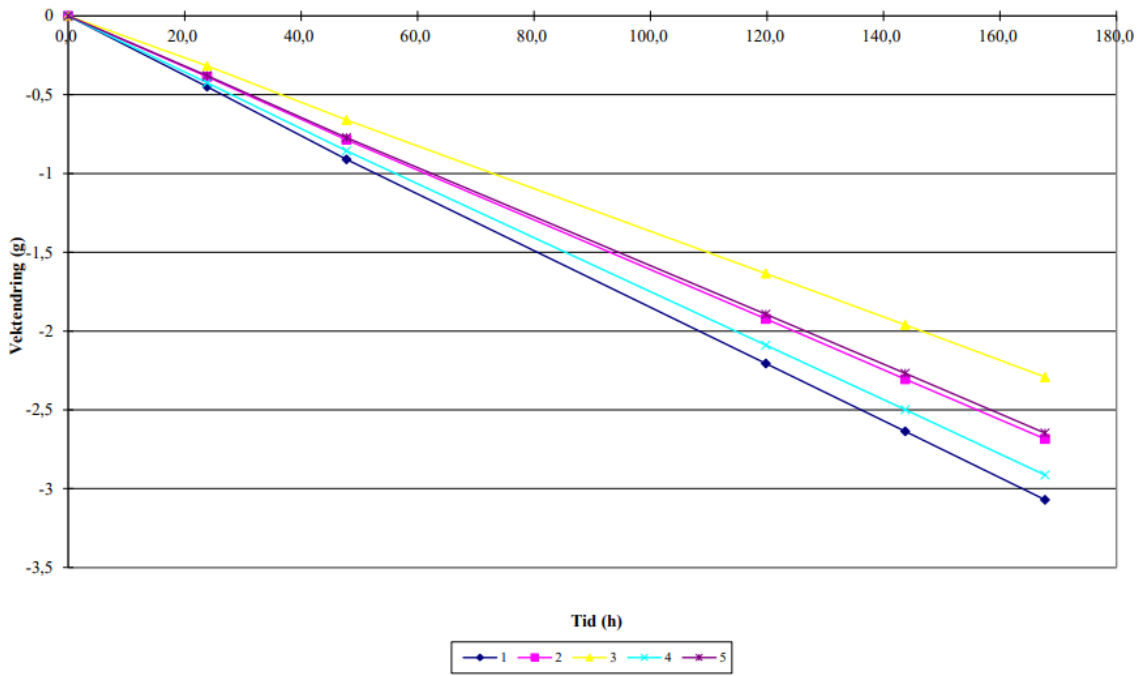Vektendring siden start for de enkelte prøvene

Figure D.12.1: Mass reduction during the period
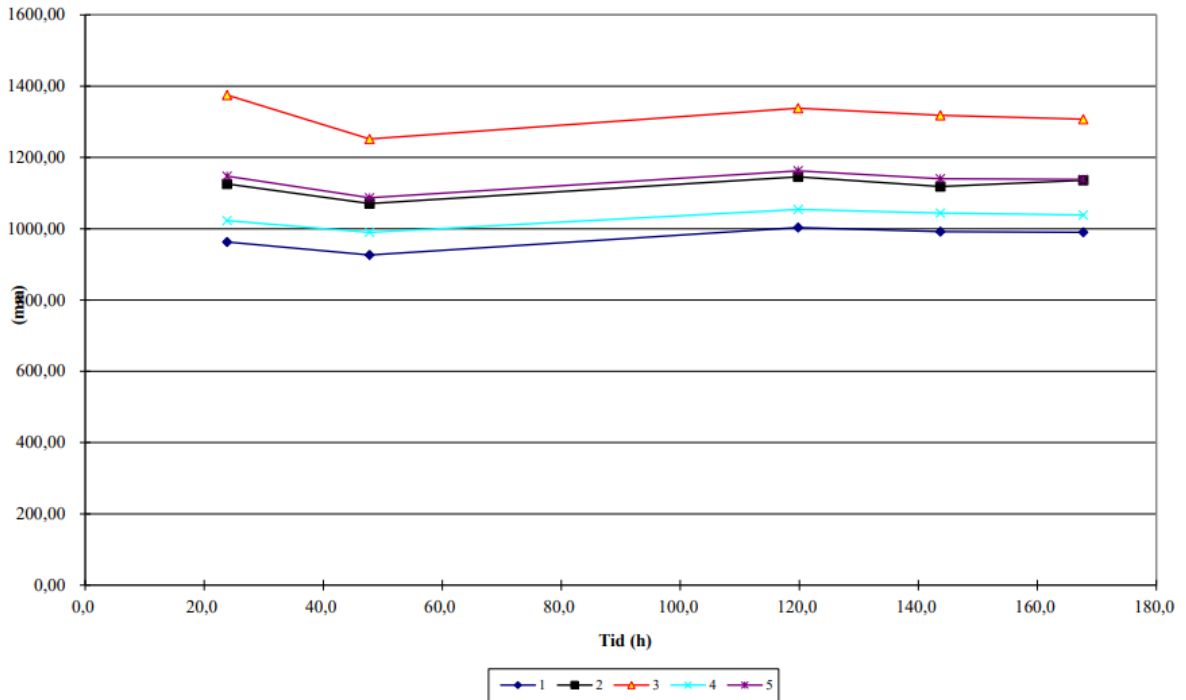
Ekvivalent luftlagstykkelse i perioden

Figure D.12.2: Equivalent air layer thickness sd-value during the period
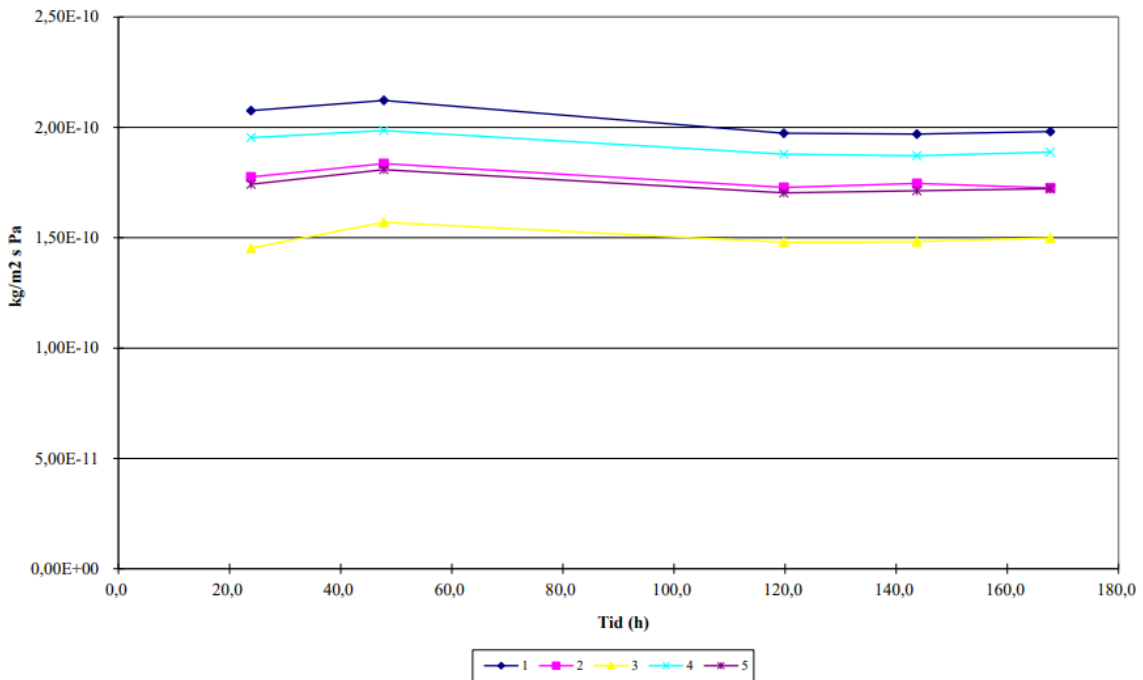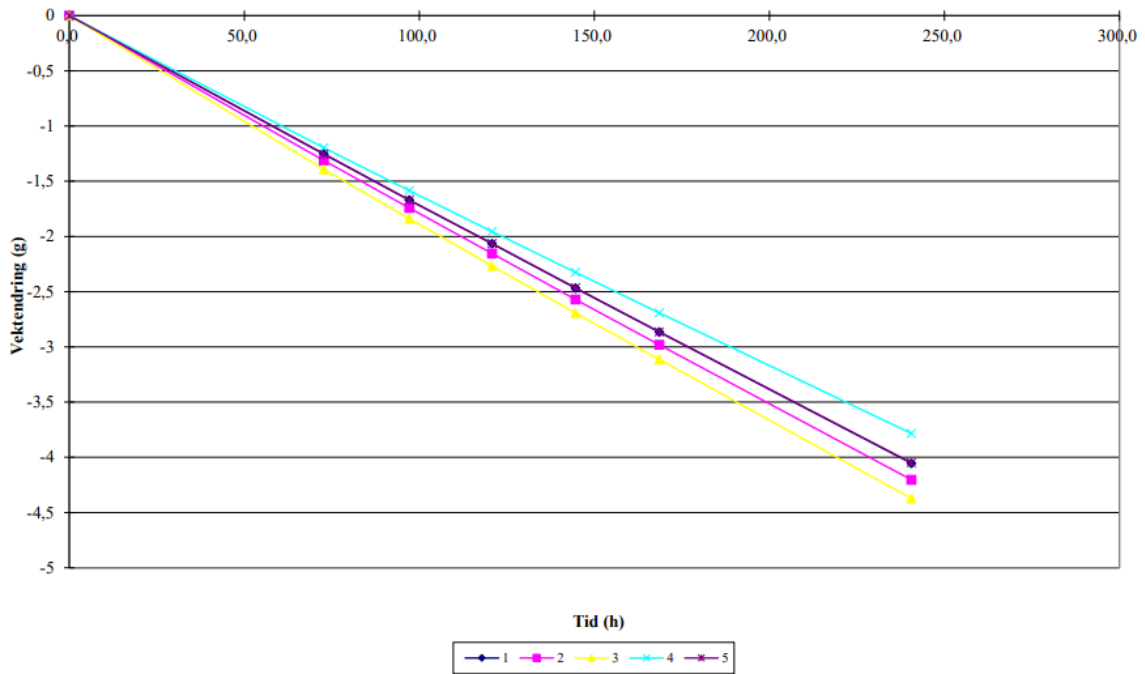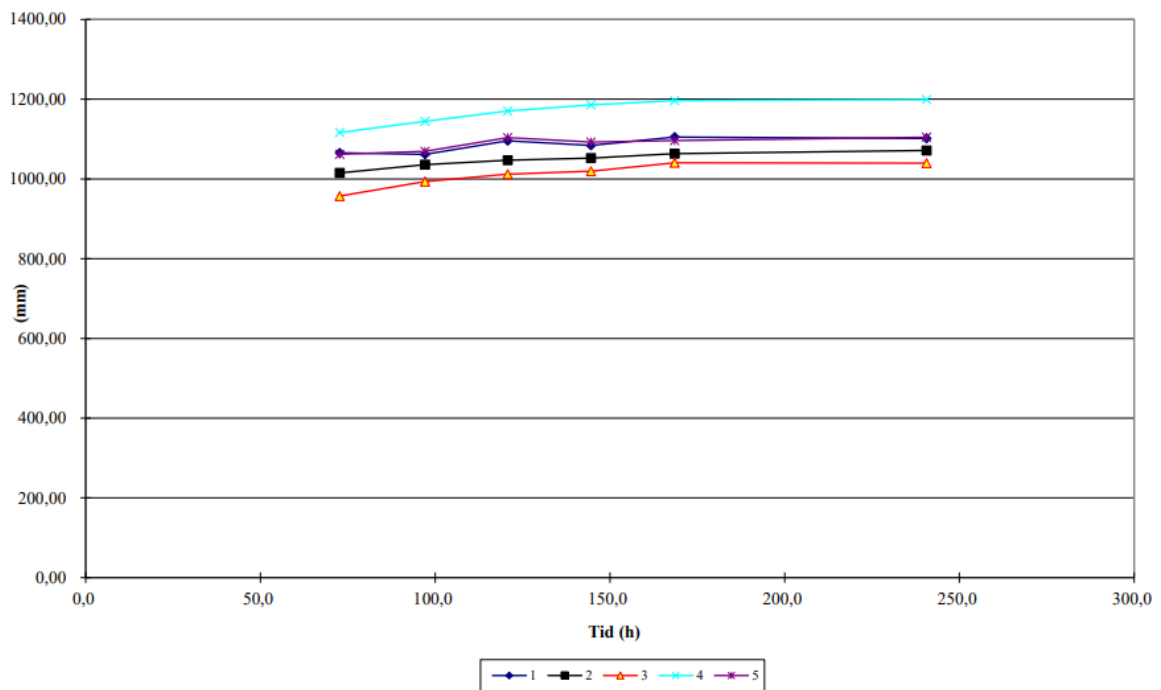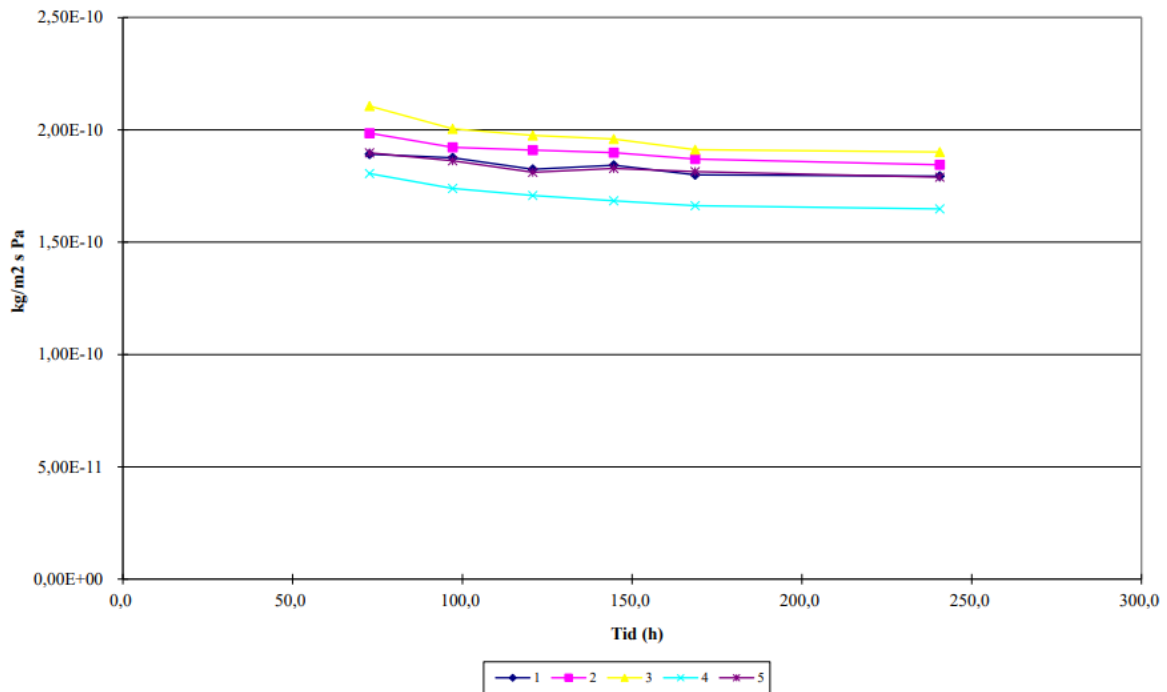
Vanndampgjennomgang i perioden

Figure D.12.3: Water vapour transmission during the period

Table D.12.1: Input data of the wet cup method

(1)Produktnavn:					Salttype:		KNO3	Prøvestykke:		1	2	3
(2)Oppdragsgiver:	Masteroppgave_Katinka		Katinka		Prøvediameter (mm):		0,164	Tykkelse:	0,40		0,36	0,49
(3)Prosjektnummer:	55B2				Luftlag salt/prøve (mm):		15	Side mot saltløsning:			Hvit side	
(4)Produktype:	Maling				Prøvest. diameter(mm):		0,174	Ferkst/Aldret:			Ferskt	
(5)Tykkelse, mm:		0,4100			Lufth. over pr.(m/s):		0,3	Start kondisjonering:			03.11.2023	
(6)Målenummer:	55B2				RF/Temp:		Vekt:		Tykkelsesmåler:			Stanse:
(12)Dato (CTRL+SHIFT+;)		02.02.2024	05.02.2024	06.02.2024	07.02.2024	08.02.2024	09.02.2024	12.02.2024	13.02.2024			
(13)Tid (CTRL+SHIFT+:)		08:44	09:26	09:51	09:30	09:19	09:19	09:22	09:20			
(14)Beregning fra veiing:	4											
(15)Barometertrykk ved veiing, hPa:		990,69	989,17	991,52	991,07	990,94	998,82	1000,01	1000,44			
(16)Barometertrykk i perioden, hPa:		990,69	981,49	993,28	989,43	990,2	994,47	1000,82	1001,08			
(17)Temperatur luft over boks,°C:		23	23,03	23,03	23,02	23,03	23,02	23,02	23,02			
(18)Temperatur i saltløsning, °C:		23	23,03	23,03	23,02	23,03	23,02	23,02	23,02			
(19)RF i rommet, %		50	50,78	50,67	50,47	50,47	50,34	50,54	50,52			
(20)Veiing nummer:		1	2	3	4	5	6	7	8	9	10
(21)Vekt,g kontrollodd før veiing:		1000,003	1000,006	1000,003	1000,005	1000,004	1000,003	1000,003	1000,001			
(22)Vekt,g prøve nr:	1	560,643	559,733	559,427	559,137	558,845	558,556	557,706	557,427			
(23)Vekt,g prøve nr:	2	521,881	520,958	520,586	520,263	519,951	519,635	518,706	518,396			
(24)Vekt,g prøve nr:	3	573,324	572,531	572,263	572,01	571,759	571,507	570,763	570,515			
(25)Vekt,g prøve nr:	4	549,08	548,152	547,852	547,569	547,285	547,004	546,176	545,899			
(26)Vekt,g prøve nr:	5	556,267	555,266	554,937	554,627	554,316	554,004	553,084	552,775			
(27)Vekt,g kontrollodd etter veiing:		1000,005	1000,006	1000,005	1000,003	1000,004	1000,004	1000,004	1000,003			

D.13. Coating 56B (Three Layers)

NB This series was fully tested (painting, conditioning, assembly, weighing) Spring 2024 due to severege leakages of the previous one)

SINTEF

PRØVINGS RAPPORT
Prøving av vanndamppermeans etter ISO/DIS 12572

Produktnavn:	▇▇▇▇▇▇	Tykkelse, mm:	0,23
Oppdragsgiver:	Masteroppgave_Katinka	Målenummer:	56BX
Prosjektnummer:	56BX	Prøvediameter: (mm)	164
Produkttype:	Maling	Salttype i boksen:	KNO3
		Prøveperiode: fra:	15.04.2024
		til:	26.04.2024

	Middel i prøveperioden		Lufth. over pr.(m/s):	0,3
Relativ luftfuktighet i boksen (%RF)	94,1		Tykkelse prøve nr	
Relativ luftfuktighet i rommet (%RF)	50,5		1	0,23
			2	0,29
Temperatur i boksen (°C)	23,1		3	0,25
			4	0,22
Temperatur i rommet (°C)	23,1		5	0,25
Barometertrykk (hPa)	1006,5		6	0,20

Tabell 1   Temperatur, relativ luftfuktighet og barometertrykk i prøveperioden.

Prøve nummer	Vanndamppermeans W_p	Vanndampmotstand sd	Z_p
	(kg/m²sPa)	(m)	(m²sPa/kg)
1	4,63E-10	0,424	2,16E+09
2	3,55E-10	0,554	2,82E+09
3	4,51E-10	0,435	2,22E+09
4	4,49E-10	0,438	2,23E+09
5	4,51E-10	0,436	2,22E+09
Middel	4,34E-10	0,453	2,31E+09
Std. dev. mean. value	1,99214E-11	0,024	1,23E+08

Tabell 2   Vanndamppermeans og vanndampmotstand for de fem prøvestykkene.
            Enkeltresultatene er et middel over fem tidsintervall med stabil fukttransport.
            Resultatene er korrigert for overgangsmotstanden over prøven,
            damptransport gjennom overlappsonen, og motstanden i luftlaget i boksen.

SIGN:
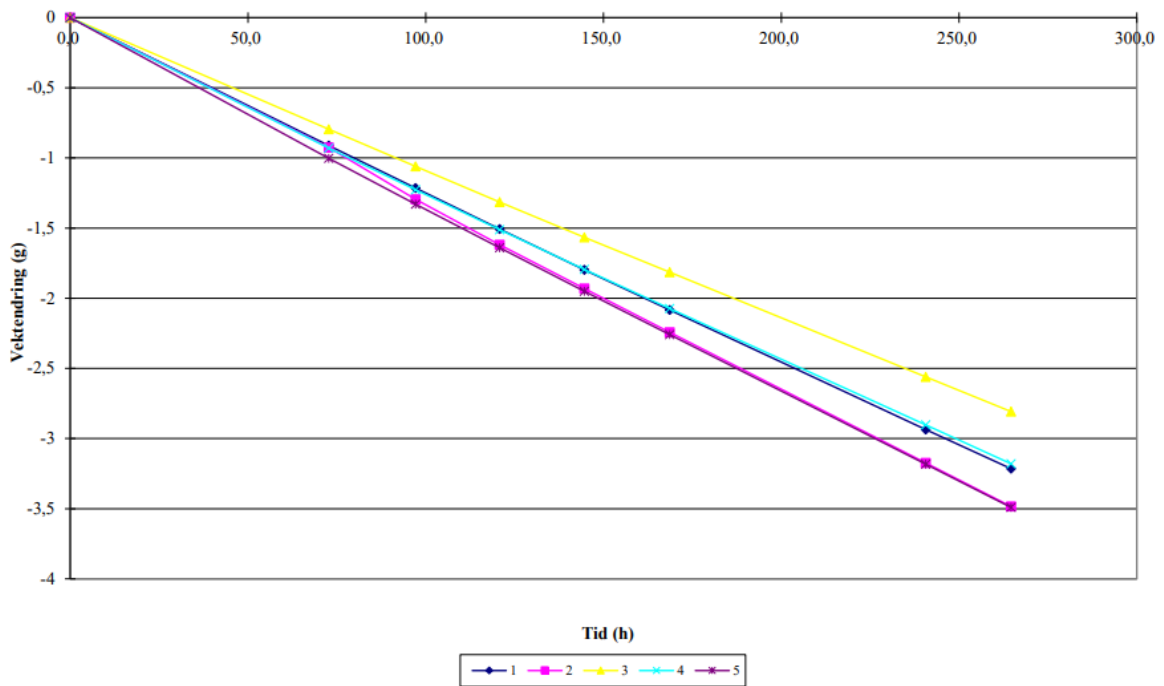
Vektendring siden start for de enkelte prøvene

Figure D.13.1: Mass reduction during the period

Ekvivalent luftlagstykkelse i perioden

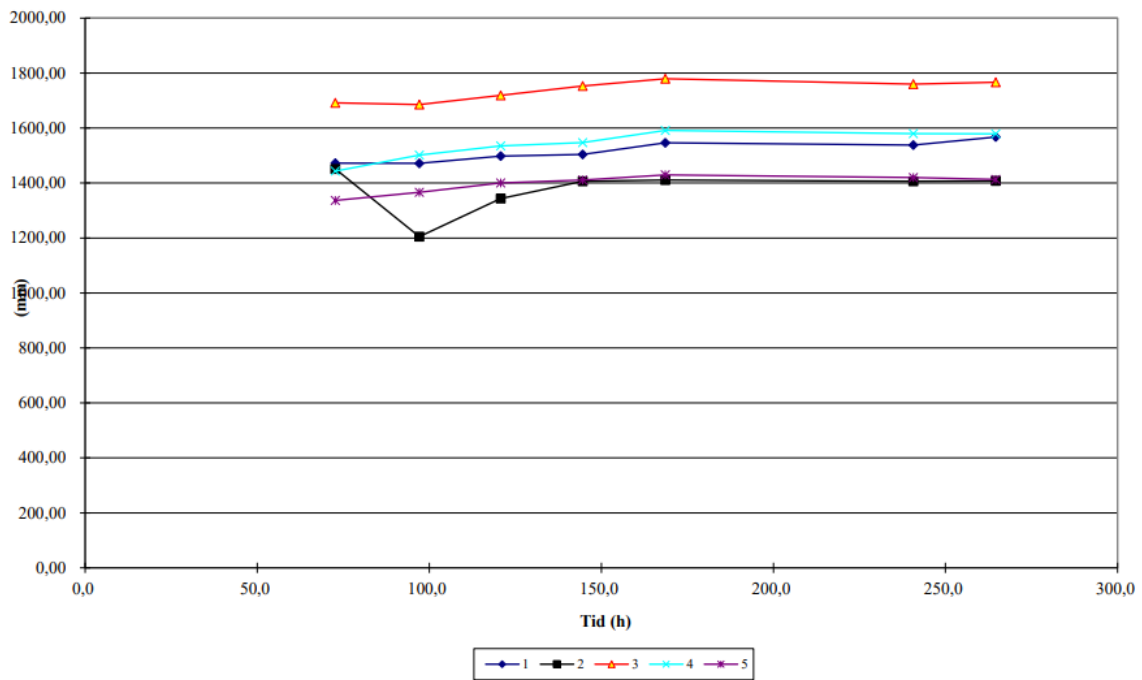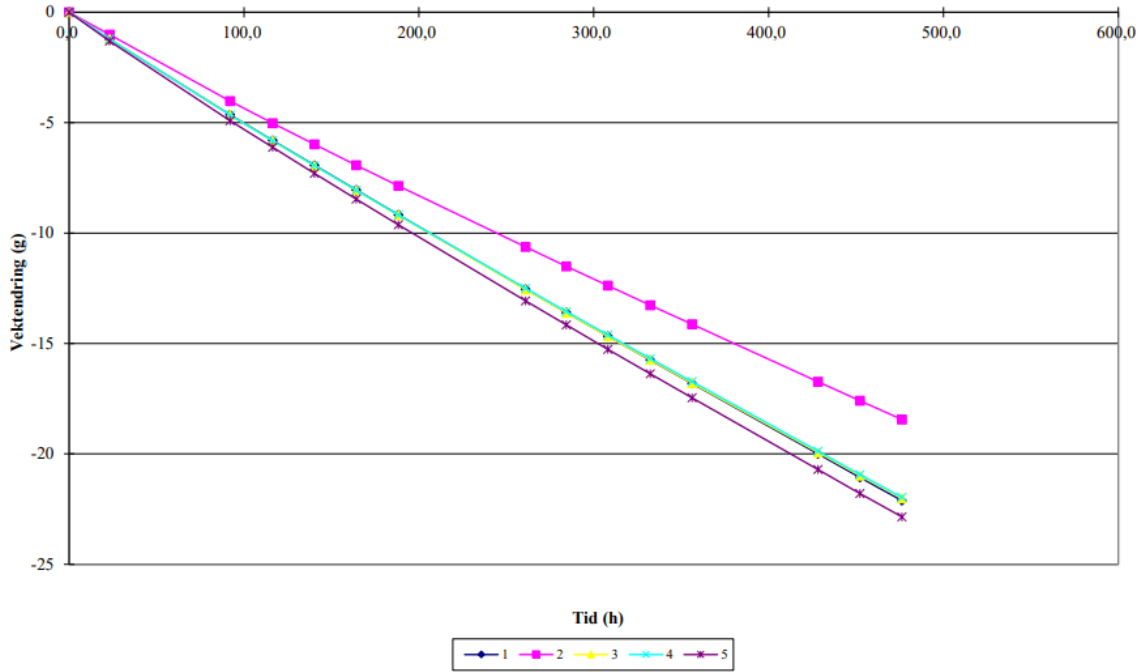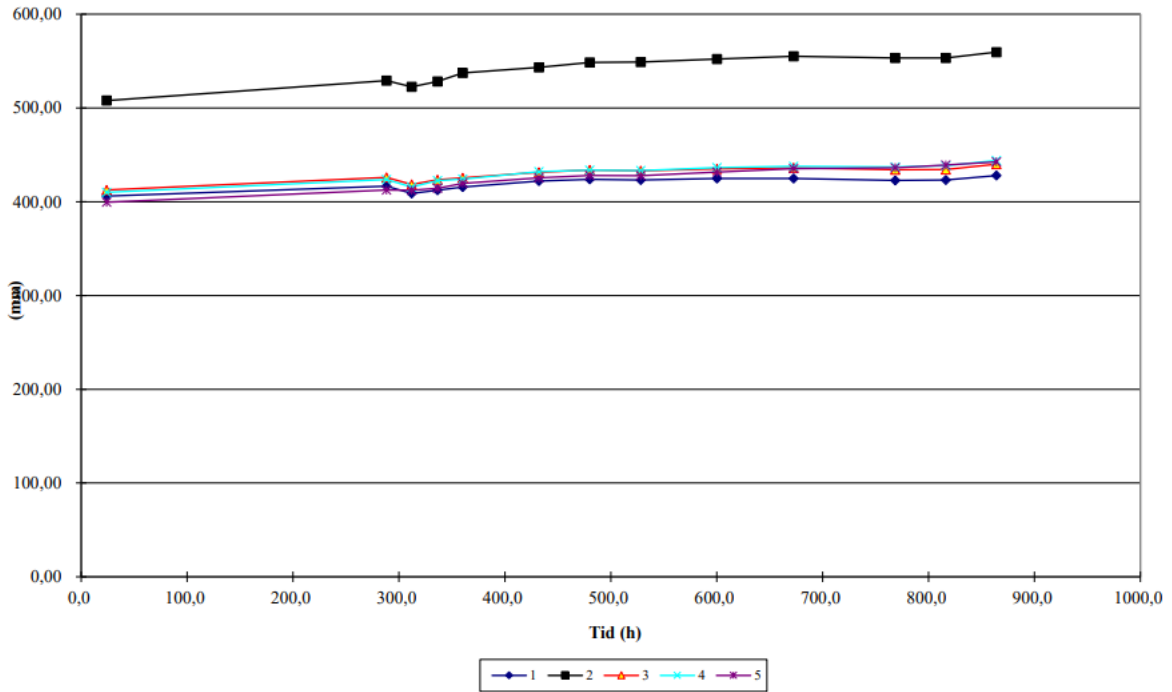**Figure D.13.2:** Equivalent air layer thickness sd-value during the period. Note that it has been continued for a longer period than the mass reduction and transmission, this to evaluate whether the value would stabilize

Figure D.13.3: Water vapour transmission during the period

Table D.13.1: Input data of the wet cup method

(1)Produktnavn:					Salttype:		KNO3
(2)Oppdragsgiver:	Masteroppgave_Katinka		Katinka		Prøvediameter (mm):		0,164
(3)Prosjektnummer:	56BX				Luftlag salt/prøve (mm):		15
(4)Produkttype:	Maling				Prøvest. diameter(mm):		0,174
(5)Tykkelse, mm:	0,2300				Lufth. over pr.(m/s):		0,3
(6)Målenummer:	56BX				RF/Temp:		Vekt:
(12)Dato (CTRL+SHIFT+ ;)		29.02.2024	01.03.2024	04.03.2024	05.03.2024	06.03.2024	07.03.2024
(13)Tid (CTRL+SHIFT+ :)		13:03	12:07	09:08	09:25	09:17	09:10
(14)Beregning fra veiing:	11						
(15)Barometertrykk ved veiing, hPa:		986,54	996,52	1016,56	1022,93	1026,34	1029,04
(16)Barometertrykk i perioden, hPa:		986,54	991,52	1007,49	1019,87	1025,04	1026,51
(17)Temperatur luft over boks,°C:		23	23,06	23,05	23,06	23,04	23,07
(18)Temperatur i saltløsning, °C:		23	23,06	23,05	23,06	23,04	23,07
(19)RF i rommet, %		50	50,66	50,67	50,69	50,22	50,16
(20)Veiing nummer:		1	2	3	4	5	6
(21)Vekt,g kontrolllodd før veiing:		1000,002	1000,001	1000	1000	999,997	999,997
(22)Vekt,g prøve nr:	1	454,091	452,865	449,444	448,288	447,162	446,039
(23)Vekt,g prøve nr:	2	444,644	443,621	440,614	439,615	438,658	437,716
(24)Vekt,g prøve nr:	3	468,542	467,324	463,882	462,714	461,578	460,467
(25)Vekt,g prøve nr:	4	468,229	467,012	463,565	462,407	461,275	460,164
(26)Vekt,g prøve nr:	5	485,636	484,329	480,716	479,516	478,335	477,17
(27)Vekt,g kontrolllodd etter veiing:		1000,002	1000,002	999,999	999,999	999,996	999,995

Prøvestykke:		1		2		3		4		5		6			
Tykkelse:	0,23		0,29		0,25		0,22		0,25		0,20				
Side mot saltløsning:			hvit side												
Ferkst/Aldret:			Ferskt												
Start kondisjonering:			13.02.2024												
	Tykkelsesmåler:				Stanse:										
08.03.2024		11.03.2024		12.03.2024		13.03.2024		14.03.2024		15.03.2024		18.03.2024		19.03.2024	20.03.2024
09:18		10:02		09:18		09:08		09:20		09:13		09:14		09:20	09:16
1024		1015,36		1011,04		1000,95		981,43		992,99		1012,34		1007,36	1009,43
1027,16		1004,23		1012,97		1006,79		989,1		986,04		1009,07		1009,38	1005,19
23,07		23,04		23,07		23,08		23,07		23,06		23,06		23,06	23,07
23,07		23,04		23,07		23,08		23,07		23,06		23,06		23,06	23,07
50,12		50,6		50,24		50,3		50,52		50,49		50,47		50,35	50,52
7		8		9		10		11		12		13		14	15
999,995		1000		1000,000		1000,005		1000,004		1000,001		1000		999,998	999,999
444,917		441,556		440,496		439,425		438,351		437,282		434,083		433,023	431,976
436,78		434,018		433,137		432,265		431,383		430,509		427,906		427,049	426,199
459,351		455,989		454,931		453,867		452,808		451,752		448,604		447,562	446,532
459,046		455,728		454,68		453,62		452,558		451,505		448,345		447,293	446,26
476,01		472,564		471,476		470,372		469,269		468,174		464,921		463,842	462,784
999,995		999,997		999,998		999,998		1000,004		1000,004		999,998		999,997	1000

D.14. Coating 56B2 (Six Layers)

NB This series was fully tested (painting, conditioning, assembly, weighing) Spring 2024 due to severege leakages of the previous one)

SINTEF

PRØVINGS RAPPORT
Prøving av vanndamppermeans etter ISO/DIS 12572

Produktnavn:	▮▮▮▮▮▮▮▮▮	Tykkelse, mm:	0,44
Oppdragsgiver:	Masteroppgave_Katinka	Målenummer:	56B2X
Prosjektnummer:	56B2X	Prøvediameter: (mm)	164
Produktype:	Maling	Salttype i boksen:	KNO3
		Prøveperiode: fra:	15.04.2024
		til:	26.04.2024

	Middel i prøveperioden
Relativ luftfuktighet i boksen (%RF)	94,1
Relativ luftfuktighet i rommet (%RF)	50,5
Temperatur i boksen (°C)	23,1
Temperatur i rommet (°C)	23,1
Barometertrykk (hPa)	1006,5

Lufth. over pr.(m/s): 0,3

Tykkelse prøve nr

1 0,49
2 0,4
3 0,44
4 0,42
5 0,45
6 0,36

Tabell 1   Temperatur, relativ luftfuktighet og barometertrykk i prøveperioden.

Prøve nummer	Vanndamppermeans W_p	Vanndampmotstand s_d	Z_p
	(kg/m²sPa)	(m)	(m²sPa/kg)
1	2,66E-10	0,738	3,75E+09
2	3,04E-10	0,647	3,29E+09
3	2,89E-10	0,681	3,46E+09
4	3,03E-10	0,648	3,30E+09
5	2,62E-10	0,751	3,82E+09
Middel	2,85E-10	0,690	3,51E+09
Std. dev. mean. value	8,93672E-12	0,022	1,12E+08

Tabell 2   Vanndamppermeans og vanndampmotstand for de fem prøvestykkene.
Enkeltresultatene er et middel over fem tidsintervall med stabil fukttransport.
Resultatene er korrigert for overgangsmotstanden over prøven,
damptransport gjennom overlappsonen, og motstanden i luftlaget i boksen.

SIGN:

Vektendring siden start for de enkelte prøvene

Figure D.14.1: Mass reduction during the period

Ekvivalent luftlagstykkelse i perioden

Figure D.14.2: Equivalent air layer thickness sd-value during the period. Note that it has been continued for a longer period than the mass reduction and transmission, this to evaluate whether the value would stabilize.
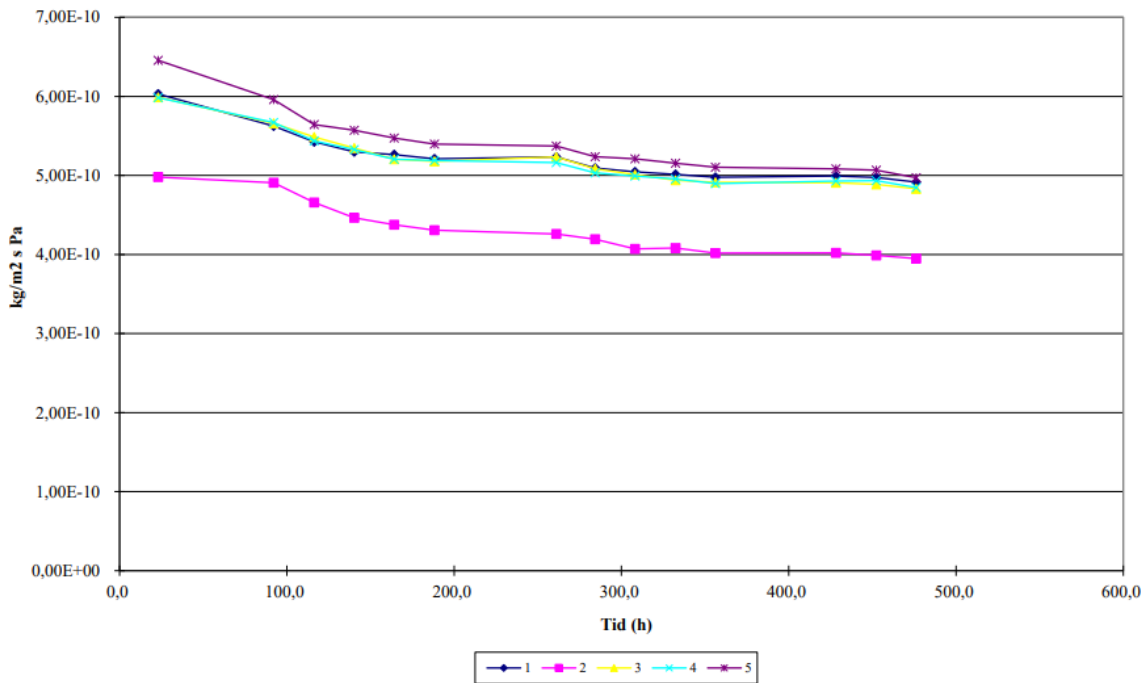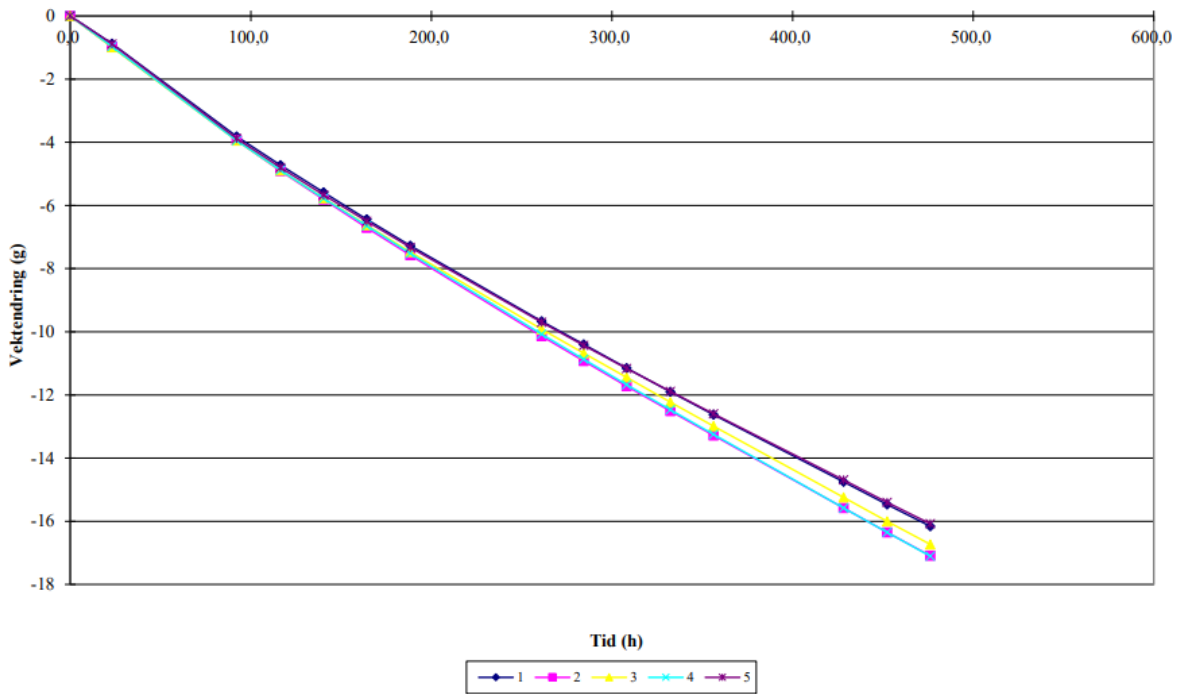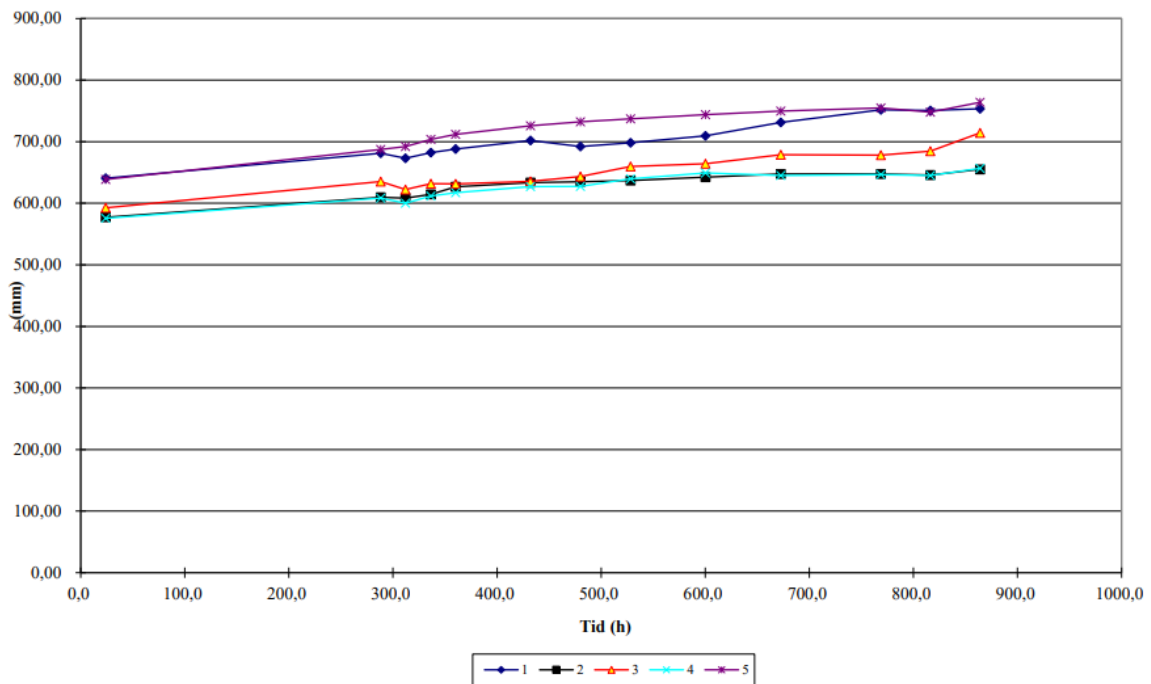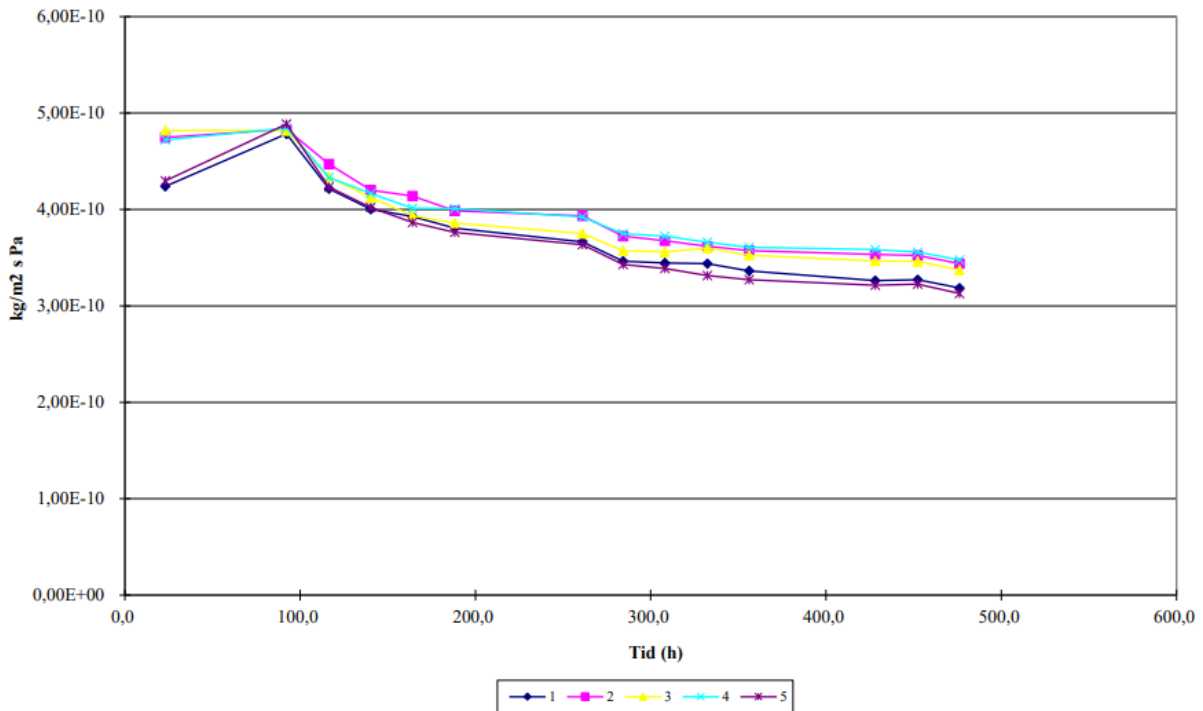
Figure D.14.3: Water vapour transmission during the period

Table D.14.1: Input data of the wet cup method

(1)Produktnavn:					Salttype:		KNO3
(2)Oppdragsgiver:	Masteroppgave_Katinka		Katinka		Prøvediameter (mm):		0,164
(3)Prosjektnummer:	56B2X				Luftlag salt/prøve (mm):		15
(4)Produktype:	Maling				Prøvest. diameter(mm):		0,174
(5)Tykkelse, mm:		0,4400			Lufth. over pr.(m/s):		0,3
(6)Målenummer:	56B2X				RF/Temp:		Vekt:
(12)Dato (CTRL+SHIFT+ ;)			29.02.2024	01.03.2024	04.03.2024	05.03.2024	06.03.2024	07.03.2024
(13)Tid (CTRL+SHIFT+ :)			13:08	12:13	09:17	09:31	09:23	09:17
(14)Beregning fra veiing:		11						
(15)Barometertrykk ved veiing, hPa:			986,54	996,52	1016,56	1022,93	1026,34	1029,04
(16)Barometertrykk i perioden, hPa:			986,54	991,53	1007,49	1019,87	1025,04	1026,51
(17)Temperatur luft over boks,°C:			23	23,06	23,05	23,06	23,04	23,07
(18)Temperatur i saltløsning, °C:			23	23,06	23,05	23,06	23,04	23,07
(19)RF i rommet, %:			50	50,65	50,67	50,69	50,22	50,16
(20)Veiing nummer:			1	2	3	4	5	6
(21)Vekt,g kontrolllodd før veiing:			1000,002	1000,003	1000	999,996	999,996	999,996
(22)Vekt,g prøve nr:		1	498,591	497,712	494,77	493,862	493,001	492,15
(23)Vekt,g prøve nr:		2	476,888	475,909	472,939	471,978	471,076	470,181
(24)Vekt,g prøve nr:		3	514,655	513,662	510,7	509,766	508,88	508,027
(25)Vekt,g prøve nr:		4	462,666	461,692	458,715	457,783	456,888	456,019
(26)Vekt,g prøve nr:		5	491,482	490,592	487,591	486,679	485,814	484,976
(27)Vekt,g kontrolllodd etter veiing:			1000,002	1000,004	999,997	999,995	999,997	999,995

Prøvestykke:		1		2		3		4		5		6			
Tykkelse:	0,49		0,4		0,44		0,42		0,45		0,36				
Side mot saltløsning:			hvit side												
Ferkst/Aldret:			Ferskt												
Start kondisjonering:			13.02.2024												
	Tykkelsesmåler:			Stanse:											
08.03.2024		11.03.2024	12.03.2024	13.03.2024	14.03.2024	15.03.2024	18.03.2024	19.03.2024	20.03.2024
09:23		10:07	09:25	09:15	09:27	09:19	09:18	09:26	09:22
1024		1015,36	1011,04	1000,95	981,43	992,99	1012,34	1007,36	1009,43
1027,16		1004,23	1012,97	1006,79	989,1	986,04	1009,07	1009,38	1005,19
23,07		23,04	23,07	23,08	23,07	23,06	23,06	23,06	23,07
23,07		23,04	23,07	23,08	23,07	23,06	23,06	23,06	23,07
50,12		50,6	50,24	50,3	50,52	50,49	50,47	50,35	50,52
7		8	9	10	11	12	13	14	15
1000		999,998	999,998	1000,002	1000,004	1000,002	999,999	999,998	999,999
491,322		488,926	488,191	487,448	486,701	485,962	483,832	483,123	482,431
469,315		466,75	465,962	465,171	464,386	463,603	461,302	460,54	459,795
507,188		504,738	503,981	503,214	502,433	501,66	499,402	498,653	497,922
455,148		452,591	451,798	450,997	450,203	449,413	447,081	446,312	445,559
484,157		481,781	481,053	480,322	479,601	478,881	476,781	476,082	475,402
1000		999,997	999,999	999,999	1000,005	1000,002	1000,001	999,998	1000,002

D.15. Coating 57B (Three Layers)

SINTEF

Produktnavn:	▮▮▮▮▮	Tykkelse, mm:	0,24
Oppdragsgiver:	Masteroppgave_Katinka	Målenummer:	57B
Prosjektnummer:	57B	Prøvediameter: (mm)	164
Produkttype:	Maling	Salttype i boksen:	KNO3
		Prøveperiode: fra:	12.02.2024
		til:	16.02.2024

Lufth. over pr.(m/s): 0,3

Tykkelse prøve nr

	1	0,19
	2	0,27
	3	0,19
	4	0,25
	5	0,22
	6	0,30

	Middel i prøveperioden
Relativ luftfuktighet i boksen (%RF)	94,1
Relativ luftfuktighet i rommet (%RF)	50,5
Temperatur i boksen (°C)	23,0
Temperatur i rommet (°C)	23,0
Barometertrykk (hPa)	1002,1

Tabell 1   Temperatur, relativ luftfuktighet og barometertrykk i prøveperioden.

Prøve nummer	Vanndamppermeans W_p	Vanndampmotstand	
		sd	Z_p
	(kg/m²sPa)	(m)	(m²sPa/kg)
1	2,05E-10	0,961	4,87E+09
2	1,69E-10	1,170	5,91E+09
3	2,27E-10	0,871	4,41E+09
4	2,02E-10	0,979	4,96E+09
5	1,85E-10	1,070	5,40E+09
Middel	1,98E-10	0,999	5,06E+09
Std. dev. mean. value	9,71652E-12	0,051	2,54E+08

Tabell 2   Vanndamppermeans og vanndampmotstand for de fem prøvestykkene.
Enkeltresultatene er et middel over fem tidsintervall med stabil fukttransport.
Resultatene er korrigert for overgangsmotstanden over prøven,
damptransport gjennom overlappsonen, og motstanden i luftlaget i boksen.

SIGN:

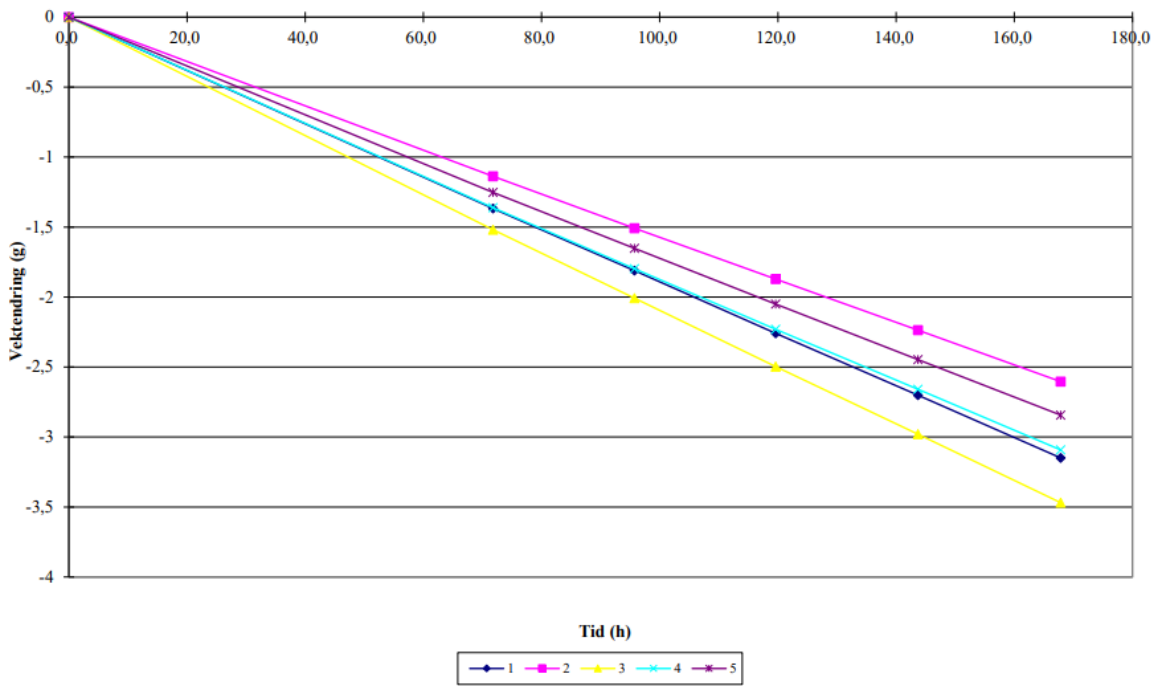Vektendring siden start for de enkelte prøvene

Figure D.15.1: Mass reduction during the period
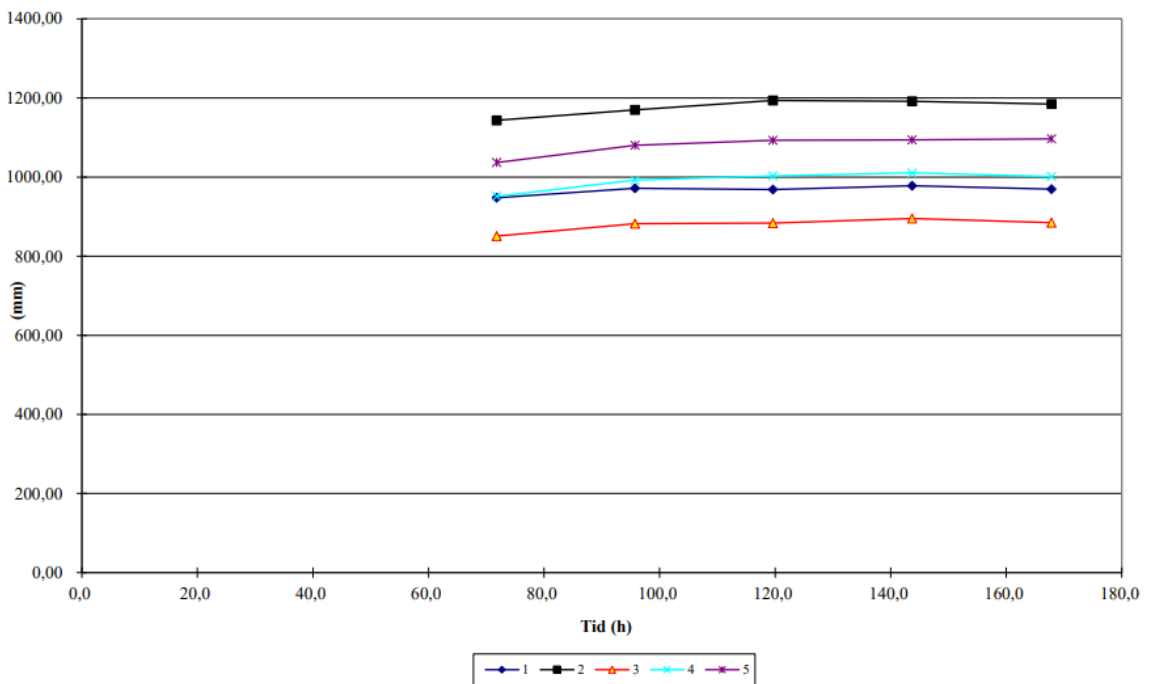
Ekvivalent luftlagstykkelse i perioden

Figure D.15.2: Equivalent air layer thickness sd-value during the period

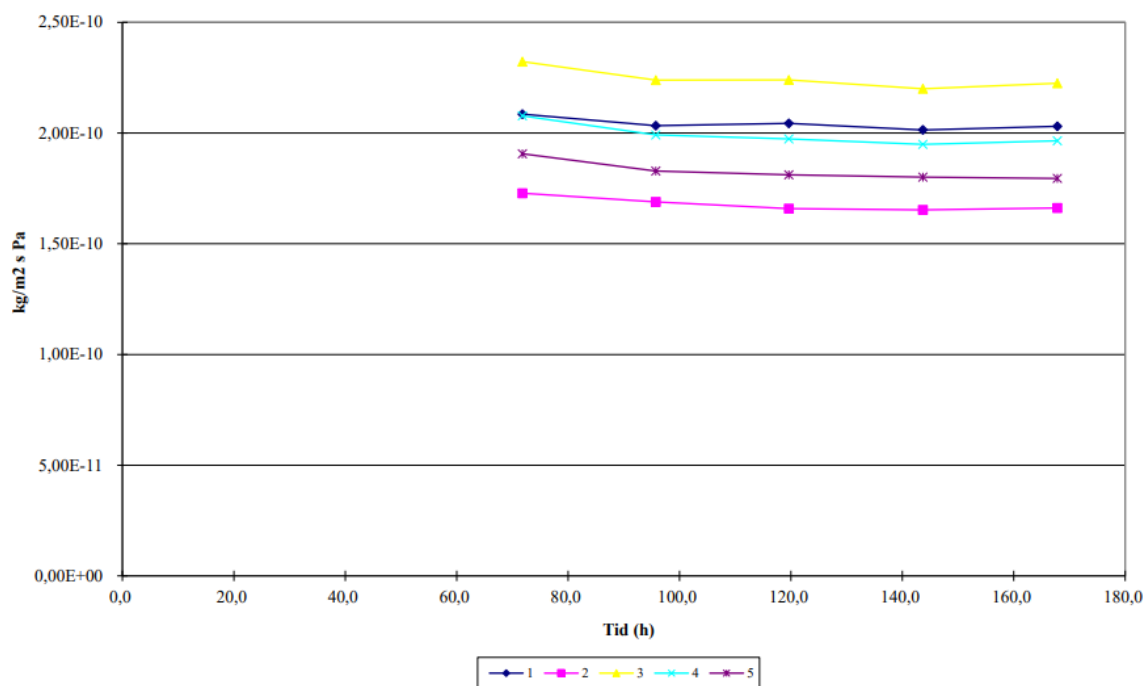**Figure D.15.3**: Water vapour transmission during the period

Table D.15.1: Input data of the wet cup method

(1)Produktnavn:	███████			Salttype:		KNO3
(2)Oppdragsgiver:	Masteroppgave_Katinka	Katinka		Prøvediameter (mm):		0,164
(3)Prosjektnummer:	57B			Luftlag salt/prøve (mm):		15
(4)Produkttype:	Maling			Prøvest. diameter(mm):		0,174
(5)Tykkelse, mm:	0,2400			Lufth. over pr.(m/s):		0,3
(6)Målenummer:	57B			RF/Temp:		Vekt:
(12)Dato (CTRL+SHIFT+ ;)		09.02.2024	12.02.2024	13.02.2024	14.02.2024	15.02.2024	16.02.2024
(13)Tid (CTRL+SHIFT+ :)		09:41	09:29	09:25	09:19	09:23	09:31
(14)Beregning fra veiing:	2						
(15)Barometertrykk ved veiing, hPa:		998,82	1000,01	1000,44	999,15	1009,77	997,81
(16)Barometertrykk i perioden, hPa:		998,82	1000,82	1001,08	999,19	1004,3	1005
(17)Temperatur luft over boks,°C:		23	23,02	23,02	23,03	23,04	23,04
(18)Temperatur i saltløsning, °C:		23	23,02	23,02	23,03	23,04	23,04
(19)RF i rommet, %:		50	50,54	50,52	50,46	50,6	50,57
(20)Veiing nummer:		1	2	3	4	5	6
(21)Vekt,g kontrolllodd før veiing:		1000,002	1000	1000,002	1000,001	1000	1000,002
(22)Vekt,g prøve nr:	1	456,675	455,307	454,864	454,417	453,969	453,531
(23)Vekt,g prøve nr:	2	445,079	443,941	443,572	443,208	442,838	442,48
(24)Vekt,g prøve nr:	3	465,969	464,449	463,962	463,473	462,985	462,505
(25)Vekt,g prøve nr:	4	463,071	461,708	461,274	460,842	460,408	459,984
(26)Vekt,g prøve nr:	5	479,308	478,055	477,656	477,259	476,857	476,47
(27)Vekt,g kontrolllodd etter veiing:		1000,001	1000	1000,004	1000,003	1000	1000,003

Prøvestykke:		1		2		3
Tykkelse:	0,19		0,27		0,19	
Side mot saltløsning:			Hvit side			
Ferkst/Aldret:			Ferskt			
Start kondisjonering:			01.11.2023			
	Tykkelsesmåler:			Stanse:		

D.16. Coating 57B2 (Six Layers)

SINTEF

Produktnavn:	████████████
Oppdragsgiver:	Masteroppgave_Katinka
Prosjektnummer:	57B2
Produkttype:	Maling

Tykkelse, mm:	0,44
Målenummer:	57B2
Prøvediameter: (mm)	164
Salttype i boksen:	KNO3
Prøveperiode: fra:	12.02.2024
til:	16.02.2024

	Middel i prøveperioden
Relativ luftfuktighet i boksen (%RF)	94,1
Relativ luftfuktighet i rommet (%RF)	50,5
Temperatur i boksen (°C)	23,0
Temperatur i rommet (°C)	23,0
Barometertrykk (hPa)	1002,1

Lufth. over pr.(m/s): 0,3

Tykkelse prøve nr

1 0,37
2 0,55
3 0,48
4 0,39
5 0,40
6 0,60

Tabell 1   Temperatur, relativ luftfuktighet og barometertrykk i prøveperioden.

Prøve nummer	Vanndamppermeans W_p	Vanndampmotstand	
		sd	Z_p
	(kg/m²sPa)	(m)	(m²sPa/kg)
1	1,48E-10	1,330	6,76E+09
2	1,25E-10	1,580	8,02E+09
3	1,17E-10	1,680	8,53E+09
4	1,41E-10	1,400	7,10E+09
5	1,37E-10	1,440	7,31E+09
Middel	1,34E-10	1,480	7,49E+09
Std. dev. mean. value	5,56532E-12	0,063	3,22E+08

Tabell 2   Vanndamppermeans og vanndampmotstand for de fem prøvestykkene.
Enkeltresultatene er et middel over fem tidsintervall med stabil fukttransport.
Resultatene er korrigert for overgangsmotstanden over prøven,
damptransport gjennom overlappsonen, og motstanden i luftlaget i boksen.

SIGN:

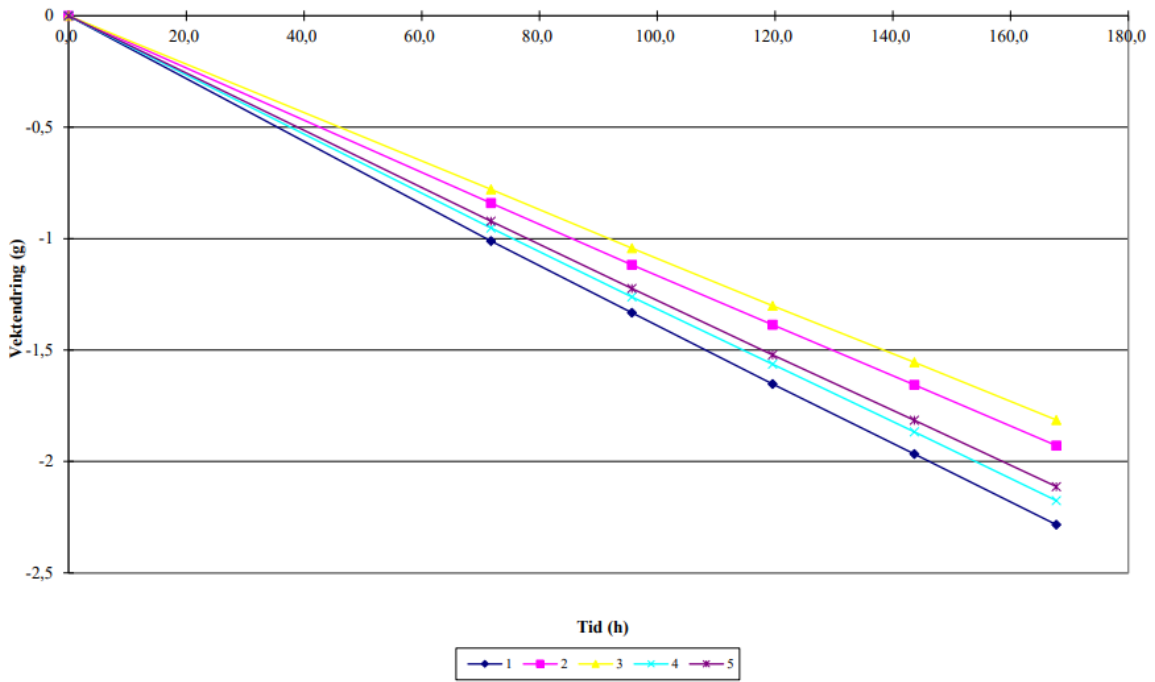Vektendring siden start for de enkelte prøvene

Figure D.16.1: Mass reduction during the period
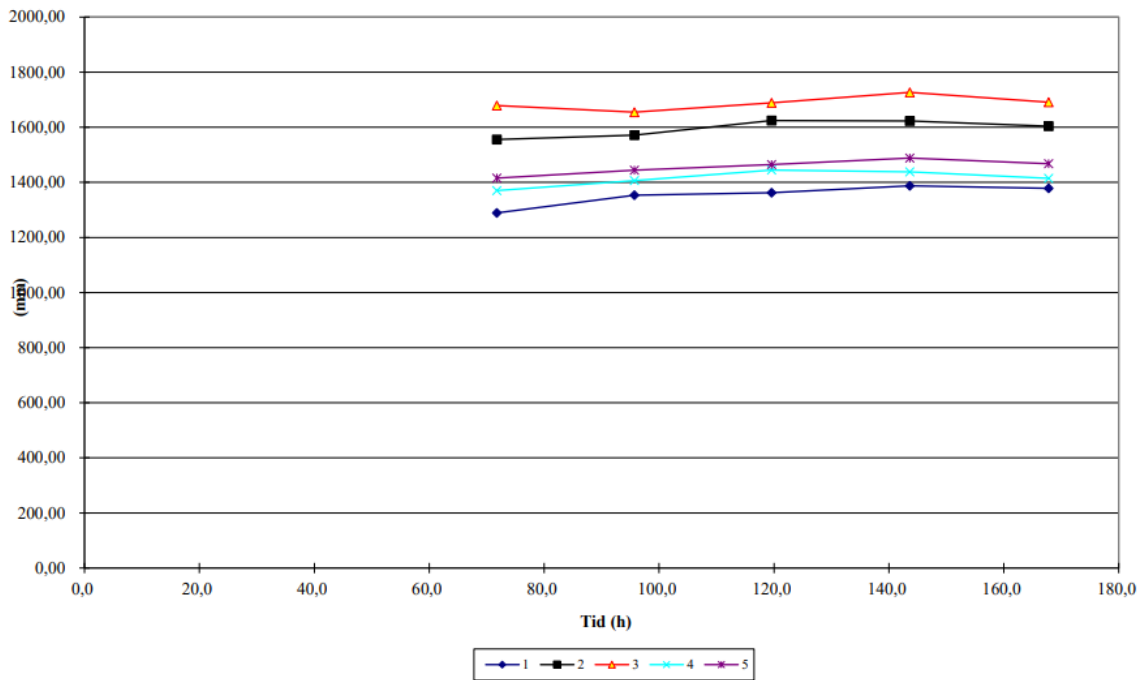
Ekvivalent luftlagstykkelse i perioden

Figure D.16.2: Equivalent air layer thickness sd-value during the period

Vanndampgjennomgang i perioden

Figure D.16.3: Water vapour transmission during the period

Table D.16.1: Input data of the wet cup method

(1)Produktnavn:		███████████████			Salttype:		KNO3
(2)Oppdragsgiver:		Masteroppgave_Katinka		Katinka	Prøvediameter (mm):		0,164
(3)Prosjektnummer:		57B2			Luftlag salt/prøve (mm):		15
(4)Produkttype:		Maling			Prøvest. diameter(mm):		0,174
(5)Tykkelse, mm:		0,4400			Lufth. over pr.(m/s):		0,3
(6)Målenummer:		57B2			RF/Temp:		Vekt:
(12)Dato (CTRL+SHIFT+ ;)			09.02.2024	12.02.2024	13.02.2024	14.02.2024	15.02.2024	16.02.2024
(13)Tid (CTRL+SHIFT+ :)			09:49	09:35	09:31	09:24	09:28	09:36
(14)Beregning fra veiing:	2							
(15)Barometertrykk ved veiing, hPa:			998,82	1000,01	1000,44	999,15	1009,77	997,81
(16)Barometertrykk i perioden, hPa:			998,82	1000,82	1001,08	999,19	1004,3	1005
(17)Temperatur luft over boks,°C:			23	23,02	23,02	23,03	23,04	23,04
(18)Temperatur i saltløsning, °C:			23	23,02	23,02	23,03	23,04	23,04
(19)RF i rommet, %:			50	50,54	50,52	50,46	50,6	50,57
(20)Veiing nummer:			1	2	3	4	5	6
(21)Vekt,g kontrolllodd før veiing:			1000,001	1000	1000,003	1000,002	1000	1000,002
(22)Vekt,g prøve nr:		1	489,344	488,332	488,012	487,692	487,373	487,065
(23)Vekt,g prøve nr:		2	475,449	474,608	474,332	474,063	473,789	473,525
(24)Vekt,g prøve nr:		3	516,562	515,782	515,52	515,261	515,003	514,753
(25)Vekt,g prøve nr:		4	462,334	461,381	461,073	460,771	460,463	460,163
(26)Vekt,g prøve nr:		5	493,352	492,429	492,129	491,831	491,533	491,244
(27)Vekt,g kontrolllodd etter veiing:			1000,002	1000,001	1000,003	1000,001	1000,002	1000,002

Prøvestykke:	1	2	3
Tykkelse:	0,37	0,55	0,48
Side mot saltløsning:		Hvit side	
Ferkst/Aldret:		Ferskt	
Start kondisjonering:		03.11.2023	
Tykkelsesmåler:		Stanse:	

D.17. Coating 58B (Three Layers)

SINTEF

Produktnavn:	████████	Tykkelse, mm:	0,2
Oppdragsgiver:	Masteroppgave_Katinka	Målenummer:	58B
Prosjektnummer:	58B	Prøvediameter: (mm)	164
Produkttype:	Maling	Salttype i boksen:	KNO3
		Prøveperiode: fra:	15.02.2024
		til:	21.02.2024

	Middel i prøveperioden		Lufth. over pr.(m/s):	0,3
Relativ luftfuktighet i boksen (%RF)	94,1		Tykkelse prøve nr	
Relativ luftfuktighet i rommet (%RF)	50,7		1	0,22
			2	0,17
Temperatur i boksen (°C)	23,0		3	0,17
			4	0,21
Temperatur i rommet (°C)	23,0		5	0,22
Barometertrykk (hPa)	1005,7		6	0,26

Tabell 1   Temperatur, relativ luftfuktighet og barometertrykk i prøveperioden.

Prøve nummer	Vanndamppermeans Wp	Vanndampmotstand	
		sd	Zp
	(kg/m²sPa)	(m)	(m²sPa/kg)
1	3,80E-10	0,517	2,63E+09
2	4,35E-10	0,452	2,30E+09
3	4,98E-10	0,395	2,01E+09
4	3,79E-10	0,519	2,64E+09
5	3,92E-10	0,502	2,55E+09
Middel	4,17E-10	0,472	2,40E+09
Std. dev. mean. value	2,25958E-11	0,024	1,21E+08

Tabell 2   Vanndamppermeans og vanndampmotstand for de fem prøvestykkene.
Enkeltresultatene er et middel over fem tidsintervall med stabil fukttransport.
Resultatene er korrigert for overgangsmotstanden over prøven,
damptransport gjennom overlappsonen, og motstanden i luftlaget i boksen.

SIGN:

Vektendring siden start for de enkelte prøvene

Figure D.17.1: Mass reduction during the period

Ekvivalent luftlagstykkelse i perioden

Figure D.17.2: Equivalent air layer thickness sd-value during the period
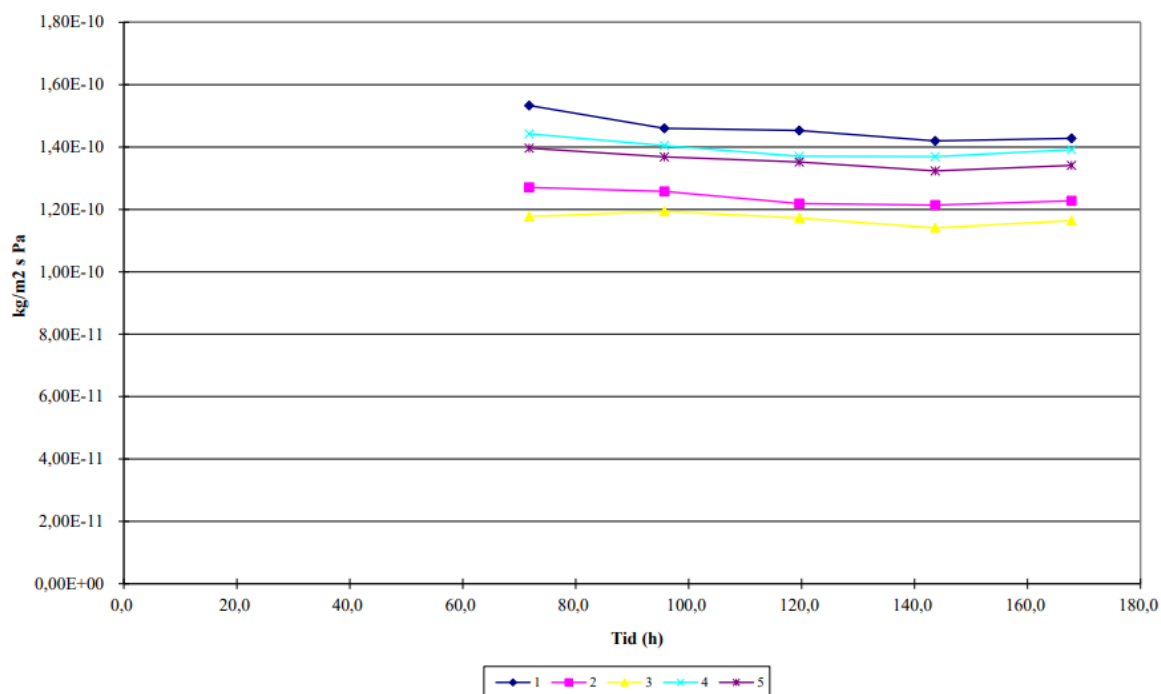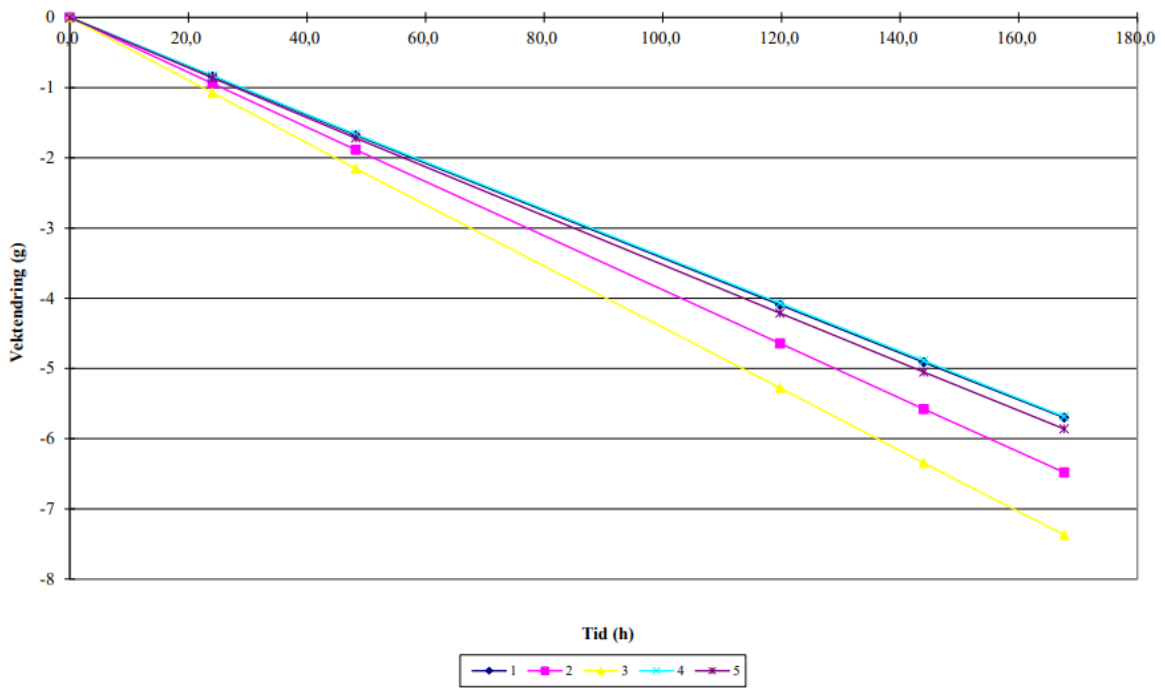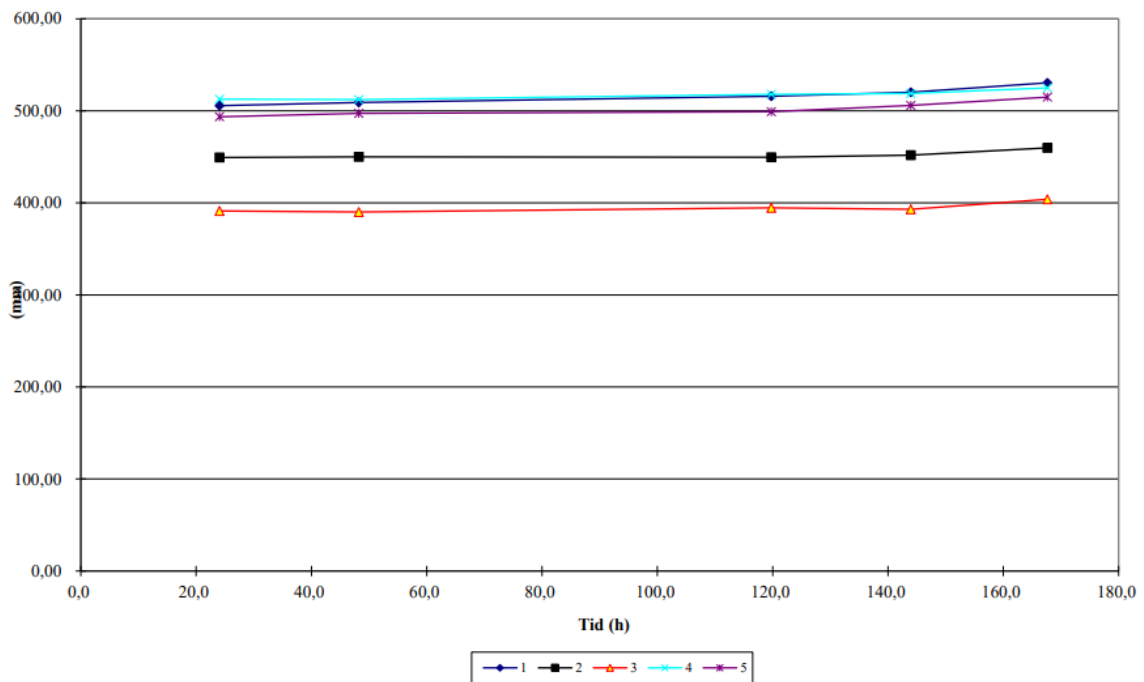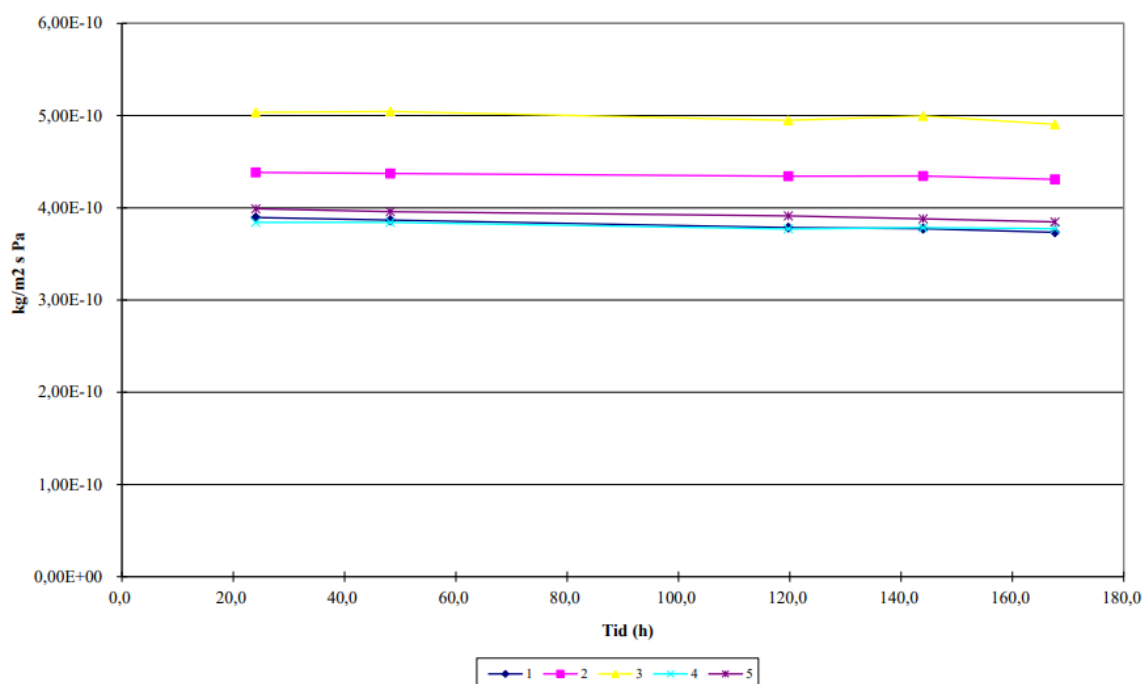
Vanndampgjennomgang i perioden

Figure D.17.3: Water vapour transmission during the period

Table D.17.1: Input data of the wet cup method

(1)Produktnavn:		████████████			Salttype:		KNO3
(2)Oppdragsgiver:		Masteroppgave_Katinka	Katinka		Prøvediameter (mm):		0,164
(3)Prosjektnummer:		58B			Luftlag salt/prøve (mm):		15
(4)Produkttype:		Maling			Prøvest. diameter(mm):		0,174
(5)Tykkelse, mm:		0,2000			Lufth. over pr.(m/s):		0,3
(6)Målenummer:		58B			RF/Temp:		Vekt:
(12)Dato (CTRL+SHIFT+ ;)		14.02.2024	15.02.2024	16.02.2024	19.02.2024	20.02.2024	21.02.2024
(13)Tid (CTRL+SHIFT+ :)		09:29	09:32	09:42	09:14	09:27	09:08
(14)Beregning fra veiing:	2						
(15)Barometertrykk ved veiing, hPa:		999,15	1009,77	997,81	1009,05	1004,78	997,79
(16)Barometertrykk i perioden, hPa:		999,15	1004,3	1005	1012,99	1007,51	998,5
(17)Temperatur luft over boks,°C:		23	23,04	23,04	23,03	23,02	23,02
(18)Temperatur i saltløsning, °C:		23	23,04	23,04	23,03	23,02	23,02
(19)RF i rommet, %		50	50,6	50,57	50,76	50,74	50,89
(20)Veiing nummer:		1	2	3	4	5	6
(21)Vekt,g kontrollodd før veiing:		1000,001	1000	999,998	999,998	1000,002	1000,000
(22)Vekt,g prøve nr:	1	453,993	453,148	452,318	449,891	449,082	448,295
(23)Vekt,g prøve nr:	2	500,239	499,293	498,358	495,59	494,663	493,76
(24)Vekt,g prøve nr:	3	502,276	501,197	500,124	496,99	495,93	494,908
(25)Vekt,g prøve nr:	4	499,904	499,07	498,245	495,827	495,016	494,221
(26)Vekt,g prøve nr:	5	530,573	529,708	528,859	526,354	525,523	524,713
(27)Vekt,g kontrollodd etter veiing:		1000,004	999,999	1000	999,998	1000	1000

Prøvestykke:		1	2	3
Tykkelse:	0,22		0,17	0,17
Side mot saltløsning:			Hvit side	
Ferkst/Aldret:			Ferskt	
Start kondisjonering:			25.10.2023	
	Tykkelsesmåler:			Stanse:

D.18. Coating 58B2 (Six Layers)

SINTEF

PRØVINGS RAPPORT
Prøving av vanndamppermeans etter ISO/DIS 12572

Produktnavn:	████████████
Oppdragsgiver:	Masteroppgave_Katinka
Prosjektnummer:	58B2
Produkttype:	Maling

Tykkelse, mm:	0,45
Målenummer:	58B2
Prøvediameter: (mm)	164
Salttype i boksen:	KNO3
Prøveperiode: fra:	15.02.2024
til:	21.02.2024

	Middel i prøveperioden
Relativ luftfuktighet i boksen (%RF)	94,1
Relativ luftfuktighet i rommet (%RF)	50,7
Temperatur i boksen (°C)	23,0
Temperatur i rommet (°C)	23,0
Barometertrykk (hPa)	1005,7

Lufth. over pr.(m/s): 0,3

Tykkelse prøve nr

1	0,45
2	0,44
3	0,41
4	0,51
5	0,45
6	0,29

Tabell 1   Temperatur, relativ luftfuktighet og barometertrykk i prøveperioden.

Prøve nummer	Vanndamppermeans Wp	Vanndampmotstand	
		sd	Zp
	(kg/m²sPa)	(m)	(m²sPa/kg)
1	2,15E-10	0,914	4,65E+09
2	2,20E-10	0,894	4,54E+09
3	2,05E-10	0,960	4,88E+09
4	1,98E-10	0,994	5,05E+09
5	2,17E-10	0,905	4,60E+09
Middel	2,11E-10	0,932	4,74E+09
Std. dev. mean. value	4,16087E-12	0,019	9,55E+07

Tabell 2   Vanndamppermeans og vanndampmotstand for de fem prøvestykkene.
Enkeltresultatene er et middel over fem tidsintervall med stabil fukttransport.
Resultatene er korrigert for overgangsmotstanden over prøven,
damptransport gjennom overlappsonen, og motstanden i luftlaget i boksen.

SIGN:

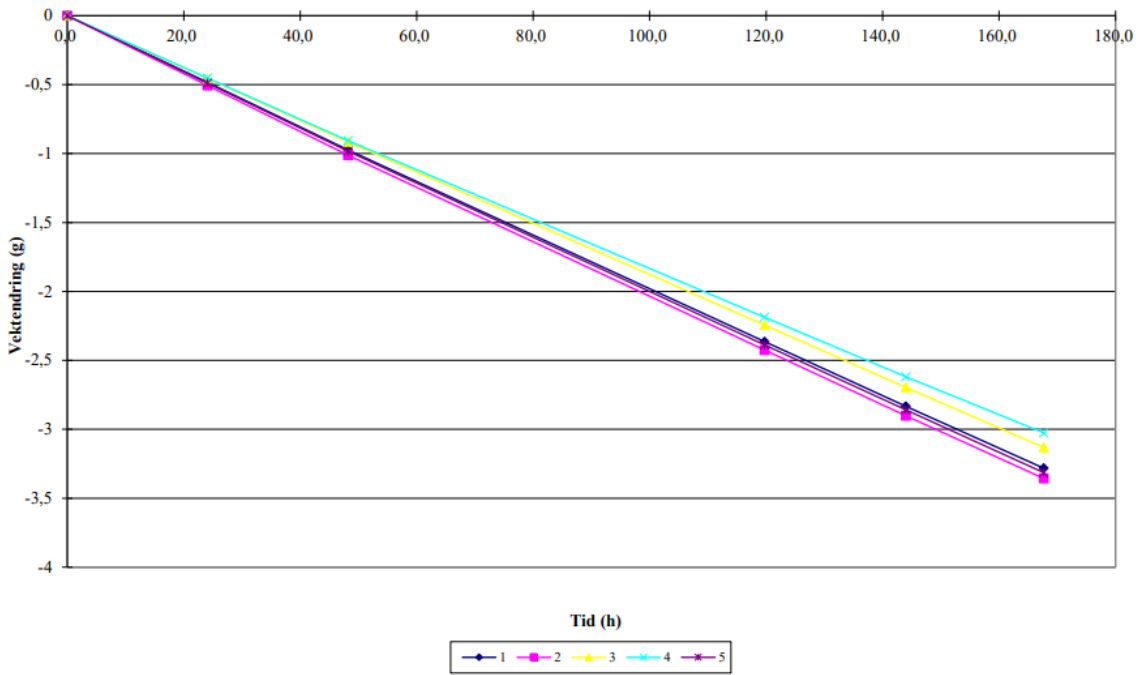Vektendring siden start for de enkelte prøvene

Figure D.18.1: Mass reduction during the period
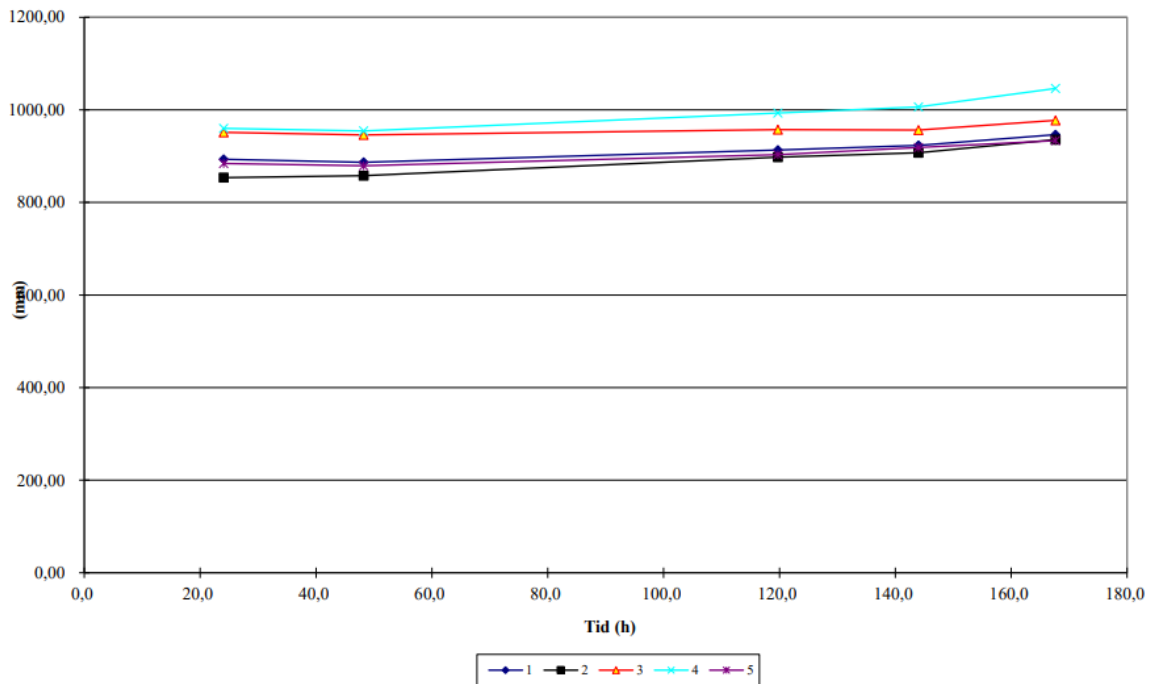
Ekvivalent luftlagstykkelse i perioden

Figure D.18.2: Equivalent air layer thickness sd-value during the period
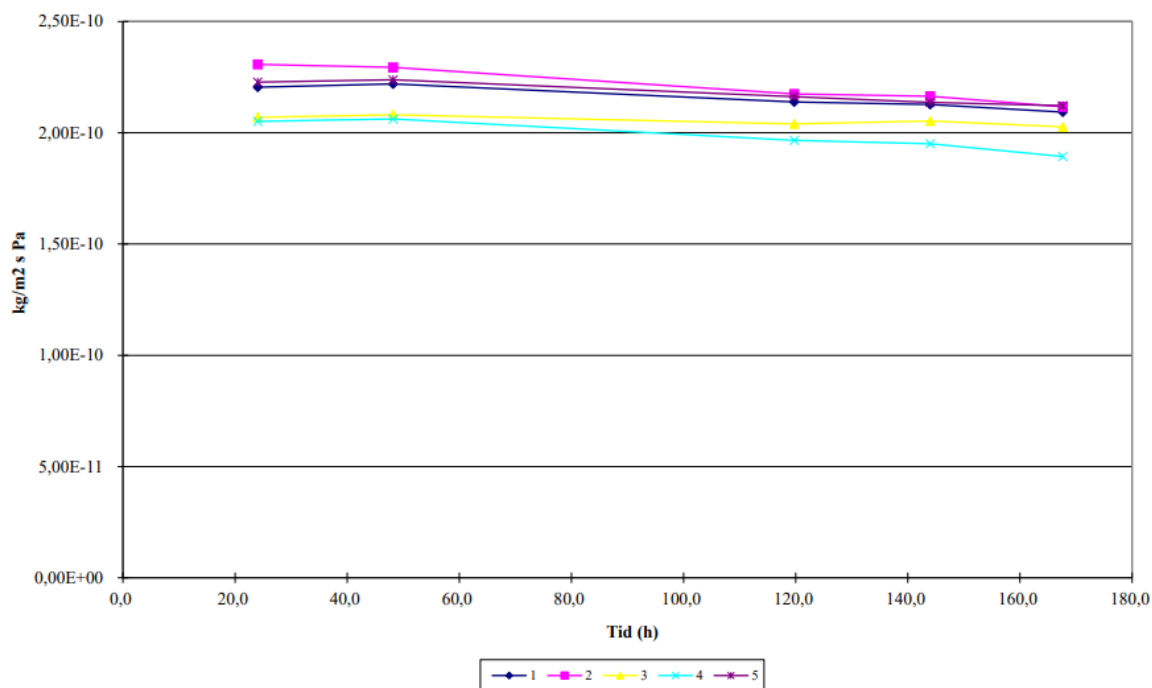
Vanndampgjennomgang i perioden

Figure D.18.3: Water vapour transmission during the period

Table D.18.1: Input data of the wet cup method

(1)Produktnavn:		███████████			Salttype:		KNO3
(2)Oppdragsgiver:		Masteroppgave_Katinka		Katinka	Prøvediameter (mm):		0,164
(3)Prosjektnummer:		58B2			Luftlag salt/prøve (mm):		15
(4)Produktype:		Maling			Prøvest. diameter(mm):		0,174
(5)Tykkelse, mm:		0,4500			Lufth. over pr.(m/s):		0,3
(6)Målenummer:		58B2			RF/Temp:		Vekt:
(12)Dato (CTRL+SHIFT+ ;)			14.02.2024	15.02.2024	16.02.2024	19.02.2024	20.02.2024	21.02.2024
(13)Tid (CTRL+SHIFT+ :)			09:35	09:38	09:47	09:19	09:34	09:14
(14)Beregning fra veiing:	2						
(15)Barometertrykk ved veiing, hPa:			999,15	1009,77	997,81	1009,05	1004,78	997,79
(16)Barometertrykk i perioden, hPa:			999,15	1004,3	1005	1012,99	1007,51	998,5
(17)Temperatur luft over boks,°C:			23	23,04	23,04	23,03	23,02	23,02
(18)Temperatur i saltløsning, °C:			23	23,04	23,04	23,03	23,02	23,02
(19)RF i rommet, %			50	50,6	50,57	50,76	50,74	50,89
(20)Veiing nummer:			1	2	3	4	5	6
(21)Vekt,g kontrolllodd før veiing:			1000	999,999	1000	999,998	1000	1000,002
(22)Vekt,g prøve nr:		1	482,963	482,474	481,994	480,594	480,132	479,685
(23)Vekt,g prøve nr:		2	501,609	501,098	500,602	499,179	498,709	498,257
(24)Vekt,g prøve nr:		3	517,127	516,667	516,217	514,88	514,434	514,001
(25)Vekt,g prøve nr:		4	476,418	475,962	475,516	474,226	473,802	473,397
(26)Vekt,g prøve nr:		5	521,773	521,279	520,795	519,38	518,916	518,463
(27)Vekt,g kontrolllodd etter veiing:			1000,001	999,998	1000	1000	1000,002	1000,004

Prøvestykke:		1	2	3
Tykkelse:	0,45		0,44	0,41
Side mot saltløsning:			Hvit side	
Ferkst/Aldret:			Ferskt	
Start kondisjonering:			27.10.2023	
	Tykkelsesmåler:			Stanse:

D.19. Coating 59B (Three Layers)

SINTEF

Produktnavn:	▉▉▉▉▉▉	Tykkelse, mm:	0,26
Oppdragsgiver:	Masteroppgave_Katinka	Målenummer:	59B
Prosjektnummer:	59B	Prøvediameter: (mm)	164
Produktype:	Maling	Salttype i boksen:	KNO3
		Prøveperiode: fra:	28.02.2024
		til:	05.03.2024

Lufth. over pr.(m/s): 0,3

	Middel i prøveperioden
Relativ luftfuktighet i boksen (%RF)	94,1
Relativ luftfuktighet i rommet (%RF)	50,7
Temperatur i boksen (°C)	23,0
Temperatur i rommet (°C)	23,0
Barometertrykk (hPa)	1001,8

Tykkelse prøve nr

1	0,28
2	0,26
3	0,23
4	0,24
5	0,27
6	0,32

Tabell 1   Temperatur, relativ luftfuktighet og barometertrykk i prøveperioden.

Prøve nummer	Vanndamppermeans W_p	Vanndampmotstand	
		sd	Z_p
	(kg/m²sPa)	(m)	(m²sPa/kg)
1	3,53E-10	0,559	2,83E+09
2	3,53E-10	0,559	2,83E+09
3	3,57E-10	0,553	2,80E+09
4	3,64E-10	0,543	2,75E+09
5	3,41E-10	0,580	2,94E+09
Middel	3,54E-10	0,559	2,83E+09
Std. dev. mean. value	3,75191E-12	0,006	3,04E+07

Tabell 2   Vanndamppermeans og vanndampmotstand for de fem prøvestykkene.
Enkeltresultatene er et middel over fem tidsintervall med stabil fukttransport.
Resultatene er korrigert for overgangsmotstanden over prøven,
damptransport gjennom overlappsonen, og motstanden i luftlaget i boksen.

SIGN:

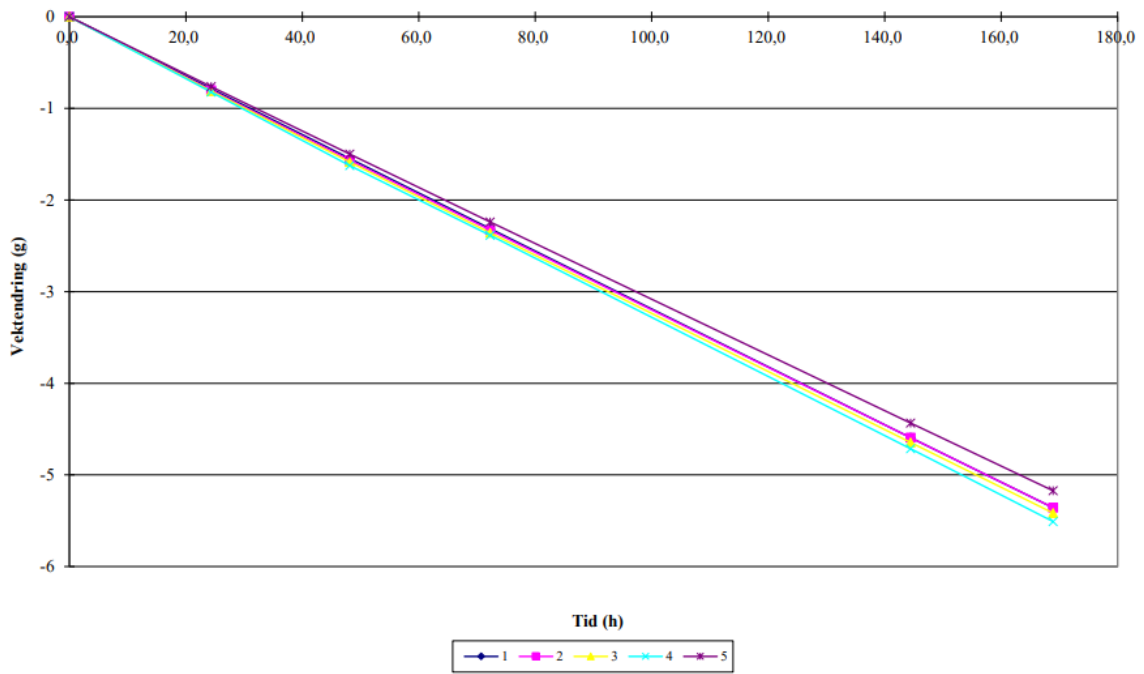Vektendring siden start for de enkelte prøvene

Figure D.19.1: Mass reduction during the period
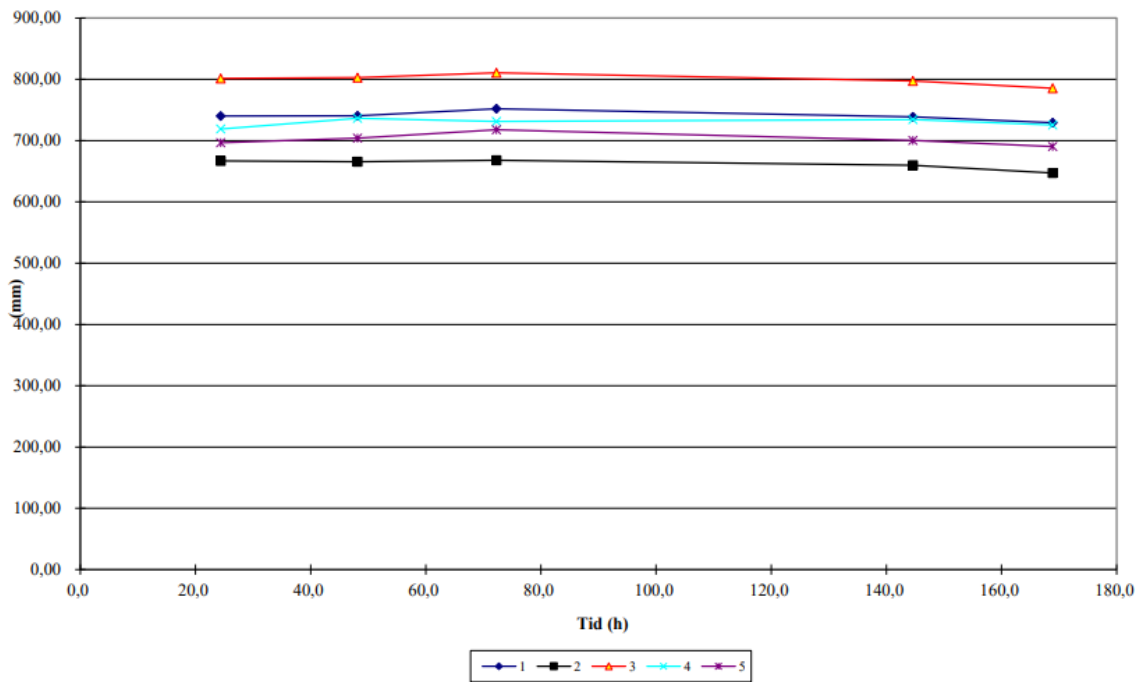
Ekvivalent luftlagstykkelse i perioden

Figure D.19.2: Equivalent air layer thickness sd-value during the period

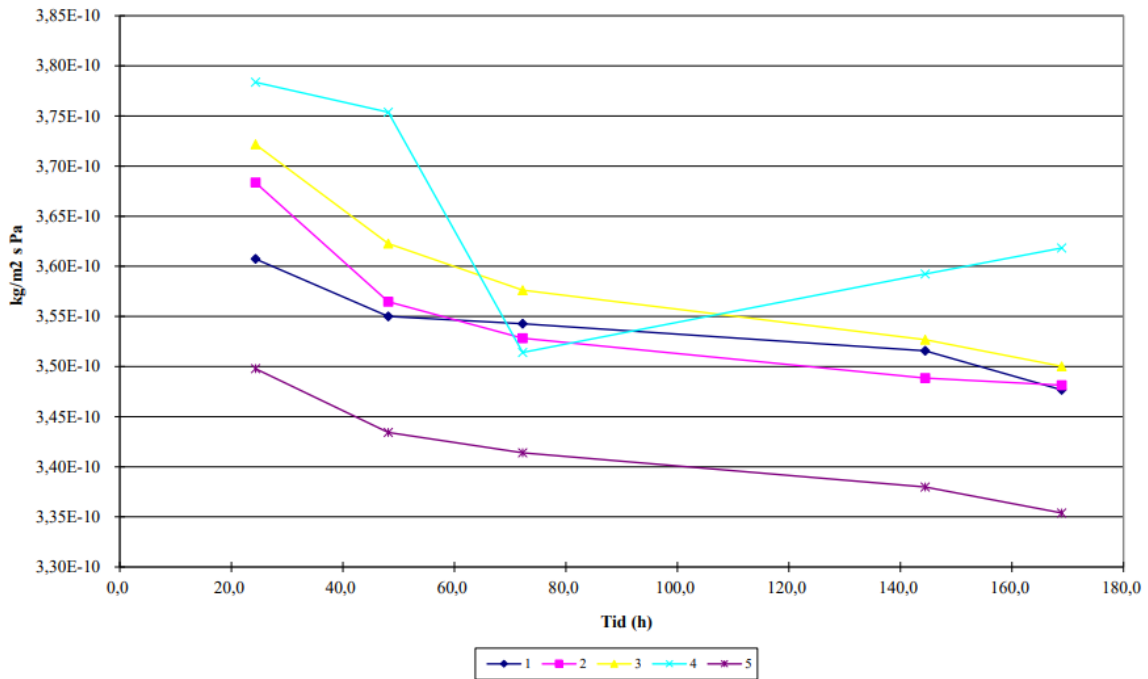**Figure D.19.3**: Water vapour transmission during the period

Table D.19.1: Input data of the wet cup method

(1)Produktnavn:		███████████			Salttype:		KNO3	
(2)Oppdragsgiver:		Masteroppgave_Katinka	Katinka		Prøvediameter (mm):		0,164	
(3)Prosjektnummer:		59B			Luftlag salt/prøve (mm):		15	
(4)Produktype:		Maling			Prøvest. diameter(mm):		0,174	
(5)Tykkelse, mm:		0,2600			Lufth. over pr.(m/s):		0,3	
(6)Målenummer:		59B			RF/Temp:		Vekt:	
(12)Dato (CTRL+SHIFT+;)			27.02.2024	28.02.2024	29.02.2024	01.03.2024	04.03.2024	05.03.2024
(13)Tid (CTRL+SHIFT+:)			08:21	08:41	08:30	08:36	08:48	09:16
(14)Beregning fra veiing:	2							
(15)Barometertrykk ved veiing, hPa:			1002,45	994,04	988,76	995,07	1016,08	1022,93
(16)Barometertrykk i perioden, hPa:			1002,45	996,97	995,34	990,02	1006,72	1019,87
(17)Temperatur luft over boks,°C:			23	23,03	23,03	23,03	23,05	23,06
(18)Temperatur i saltløsning, °C:			23	23,03	23,03	23,03	23,05	23,06
(19)RF i rommet, %			50	50,78	50,62	50,65	50,68	50,69
(20)Veiing nummer:			1	2	3	4	5	6
(21)Vekt,g kontrollodd før veiing:			1000,001	1000,002	1000	1000,003	1000	999,996
(22)Vekt,g prøve nr:		1	477,654	476,871	476,11	475,339	473,051	472,291
(23)Vekt,g prøve nr:		2	479,07	478,271	477,507	476,739	474,468	473,707
(24)Vekt,g prøve nr:		3	485,12	484,313	483,537	482,759	480,464	479,699
(25)Vekt,g prøve nr:		4	486,256	485,436	484,633	483,868	481,532	480,742
(26)Vekt,g prøve nr:		5	515,342	514,582	513,845	513,101	510,898	510,164
(27)Vekt,g kontrollodd etter veiing:			1000,003	1000	1000,003	1000,002	999,997	999,997

Prøvestykke:		1		2		3
Tykkelse:	0,28		0,26		0,23	
Side mot saltløsning:			Hvit side			
Ferkst/Aldret:			Ferskt			
Start kondisjonering:			01.11.2023			

D.20. Coating 59B2 (Six Layers)

SINTEF

Produktnavn:	▮▮▮▮▮▮▮▮	Tykkelse, mm:	0,38
Oppdragsgiver:	Masteroppgave_Katinka	Målenummer:	59B2
Prosjektnummer:	59B2	Prøvediameter: (mm)	164
Produkttype:	Maling	Salttype i boksen:	KNO3
		Prøveperiode: fra:	28.02.2024
		til:	05.03.2024

	Middel i prøveperioden
Relativ luftfuktighet i boksen (%RF)	94,1
Relativ luftfuktighet i rommet (%RF)	50,7
Temperatur i boksen (°C)	23,0
Temperatur i rommet (°C)	23,0
Barometertrykk (hPa)	1001,8

Lufth. over pr.(m/s): 0,3

Tykkelse prøve nr
1 0,36
2 0,37
3 0,41
4 0,38
5 0,39
6 0,34

Tabell 1 Temperatur, relativ luftfuktighet og barometertrykk i prøveperioden.

Prøve nummer	Vanndamppermeans Wp	Vanndampmotstand	
		sd	Zp
	(kg/m²sPa)	(m)	(m²sPa/kg)
1	2,67E-10	0,741	3,75E+09
2	2,98E-10	0,662	3,35E+09
3	2,47E-10	0,800	4,05E+09
4	2,70E-10	0,732	3,70E+09
5	2,81E-10	0,702	3,56E+09
Middel	2,73E-10	0,724	3,67E+09
Std. dev. mean. value	8,48919E-12	0,023	1,15E+08

Tabell 2 Vanndamppermeans og vanndampmotstand for de fem prøvestykkene.
Enkeltresultatene er et middel over fem tidsintervall med stabil fukttransport.
Resultatene er korrigert for overgangsmotstanden over prøven,
damptransport gjennom overlappsonen, og motstanden i luftlaget i boksen.

SIGN:
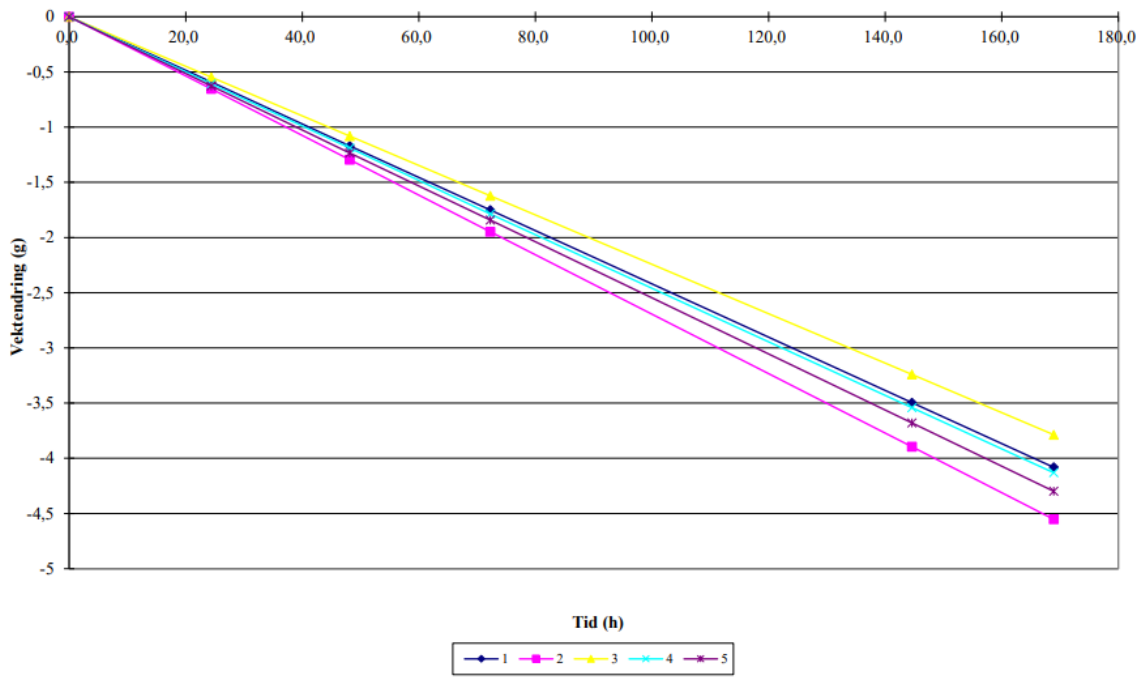
Vektendring siden start for de enkelte prøvene

Figure D.20.1: Mass reduction during the period
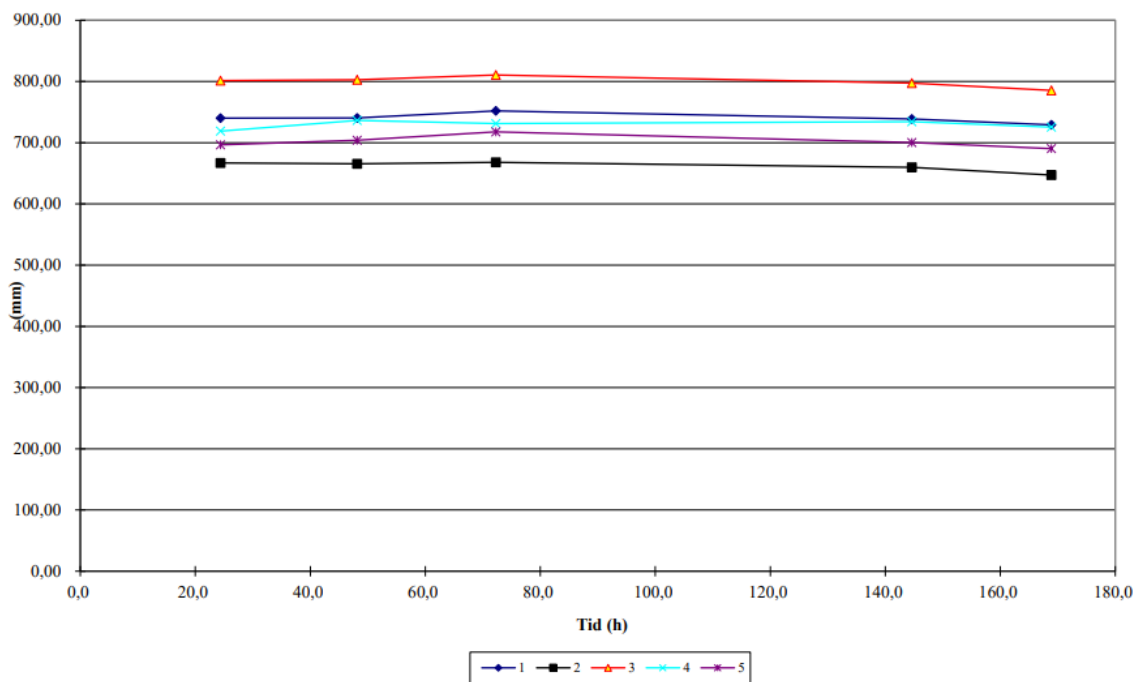
Ekvivalent luftlagstykkelse i perioden

Figure D.20.2: Equivalent air layer thickness sd-value during the period
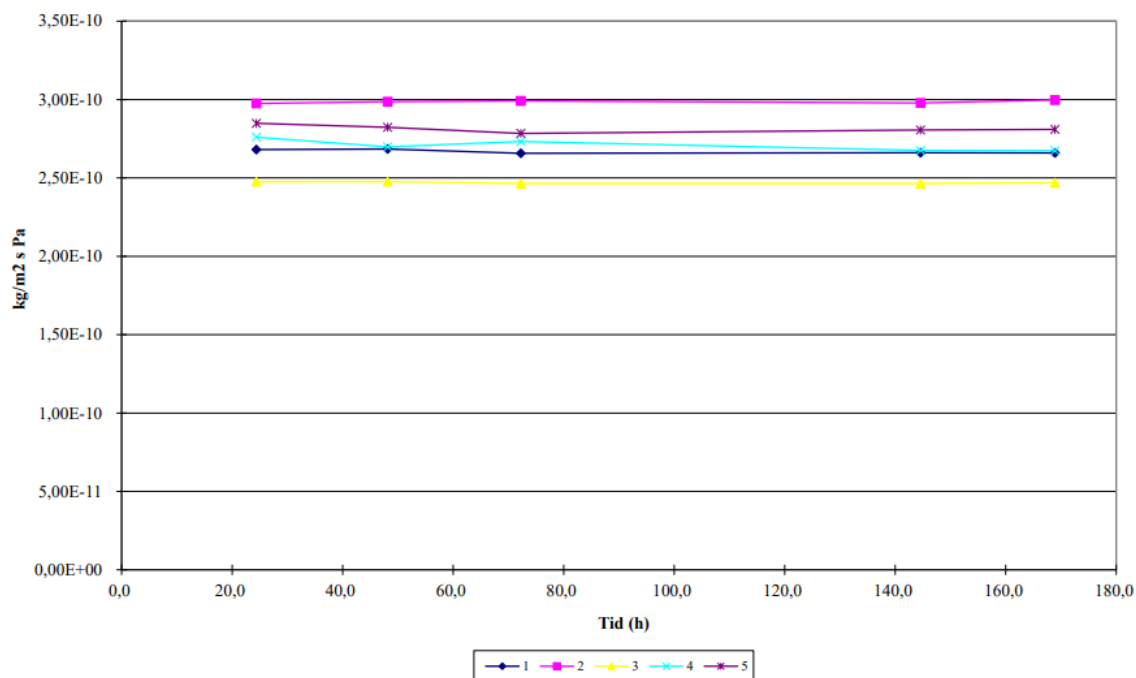
Figure D.20.3: Water vapour transmission during the period

Table D.20.1: Input data of the wet cup method

(1)Produktnavn:					Salttype:		KNO3
(2)Oppdragsgiver:	Masteroppgave_Katinka		Katinka		Prøvediameter (mm):		0,164
(3)Prosjektnummer:	59B2				Luftlag salt/prøve (mm):		15
(4)Produkttype:	Maling				Prøvest. diameter(mm):		0,174
(5)Tykkelse, mm:	0,3800				Lufth. over pr.(m/s):		0,3
(6)Målenummer:	59B2				RF/Temp:		Vekt:
(12)Dato (CTRL+SHIFT+ ;)		27.02.2024	28.02.2024	29.02.2024	01.03.2024	04.03.2024	05.03.2024
(13)Tid (CTRL+SHIFT+ :)		08:26	08:49	08:35	08:42	09:02	09:20
(14)Beregning fra veiing:	2						
(15)Barometertrykk ved veiing, hPa:		1002,45	994,04	988,76	995,07	1016,08	1022,93
(16)Barometertrykk i perioden, hPa:		1002,45	996,97	995,34	990,02	1006,72	1019,87
(17)Temperatur luft over boks,°C:		23	23,03	23,03	23,03	23,05	23,06
(18)Temperatur i saltløsning, °C:		23	23,03	23,03	23,03	23,05	23,06
(19)RF i rommet, %		50	50,78	50,62	50,65	50,68	50,69
(20)Veiing nummer:		1	2	3	4	5	6
(21)Vekt,g kontrolllodd før veiing:		1000,003	1000,002	1000,003	1000,002	999,996	999,998
(22)Vekt,g prøve nr:	1	467,53	466,942	466,363	465,777	464,024	463,444
(23)Vekt,g prøve nr:	2	492,405	491,754	491,112	490,455	488,5	487,848
(24)Vekt,g prøve nr:	3	513,875	513,331	512,796	512,251	510,623	510,084
(25)Vekt,g prøve nr:	4	464,583	463,978	463,396	462,794	461,031	460,448
(26)Vekt,g prøve nr:	5	512,459	511,835	511,227	510,614	508,768	508,156
(27)Vekt,g kontrolllodd etter veiing:		1000,001	1000	1000,003	1000,002	999,997	999,998

Prøvestykke:		1		2		3
Tykkelse:	0,36		0,37		0,41	
Side mot saltløsning:			Hvit side			
Ferkst/Aldret:			Ferskt			
Start kondisjonering:			03.11.2023			
	Tykkelsesmåler:			Stanse:		